# Innovative Assessment Tests and Indicators for Performance-Based Asphalt Mix Design

A Dissertation

Presented in Partial Fulfillment of the Requirements for the

Degree of Doctor of Philosophy

with a

Major in Civil Engineering

in the

College of Graduate Studies

University of Idaho

by

Hamza Alkuime

Major Professor: Emad Kassem, Ph.D., P.E.

Committee Members: Fouad M.S. Bayomy, Ph.D., P.E.; Richard Nielsen, Ph.D., P.E.; Gabriel Potirniche, Ph.D., P.E.

Department Administrator: Patricia J. S. Colberg, Ph.D., P.E.

December 2019

**Authorization to Submit Dissertation**

This dissertation of Hamza Alkuime, submitted for the degree of Doctor of Philosophy with a Major in Civil Engineering and titled "Innovative Assessment Tests and Indicators for Performance-Based Asphalt Mix Design," has been reviewed in final form. Permission, as indicated by the signatures and dates below, is now granted to submit final copies to the College of Graduate Studies for approval.

Major Professor: _____ Date: _____
Emad Kassem, Ph.D., P.E.

Committee Members: _____ Date: _____
Fouad M.S. Bayomy, Ph.D., P.E.

_____ Date: _____
Richard Nielsen, Ph.D., P.E.

_____ Date: _____
Gabriel Potirniche, Ph.D., P.E.

Department Administrator: _____ Date: _____
Patricia J. S. Colberg, Ph.D., P.E.

## Abstract

Asphalt mixes are designed to provide adequate resistance to various distresses including cracking, rutting, and moisture damage. Recently, more efforts are directed towards including performance assessment tests during the design and production of asphalt mixes. Performance-Engineered Mix Design (PEMD) or Balanced Mix Design (BMD) is a new and innovative design approach that incorporates performance assessment tests to optimize the design of asphalt mixes to provide adequate performance. Although transportation agencies are motivated to implement the PEMD approach, several research knowledge gaps and concerns need to be addressed before PEMD successful implementation. This research study aims to advance, develop, and implement performance-engineered design approach and specifications to extend the service life of asphalt pavements.

The first phase of this research developed and evaluated a new and innovative monotonic cracking performance indicator called Weibull Cracking Resistance Index ($Weibull_{CRI}$). The proposed indicator describes the entire load-displacement curve, which overcomes the limitations of the existing performance indicators. First, $Weibull_{CRI}$ was examined using an extensive laboratory evaluation of 16 different asphalt mixes. The results indicated that $Weibull_{CRI}$ was sensitive to variation in binder content and binder PG and the results were in good agreement with the expected cracking resistance based on the composition of the studied mixes. In addition, $Weibull_{CRI}$ had low variability in test results and higher number of various statistical groups. Next, the applicability of $Weibull_{CRI}$ as a unified approach to analyze the results of various monotonic assessment tests was investigated using data generated by other researchers and reported in the literature. The results indicated that $Weibull_{CRI}$ is able to interpret the testing results of various monotonic performance assessment tests (i.e., IDT- intermediate temperature, Semi-Circle Bending [SCB]- intermediate temperature, SCB-low temperature, Disk-Shaped Compact Tension [DCT], and Simple Punching Shear Test [SPST]) and various displacement measurement methods (i.e., actuator vertical displacement and Crack Mouth Opening Displacement [CMOD]). $Weibull_{CRI}$ was also sensitive to variation in test conditions (i.e., specimen notch depth, thickness, and air void content) and mix composition proportions (i.e., binder content,

binder grade, aggregate type, NMAS, aging, rejuvenator dosages, and Recycled Asphalt Pavement [RAP] materials).

The second phase of this study reviewed and evaluated the current monotonic cracking performance assessment tests and indicators including the developed $Weibull_{CRI}$ used to assess asphalt mix resistance to cracking. In this phase, the testing requirements of various test standards, key publications, concepts, calculation methods, physical meaning, and advantages and disadvantages of various performance indicators were reviewed. Then, the study investigated the validity of the most promising testing standards and indicators. Three testing standards and 12 performance indicators were considered. Several aspects were examined including 1) investigate the fundamental meaning of the variation in the load-displacement curve in terms of the change in mix resistance to cracking, 2) sensitivity of performance indicators to mix compositions, 3) variability in test results, 4) number of various statistical groups, 5) correlation between various performance indicators, 6) direct correlation between laboratory results of monotonic performance tests and indicators with the observed field cracking, and 7) ability to develop PEMD specifications. A comprehensive laboratory investigation was conducted using 33 different asphalt mixes included six Laboratory Mixed-Laboratory Compacted (LMLC) and 10 Plant Mixed-Laboratory Compacted (PMLC) asphalt mixes, and 17 field projects with known cracking performance. The results showed that $Weibull_{CRI}$ calculated from the IDT test to have the lowest test variability, maximum number of Tukey's honestly significant difference (HSD) groups, and have excellent correlation with cyclic cracking resistance assessment indicators as compared to the other monotonic performance indicators. In addition, the results demonstrated that there was no direct correlation between all monotonic performance indicators and the observed field cracking performance, therefore an alternative approach was proposed, evaluated, and validated to develop performance thresholds for the selected performance indicators. Three pass/fail cracking performance thresholds were proposed for $Weibull_{CRI}$ to distinguish between asphalt mixes with good, fair, and poor cracking resistance using the proposed approach.

The third phase of this study focused on the development and evaluation of a new cyclic cracking assessment test called Multi-Stage Semi-circle bending Dynamic (MSSD). The test offers advantages over the available monotonic and dynamic cracking assessment tests and addresses major concerns to implement the PEMD (i.e., performance test validity, complex specimen preparation, and testing time). The developed MSSD test simulates the repeated loading (cyclic) in a reasonable testing time (less than 9 hours per test regardless of mix type), has a fixed loading sequence that works for mixes with different characteristics (e.g., mix composition, percent air void content, thickness, etc.), and utilizes testing equipment and specimen geometry similar to that used in monotonic tests. The laboratory evaluation results showed that the proposed test and its derived performance indicators were sensitive to mix composition and had lower variability compared to other dynamic tests. In addition, the MSSD performance indicators correlated well with the observed cracking performance in the field and were able to distinguish between projects with good and poor resistance to cracking. Based on the evaluation results, three pass/fail cracking performance thresholds were proposed to distinguish between asphalt mixes with good, fair, and poor resistance to cracking.

The fourth phase of this research examined the most promising tests and performance indicators to evaluate the resistance of asphalt mixtures to rutting. Two tests (i.e., Hamburg Wheel Tracking test [HWTT], and Asphalt Pavement Analyzer [APA] rut test) and three rutting performance indicators (i.e., HWTT rut depth after 15,000 passes [$HWTT_{15000}$], HWTT rut depth at 20,000 passes [$HWTT_{20000}$], and APA rut depth after 8,000 cycles [$APA_{8000}$]) were considered. An intensive laboratory investigation was conducted that included six LMLC, 10 PMLC, and field cores extracted from 17 field projects. The research findings showed that both HWTT and APA rut test provided similar rutting assessment for the evaluated mixes. The study recommended using the HWTT over the APA rut test since HWTT can be also used to assess the resistance of asphalt mixtures to moisture damage to moisture damage. Also, the study recommended using $HWTT_{15000}$ over $HWTT_{20000}$ as a performance indicator since it requires less testing time.

The final phase of this research provided recommendations of the best testing standards, performance indicators, and performance specifications to assess asphalt mix resistance to cracking and rutting. In addition, it provided guidelines to demonstrate the use of the proposed tools during the design and/or production of asphalt mixes. It also proposed standards testing procedures for the newly developed $Weibull_{CRI}$ performance indicator and MSSD test.

## Acknowledgments

In the name of Allah, the Entirely Merciful, the Especially Merciful.

First of all, I thank Allah for giving me strength, ability, faith, and patient to complete this dissertation.

In my journey towards this degree, I have found a friend, a teacher, a role model and an adviser, Dr. Emad Kassem. I am deeply indebted to his invaluable support, guidance, help, and comments, enduring patience, continuous encouragement and motivation, insightful suggestions, and outstanding mentorship. Dr. Emad has been always happy to generously contribute his time and effort to answer my many and long questions and inquiries for knowledge. I am extremely grateful to his profound belief in my abilities and being an excellent example of hard-working researcher, which encouraged me to suppress my limits to become the researcher who how I am today. I have been lucky to have a supervisor like Dr. Emad Kassem. My research achievements would not have been possible without the support and nurturing of Dr. Emad Kassem.

Also, I would like to extend my deepest gratitude to the other members of my dissertation committee; Dr. Fouad Bayomy, Dr. Richard Nielsen, and Dr. Gabriel Potirniche for their invaluable contribution, suggestions, and guidance and for serving as members of my committee. Also, I would like to extend my appreciation to Dr. Fouad Bayomy, Dr. Richard Nielsen, and Dr. Gabriel Potirniche, and Dr. Sunil Sharma. Their courses provided me with extensive knowledge of pavement and soil materials and finite element analysis and application. I am delighted to thank Dr. S.J. Jung for allowing me using his laboratory for studying and testing. I am extremely grateful for Dr. Patricia J. S. Colberg for her continuous support and guidance. Thanks also to Dr. Ahmad Muftah for his support and advice. Special thanks to Mr. Don Parks for helping me in the lab when I needed. Many thanks to Mr, Brian Petty and Mr. Charles Cornwall for making numerous scientific instruments that I needed in my research.

I would like also to extend my sincere thanks to my friends Mohamed Elsayed, Khaled Alshriedeh, and Arowojolu Niyi. In addition, I would like to extend my sincere thanks to my

colleagues at the University of Idaho, and in particular Simpson Lamichhane, Robinur Chowdhury, Charles Whizzy, Mumtahin Hasnat, Eben Fanijo, Fahmid Tousif, Chaz Woo, Wahid Hassan, Sandarva Sharma, Eric Saasita and Mohammad Al-Assi. I would like also to acknowledge the support provided by Idaho Transportation Department (ITD) research project RP261 and the Hashemite University.

My acknowledgment would be incomplete without thanking the biggest source of my strength, my family. The blessing, love, and care of my parents (Mohammad and Kutna) and my brothers ( Abdul Al-Kareem, and Akram), my sisters (Amira, Amani, Tahani, and Malak). I thank them for their heartfelt support, love, and patience during my study and provide me with invaluable encouragement to follow my dream of getting this degree. This research would not have been possible without their encouragement, unwavering and unselfish love and support, and belief in me.

**Dedication**

I dedicate this dissertation

to who guided me to my faith

to who invested in educating me

to who always had confidence in me

to who profound belief in my abilities

to who taught me Arabic alphabets at the age of four

to who taught me how to be passionate, alive, and committed

to who taught me patience, hard work, and diligence

to who is the secret of my success

to who the source of my happiness

to who gave me the fruits of his life

to who raise me to become the person who I am

to my parents

To my beloved $\frac{Dad}{Mom}$, this is for YOU.

I pray to Allah to guide me to treat you with humility and tenderness

“And lower to them the wing of humility out of mercy and say, "My Lord, have mercy upon them as they brought me up [when I was] small." “

—Quran 17:24

Table of Contents

Authorization to Submit Dissertation ..... ii

Abstract ..... iii

Acknowledgments ..... vii

Dedication ..... ix

Table of Contents ..... x

List of Tables ..... xv

List of Figures ..... xvii

Statement of Contribution ..... xxiii

Chapter 1: Introduction ..... 1

1.1. Overview ..... 1

1.2. Problem Statement and Research Goal ..... 4

1.3. Research Objectives ..... 6

1.4. Research Tasks ..... 7

1.5. Dissertation Organization ..... 9

1.6. References ..... 11

Chapter 2: Development of a New Performance Indicator to Evaluate the Resistance of Asphalt Mixes to Cracking ..... 12

2.1. Abstract ..... 12

2.2. Introduction ..... 12

2.3. Objectives ..... 14

2.4. Development of Weibull Cracking Resistance Index (WeibullCRI) ..... 15

2.5. Experimental Program ..... 19

2.6. Analysis and Discussion ..... 24

2.7. Summary and Conclusions ..... 34

2.8. References ..... 36

Chapter 3: Review and Evaluation of Cracking Testing Standards and Performance Indicators for Asphalt Mixes ..... 40

3.1. Abstract ..... 40

3.2. Introduction ..... 40

3.3. Objectives ..... 42

3.4. Review of Monotonic Intermediate Temperature Cracking Assessment Standards ..... 43

3.5. Review of Current Performance Indicators ..... 45

3.6. Laboratory Experimental Program ..... 56

3.7. Analysis of Results and Discussion ..... 58

3.8. References ..... 78

Chapter 4: Development and Evaluation of Multi-Stage Semi-Circle Bending Dynamic (MSSD) Test to Assess the Cracking Resistance of Asphalt Mixes ..... 83

4.1. Abstract ..... 83

4.2. Introduction ..... 83

4.3. Study Objectives ..... 86

4.4. MSSD Development ..... 87

4.5. Experimental Evaluation ..... 99

4.6. Analysis and Discussion of Test Results ..... 104

4.7. Conclusions ..... 123

4.8. References ..... 124

Chapter 5: Evaluation and Development of Performance-Engineered Specifications for Monotonic Loading Cracking Performance Assessment Tests ..... 129

5.1. Abstract ..... 129

5.2. Introduction ..... 130

5.3. Study Objectives ..... 132

5.4. Results and Discussion ..... 138

5.5. Examine the Cracking Resistance of Currently Produced Asphalt Mixes in Idaho ..... 152

5.6. Selection Recommendation of the Best Monotonic Performance Assessment Test(s) and Indicator(s) to Assess Asphalt Mix Resistance to Cracking ..... 153

5.7. Conclusions and Recommendations ..... 153

5.8. References ..... 154

Chapter 6: Comprehensive Evaluation of Wheel-Tracking Rutting Performance Assessment Tests ..... 158

6.1. Abstract ..... 158

6.2. Introduction ..... 159

6.3. Study Objectives ..... 160

6.4. Review Testing Standards ..... 160

6.5. Experimental Testing Plan ..... 167

6.6. Rutting Performance Evaluation ..... 171

6.7. Analysis and discussion ..... 173

6.8. Summary and Conclusions ..... 189

6.9. References ..... 190

Chapter 7: Investigate the Applicability of Weibull Cracking Resistance Index Using Data Generated by Other Researchers and Reported in The Literature ..... 194

7.1. Abstract ..... 194

7.2. Introduction ..... 195

7.3. Evaluation Plan and Weibull CRI Calculation ..... 196

7.4. Analysis and Discussion ..... 199

7.5. Conclusions ..... 223

7.6. References ..... 224

Chapter 8: Recommendations and Guidelines for PEMD Implementation ..... 228

8.1. Recommendations ..... 228

8.2. Proposed Standard Test Method Drafts ..... 230

8.3. Implementation Guidelines ..... 231

Chapter 9: Conclusions ..... 234

9.1. Conclusions ..... 234

9.2. Research Significance and Contributions to Knowledge ..... 240

9.3. Future Recommendations ..... 241

Appendix A - Detailed Example of Statistical Analysis Results ..... 242

Appendix B - Sensitivity of Monotonic Indicators for Binder Content and PG ..... 250

Appendix C - Correlation between Field Cracking Resistance and Monotonic Indicators .. 256

Appendix D - Correlation Between Monotonic and MSSD Performance Indicators ..... 267

Appendix E - Standard Test Method for Determination of Weibull Cracking resistance Index to Evaluate the Resistance of Asphalt Mixtures to Intermediate Temperature Cracking using Monotonic Loading Cracking Assessment tests ..... 279

Appendix F - Standard Test Method for Evaluation of Asphalt Mixture Resistance to Intermediate Temperature Cracking using Multi-Stage Semi-Circle Bending Dynamic Test ..... 284

Appendix G - Permissions ..... 290

## List of Tables

Table 2.1. Initial values for fitting parameters based on different test data sources ..... 17

Table 2.2. Properties of LMLC mixes ..... 23

Table 2.3. Properties of received PMLC materials ..... 24

Table 2.4. Comparison between WeibullCRI (SC) and WeibullCRI (IDT) ..... 32

Table 3.1 Specified important requirements for intermediate temperature cracking protocols ..... 45

Table 3.2 Selected performance indicator and test data source ..... 57

Table 3.3 LMLC asphalt mixture characteristics [32] ..... 58

Table 3.4 PMLC asphalt mixture characteristics [32] ..... 58

Table 3.5 The sensitivity of monotonic performance indicators to binder content and binder PG ..... 64

Table 3.6 Estimated mix cracking resistance based on its composition ..... 67

Table 3.7 Sensitivity of monotonic performance indicators to PMLC mixe ranking ..... 69

Table 3.8 Pearson coefficient (r) for monotonic performance indicators ..... 74

Table 3.9 Spearman coefficient (rs) for monotonic performance indicators ..... 74

Table 3.10. Monotonic performance indicators comparison summary ..... 75

Table 4.1. Comparison between monotonic, bending beam fatigue, and MSSD tests. ..... 88

Table 4.2. PMLC project information ..... 101

Table 4.3. Properties of received PMLC materials [13] ..... 102

Table 4.4 .Location of selected field projects ..... 103

Table 4.5. Mix properties of selected field projects ..... 103

Table 4.6. Summary of proposed performance thresholds ..... 122

Table 5.1. Identified field projects [15] ..... 135

Table 5.2. Intermediate Temperature Cracking Most Promising Performance Indicators and Its Associate Testing Standards [11]..... 136

Table 5.3. Properties of received PMLC materials..... 148

Table 5.4. Correlation results between MSSD parameters and monotonic cracking resistance indicators..... 151

Table 5.5. Estimated cracking resistance of currently produced mixes in the state of Idaho using the developed performance thresholds for monotonic and cyclic assessment tests.... 152

Table 6.1 Selected testing protocols for rutting assessments [16,22]..... 162

Table 6.2. HWTT rutting performance thresholds [3,4,13–15,5–12]..... 164

Table 6.3 APA rut pass/fail performance thresholds [23,24,33–39,25–32] ..... 165

Table 6.4 Properties of evaluated asphalt mixes..... 170

Table 7.1 Properties of mixes evaluation by Moon et al. (2019) [19]. ..... 200

Table 7.2. The sensitivity of WeibullCRI to the variation in test loading rate using data published in [24–26] ..... 207

Table 7.3. The sensitivity of WeibullCRI to the variation in specimen thickness using data published in [24,25,27] ..... 209

Table 7.4. The sensitivity of WeibullCRI to the variation in specimen air void content using data published in [25–27]..... 211

## List of Figures

Figure 1.1 BMD design approaches [5] ..... 3

Figure 1.2 Implementation of PEMD design approaches or performance assessments test by different stats [5] ..... 3

Figure 1.3 Identified concerns by state DOTs and contractors regarding PEMD implementations ..... 5

Figure 1.4 Identified future research needs by state DOTs and contractors regarding the PEMD design approach. ..... 6

Figure 1.5 Study experimental testing design. ..... 8

Figure 2.1. Fitting the Load-displacement curve using the modified Weibull function ..... 17

Figure 2.2. Example of variation in load-displacement curve with the decrease in binder content; (A) increasing pre-peak slope, (B) increasing peak, (C) increasing post-peak slope, and (D)decreasing failure displacement ..... 20

Figure 2.3. Effects of Weibull parameters on the stress-strain curve shape, A) $A$ parameter, B) $\beta$ parameter, and C) $\eta$ parameter ..... 21

Figure 2.4. Study testing experimental plan ..... 22

Figure 2.5. LMLC aggregate gradation (SP3-12.5mm) ..... 23

Figure 2.6. (A1, A2) the sensitivity of $Weibull_{CRI}$ calculated from the IDT test and SCB test to the binder content, respectively. (B1, B2) the sensitivity of $Weibull_{CRI}$ calculated from IDT test and SCB test to the binder grade, respectively ..... 26

Figure 2.7. A) $Weibull_{CRI}$ (IDT) and B) $Weibull_{CRI}$ (SC) results for the PMLC mixes ..... 28

Figure 2.8. The proposed resistance to cracking thresholds using $Weibull_{CRI}$ (IDT) results. 34

Figure 3.1. Load-displacement basic curve elements ..... 46

Figure 3.2. Laboratory testing plan ..... 57

Figure 3.3. Monotonic tests load-displacement curve at different binder contents ..... 60

Figure 3.4. Monotonic tests load-displacement curve at binder PG and contents ..... 61

Figure 3.5. Monotonic tests load-displacement curve at different RAP content using data published in [14,19] ..... 62

Figure 3.6. Sensitivity of total fracture energy calculated from the IDT test to the binder PG and binder content ..... 63

Figure 3.7 The changes in Load-displacement curve from the IDT test for different PMLC mixes ..... 68

Figure 3.8 Total fracture energy calculated from the IDT test for the PMLC mixes ..... 68

Figure 3.9. COV average, median, and range for different performance indicators using LMLC and PMLC data ..... 70

Figure 4.1. Schematic MSSD test specimen and fixture ..... 88

Figure 4.2. MSSD test fixture inside the AMPT chamber ..... 88

Figure 4.3. Flow chart for MSSD testing stage identification procedures ..... 89

Figure 4.4. Computed fracture toughness for monotonic SCB specimens ..... 92

Figure 4.5. MSSD continuous haversine loading wave ..... 92

Figure 4.6. Selected Kmax value for each loading stage ..... 93

Figure 4.7. ΔK, Kmax, and Kmin for each loading stage ..... 93

Figure 4.8. MSSD test typical output ..... 94

Figure 4.9. Typical vertical displacement S-shaped curve and Inflection points ..... 95

Figure 4.10. Fitting the S-curve with $6^{th}$-degree polynomial function ..... 97

Figure 4.11. Determination of MSSD performance indicators ..... 97

Figure 4.12. Study experimental plan ..... 99

Figure 4.13. The variation in the rate of change of vertical actuator displacement and number of cycles versus the change in SIF (ΔK) for all field projects ..... 104

Figure 4.14. Example of MSSD performance indicators (H and z) for mixes with good and poor observed field cracking resistance. ..... 105

Figure 4.15. MSSD Slope (z) performance indicator results and proposed performance thresholds for field projects ..... 105

Figure 4.16. MSSD absolute intercept (Abs [Log H]) performance indicator and proposed performance thresholds for field projects ..... 106

Figure 4.17. Subjective cracking performance evaluation for all field test projects ..... 108

Figure 4.18. Correlation between the Slope (z) performance indicator with the observed field cracking resistance and developing the performance thresholds ..... 111

Figure 4.19. Correlation between the Abs (Log *H*) performance indicator with the observed field cracking resistance and developing the performance thresholds using field projects results ..... 111

Figure 4.20. Determination of MSSD performance indicators (z and Abs [log H]) for PMLC mixes ..... 113

Figure 4.21. MSSD slope (z) performance indicator for PMLC mixes ..... 113

Figure 4.22. MSSD Abs (Log H) performance indicator for PMLC mixes ..... 114

Figure 4.23. Correlation between MSSD test performance indicators (z and abs [log H]) for both field and PMLC mixes ..... 118

Figure 4.24. Initial estimation of cracking resistance for slope (z) performance indicator using PMLC mixes laboratory results ..... 120

Figure 4.25. Initial estimation of cracking resistance for Abs (log H) performance indicator using PMLC mixes laboratory results ..... 120

Figure 5.1. Measured (A) average Air void content, (B) average thickness for the extracted field cores ..... 137

Figure 5.2. Correlation between subjective performance groups and (A) $G_{fracture}$ [IDT]), (B) CRI(SCB-FI), (C) FI (SCB-FI), (D) IDEAL-$CT_{Index}$, (E) Nflex, (F) $IDT_{Modulus}$, (G) $J_c$, and (H) $Weibull_{CRI}$ ..... 139

Figure 5.3. The variation in the load-displacement curve of SCB test with A) specimen air void content and B) specimen thickness; (1) increasing pre-peak slope, (2) increasing peak, (3) increasing post-peak slope, and (4) decreasing failure displacement using data published in Rivera (2017) [19] ..... 142

Figure 5.4. Correlation observed field project performance with corrected (A) $G_{fracture}$ [IDT]), (B) CRI(SCB-FI), (C) FI (SCB-FI), (D) IDEAL-$CT_{Index}$, (E) Nflex, (F) $IDT_{Modulus}$, (G) $J_c$, and (H) $Weibull_{CRI}$..... 145

Figure 5.5. (A) Correlation between MSSD parameters (slope, and absolute intercept) and $Weibull_{CRI,}$(B) Proposed $Weibull_{CRI}$ performance thresholds based on the MSSD slope ($z$) parameter..... 148

Figure 6.1. Cycle-deformation curves for A) HWTT and B) APA rut test, respectively ..... 161

Figure 6.2. Study experimental design ..... 167

Figure 6.3. Hamburg test specimen preparation; a) placing the specimen in the casting mold, b) mixing the plastering materials, c) filling the gap with plastering materials and smoothing the surface, d) the bottom surface after plastering, e) levelling the Hamburg test specimens. ..... 169

Figure 6.4. Field rut depth measurements for selected locations..... 172

Figure 6.5. Sensitivity to binder PG A1) $HWTT_{15000}$, B1) $HWTT_{20000}$, and C1) $APA_{8000}$ and sensitivity to binder content A2) $HWTT_{15000}$, B2) $HWTT_{20000}$, and C2) $APA_{8000}$ ..... 175

Figure 6.6. PMLC mixes results for performance A) $HWTT_{15000}$, B) $HWTT_{20000}$, and C) $APA_{8000}$ ..... 176

Figure 6.7. Rutting results for field cores for A) $HWTT_{15000}$, B) $HWTT_{20000}$, and C) $APA_{8000}$ ..... 177

Figure 6.8. Moisture damage in A) D5C2 field project and B) D2C11 field project ..... 178

Figure 6.9. Testing results variability for all mixes (LMLC, PMLC, and field cores) for A) $HWTT_{15000}$, B) $HWTT_{20000}$, and C) $APA_{8000}$ ..... 183

Figure 6.10. Correlation between A) $HWTT_{15000}$ and $HWTT_{20000,}$ B) $HWTT_{15000}$ and $APA_{8000,}$ $HWTT_{20000}$ and $APA_{8000}$ indicators ..... 184

Figure 6.11. Laboratory versus field performance A) $HWTT_{15000}$, B) $HWTT_{20000}$, and C) $APA_{8000}$ ..... 185

Figure 6.12. rut depth for all test mixes (LMLC, PMLC, and field cores) for A) $HWTT_{15000}$, B) $HWTT_{20000}$, and C) $APA_{8000}$ ..... 186

Figure 7.1. Research plan for Task ..... 195

Figure 7.2. Data extraction procedure using WebPlotDigitizer ..... 196

Figure 7.3. $Weibull_{CRI}(SCB_{Low\text{-}temperature})$ for mixes prepared with different RAP content at a test temperature of A) -12 °C and B) -24 °C using data published in [19]. ..... 200

Figure 7.4. $Weibull_{CRI}$ from SPST using data collected from Faruk et al. (2015) [20] ..... 201

Figure 7.5. A) correlation between $Weibull_{CRI}(SCB_{CMOD})$ and $Weibull_{CRI}$ $(SCB_{LLD})$ and B) correlation between $Weibull_{CRI}(DCT_{CMOD})$ and $Weibull_{CRI}(SCB_{CMOD})$ and between $Weibull_{CRI}$ $(DCT_{CMOD})$ and $Weibull_{CRI}(SCB_{LLD})$ using data published in [23]. ..... 203

Figure 7.6. The sensitivity of $Weibull_{CRI}$ to the variation in specimen notch depth using data published in [24,25] ..... 204

Figure 7.7. The sensitivity of $Weibull_{CRI}$ to the variation in binder content using data published in [13,26] ..... 210

Figure 7.8. The sensitivity of $Weibull_{CRI}$ to the variation in aggregate type and binder grade using data published in [18]. ..... 212

Figure 7.9. The sensitivity of $Weibull_{CRI}$ to the variation in NMAS at A) different specimen thickness and B) at different specimen air void content using data published in [27] ..... 213

Figure 7.10. The sensitivity of $Weibull_{CRI}$ to the variation in aggregate type and binder grade using data published in [32] ..... 214

Figure 7.11. The sensitivity of $Weibull_{CRI}$ to A) different rejuvenator dosages and B) rejuvenator and aging effects using data published in [27] ..... 216

Figure 7.12. The sensitivity of $Weibull_{CRI}$ to the variation in Recycled Binder Replacement (RBR) percentages using data published in [2,4,18]. ..... 217

Figure 7.13. $Weibull_{CRI}$ from the Disk-shaped compact tension using data collected from Chiangmai, (2010) [21]..... 218

Figure 7.14. Correlation between $Weibull_{CRI}$ for the Disk-shaped compact tension and A) $Nf_{50}$ and B) PV using data collected from Chiangmai, (2010) [21]..... 219

Figure 7.15. Correlation between $Weibull_{CRI}$ from IDT and SCB tests with MSSD performance indicators [13,14,22]..... 221

Figure 8.1. Schematic of implementation of the proposed HWTT rutting and cracking thresholds ..... 230

Figure 8.2. Implementation of performance tests as quality control tools..... 231

## Statement of Contribution

Dr. Emad Kassem advised me throughout all research phases including research concept, design, data collection, analysis and interpretation, and manuscript preparation.

Dr. Fouad Bayomy and Dr. Richard Nielsen guided me during my research and assisted me in preparing research manuscripts.

Mr. Fahmid Tousif assisted me in test sample preparation and testing for Chapter 3.

# Chapter 1: Introduction

## 1.1. Overview

The Superpave mix design system was developed under the Strategic Highway Research Program (SHRP) in the early 1990s. It aimed to produce economical asphalt mixes that have adequate asphalt content, air voids, voids in the mineral aggregate, workability, and acceptable field performance [1]. Three design levels (Level 1, 2, and 3) were initially proposed for the Superpave mix design. Level 1 addressed material selection and compaction procedures to produce mixes that satisfy basic volumetric requirements without evaluation of mix performance. Levels 2 and 3 included additional mix performance specifications. Mixes were evaluated for rutting, fatigue cracking, and thermal cracking using laboratory performance assessment tests [1]. Meanwhile, the Superpave implementation is often limited to Level 1 since it required less time and efforts. However, pavement distresses (e.g., rutting and cracking) are observed in pavements designed using the Superpave procedures.

Currently, more efforts are being paid for including performance assessment tests during the design and production of asphalt mixes. Performance-Engineered Mix Design (PEMD) or Balanced Mix Design (BMD) is an innovative design approach that incorporates performance assessment tests to ensure that asphalt mixes have adequate resistance to specific distresses (e.g., cracking and rutting). Recently, Federal Highway Administration (FHWA) initiated a special task force group aimed to define the PEMD approach and to identify the current implementation of PEMD specifications, the available performance assessment tests, and the future research needs for PEMD approach [2].

PEMD is defined as *"Asphalt mix design using performance tests on appropriately conditioned specimens that address multiple modes of distress taking into consideration mix aging, traffic, climate and location within the pavement structure"* [3]. There are three main approaches for PEMD (Figure 1.1) [4].

(1) *Volumetric Design with Performance Verification*: In this approach, asphalt mix is designed using the currently Superpave volumetric specifications. The performance assessment tests are conducted to verify the performance (resistance) of the designed

mix to specific distress (e.g., cracking and rutting). The designed mix should meet the Superpave volumetric as well as PEMD performance specifications to be accepted. Otherwise, it should be redesigned starting from the Superpave volumetric analysis. This approach is the simplest and frequently used by different transportation agencies.

(2) *Performance-Modified Volumetric Mix Design*: In this approach, asphalt mix is initially designed using the currently Superpave volumetric specifications to determine initial mix proportions (e.g., binder content, Recycled Asphalt Pavement [RAP], aggregate gradation., etc.). Then, performance assessment tests are conducted to assess the performance (resistance) of the designed mix to specific distress (e.g., cracking and rutting). The designed mix should meet the PEMD specifications only to be accepted without any further considerations to the Superpave volumetric design specifications. Otherwise mix proportions (e.g., binder content) should be modified until achieving PEMD requirements.

(3) *Performance Design*: In this approach, the asphalt mix is fully designed using performance assessment tests. The Superpave volumetric design specifications are not required to be achieved, but it may be used as design guidelines only. The mix is designed and prepared using different proportions and evaluated using performance assessment tests to select the proper mix design proportions.

Transportation agencies are interested in implementing either one of the PEMD design approaches and incorporating performance assessment tests (Figure 1.2) [5]. In fact, some states DOTs implemented either one of the first or the second PEMD approaches (Figure 1.2). The first PEMD design approach is being implemented by state DOTs in Texas, Wisconsin, New Jersey, Louisiana, and Illinois, while the second approach is being implemented by California state DOT. In addition, 20 state DOTs are currently implementing a performance assessment test to assess mixes resistance to either rutting or cracking (Figure 1.2).

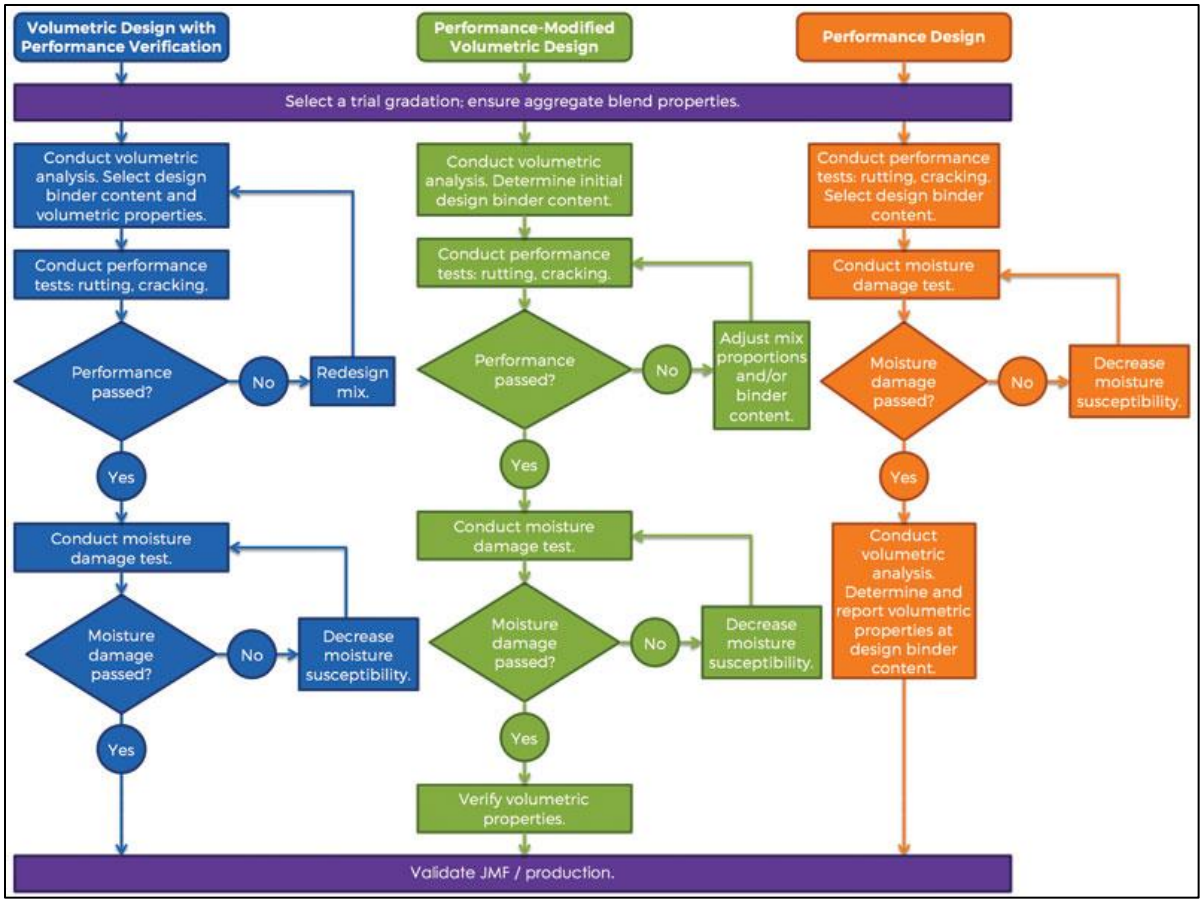


**Figure 1.1** Schematic illustration of three BMD approaches [5].

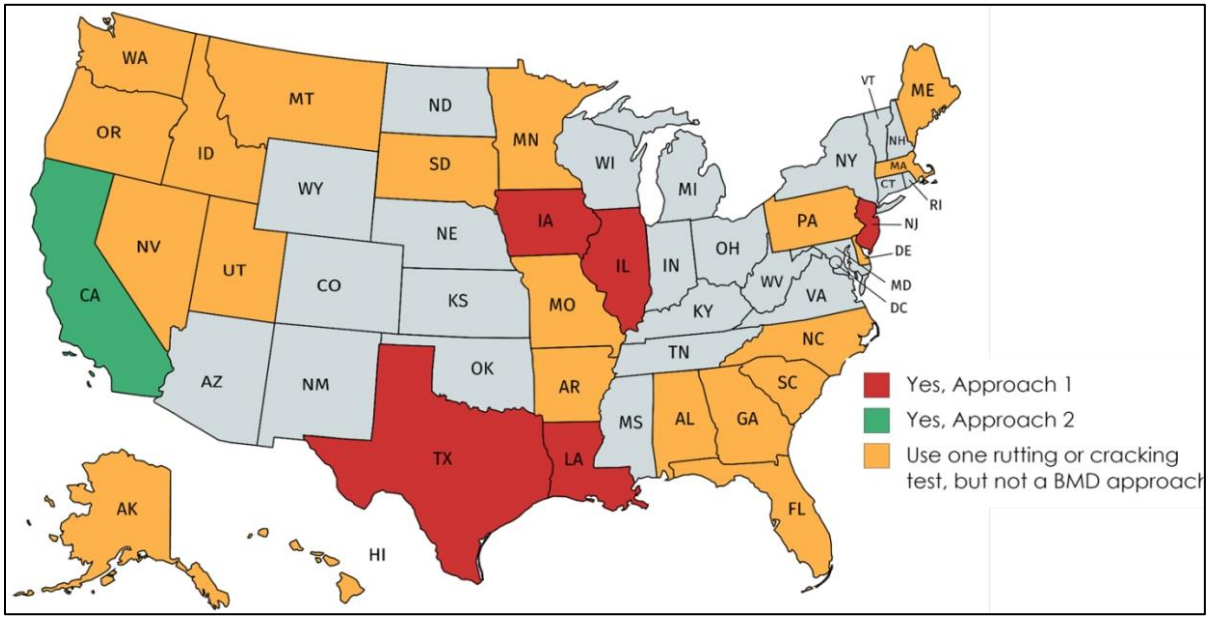


**Figure 1.2** U.S. map of current use of BMD approaches [5].

### 1.2. Problem Statement and Research Goal

Although many state DOTs are interested in PEMD implementation, there are several research knowledge gaps, concerns, and needs related to the PEMD design approach that needs to be addressed by the asphalt research community. Recently, the National Cooperative Highway Research Program (NCHRB) project 20-07 was conducted to develop a framework for the PEMD (or BMD) design approach [5]. As part of this project, the current practice, research knowledge gaps, concerns, and needs related to the BMD (or PEMD) design approach were identified.

The study distributed a national online survey to collect information related to the PEMD approach. The survey showed that state DOTs and contractors have several concerns about implementing the PEMD approach as can be seen in Figure 1.3. The main concern is related to the validity of the current performance assessment tests such as the ability to correlate with the observed field performance, ability to develop PEMD specifications (i.e., pass/fail performance assessment thresholds), statistical mix performance grouping, test result variabilities, and sensitivity to mix composition. In addition, they had concerns with specimen long preparation and testing time for performance assessment tests such as cyclic (dynamic) cracking resistance assessment tests, and concerns with the acceptance testing standards of PEMD and not enough understanding of PEMD approach. In addition, they informed that the priority of PEMD future research should be to identify the best performance assessment tests, to develop training materials, and implementation plan for PEMD (Figure 1.4). Furthermore, the survey also indicated that the fatigue cracking and rutting were identified as being the main pavement distresses that need to be addressed in the PEMD process. About 40 and 30 state DOTs are interested in implementing fatigue cracking and rutting assessment tests, respectively.

It can be observed from the survey outcomes that most of the state DOTs and contractors were uncertain about the appropriate selection of test type, testing standards, performance indicators, and test evaluation criteria (i.e., pass/fail performance thresholds) to be implemented, especially to assess asphalt mix resistance to cracking and rutting. These assessment tools contribute to the core design step within all proposed PEMD design

approaches ( i.e., conduct performance tests) as can be seen in Figure 1.1. Therefore, the success of PEMD design approach depends mainly on the efficiency of the incorporated performance assessment tests, indictors (i.e., analysis methods), and PEMD specifications (i.e., performance thresholds) to assess asphalt mix resistance to required distress (e.g., cracking and rutting), regardless of what approach is being used. Therefore, it is necessary to address these concerns and needs to ensure a successful implementation of the PEMD design approach.

The goal of this research study was to advance, develop, and implement performance-engineered design approach and specifications to extend the service life of asphalt pavements.

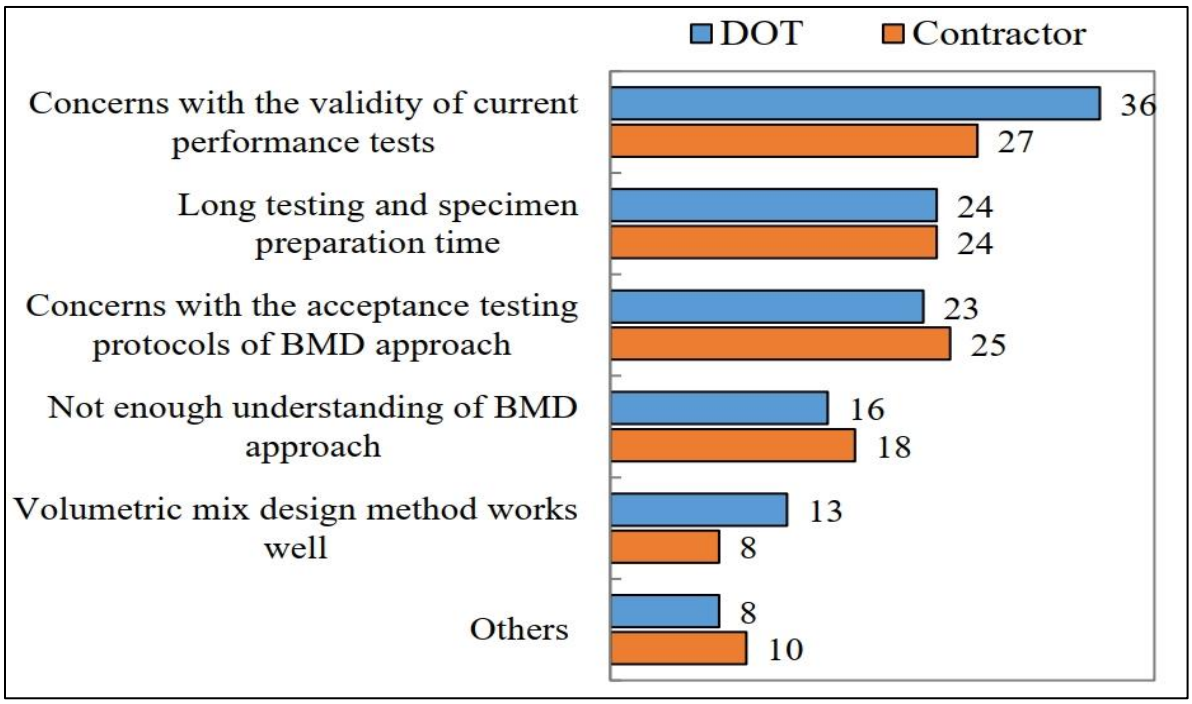


**Figure 1.3** Concerns regarding BMD implementation [5].

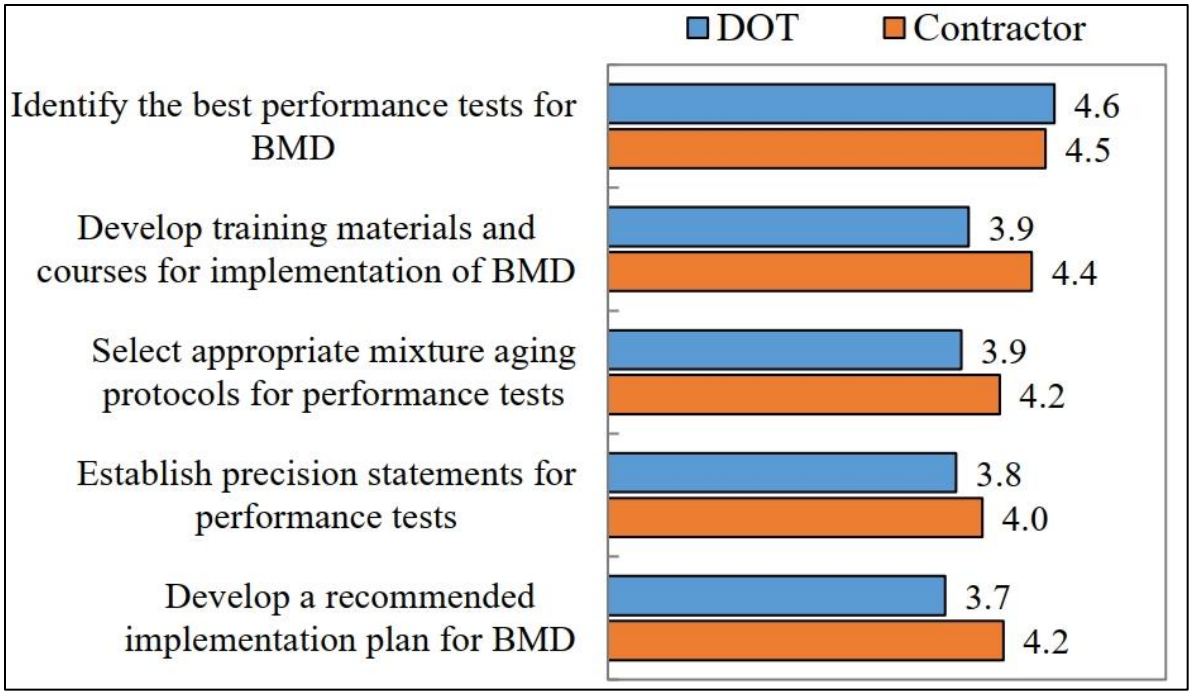


**Figure 1.4** Concerns regarding BMD implementation [5].

### 1.3. Research Objectives

To meet the research goal, the following objectives were identified:

(1) Review and document the most promising performance assessment tests and indicators to assess asphalt mix resistance to cracking and rutting. The review included testing requirements, conditions, and concept, calculation method, physical meaning, and advantages and disadvantages of the available performance indicators. In addition, the review identified the limitations of these methods.

(2) Develop and evaluate a new innovative dynamic cracking assessment test that overcomes the limitations of the current monotonic and dynamic cracking assessment tests and address the concerns of state DOTs and contractors (e.g., long specimen preparation and testing time) to evaluate the resistance of asphalt mix to cracking.

(3) Develop and evaluate a new innovative monotonic cracking performance assessment indicator that overcomes the limitations of the existing performance indicators to evaluate the resistance of asphalt mix to cracking.

(4) Investigate the applicability of the proposed monotonic cracking performance indicator as a unified approach to interpret and analyze the output of various monotonic assessment tests using data generated by other researchers and reported in the literature.

(5) Conduct a comprehensive laboratory evaluation using laboratory-prepared specimens to investigate the validity of the most promising performance tests and indicators as well as the newly developed dynamic cracking assessment test and monotonic cracking performance indicator to assess asphalt mix resistance to cracking and rutting.

(6) Conduct a comprehensive laboratory evaluation using extracted field cores to develop PEMD specifications for the most promising performance tests and indicators as well as the newly developed dynamic cracking assessment test and monotonic cracking performance indicator to assess asphalt mix resistance to cracking and rutting.

(7) Develop, propose, and evaluate an alternative approach to develop PEMD specifications for monotonic cracking performance assessment indicators.

(8) Develop recommendations and guidelines for the implementation of PEMD in the state of Idaho based on the results of this study.

### 1.4. Research Tasks

In order to achieve the main objectives of this study, the following tasks were performed.

Task 1: *Conduct a literature review*. This task involved reviewing and documenting the most promising current performance tests and performance indicators used to evaluate cracking and rutting resistance of asphalt mix.

Task 2: *Develop new and innovative cracking assessment tests*. In this task, the author proposed and developed a new and innovative unified performance indicator (analysis method) to interpret and analyze the output of the monotonic cracking assessment tests (i.e., load-displacement curve). In addition, the author developed a new dynamic loading cracking

assessment test. These methods are designed and proposed to overcome the limitations of the current cracking assessment tests and performance indicators identified in Task 1.

Task 3: *Identify and select testing materials and conduct field performance evaluation*. In this research, two types of testing specimens were evaluated; laboratory-prepared specimens and extracted field cores. The laboratory-prepared specimens include six Laboratory Mixed-Laboratory Compacted (LMLC) and 10 Plant Mixed-Laboratory Compacted (PMLC) asphalt mixes, while the field cores were obtained from 17 field pavement projects with known field cracking and rutting performance. This task also documented the properties of the selected test materials, specimen preparation procedures, and the procedures used to evaluate the field cracking and rutting performance of the selected projects.

Task 4: *Conduct laboratory performance tests*. This task involved designing and conducting a comprehensive laboratory testing program that included laboratory-prepared specimens and extracted field cores in accordance with the selected cracking and rutting performance assessment testing standards as shown in Figure 1.5.

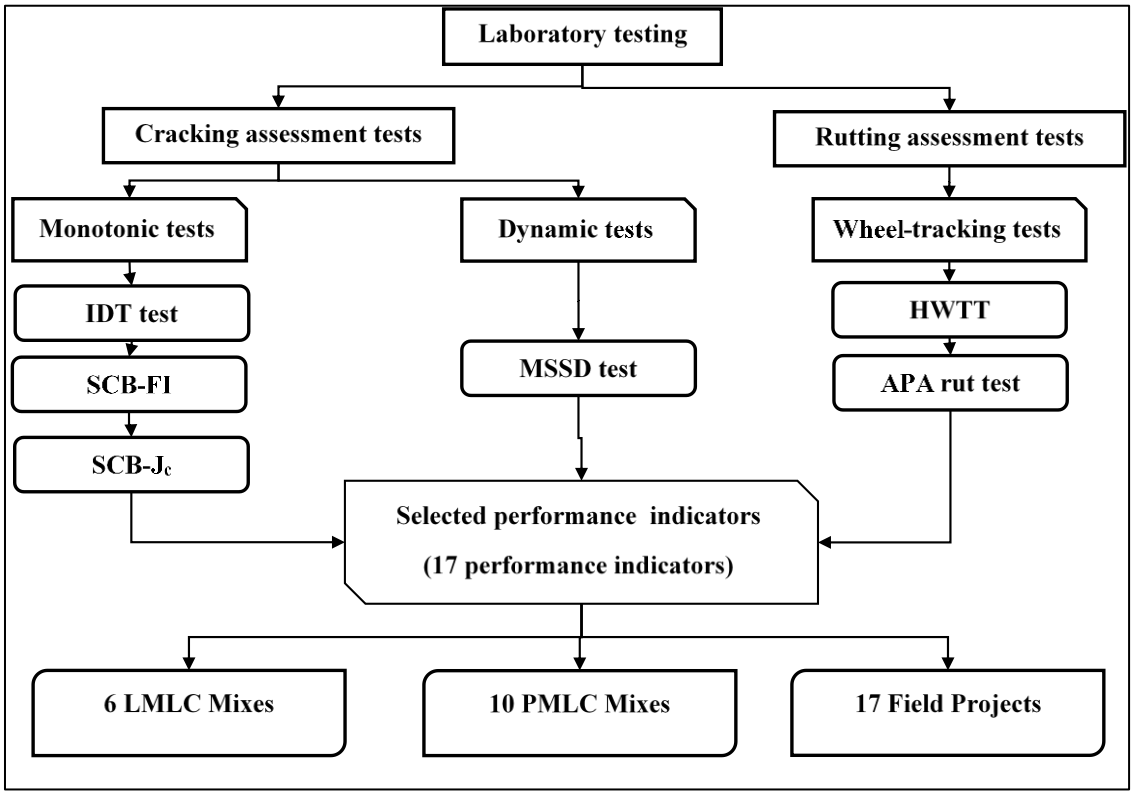


**Figure 1.5** Study experimental testing design.

Task 5: *Conduct a comprehensive evaluation of cracking and rutting performance of laboratory-prepared specimens*. This task analyzes the testing results of laboratory-prepared specimens to examine various cracking and rutting performance tests and indicators in terms of 1) sensitivity to mix compositions (i.e., binder content, binder Performance Grade [PG]), 2) statistical grouping for mixes performance, 3) indicators variability, 4) correlation between various indicators, and 5) the performance of the currently produced PMLC mixes.

Task 6: *Develop PEMD specifications to assess mix resistance to cracking and rutting*. This task analyses the results of the extracted field cores as well as the observed field performance to develop PEMD specifications (i.e., performance assessment thresholds) for cracking and rutting performance. This task also developed, proposed and evaluated a new alternative approach to identify proper performance thresholds for monotonic cracking assessment tests and indicators.

Task 7: *Develop recommendations and guidelines for PEMD*. This task provided recommendations on the selected testing standards, performance indicators, and performance specifications to assess asphalt mix resistance to cracking and rutting. Also, it provided guidelines to demonstrate the use of the proposed methods during the design and/or production of asphalt mix.

Task 8: *Investigate and propose a universal analysis method for monotonic performance assessment tests*. This task examined and evaluated the applicability of the proposed performance analysis method, developed in Task 2, as a unified approach to analyze the results of various monotonic assessment tests using data generated by other researchers and reported in the literature. The evaluation covered three main aspects including 1) sensitivity to the change in testing conditions (e.g., specimen notch depth), 2) sensitivity to the change in mix properties (e.g., Recycled Asphalt Pavement [RAP]), and 3) ability to analyze other monotonic assessment tests (e.g., low-temperature cracking monotonic assessment tests).

### 1.5. Dissertation Organization

This dissertation consists of nine chapters and six appendices.

**Chapter 1** provides an introduction to this research, presents the research problem statement, goal, objectives, and tasks, and the dissertation organization.

**Chapter 2** (*Manuscript No. 1*) presents the development of a new innovative monotonic cracking performance assessment indicator that overcomes the limitations of the existing performance indicators. In addition, it presents the laboratory evaluation results using laboratory-prepared specimens.

**Chapter 3** (*Manuscript No. 2*) documents the available monotonic cracking assessment tests and performance indicators. In addition, it presents the laboratory evaluation results of the most promising monotonic testing standards and performance indicators as well as the newly developed monotonic performance indicator using laboratory-prepared specimens.

**Chapter 4** (*Manuscript No. 3*) presents the development of a new innovative dynamic cracking assessment test that overcomes the limitations of the current monotonic and dynamic cracking assessment tests and addresses the concerns of state DOTs and contractors. In addition, it presents the laboratory evaluation results and the developed PEMD specifications using laboratory-prepared specimens and extracted field cores, respectively.

**Chapter 5** (*Manuscript No. 4*) presents the development of PEMD specifications for monotonic cracking assessment tests and performance indicators based on the performance evaluation of the laboratory-prepared specimens and extracted field cores.

**Chapter 6** (*Manuscript No. 5*) documents the most promising wheel-tracking rutting performance assessment tests and indicators. In addition, it presents the laboratory evaluation results and the developed PEMD specifications using laboratory-prepared specimens and extracted field cores, respectively.

**Chapter 7** (*Manuscript No. 6*) summarizes the investigation outcomes of the applicability of the proposed monotonic cracking performance indicator as a unified approach to interpret

and analyze the output of various monotonic assessment tests using data generated by other researchers and reported in the literature.

**Chapter 8** provides recommendations of the best testing standards, performance indicators, and performance specifications to assess the resistance of asphalt mix to cracking and rutting. Also, it provides guidelines to demonstrate the use of the proposed methods during the design and/or production of asphalt mix.

**Chapter 9** summarizes the main findings of this study and its significance and contributions to the practice. In addition, it provides recommendations for future research.

## 1.6. References

[1] R. Cominsky, G. a Huber, T.W. Kennedy, M. Anderson, The Superpave Mix Design Manual for New Construction and Overlays, Publication NO SHRP-S-407 Strategic Highway Research Program, U.S. (1994) 184.

[2] S. Buchanan, R.F. Bonaquist, J. Bukowski, C. Abadie, FHWA Asphalt Mixture Expert Task Group annual meeting, 2015.

[3] S. Buchanan, Balanced Mix Design Task Force Update of Activities, Presented at Asphalt Mixture Expert Task Group(ETG) Meeting. (2016).

[4] NCAT, Moving Towards Balanced Mix Design for Asphalt Mixtures, (2019). http://www.eng.auburn.edu/research/centers/ncat/newsroom/2017-spring/balanced-mix.html.

[5] R.C. West, C. Rodenzo, F. Leiva, F. Yin, Development of a framework for balanced mix design, NCHRP project 20-07/task 406, 2018. http://apps.trb.org/cmsfeed/TRBNetProjectDisplay.asp?ProjectID=4324.

# Chapter 2: Development of a New Performance Indicator to Evaluate the Resistance of Asphalt Mixes to Cracking

Hamza Alkuime[1]; Emad Kassem[1], Ph.D., P.E., M.ASCE; Fouad M.S. Bayomy[1], Ph.D., P.E., M.ASCE; Richard J. Nielsen[1], Ph.D., P.E, M.ASCE.

(Submitted to Journal of Transportation Engineering, Part B: Pavements)

## 2.1. Abstract

Several monotonic performance indicators that use one or more elements of the load-displacement curve (e.g., area under the curve, curve peak, etc.) are used to assess the resistance of asphalt mix to cracking. While these indicators have their own merits, they lack the full description of the load-displacement curve. This study developed a new performance indicator called Weibull Cracking Resistance Index ($Weibull_{CRI}$), which describes the entire load-displacement curve. The study performed an extensive laboratory evaluation of 16 different asphalt mixes tested in two different testing protocols (i.e., Indirect Tension test [IDT] and Semi – Circle bending [SCB test]) to evaluate the proposed indicator. The findings of this study demonstrated that $Weibull_{CRI}$ results were sensitive to the variation in binder content and binder PG and were in good agreement with expected cracking resistance based on the composition of the studied mixes. In addition, the $Weibull_{CRI}$ had low variability and provided a good statistical grouping of mix resistance to cracking. The study recommended the IDT test to determine $Weibull_{CRI}$ in order to assess asphalt mix resistance to cracking.

Keywords: semi-circular bending; indirect tension test, performance-engineered mix design (PEMD); balanced mixed design (BMD)

## 2.2. Introduction

The Superpave design system was introduced through the Strategic Highway Research Program (SHRP) in the late 1990s. It aimed to produce economical asphalt mixes that have adequate asphalt binder content, air void content, voids in mineral aggregates, workability,

[1] Department of Civil and Environmental Engineering, University of Idaho, Moscow, ID 83844 USA.

and acceptable field performance [1]. Pavement distresses (e.g., rutting and cracking) are observed in pavements designed using the Superpave procedures. Currently, performance assessment tests are increasingly being included during the design and production process of asphalt mixes. Performance-Engineered Mix Design (PEMD) or Balanced Mix Design (BMD) is an innovative design approach that incorporates the performance assessment tests in the mix design process to ensure that asphalt mixes have adequate resistance to specific distresses (e.g., cracking, rutting, or moisture damage). BMD is defined as "*Asphalt mix design using performance tests on appropriately conditioned specimens that address multiple modes of distress taking into consideration mix aging, traffic, climate and location within the pavement structure*" [2]. A recent survey showed that six state departments of transportation (DOTs) are currently using the BMD and there are 29 state DOTs are willing to use the BMD in the future [3].

In the United States, pavement cracking distresses are the main concern since the Superpave mainly focused on improving the resistance of asphalt mix to rutting [3]. The survey results showed that 40, 30, and 29 state DOTs are planning to address fatigue-, thermal-, and reflection-related cracking, respectively using laboratory cracking assessment tests [3]. In the state of Idaho, a local survey, distributed by the authors to Idaho Transportation Department (ITD) Materials Engineers, reported that cracking is the main distress in the state of Idaho. In addition, ITD Materials Engineers show interest in implementing a cracking performance assessment test in addition to the currently specified rutting performance assessment test.

Assessment tests for asphalt mix resistance to cracking include monotonic as well as cyclic tests based on the mode of loading. The monotonic loading tests apply the load at a constant displacement rate, while the cyclic tests apply a repeated load at a given frequency and wave shape. The cyclic tests require complex and costly testing systems, long testing times, and complicated specimen preparation procedures [4]. These requirements make the cyclic tests less preferable to be used by the asphalt industry or transportation agencies. On the other hand, monotonic tests require simpler and less expensive testing systems, shorter testing time, and simpler specimen preparation procedures [4]. Although monotonic tests are

not true fatigue cracking tests, several research studies reported that monotonic tests had good correlation with the observed field cracking resistance [5–9].

Several monotonic tests were proposed and standardized to assess asphalt mix resistance to cracking (e.g., AASHTO TP105 and TP124, ASTM D8044, D6931, and D8225, and LADOTD TR330). These tests have a similar loading concept (i.e., constant displacement rate) and outputs (i.e., load-displacement curve), but they have different testing conditions (e.g., loading rate, specimen geometry, and test temperature. etc.). In the monotonic tests, the applied load and the associated actuator vertical displacement are recorded and used to generate the load-vertical displacement curve. The monotonic tests use the variation in the load-displacement curve to assess the variation in mix resistance to cracking.

Several performance indicators derived from the load-displacement curve were proposed to assess the resistance of asphalt mix to cracking. These indicators include total fracture energy ($G_{fracture}$), Indirect tensile strength ($IDT_{strength}$), Indirect tensile modulus ($IDT_{Modulus}$), Indirect tensile asphalt cracking test ($IDEAL\text{-}CT_{Index}$ ), Cracking Resistance Index (CRI), Flexibility Index (FI), Nflex factor, and Critical strain energy release rate ($J_C$) [5,7,8,10–17]. These performance indicators use one or more elements of the load-displacement curve (e.g., area under the curve, curve peak, post- and pre-peak slopes, termination displacement, etc.) to describe the resistance of asphalt mix to cracking (i.e., variation in load-displacement shape). For instance, the $IDT_{strength}$ uses the curve peak, the $G_{fracture}$ uses the area under the curve, the CRI uses the area under the curve and the peak load, while the FI uses the area under the curve and the post-peak slope. While these methods have their own merits, they lack the full description of the load-displacement curve. Therefore, there is a need to develop an alternative method to describe the entire load-displacement curve and propose a performance indicator that can be used to assess the resistance of asphalt mix to cracking.

## 2.3. Objectives

The main objectives of this study were:

- Propose a method to fit the overall load-displacement (or stress-vertical strain) curve for any monotonic test (e.g., Indirect tension test [IDT], Semi-Circle Bending test [SCB], IDT, etc.) output and derive a performance indicator to assess the cracking resistance of asphalt mix.

- Evaluate the sensitivity of the proposed performance indicator to mix properties such as the binder content, binder performance grade (PG), and composition of the mix (e.g., using RAP). In addition, this study evaluated the indicator variability and statistical grouping for mixes cracking resistance.

- Select the best standardized monotonic cracking assessment testing protocol to calculate the proposed performance indicator.

- Propose initial cracking resistance performance thresholds for asphalt mixes produced in Idaho.

## 2.4. Development of Weibull Cracking Resistance Index (Weibull$_{CRI}$)

### *2.4.1. Fitting of the Load-Displacement Curve of The Monotonic Cracking Assessment Tests*

The load-displacement (or stress-strain) curve can be described using the two-parameter Weibull probability density function [18]. This function has two parameters: the shape parameter ($\beta$) and the scale parameter ($\eta$) as presented in Equation 2.1.

$$f(x) = \left(\frac{\beta}{\eta}\right)\left(\frac{x}{\eta}\right)^{\beta-1} \times e^{-(\frac{u}{\eta})^{\beta}} \quad 2.1$$

where $f(x)$ is the dependent variable, $x$ is the independent variable, $\beta$ is the shape parameter (Weibull slope), $\eta$ is the scale parameter.

A third parameter (i.e., parameter *A*) equivalent to the area under the load-displacement curve was added to be able to describe any load-displacement curve as presented in Equation 2.2.

$$P = A \times \left(\frac{\beta}{\eta}\right)\left(\frac{u}{\eta}\right)^{\beta-1} \times e^{-(\frac{u}{\eta})^{\beta}} \quad 2.2$$

where $P$ is the applied load or stress, A is the area parameter (equivalent to the area under the load-displacement curve or stress-strain curve), $\beta$ is the shape parameter (Weibull slope), $\eta$ is the scale, $u$ is the measured displacement (vertical actuator displacement, LVDT or CMOD) or strain.

The load-displacement curve fitting is performed using the Nonlinear Least Square Fitting (NLSF) regression method. In this approach, the NLSF fitting is optimized to provide a minimum Sum of Squared Errors (SSR) between the measured and the predicted load/stress values (Equation 2.3). The fitting accuracy is checked using the Standard Error (SE), the coefficient of determination ($R^2$), and the 95% Confidence Intervals (CI) as presented in Equations 2.4, 2.5, and 2.6, respectively. The NLSF fitting can be performed using commercial software (e.g., OriginLab) or using Excel's SOLVER tool. In this study, the procedures provided by Brown (2001) for performing the NLSF using Excel SOLVER were followed [19]. The Excel SOLVER requires an initial estimation of the fitting parameters (i.e., $A$, $\beta$, and $\eta$). Table 2.1 presents values for initial estimations of model parameters found to work properly for various monotonic tests.

$$\text{SSR} = \sum_{i=1}^{n}\left[P_{measured} - P_{predicted}\right]^2 \quad 2.3$$

$$\text{SE} = \frac{SSR}{df} \quad 2.4$$

$$R^2 = 1 - \frac{SSR}{\sum_{i=1}^{n}[P_{measured} - P_{mean}]^2} \quad 2.5$$

$$\text{CI} = t_{critial} \times SE \quad 2.6$$

where $SSR$ is the sum of squared error, $P_{measured}$ is the measured load/stress at displacement/strain, $P_{predicted}$ is the predicted load/stress at displacement/strain I, $i$ is a counter, $n$ is the number of measured data points, $df$ is the degrees of freedom ($df = n -$

3), $P_{mean}$ is the average value of the measured load, $t_{critial}$ is the critical t-value at 95% confidence interval.

Figure 2.1 shows an example of using the modified Weibull function (Equation 2.2) to fit the load-vertical actuator displacement curve generated from IDT test data. The function fits the entire curve data with excellent accuracy (coefficient of determination [$R^2$] = 0.997). In addition, Figure 2.1 demonstrates that the 95% CI bands provide an accurate estimation of the measured load values.

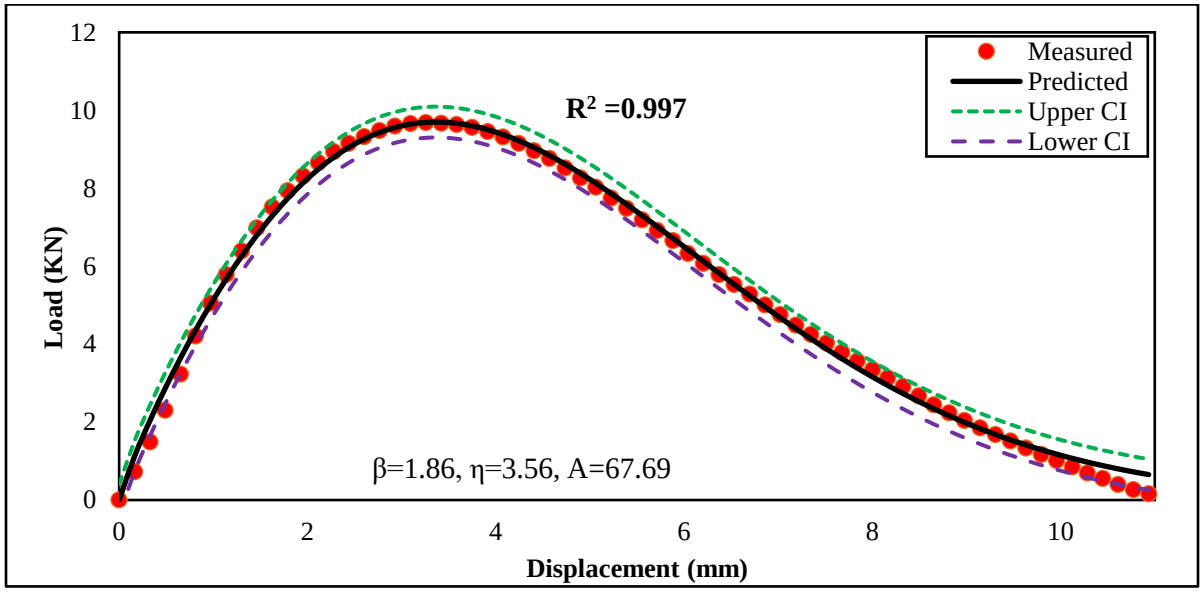


**Figure 2.1**. Fitting the Load-displacement curve using the modified Weibull function

**Table 2.1**. Initial values for fitting parameters based on different test data sources

| Testing protocol | Curve | Initial proposed values | | |
|---|---|---|---|---|
| | | Fitting Parameters | | |
| | | $A$ | $\beta^1$ | $\eta$ |
| IDT | Stress-strain | 2000.0 | 1.80 | 2.30 |
| IDT | Load- actuator vertical Displacement | 50.0 | 1.80 | 2.30 |
| SCB at intermediate temperature | Load- actuator vertical Displacement | 3.0 | 1.80 | 1.60 |
| SCB at Low temperature | Load- CMOD displacement | 0.5 | 1.30 | 0.10 |
| Disk shaped (Load -CMOD) | Load- CMOD displacement | 0.8 | 2.00 | 0.30 |

Note: Load is in N, Displacement in mm, the stress in kPa, strain in %, CMOD in mm,
[1] $\beta$ shall be larger than 1

*2.4.2. Interpretation of the Variation in the Load-Displacement Curve Shape Using Weibull Fitting Parameters*

The shape of the load-displacement curve changes with the variation in the composition of asphalt mixes. Figure 2.2 demonstrates the change in the load-displacement curve for the IDT test at different binder contents. As the binder content decreased, the curve peak, the pre- and post-peak slopes increased, while the termination (final) displacement decreased as shown in Figure 2.2. Such changes in these basic elements indicate an overall decline in the mix resistance to cracking. For instance, a steeper post-peak slope indicates that the cracks are propagating faster. Therefore, the specimen would fail earlier which indicates a decline in the mix resistance to cracking. This understanding of the relation between changes in load-displacement curve basic elements (e.g., post-peak slope) and the change in mix resistance to cracking was used to investigate the relation between Weibull fitting parameters (i.e., *A*, $\beta$, and $\eta$) and the mix resistance to cracking.

Figure 2.3 demonstrates the effect of model parameters *A*, $\beta$, and $\eta$ on the shape of the stress versus unit vertical deformation, respectively. In Figure 2.3, the stress (${\sigma_{tesnile}}^{IDT}$) and unit vertical deformation ($l_{v_i}$) were computed using Equations 2.7 and 2.8 respectively. It can be observed that the increase in the area parameter "*A*" pulls the peak of the curve upwards causing increased area under the curve, increased peak load, and increased pre-and post-peak slopes (Figure 2.3-A), which indicates an overall improved mix resistance to cracking. The increase in the shape parameter "$\beta$", pulls the curve peak upwards and to the right causing increased pre- and post-peak and decreased terminal strain (i.e., strain at 20 kPa), which demonstrates an overall reduction in mix resistance to cracking (Figure 2.3-B). The increase in the scale parameter "$\eta$" pulls the curve downward resulting in decreased pre- and post-peak slopes and increased terminal strain, which demonstrates improved mix resistance to cracking (Figure 2.3-C).

$$ {\sigma_{tesnile}}^{IDT} = \frac{2000\text{xP}}{\pi \times \text{t} \times \text{D}} \qquad 2.7 $$

$$ l_{v_i} = \frac{\Delta l_i}{\text{D}} \times 100\% \qquad 2.8 $$

where $\sigma_{tesnile}{}^{IDT}$ is the tensile stress (kPa), $P$ is the applied load (N), t is the specimen thickness (mm), D is the specimen diameter (mm), F is the load per unit specimen width at failure (N/mm), $l_{v_i}$ is unit vertical deformation at load i (%), (mm), $\Delta l_i$ is the change in vertical displacement (mm), $D$ is the initial specimen diameter (mm). Weibull Cracking Resistance Index ($Weibull_{CRI}$)

Based on the findings on the relation between Weibull parameters (i.e., $A$, $\beta$, and $\eta$) and mix resistance to cracking, the authors proposed a performance indicator called Weibull Cracking Resistance Index ($Weibull_{CRI}$) as presented by Equation 2.9. The $Weibull_{CRI}$ increases with the scale parameter "$\eta$" and area parameter "$A$", while it decreases with the increase in the shape parameter "$\beta$". The $Weibull_{CRI}$ is proposed as a performance indicator to evaluate asphalt mix resistance to cracking, where higher $Weibull_{CRI}$ values indicate better or improved resistance of asphalt mix to cracking.

$$Weibull_{CRI} = \left(\frac{\eta}{\beta}\right) \times log[A] \qquad 2.9$$

where $\beta$ is the shape parameter (Weibull slope), $\eta$ is the scale parameter, $A$ is the area parameter equals to the area under the load-displacement curve.

## 2.5. Experimental Program

In order to evaluate the $Weibull_{CRI}$, a testing experimental plan was developed as shown in Figure 2.4. The plan included an extensive laboratory evaluation of 112 specimens that were prepared from 16 different asphalt mixes.

### *2.5.1. Testing* Standards

The monotonic tests have a similar loading concept (constant displacement rate) and test outputs (i.e., time, load, and vertical actuator displacement), but they have different requirements on the geometry of the testing specimen (e.g., specimen shape, thickness, or diameter). For cracking assessment tests, two specimen geometries are being used: the circular (or IDT) specimen and the notched Semi-Circle (SC) specimen. In this study, both specimen geometries were evaluated. The IDT specimen was evaluated in accordance with

ASTM D6931 *'Standard Test Method for Indirect Tensile (IDT) Strength of Asphalt Mixtures*, or the newly developed ASTM D8225 'Standard *Test Method for Determination of Cracking Tolerance Index of Asphalt Mixture Using the Indirect Tensile Cracking Test at Intermediate Temperature'.* The SC specimen was evaluated in accordance with AASHTO TP 124 '*Standard Method of Test for Determining the Fracture Potential of Asphalt Mixtures Using the Flexibility Index Test (FIT)'.*

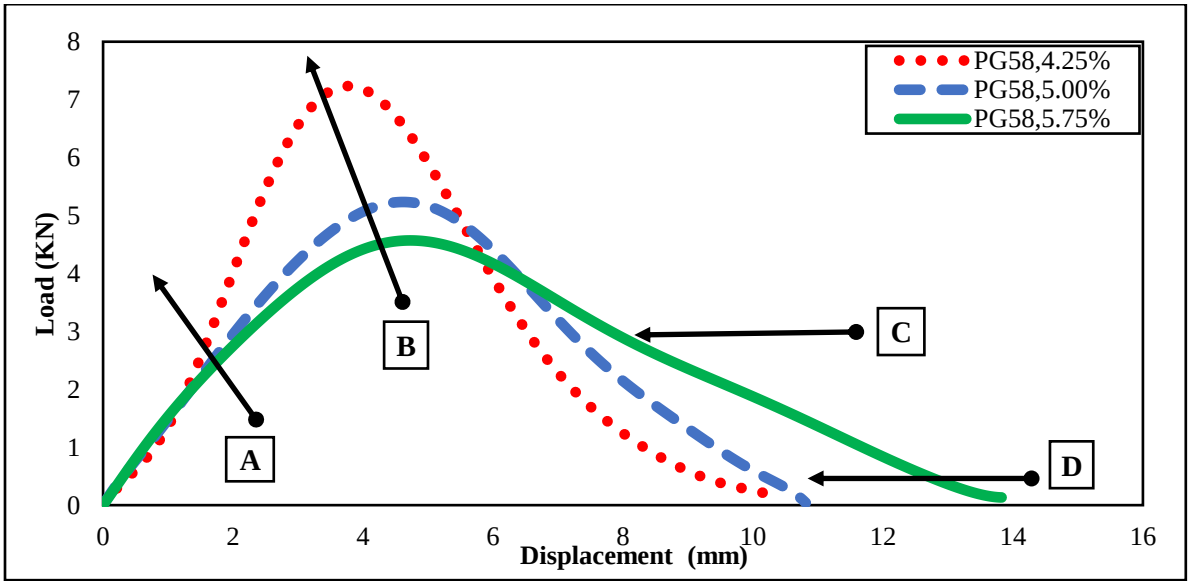


**Figure 2.2.** Example of variation in load-displacement curve with the decrease in binder content; (A) increasing pre-peak slope, (B) increasing peak, (C) increasing post-peak slope, and (D)decreasing failure displacement

The determination of $Weibull_{CRI}$ does not require any additional or modification on testing standard requirements or procedures. However, in this study, the requirements on the testing system and specimen geometry (i.e., diameter and thickness) were unified between the two testing standards to remove any bias in the results of the tests from these sources (i.e., IDT and SCB). Tests were performed using a servohydraulic testing system (i.e., Material Testing System [MTS]) at the University of Idaho laboratory. The IDT and SC test specimens had a thickness of 50 mm and they were 150 mm in diameter. Other testing standard requirements were followed as specified such as test loading rate (50 mm/min), test temperature (25 °C), SC notch depth (15 mm), and loading fixtures.

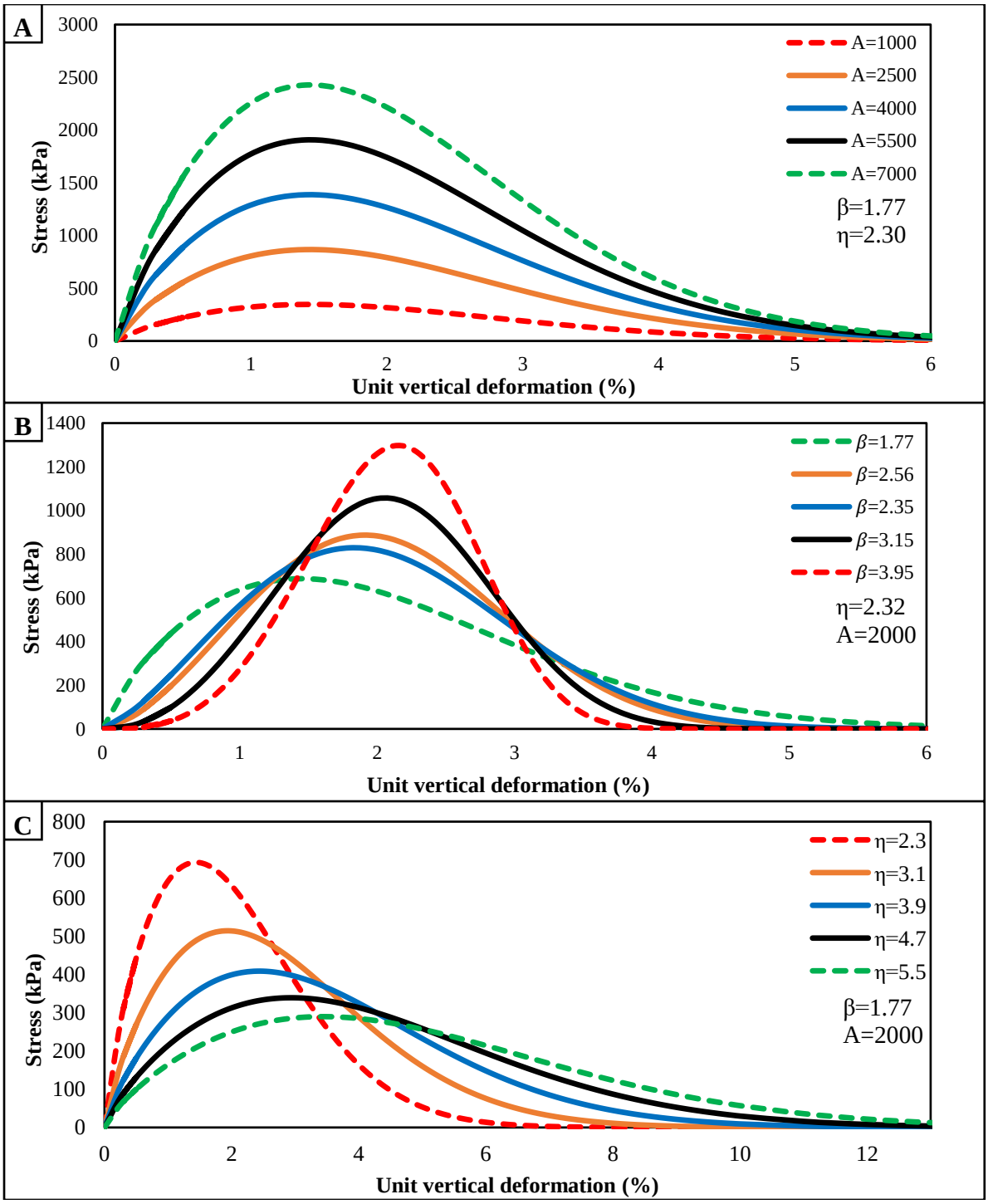


**Figure 2.3**. Effects of Weibull parameters on the stress-strain curve shape, A) $A$ parameter, B) $\beta$ parameter, and C) $\eta$ parameter

The $Weibull_{CRI}$ was calculated using each testing protocol results included $Weibull_{CRI}$ (IDT) calculated from ASTM-D6931 or ASTM-D8225 (i.e., IDT specimen) results and $Weibull_{CRI}$ (SC) calculated from AASHTO TP 124 (i.e., SC specimen) results. The indicators

were compared in terms of sensitivity to binder content, binder PG, and composition of PMLC mixes, and statistical grouping and variability. The findings were then used to identify the appropriate testing protocols and conditions (e.g., specimen shape [IDT, or SC]) to measure the newly proposed performance indicator (i.e., $Weibull_{CRI}$).

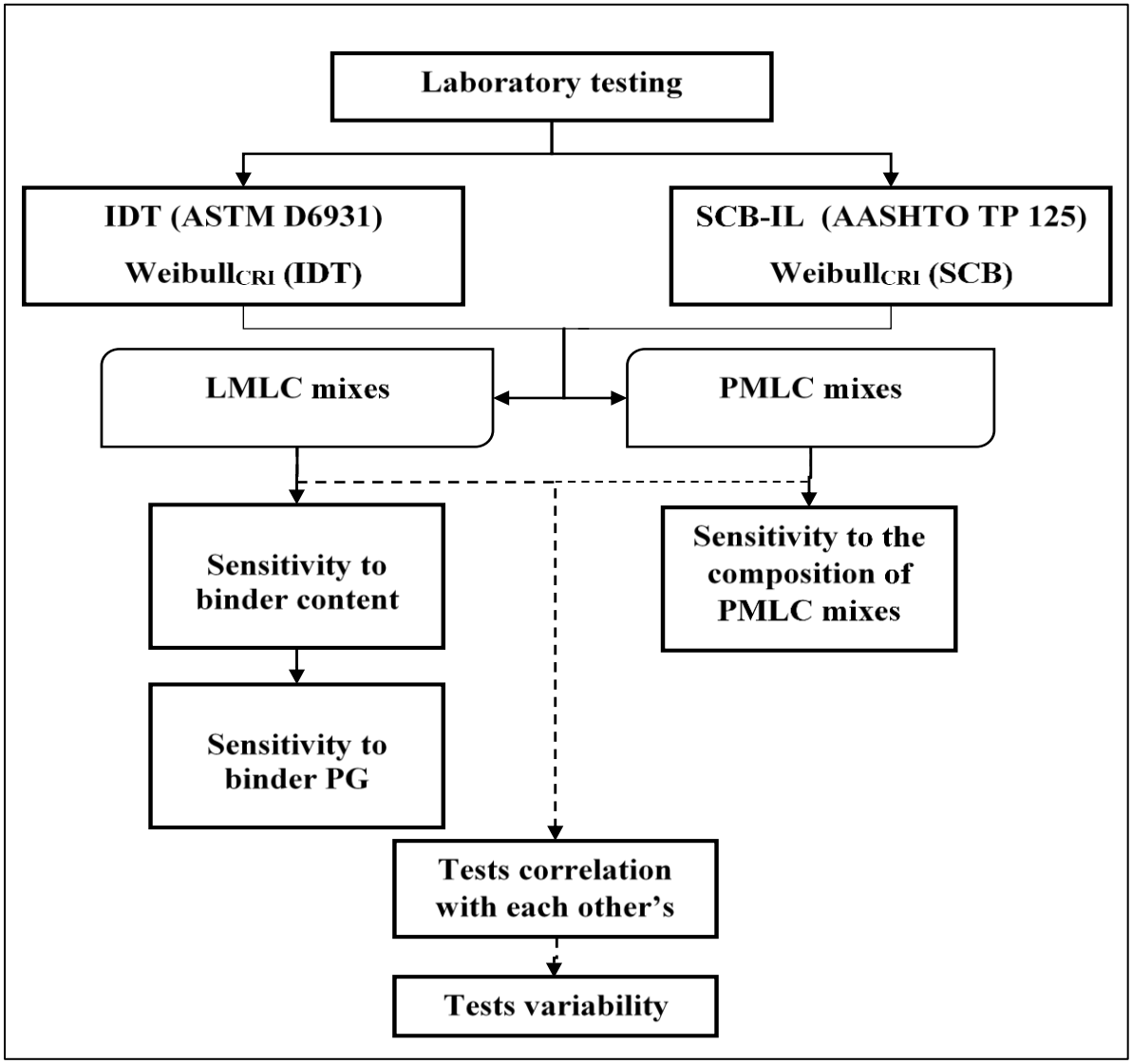


**Figure 2.4.** Study testing experimental plan

*2.5.2. Asphalt Mix Characteristics*

In this study, Laboratory Mixed-Laboratory Compacted (LMLC) and Plant Mixed-Laboratory Compacted (PMLC) asphalt mixes were prepared and tested. The testing results of LMLC mixes were used to examine the sensitivity of $Weibull_{CRI}$ to binder PG and content. The LMLC testing matrix included six mixes as presented in Table 2.2. Properties of LMLC

mixes. Mixes were designed using two binder PG (i.e., PG 58-34 and PG 70-28) and three binder contents (i.e., Optimum Binder Content [OBC], OBC-0.75%, and OBC+0.75%). Other mix properties were kept constant for all test mixes (e.g., aggregate type [Basalt], aggregate gradation [Figure 2.5], NMAS [12.5 mm], Recycled Binder Replacement [RBR] [0%], and mix type [SP3 in accordance with Idaho Transportation Department [ITD 2017] [20].

**Table 2.2.** Properties of LMLC mixes

| Mixes ID | Binder Type | Binder Content |
|---|---|---|
| PG 70-4.25% | PG 70-28 | 4.25% |
| PG 70-5.00% | PG 70-28 | 5.00% |
| PG 70-5.75% | PG 70-28 | 5.75% |
| PG 58-4.25% | PG 58-34 | 4.25% |
| PG 58-5.00% | PG 58-34 | 5.00% |
| PG 58-5.75% | PG 58-34 | 5.75% |

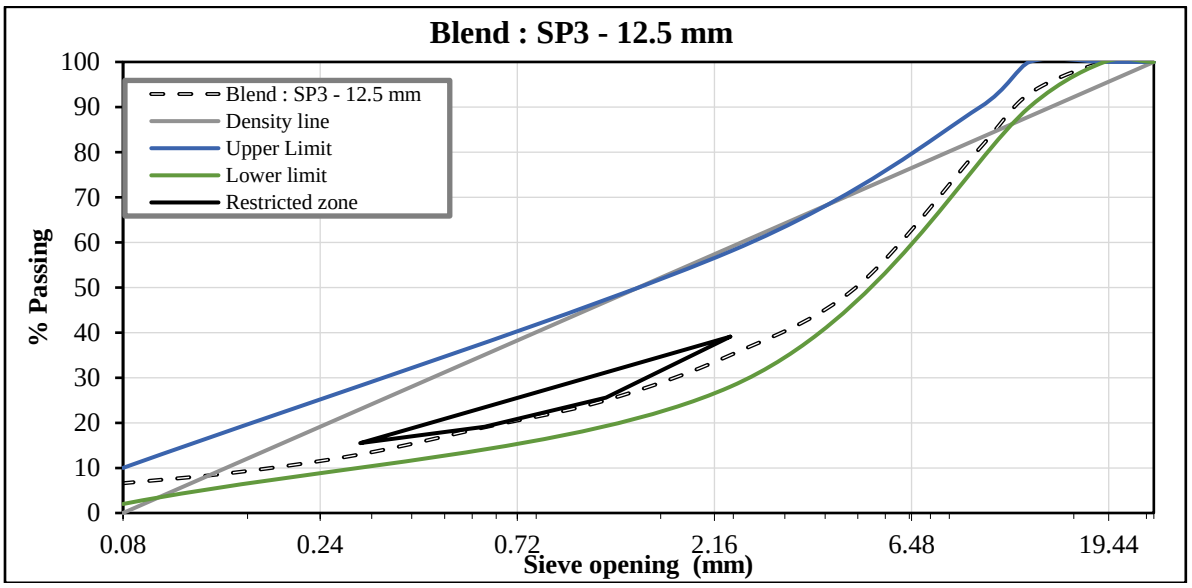


**Figure 2.5**. LMLC aggregate gradation (SP3-12.5mm)

The testing results of PMLC mixes were used to examine the sensitivity of $Weibull_{CRI}$ to the composition of the test mixes and to propose an initial cracking resistance performance threshold. The testing matrix included 10 PMLC mixes collected from new paving projects across the state of Idaho (Table 2.3). About 200 lb of loose materials were sampled and delivered to the laboratory. Table 3 summarizes the main properties of the collected PMLC mixes. The PMLC mixes properties included two mix designs (SP3 and SP5), two NMAS

(12.5 mm and 19.0 mm), five binder grades (PG 58-28, PG 64-28, PG 64-34, PG 70-28, and PG 76-28), five binder contents (4.8%, 5.2%, 5.3%, 5.4%, and 5.7%), and four RBR percent (0%, 29%, 30%, and 50%). The testing results of LMLC and PMLC together were used to examine $Weibull_{CRI}$ variability and statistical grouping of mixes resistance to cracking.

**Table 2.3**. Properties of received PMLC materials

| # | District | Project ID | Mix Type | Specified Binder PG | Virgin Binder PG | Binder content Pb% | RAP % | NMAS |
|---|---|---|---|---|---|---|---|---|
| 1 | 1 | D1L1 | SP5 | 64-28 | 58-34 | 5.30% | 30% | 12.5 |
| 2 | 2 | D2L1 | SP3 | 70-28 | 64-34 | 5.70% | 50% | 12.5 |
| 3 | | D2L2 | SP3 | 64-28 | 58-34 | 5.70% | 30% | 12.5 |
| 4 | 3 | D3L1 | SP3 | 70-28 | 52-34 | 5.20% | 50% | 12.5 |
| 5 | | D3L2 | SP3 | 70-28 | 64-34 | 5.20% | 30% | 12.5 |
| 6 | | D3L3 | SP3 | 64-28 | 58-34 | 5.30% | 30% | 12.5 |
| 7 | | D3L4 | SP3 | 70-28 | 64-34 | 5.30% | 30% | 12.5 |
| 8 | | D3L5 | SP5 | 76-28 | 70-34 | 5.30% | 30% | 12.5 |
| 9 | 5 | D5L1 | SP5 | 70-28 | 70-28 | 4.80% | 30% | 19.0 |
| 10 | 6 | D6L1 | SP5 | 64-34 | 64-34 | 5.40% | 0% | 12.5 |

## 2.6. Analysis and Discussion

Figure 2.6 and Figure 2.7 show the results of $Weibull_{CRI}$ for the LMLC and PMLC test specimens. The $Weibull_{CRI}$ (IDT) was calculated from the stress-unit deformation curve, while the $Weibull_{CRI}$ (SC) was calculated from the load-vertical actuator displacement curve. Figure 2.6 and Figure 2.7 report the average results of three replicates of IDT specimens and four replicates of SC specimens. The error bars represent ± one standard deviation (SD) from the average value. In addition, statistical analysis of the mixes results was performed. The t-test was used to evaluate the sensitivity of both ($Weibull_{CRI}$ [IDT]) and $Weibull_{CRI}$ [SC]) to binder PG. Analysis of Variance (ANOVA) and Tukey's Honestly Significant Difference (Tukey' HSD) tests were used to evaluate the sensitivity for the composition of PMLC mixes and the binder content (at each binder PG [three binder content groups at each binder grade]). Both tests (t-test and Tukey's HSD) were performed at a 95% confidence interval. The statistical analysis results (Tukey's HSD groups) were included in the form of letters or numbers at the bottom of each bar. Mixes that do not share the same letter/number were

significantly different in terms of their $Weibull_{CRI}$. Detailed examples of analyses result of the selected statistical tests are provided in Appendix A.

### *2.6.1. Sensitivity to Binder Content and Binder Grade*

$Weibull_{CRI}$ (IDT) and $Weibull_{CRI}$ (SC) indicators were both sensitive to the variation in binder content as shown in Figure 2.6. It can be seen that mixes with higher binder content had higher $Weibull_{CRI}$ (Figure 2.6-A1 and Figure 2.6-A2), which indicates improved resistance to cracking. One can expect that increasing the mix binder content, up to a limit, would make the specimens more flexible leading to improved resistance to cracking. Therefore, the $Weibull_{CRI}$ results were in agreement with the expected effects of binder content in terms of resistance to cracking. The ANOVA results for $Weibull_{CRI}$ (IDT) and $Weibull_{CRI}$ (SC) showed that there is a statistically significant difference ($p$-value < 0.05) between the specimens prepared with 4.25% binder content and the specimens prepared with 5.75% binder content at the corresponding binder PG (i.e., PG 70-28 and PG 58-34). There was no statistically significant difference between specimens prepared with 5.00% binder content and the specimens prepared with 5.75% or 4.25% for both indicators (i.e., $Weibull_{CRI}$ [IDT] and $Weibull_{CRI}$ [SC]).

The $Weibull_{CRI}$ (IDT) and $Weibull_{CRI}$ (SC) results were also sensitive to binder PG at the corresponding binder content (i.e., 4.25%, 5.00%, and 5.75%) as shown in Figure 2.6-B1 and Figure 2.6-B2. $Weibull_{CRI}$ (SC) results indicated that the specimens prepared with the PG 58-34 binder had better resistance to cracking as compared to specimens prepared with the PG 70-28 binder at the corresponding binder content. In general, one can expect a softer binder (e.g., PG 58-34) to provide better resistance to cracking when compared with a stiffer binder (i.e., PG 70-28) which was observed from $Weibull_{CRI}$ (SC) results. The $Weibull_{CRI}$ (IDT) results indicate a similar trend at 5.0% binder content where specimens prepared with PG 58-34 had higher $Weibull_{CRI}$ (IDT) compared to specimens prepared with PG 70-28. However, the difference between the specimens prepared with PG 58-34 binder and the specimens prepared with PG 70-28 binder was very small (less than 4.3%) at the other binder contents (4.25%, and 5.75%). The t-test results showed that there was a statistically

significant difference ($p$-value < 0.05) of $Weibull_{CRI}$ (SC) and $Weibull_{CRI}$ (IDT) results between PG 58-34 and PG 70-28 specimens at binder content of 5.00% only.

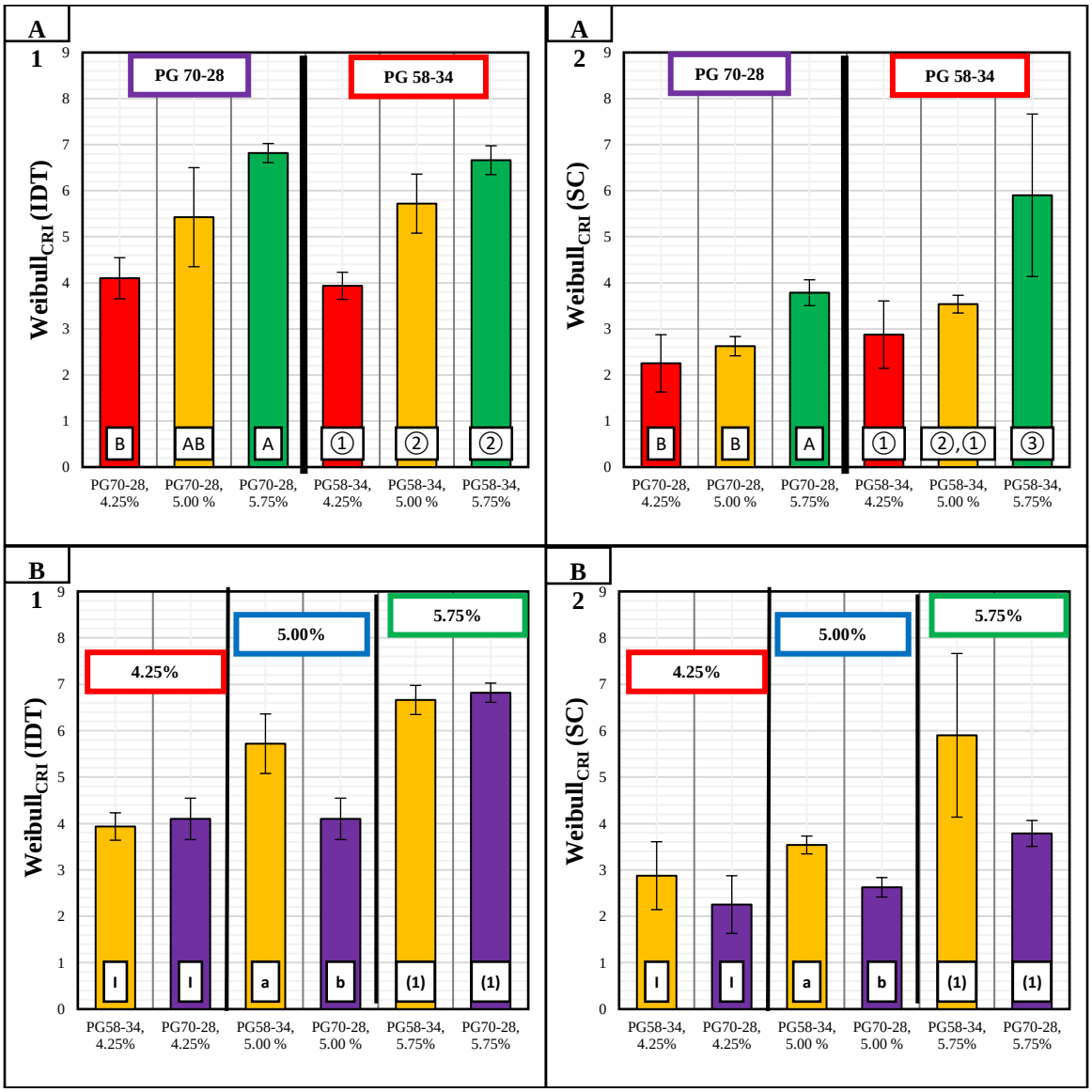


**Figure 2.6.** (A1, A2) the sensitivity of $Weibull_{CRI}$ calculated from the IDT test and SCB test to the binder content, respectively. (B1, B2) the sensitivity of $Weibull_{CRI}$ calculated from IDT test and SCB test to the binder grade, respectively

### *2.6.2. Cracking Resistance Evaluation of PMLC Using $Weibull_{CRI}$*

Figure 2.7-A and Figure 2.7-B show the $Weibull_{CRI}$ (IDT) and $Weibull_{CRI}$ (SC) results for the PMLC mixes, respectively. The $Weibull_{CRI}$ (IDT) average values ranged from 2.93 to 5.59 with SD range between 0.02 and 0.79 (Figure 2.7-A). The $Weibull_{CRI}$ (SC) average values ranged from 1.48 to 3.03 with SD range between 0.13 and 0.83 (Figure 2.7-B). The ANOVA

statistical analysis showed a significant difference ($p$-value < 0.05) between mix's estimated resistance to cracking for both $Weibull_{CRI}$ (IDT) and $Weibull_{CRI}$ (SC). Tukey's HSD test classified mixes estimated resistance to cracking into different statistical groups A, B, C, and D, where mixes within group A have the best cracking resistance, while mixes within group D have the worst cracking resistance based on $Weibull_{CRI}$ (IDT). Tukey's HSD results of $Weibull_{CRI}$ (SC) showed three statistical groups; A, B, and C, where mixes within group A have the best cracking resistance, while mixes within group C have the worst cracking resistance based on $Weibull_{CRI}$ (SC).

Asphalt mix's resistance to cracking depends on the composition of the mixes. The variation in one or more of the mix design parameters affect the mix resistance to cracking. Several research studies examined the effect of the design parameters on mix resistance to cracking. It was reported that the cracking resistance improves with increasing binder content, aggregate angularity, using the softer and unaged binder, or polymer-modified binder, decreasing NMAS, air void content, or RBR percent, and replacing sand with crushed aggregate [21–24]. The authors studied the resistance of the PMLC to cracking and correlated the results to their composition. Table 2.3 summarizes the properties of PMLC evaluated in this study. The main findings of the comparison are presented.

Either D2L2 or D6L1 mixes are expected to have better resistance to cracking compared to other mixes. D2L2 mix had the highest binder content (5.70%) and the smallest NMAS (12.5 mm) compared to all other mixes. It also had the second softest virgin binder PG (PG 58-34) and design binder PG (PG 64-28) as provided in Table 2.3. Mix D6L1 is the only mix designed without RAP materials. It had the second highest binder content (5.40%), softer specified binder PG (PG 64-34), small NMAS (12.5mm), and better mix type (SP5) (SP5 mix is designed for higher traffic level as compared to SP3 mix). Therefore, it is expected that mixes D2L2 and D6L1 to have good resistance to cracking. Both D2L2 and D6L1 mixes had higher $Weibull_{CRI}$ (IDT) compared to other mixes (Figure 2.7-A) which agrees with the expected resistance to cracking based on the compositions of the two mixes. On the other hand, mix D2L2 had a higher $Weibull_{CRI}$ (SC); however, D6L1 had the lowest $Weibull_{CRI}$ (SC) as shown in Figure 2.7-B. The findings of $Weibull_{CRI}$ (SC) agreed with the

expected resistance to cracking based on the compositions of mix D2L2 only while it contradicts the expected cracking performance of mix D6L1.

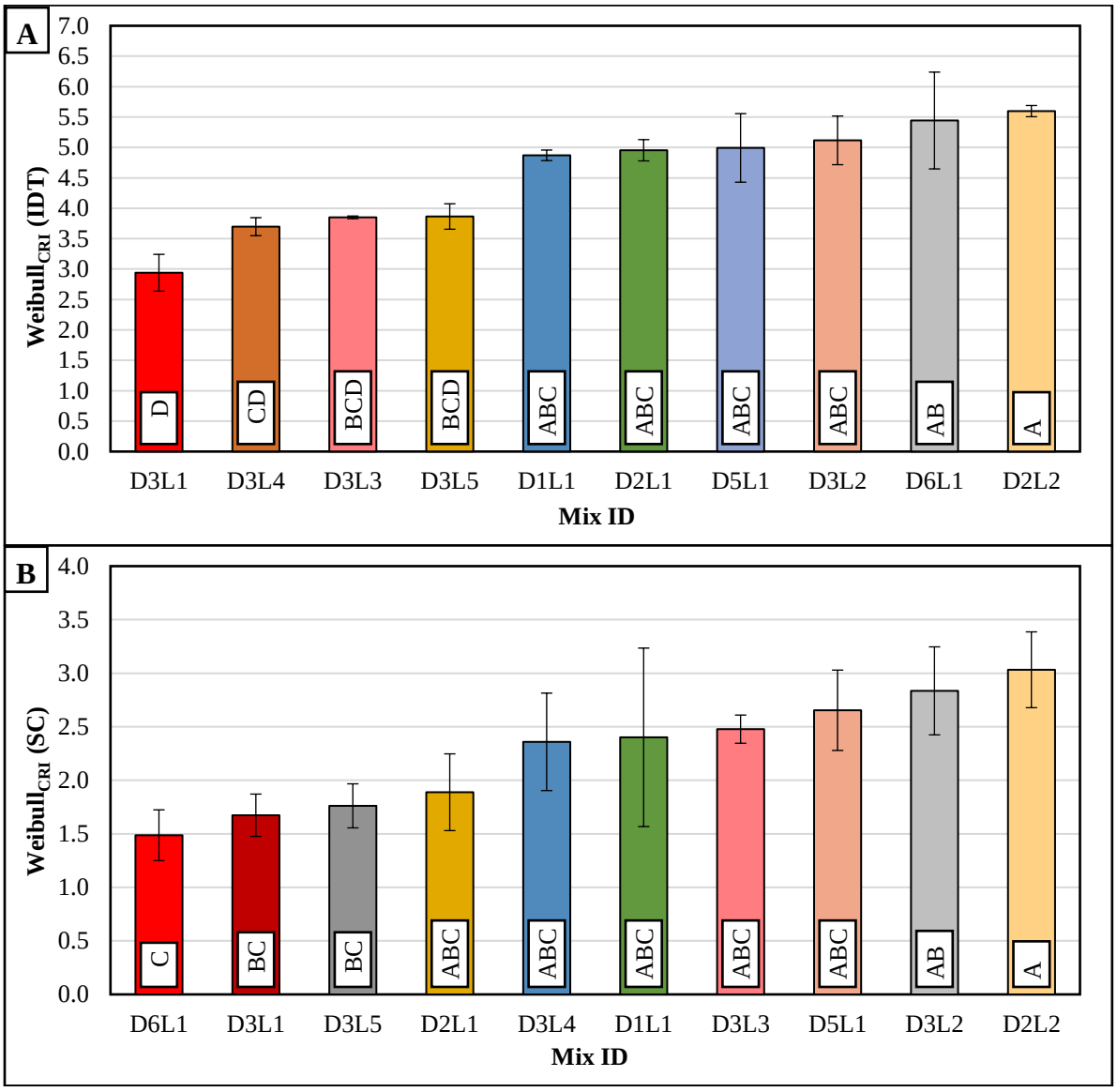


**Figure 2.7.** A) Weibull$_{CRI}$ (IDT) and B) Weibull$_{CRI}$ (SC) results for the PMLC mixes

Mix D3L1 is expected to have poor resistance to cracking since it had the highest RBR content (50%), third lowest binder content (5.20%) and stiffer design binder PG (PG 70-28) compared to other PMLC mixes; therefore it is expected to have poor resistance to cracking. Mix D3L1 had the lowest Weibull$_{CRI}$ (IDT), in addition, it had the second lowest Weibull$_{CRI}$ (SC). The Weibull$_{CRI}$ (IDT) and Weibull$_{CRI}$ (SC) findings agreed with the expected resistance to cracking based on the compositions of mix D3L1 (Figure 2.7).

Mix D1L1 is expected to have better resistance to cracking compared to mix D3L3. Mixes D1L1 and D3L3 had the same specified binder PG (PG 64-28), virgin binder PG (PG 58-34), binder content (5.30%), RBR content (30%), and NMAS (12.5mm) but D1L1 is SP5 mix while D3L3 is SP3 mix. The SP5 mix is designed and used in Idaho for pavements with higher traffic levels as compared to SP3 mixes; therefore, it was expected that D1L1 (SP5 mix) would have better resistance to cracking than mix D3L3 (SP3 mix). The $Weibull_{CRI}$ (IDT) findings agreed with the expected resistance to cracking based on the compositions of D1L1 and D3L3 mixes (Figure 2.7-A). On the other hand, $Weibull_{CRI}$ (SC) findings showed an opposite trend with the expected resistance to cracking based on the compositions of the mixes as shown in Figure 2.7-B, where the D3L3 mix is expected to have better resistance to cracking compared to the D1L1 mix.

Mix D1L1 is expected to have better resistance to cracking compared to mix D3L5. Both D1L1 and D3L5 mixes had the same mix type (SP5), binder content (5.30%), RBR content (30%), and NMAS (12.5 mm). The specified binder PG for mix D1L1 is PG 64-28, while the binder for mix D3L5 is PG 76-28. Also, the virgin binder for mix D1L1 was PG 58-34, while it was PG 70-34 for mix D3L5. Mix D1L1 had softer specified and virgin binder PG than mix D3L5; therefore, it is expected that mix D1L1 to have better resistance to cracking than mix D3L5. The $Weibull_{CRI}$ (IDT) and $Weibull_{CRI}$ (SC) findings agreed with the expected resistance to cracking based on the compositions of these two mixes (i.e., D1L1 and D3L5) as shown in Figure 2.7.

Mix D2L1 is expected to have better resistance to cracking compared to mix D3L1. Both D2L1 and D3L1 mixes had the same mix type (SP3), specified binder PG (PG 70-28), RBR content (50%), and NMAS (12.5 mm). The virgin binder for mix D2L1 was PG 64-34, it was PG 52-34 for mix D3L1. Also, the binder content for mix D2L1 was 5.7%, while it was 5.2% for mix D3L1. Since mix D2L1 had softer virgin binder PG and higher binder content than mix D3L1, it is expected that mix D2L1 would have better resistance to cracking than mix D3L1. The $Weibull_{CRI}$ (IDT) and $Weibull_{CRI}$ (SC) findings agreed with the expected resistance to cracking based on the compositions of the mixes (Figure 2.7).

Mix D2L2 is expected to have better resistance to cracking than mix D2L1. Both mixes had the same mix type (SP3), binder content (5.7%) and NMAS (12.5 mm). The RBR% for mix D2L2 was 30%, while it was 50% for mix D2L1. Also, the specified binder PG for mix D2L2 was PG 64-28, while it is PG 70-28 for mix D2L1. In addition, the virgin binder PG for mix D2L2 was PG 58-34, while it is PG 64-34 for mix D2L1. Mix D2L2 had lower RBR content, softer specified binder PG, and virgin binder PG as compared to D2L1, therefore it is expected that mix D2L2 to have better resistance cracking than mix D2L1. The $Weibull_{CRI}$ (IDT) and $Weibull_{CRI}$ (SC) findings agreed with the expected resistance to cracking based on the compositions of the mixes (Figure 2.7).

It can be concluded that in general, both $Weibull_{CRI}$ (IDT) and $Weibull_{CRI}$ (SC) findings agreed with the expected resistance to cracking based on the compositions of PMLC. The $Weibull_{CRI}$ (IDT) results agreed with the expected cracking resistance for all six cases discussed above, while $Weibull_{CRI}$ (SC) agreed with only four cases. Based on these results, the $Weibull_{CRI}$ (IDT) has better agreement with expected cracking resistance based on the composition than the $Weibull_{CRI}$ (SC).

### *2.6.3. Correlation Between $Weibull_{CRI}$ (IDT) and $Weibull_{CRI}$ (SC)*

The researchers examined the correlation between $Weibull_{CRI}$ (IDT) and $Weibull_{CRI}$ (SC) using the Pearson product-moment correlation coefficient (r) and the Spearman rank correlation coefficient ($r_s$). The Pearson coefficient studies the relationship between indicators values, while the Spearman coefficient studies the relationship between indicators' ranking of mixes' resistance to cracking. These coefficients represent the relationship type and strength between indicators using the sign and magnitude of the coefficient, respectively. The coefficient magnitude ranges between 1 and +1, where a higher magnitude indicates stronger relation and a positive sign indicates direct relationship [25]. In this study, the correlation coefficients between $Weibull_{CRI}$ (IDT) and $Weibull_{CRI}$ (SC) were calculated for LMLC and PMLC testing results together using Minitab statistical analysis software. The results showed that the indicators had a good correlation with each other ($r = 0.74$) and good ranking agreements of mixes' resistance to cracking ($r_s = 0.65$).

### *2.6.4. Variability*

The variability of $Weibull_{CRI}$ (IDT) and $Weibull_{CRI}$ (SC) results were examined using the Coefficient of Variation (COV). $Weibull_{CRI}$ (IDT) and $Weibull_{CRI}$ (SC) values were calculated from three and four replicates for each mix, respectively. A total number of 16 asphalt mixes were evaluated (i.e., six LMLC and 10 PMLC mixes); therefore 16 COV values were reported for each indicator (i.e., $Weibull_{CRI}$ [IDT] and $Weibull_{CRI}$ [SC]). The $Weibull_{CRI}$ (IDT) results had an average COV value of 7.4% and ranged between 0.6% and 19.8%. The $Weibull_{CRI}$ (SC) results had an average COV value of 16.4% and ranged between 5.3% and 34.7%. The $Weibull_{CRI}$ (IDT) results had low variability, while the $Weibull_{CRI}$ (SC) results had moderate variability; therefore the $Weibull_{CRI}$ (IDT) is recommended over the $Weibull_{CRI}$ (SC) for more repeatable performance results which provides a more accurate assessment of mixes' resistance to cracking.

### *2.6.5. Selection of Testing Protocol for Determining $Weibull_{CRI}$*

One of the objectives of this study was to determine the most appropriate testing protocol for determining the $Weibull_{CRI}$. Two specimen geometries were evaluated; the IDT geometry in accordance with ASTM D6931 or ASTM D8225 and SC geometry in accordance with AASHTO TP 124. The testing standards were evaluated using two main criteria: 1) the testing protocol requirements (i.e., equipment cost, specimen preparation, and testing time) and 2) the capabilities of the calculated $Weibull_{CRI}$ indicators (i.e., sensitivity to binder content, binder grade, and composition of PMLC mixes, indicators' statistical sensitivity [number of Tukey's HSD groups], and indicator variability).

Table 2.4 summarizes the comparison results. It can be concluded that the IDT testing standards and the $Weibull_{CRI}$ (IDT) are recommended over the SC testing protocol and the $Weibull_{CRI}$ (SC). Despite the fact that both standards are simple and performed on the same testing system, the IDT specimen does not require any additional specimen preparation after compaction, while the SC test requires cutting and notch making. Moreover, the $Weibull_{CRI}$ (IDT) and $Weibull_{CRI}$ (SC) findings agreed with the expected resistance to cracking based on the compositions of the PMLC mixes; however, the $Weibull_{CRI}$ (IDT) results were in better agreement. In addition, $Weibull_{CRI}$ (IDT) had a higher number of Turkey's HSD statistical

groups than the $Weibull_{CRI}$ (SC) results; therefore, the $Weibull_{CRI}$ (IDT) provided a better comparison between PMLC mixes' resistance to cracking than $Weibull_{CRI}$ (SC). In addition, the $Weibull_{CRI}$ (IDT) results had lower variability as compared to $Weibull_{CRI}$ (SC); therefore, it is expected to provide more repeatable results. Based on these findings, the IDT testing standards and $Weibull_{CRI}$ (IDT) are proposed and recommended to evaluate the resistance of asphalt mixes to cracking.

**Table 2.4**. Comparison between $Weibull_{CRI}$ (SC) and $Weibull_{CRI}$ (IDT)

| Comparison Criteria's | | SC | IDT |
|---|---|---|---|
| Testing protocol requirements | Equipment cost | Not expensive | Not expensive |
| | Specimen preparation | Simple | Simpler than SC |
| | Testing time | Short (< 2 min) | Short (< 2 min) |
| Testing performance capabilities | Sensitivity to binder content | Yes | Yes |
| | Sensitivity to binder grade | Yes | Yes |
| | Sensitivity to Mixes composition | Yes | Yes, but better than SC |
| | Number of Tukey groups | 3 | 4 |
| | Variability | Moderate | Low |

*2.6.6. Initial Estimation of Cracking Resistance Performance Threshold for PMLC Mixes*

Asphalt mixes performance assessment tests aim to identify mixes with poor resistance to cracking during the mix design or production processes by comparing the results to performance thresholds. These thresholds are the pre-specified limits for a given performance indicator to be achieved. These thresholds are often developed based on the correlation between the laboratory results and observed field performance, which requires additional effort and resources. Alternatively, Diefenderfer and Bowers (2019) proposed three statistical methods for developing initial performance thresholds using limited laboratory testing results of PMLC mixes (e.g., five PMLC mixes). In this study, the suggested methods were followed, and an initial cracking performance threshold using $Weibull_{CRI}$ (IDT) (the selected indicator) was proposed for the 10 PMLC mixes evaluated in this study as shown in Figure 2.8. The methods and their proposed thresholds were as follows:

- *Method 1*: this method assumes that the currently produced mixes would have a good estimated field resistance to cracking and the threshold is specified to achieve this

assumption. In case of $Weibull_{CRI}$ (IDT) (where a higher value indicates better resistance to cracking), the threshold is specified as the minimum $Weibull_{CRI}$ (IDT) value of the evaluated PMLC mixes; therefore, the threshold was specified as a minimum $Weibull_{CRI}$ (IDT) of 2.94. Applying this threshold assumes that the resistance to cracking of the currently produced mixes in Idaho is acceptable and the DOT aims to preserve this level of performance. The threshold proposed using Method 1 is considered a less conservative threshold when compared to the thresholds proposed using Methods 2 and 3.

- *Method 2*: this method assumes that the average resistance to cracking of the currently produced mixes is minimally acceptable; therefore, the performance threshold is specified as the average indicator value of the evaluated PMLC mixes. Based on this assumption, the threshold was specified as a minimum $Weibull_{CRI}$ (IDT) of 4.53. This threshold reduces the possibility of accepting mixes with poor estimated field resistance to cracking when compared to the threshold proposed using Method 1, but it may eliminate mixes with good or fair estimated field resistance to cracking. The threshold proposed using Method 2 is considered as the highest threshold when compared to the thresholds proposed using Methods 1 and 3.

- *Method 3*: This method assumes that the current resistance to cracking of the currently produced mixes is acceptable but mixes with a low resistance to cracking should be improved. The proposed threshold lies between Method 1 and Method 2 thresholds. The performance thresholds are specified as the average value +/- one SD based on the indicator concept (i.e., the $Weibull_{CRI}$ [IDT] threshold is specific as average value minus one SD). The evaluated PMLC mixes had an average $Weibull_{CRI}$ (IDT) value of 4.53 and SD of 0.83, therefore the threshold was specified as minimum $Weibull_{CRI}$ (IDT) of 3.70. The threshold proposed using Method ٣ is considered a moderate threshold compared to the thresholds proposed using Methods 1 and 2.

The above-proposed thresholds need to be compared with field performance, but they are considered as initial proposed performance thresholds for the cracking resistance of PMLC mixes.

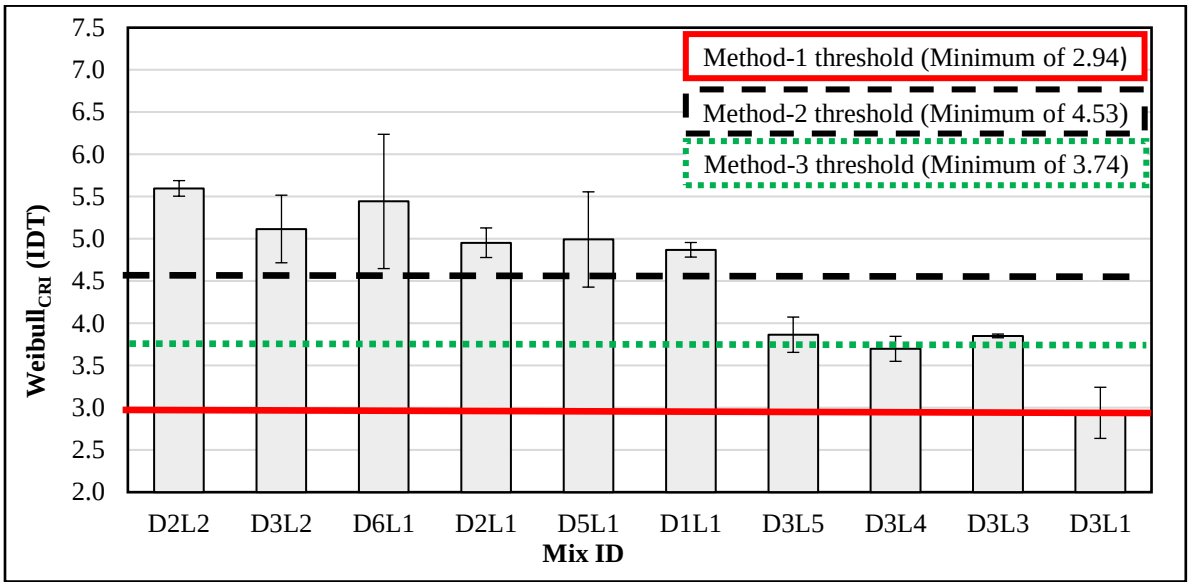


**Figure 2.8.** The proposed resistance to cracking thresholds using Weibull$_{CRI}$ (IDT) results.

The authors also compared the Weibull$_{CRI}$ (IDT) results with other monotonic performance indicators including $G_{fracture}$, CRI, FI, IDEAL-CT$_{Index}$, Nflex factor, IDT$_{Strength}$, IDT$_{Modulus}$, and $J_C$. The Weibull$_{CRI}$ (IDT) was found to have the lowest variability (average COV = 7.4%), and the highest number of Turkey's groups compared to all other performance indicators. Further details about these findings will be discussed in chapter 3.

In addition, the authors studied the correlation between cyclic and monotonic cracking assessment tests. The study showed that the Weibull$_{CRI}$ (IDT) had the best correlation with cyclic fatigue cracking parameters compared to the other monotonic performance indicators ($G_{fracture}$, CRI, FI, IDEAL-CT$_{Index}$, Nflex factor, IDT$_{Strength}$, IDT$_{Modulus}$, and $J_C$). Further details about these findings will be discussed in chapter 5.

## 2.7. Summary and Conclusions

Several performance indicators are proposed to analyze the load-displacement curve to assess the resistance of asphalt mixes to cracking. However, none of the current indicators can describe the overall variation in the load-displacement curve. This study introduced a new

performance indicator called Weibull Cracking Resistance Index ($Weibull_{CRI}$) that describes the entire load-displacement curve and can be used to evaluate the resistance of asphalt mixes to cracking. The study performed an extensive laboratory evaluation of 16 different asphalt mixes from two different mix types (LMLC and PMLC) using two different testing protocols (i.e., ASTM D6931 and AASHTO TP 125). Based on the findings of this study, the following conclusions can be made:

- A modified Weibull function fitted the load-displacement curve with excellent accuracy and provided an accurate estimate of the measured load and displacement values. The shape of the load-displacement curve changed with the variation in the composition of asphalt mixes. The curve peak, the pre-peak, and post-peak slopes increase with the reduction in binder content while the termination displacement increases with binder content. The modified Weibull function parameters (i.e., $A$, $\beta$, $\eta$) were used to assess mix resistance to cracking. It was observed that better cracking resistance is associated with higher "$A$", and "$\eta$" and lower "$\beta$".

- A new index named the Weibull Cracking Index ($Weibull_{CRI}$) was proposed for the IDT and SCB tests. Both, The $Weibull_{CRI}$ (IDT) and $Weibull_{CRI}$ (SC) were found to be sensitive to the variation in binder content and binder grade.

- The resistance of asphalt mixes to cracking depends on mix composition. The $Weibull_{CRI}$ results were compared to expected cracking resistance based on mix composition (e.g., D2L2 mix is expected to have the best cracking resistance). The $Weibull_{CRI}$ (IDT) results were in good agreement with all comparisons made between mix with different compositions – a total of six comparisons. The $Weibull_{CRI}$ (SC) agreed with four comparisons; therefore, the $Weibull_{CRI}$ (IDT) had better agreement with expected resistance to cracking based on the composition of PMLC mixes compared to $Weibull_{CRI}$ (SC).

- The correlation coefficients between $Weibull_{CRI}$ (IDT) and $Weibull_{CRI}$ (SC) were calculated using LMLC and PMLC testing results. The results showed that the indicators had a good correlation with each other ($r = 0.74$) and good mix cracking resistance ranking agreements based on Spearman ranking analysis ($r_s = 0.65$). Also,

the findings showed that the $Weibull_{CRI}$ (IDT) results had low variability, while the $Weibull_{CRI}$ (SC) results had a moderate variability, therefore $Weibull_{CRI}$ (IDT) would provide a more accurate cracking assessment.

- The IDT testing standard and $Weibull_{CRI}$ (IDT) are recommended to assess asphalt mix resistance to cracking. The IDT specimen was easier to prepare compared to the SC specimen. The $Weibull_{CRI}$ (IDT) results were in better agreement with expected cracking performance based on the compositions of the PMLC mixes. Also, the $Weibull_{CRI}$ (IDT) had a higher number of Turkey's HSD statistical groups and low variability as compared to $Weibull_{CRI}$ (SC) results.

- Three initial cracking performance thresholds were proposed using the $Weibull_{CRI}$ (IDT). The first threshold was specified as minimum $Weibull_{CRI}$ (IDT) of 2.94, but it is considered a less conservative threshold when compared to the second and third threshold. The second threshold was specified as a minimum of 4.53, but it is considered the high threshold when compared to the first and third thresholds. The third threshold was specified as a minimum of 3.70, which is considered as a moderate threshold when compared to the first and second thresholds. These thresholds were initial estimations and they need further validation and calibration by field performance evaluation of PMLC mixes.

## 2.8. References

[1] R. Cominsky, G. a Huber, T.W. Kennedy, M. Anderson, The Superpave Mix Design Manual for New Construction and Overlays, Publication NO SHRP-S-407 Strategic Highway Research Program, U.S. (1994) 184.

[2] S. Buchanan, Balanced Mix Design Task Force Update of Activities, Presented at Asphalt Mixture Expert Task Group(ETG) Meeting. (2016).

[3] R.C. West, C. Rodenzo, F. Leiva, F. Yin, Development of a framework for balanced mix design, NCHRP project 20-07/task 406, 2018. http://apps.trb.org/cmsfeed/TRBNetProjectDisplay.asp?ProjectID=4324.

[4] F. Zhou, D. Newcomb, C. Gurganus, S. Banihashemrad, M. Sakhaeifar, E.S. Park, R.L. Lytton, Field Validation of Laboratory Tests to Assess Cracking Resistance of Asphalt Mixtures: An Experimental Design, 2016. doi:10.17226/23608.

[5] I. Al-Qadi, H. Ozer, J. Lambros, A. El Khatib, D. Singhvi, Testing protocols to ensure performance of high asphalt binder replacement mixes using RAP and RAS, Urbana, IL: Illinois Center for Transportation, Illinois Dept. of Transportation. (2015).

[6] L. Mohammad, M. Kim, M. Elseifi, Characterization of asphalt mixture's fracture resistance using the Semi-Circular Bending (SCB) test, 7th RILEM International Conference on Cracking in Pavements SE - 1. 4 (2012) 1–10. doi:10.1007/978-94-007-4566-7_1.

[7] R.C. West, C. Van Winkle, S. Maghsoodloo, S. Dixon, Relationships between simple asphalt mixture cracking tests using ndesign specimens and fatigue cracking at FHWA's accelerated loading facility, Road Materials and Pavement Design. 86 (2017) 579–602. doi:10.1080/14680629.2017.1389083.

[8] F. Zhou, S. Im, L. Sun, T. Scullion, Development of an IDEAL cracking test for asphalt mix design and QC/QA, Asphalt Paving Technology: Association of Asphalt Paving Technologists-Proceedings of the Technical Sessions. 86 (2017) 549–577. doi:10.1080/14680629.2017.1389082.

[9] R. West, D. Timm, B. Powell, M. Heitzman, N. Tran, C. Rodezno, D. Watson, F. Leiva, A. Vargas, NCAT draft Report 18-04 PHASE VI (2012-2015) NCAT test track findings, 2018.

[10] F. Kaseer, F. Yin, E. Arámbula-Mercado, A.E. Martin, J.S. Daniel, S. Salari, Development of an index to evaluate the cracking potential of asphalt mixtures using the semi-circular bending test, Construction and Building Materials. 167 (2018) 286–298. doi:10.1016/j.conbuildmat.2018.02.014.

[11] F. Bayomy, A. abdo Ahmad, M. Ann Mull, Evaluation of hot mix asphalt ( HMA ) fracture resistance using the critical strain energy release rate, 2006.

[12] W.G. Buttlar, R. Roque, N. Kim, Accurate asphalt mixture tensile strength, in: Proceedings of the Materials Engineering Conference, 1996.

[13] AASHTO, Standard method of test for determining the creep compliance and strength of hot mix asphalt (HMA) using the indirect tensile test device AASHT322-07:, Washington D.C., 2011.

[14] A.A.A. Molenaar, A. Scarpas, X. Liu, S.M.J.G. Erkens, Semi-circular bending test; simple but useful, Asphalt Paving Technology: Association of Asphalt Paving Technologists. (2002). https://trid.trb.org/view.aspx?id=698764.

[15] L. Huang, K. Cao, M. Zeng, Evaluation of semicircular bending test for determining tensile strength and stiffness modulus of asphalt mixtures, Journal of Testing and Evaluation. 37 (2009) 122–128.

[16] R. Hofman, B. Oosterbaan, S.M.J.G. Erkens, J. Van der Kooij, Semi-circular bending test to assess the resistance against crack growth, 6th International Rilem Symposium. (2003) 257–263.

[17] R.C. West, A. Copeland, High RAP asphalt pavements: Japan practice-lessons learned, National Asphalt Pavement Association. 139 (2015) 62.

[18] W. Weibull, S. Sweden, A Statistical Distribution Function of Wide Applicability, Journal of Applied Mechanics. 18 (1951) 293–297. https://pdfs.semanticscholar.org/88c3/7770028e7ed61180a34d6a837a9a4db3b264.pdf.

[19] A.M. Brown, A step-by-step guide to non-linear regression analysis of experimental data using a Microsoft Excel spreadsheet, Computer Methods and Programs in Biomedicine. 65 (2001) 191–200. doi:10.1016/S0169-2607(00)00124-3.

[20] Idaho Transportation Department (ITD), Standard specification for highway construction, 2017.

[21] M. Zaumanis, L.D. Poulikakos, M.N. Partl, Performance-based design of asphalt mixtures and review of key parameters, Materials and Design. 141 (2018) 185–201. doi:10.1016/j.matdes.2017.12.035.

[22] R. AWu, J. Harvey, J. Buscheck, A. Mateos, Mechanistic-Empirical (ME) design: mix design guidance for use with asphalt concrete performance-related specifications, 2018.

[23] L. Barros, Influence of mix design parameters on performance of balanced asphalt concrete, University of Texas at El Paso, 2018.

[24] F. Bayomy, A.A. Abdo, Performance evaluation of Idaho HMA mixes using gyratory stability, University of Idaho , Idaho Transportation Department, Idaho. (2007).

[25] N.J. Salkind, Encyclopedia of research design, 2010.

[26] S.D. Diefenderfer, B.F. Bowers, Initial approach to performance (balanced) mix design : the Virginia experience, Transportation Research Board. (2019). doi:10.1177/0361198118823732.7

# Chapter 3: Review and Evaluation of Cracking Testing Standards and Performance Indicators for Asphalt Mixes

Hamza Alkuime[2]; Fahmid Tousif[1], Emad Kassem[1]; and Fouad M.S. Bayomy[1]

(Submitted to International Journal of Construction and Building Materials)

## 3.1. Abstract

The main objective of this study was to review and evaluate the current monotonic cracking performance assessment tests and indicators. The testing requirements of various test standards were compared. Also, key publications, concepts, calculation methods, physical meaning, and advantages and disadvantages of various performance indicators were documented. In addition, a comprehensive laboratory evaluation was conducted to examine indicators sensitivity to mix compositions, variability, and statistically grouping as well as mix performance ranking. The results showed that the indirect tension test provided better cracking assessment as compared to semi-circle bending tests. In addition, the Weibull cracking resistance indicator was recommended over other performance indicators.

Keywords**:** Asphalt Mixture; Balanced mixed design; Fatigue cracking; Semi-circular bending; Indirect tension test; Intermediate temperature fatigue cracking assessment

## 3.2. Introduction

Asphalt pavements experience various distresses such as cracking, rutting, and moisture damage in the field. These distresses could be related to design-related issues (e.g., poor mix design or inadequate structural design) and/or non-design related problems (e.g., construction and environmental conditions). Fatigue cracking occurs commonly in the wheel path since it is subjected to repeated traffic loading. The fatigue cracking starts as a series of interconnected cracks before it develops in many-sided, sharp-angled pieces [1]. Several causes may lead to fatigue cracking including inadequate structural design, inadequate mix design, overloading, poor construction, or poor drainage.

[2] Department of Civil and Environmental Engineering, University of Idaho, Moscow, ID 83844 USA.

There are several testing methods and performance indicators that have been proposed to assess asphalt mixes resistance to intermediate temperature cracking. These tests have different loading application modes (repeated or monotonic), specimen geometries (beam, cylindrical [or Indirect Tension Test IDT], trapezoidal, dogbone, semi-circle notched (SC), and disk-shaped), and analysis theories (general fatigue approach, energy and energy-inspired methods, continuum damage method, and fracture methods) [2]. Generally, the monotonic loading assessment tests require a relatively low-cost testing system, easy specimen preparation process, simple data analysis process, and its results have low variability when compared to the dynamic loading tests. Also, it correlated well with the observed field cracking performance [3,4].

Several monotonic testing standards were proposed to assess asphalt mix resistance to intermediate temperature cracking including ASTM D6931 *'Standard Test Method for Indirect Tensile (IDT) Strength of Asphalt Mixtures,* ASTM D8225 ' *Standard Test Method for Determination of Cracking Tolerance Index of Asphalt Mixture Using the Indirect Tensile Cracking Test at Intermediate Temperature',* AASHTO TP 124 '*Standard Method of Test for Determining the Fracture Potential of Asphalt Mixes Using the Flexibility Index Test (FIT)',* and ASTM D8044 *' Standard Test Method for Evaluation of Asphalt Mixture Cracking Resistance using the Semi-Circular Bend Test (SCB) at Intermediate Temperatures'.* These standards may have different requirements (e.g., test specimen geometry), but it collects similar data (i.e., time, load, and vertical actuator displacement). This data is used to generate the load-displacement curve to represent mix resistance to cracking. Performance parameters or indicators are used to interpret the load-displacement curve to estimate the mix resistance to cracking. Several performance indicators were specified or proposed using each standard (i.e., Indirect tensile asphalt cracking test [IDEAL-$CT_{Index}$ ], indirect tension strength [$\sigma_{tesnile}{}^{IDT}$], Flexibility Index [FI], and critical strain energy release rate [$J_c$] indicators were specified by ASTM D8225, ASTM D6931, AASHTO TP 124, and ASTM D8044 , respectively.

Several state Departments of Transportation (DOTs) are using performance indicators as part of the Balanced Mix Design (BMD) or performance-engineered mix design. A recent survey demonstrated that six DOTs are applying the BMD, while 29 DOTs are interested in

applying the BMD [5]. However, the interested DOTs may confront several difficulties as they develop their BMD specifications. For example, there are three test standards and over 10 performance indicators to assess asphalt mix resistance to intermediate temperature cracking. It could be difficult to select the appropriate testing standard and performance indicator that would provide the best assessment of cracking resistance.

Therefore, there is a need to document and compare the testing requirements (e.g., specimen geometry) and conditions (testing temperature) of the available testing standards as well as the concept, calculation methods, physical meaning, and advantages and disadvantages of the available performance indicators. In addition, these testing standards and performance indicators should be compared for the same mixes thus pros and cons of each standard and performance indicators should be identified.

### 3.3. Objectives

The objectives of this study were as following:

- Review of the available monotonic intermediate temperature cracking assessment tests to identify the similarities and differences between available standards.
- Review of the most promising current performance indicators to interpret the outputs of monotonic intermediate temperature cracking assessment (i.e., load-displacement curve).
- Laboratory evaluation of the available monotonic intermediate temperature cracking assessment standards and performance indicators using 16 asphalt mixes with different characteristics.
- Explain the variation in the shape of the load-displacement curves in terms of their relation to asphalt mix resistance to cracking
- Provide recommendations on the best testing standard(s) and performance indicator(s) that would provide the appropriate assessment for asphalt mixes resistance to cracking.

### 3.4. Review of Monotonic Intermediate Temperature Cracking Assessment Standards

Currently, there are four intermediate temperature cracking assessment standards including AASHTO TP 124, ASTM D6931, ASTM D8044, and ASTM D8225 standards. This section reviewed the specified important requirements including:

- *Loading rate:* The standards are performed at a constant displacement loading rate. ASTM D8044 specifies loading rate of 0.5 mm/min, while other standards (i.e., AASHTO TP 124, ASTM D6931, and ASTM D8225) specify loading rate of 50 mm/min.

- *Testing system and fixtures:* Each standard has specific requirements on the testing system and loading fixture. However, some testing systems are capable to perform all tests using suitable loading fixture such as Material Testing System (MTS), or Asphalt Mixture Performance Tester (AMPT).

- *Testing temperature:* The standards are performed at the asphalt intermediate temperature. AASHTO TP 124 and ASTM D6931 specify a fixed testing temperature of 25 °C, while ASTM D8044 specifies the test temperature equivalent to binder intermediate performance temperature grade (PG IT) as shown in Equation 3.1. ASTM D8225 specifies a typical test temperature of 25 ̊C, but it can be performed at any other intermediate temperature such as PG IT (Equation 3.1).

$$\text{PG IT} = \frac{\text{PG High} - \text{PG Low}}{2} + 4 \qquad 3.1$$

where PG IT is the intermediate binder performance grade (PG) temperature (selected test temperature, °C), PG High is the climatic high binder performance grade temperature (°C), and PG Low is the climatic low binder performance grade temperature (°C)

- Testing specimens

    - *Geometries:* ASTM D6931 and ASTM D8225 use a circular (or IDT) specimen geometry, while AASHTO TP124 and ASTM D8044 use a notched Semi-Circle (SC) specimen geometry. AASHTO TP 124 requires using one notch depth (15

mm), while ASTM D8044 requires using three notch depths (25.4 mm, 31.8 mm, and 38.4 mm).

- *Laboratory prepared specimens size:* AASHTO TP 124 requires laboratory prepared specimen to have 50 mm thickness (t) and 150 mm diameter (D), while ASTM D8044 requires laboratory prepared specimens to have 57 mm thickness and 150 mm diameter. ASTM D8225 and ASTM D6931 require two specimen sizes depending on the NMAS of the mix. For mixes with NMAS≤19 mm, ASTM D8225 requires laboratory prepared specimen to have a thickness of 62 mm and a diameter of 150 mm, while ASTM D6931 requires laboratory prepared specimens that are 101.6 in diameter and 50.8 mm thick (minimum thickness). For mixes with NMAS>19 mm, ASTM D8225 requires laboratory prepared specimen to have 95 mm thickness and 150 mm diameter, while ASTM D6931 requires laboratory prepared specimens to have 150 diameter and minimum thickness 75 mm.
- *Extracted field cores specimens:* AASHTO TP 124 allows testing field cores with 150 mm diameter and thickness between 25 mm and 50 mm. ASTM D8225 allows testing field cores with 150 mm and a minimum thickness of 38 mm. ASTM D8044 allows using field cores with 150 mm diameter and thickness between 38 mm and 75 mm. ASTM D6931 requires using either cores with 101.6 mm diameter and minimum thickness of 38 mm or with 150 mm and 75 mm minimum thickness.
- *Number of testing specimen replicates:* ASTM -D6931, and -D8225 requires a minimum of three replicates, AASHTO TP 124 require four replicates, while ASTM D8044 requires 12 replicates (four replicates at each notch depth [i.e., three notches]). These requirements were specified for both laboratory prepared specimens and the extracted field cores.
- *Selected performance indicator:* ASTM D8225, ASTM D6931, AASHTO TP 124, ASTM D8044 propose IDEAL-$CT_{Index}$, $\sigma_{tesnile}{}^{IDT}$, FI, and $J_c$ performance indicators, respectively. These indicators will be discussed in the next section.

Table 3.1 summarizes important requirements for various intermediate temperature cracking protocols.

**Table 3.1** Specified important requirements for intermediate temperature cracking protocols

| Requirements | | ASTM D8225 | ASTM D6931 | AASHTO TP 124 | ASTM D8044 |
|---|---|---|---|---|---|
| Loading rate (mm/min) | | 50 | 50 | 50 | 0.5 |
| Testing temperature | | 25 °C, but can at any other intermediate temperature | 25 °C | 25 °C | PG IT |
| Specimen geometry | | IDT | IDT | notched SC | notched SC |
| Laboratory prepared specimens | Thickness (mm) | 62 or 95 | 50.8 or 75 | 50 | 50 |
| | Diameter (mm) | 150 | 101.6 or 150 | 150 | 150 |
| Extracted field cores specimens | Thickness (mm) | > 38 | > 38 or > 75 | 25 - 50 | 38 - 75 |
| | Diameter (mm) | 150 | 101.6 or 150 | 150 | 150 |
| Number of testing specimen replicates/mix | | 3 | 3 | 4 | 12 |
| Selected performance indicator | | IDEAL-CTIndex | $\sigma_{tesnile}{}^{IDT}$ | FI | Jc |
| Testing system | | A system capable to provide a constant displacement load | | | |
| Testing fixture | | Suitable testing fixtures are required for each design | | | |

### 3.5. Review of Current Performance Indicators

Several performance parameters or indicators are currently used to analyze the load-displacement curve to assess the resistance of asphalt mixes to cracking. In this section, the researchers documented the most used performance indicators that those recently proposed in the literature. The key publications, concept, calculation method, and findings of previous studies for each performance indicator were documented in this section. It should be noted that these indicators can be calculated for the load-displacement curve obtained from all intermediate temperature monotonic tests.

*3.5.1. Peak Load*

The peak load ($P_{Peak}$) is the maximum load applied to the specimen until failure (Figure 3.1). The peak load is a measurement of the material's strength. Stiffer mixes often exhibit a higher peak load compared to softer mixes. The peak load is determined as the maximum recorded load during the test.

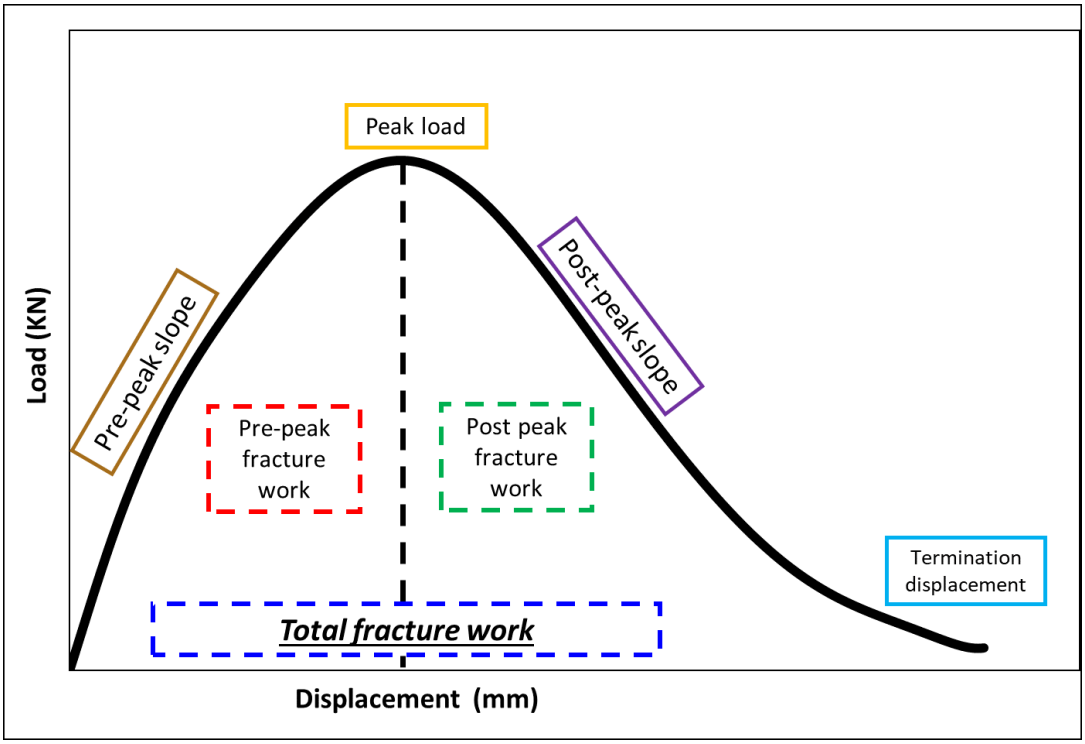


**Figure 3.1.** Load-displacement basic curve elements

*3.5.2. Tensile strength*

The tensile strength is a normalization of the peak load ($P_{peak}$) with respect to specimen geometry. Several research studies investigated the calculations of the tensile stress of asphalt mixes using IDT and SCB tests [6–10]. Equation 3.2 is used to calculate the tensile strength using the IDT test [6]. Molenaar et al. (2002) proposed an indicator for SCB tensile strength for specimen without a notch (Equation 3) [8]. Equation 3.3 is valid when the support span is 0.8 of specimen diameter. Huang et al. (2009) presented a generalized model that computes the tensile stress at various support span distances for specimen without a notch (Equation 3.4) [9]. Hofman et al. (2003) proposed a simple model for notched SCB

specimen (Equation 3.5) [10]. ASTM D6931 uses $\sigma_{tesnile}{}^{IDT}$ as performance indicator to assess the resistance to cracking.

$$\sigma_{tesnile}{}^{IDT} = \frac{2000xP_{Peak}}{\pi \times t \times D} \quad 3.2$$

$$\sigma_{tensile}{}^{SCB_{unnotched}} = \frac{4.8F}{\mathrm{D}} \quad 3.3$$

$$\sigma_{tensile}{}^{SCB_{unnotched}} = \frac{6 \times P_{Peak} \times L_{support}}{\mathrm{t}\times\mathrm{D}^2} \quad 3.4$$

$$\sigma_{tensile}{}^{SCB_{notched}} = \frac{4.263 \times P_{Peak}}{\mathrm{t}\times\mathrm{D}} \quad 3.5$$

where $\sigma_{tesnile}{}^{IDT}$ is the tensile strength (kPa) determined from IDT test, $\sigma_{tensile}{}^{SCB_{unnotched}}$ is the tensile strength from SCB test using specimen without a notch, $P_{Peak}$ is the peak load (N), t is the specimen thickness (mm), D is the specimen diameter (mm), F is the load per unit specimen width at failure (N/mm), $L_{support}$ is the distance between the support span (mm).

### *3.5.3. IDT$_{Modulus}$ (IDT Japan coefficient)*

The IDT$_{Modulus}$ is a normalization of IDT tensile strength with respect to the displacement at the peak load as presented in (Equation 3.6). This index is developed in Japan to assess the resistance of mixes with RAP to cracking [11]. It serves as a measurement of material strength and ductility. Asphalt mixes test specimens are prepared using 100% RAP and tested using a constant displacement rate of 50 mm/min at 20°C. The test specimens should have a maximum IDT$_{Modulus}$ of 1.7 MPa/mm for acceptance [11]. A recent study by West et al. (2017) found that IDTModulus had a moderate correlation ($R^2$ = 0.47) with field performance of eight Accelerated Loading Facility (ALF) test sections [12].

$$\mathrm{IDT_{modulus}} = \frac{\sigma_{\mathrm{Tensile}}{}^{\mathrm{IDT}}}{\mathrm{L_{Peak\ load}}} \quad 3.6$$

where $IDT_{Modulus}$ is the ratio of the tensile strength to the displacement at the peak load (MPa/mm, $\sigma_{Tensile}{}^{IDT}$ is the IDT tensile strength (MPa), and $L_{Peak\ load}$ is the displacement at the peak load (mm)

### *3.5.4. Work of fracture*

The work of fracture is the area under the load-displacement curve (Figure 3.1). Three performance indicators have been identified: pre-peak work of fracture ($W_{Fracture}^{Pre-peak}$), post-peak work of fracture ($W_{Fracture}^{Post-peak}$) and total work of fracture ($W_{Fracture}^{Total}$). The pre-peak work refers to the work required to initiate the cracks inside the specimen, and it is computed as the area under the load-displacement curve until the peak load (Equation 3.7). The post-peak work refers to the work required for crack propagation and it is determined as the area under the load-displacement curve from the peak load until failure (test termination point) (Equation 3.8). The total work of fracture refers to the total work needed to initiate and propagate the cracks and it is the summation of pre- and post-peak work (Equation 3.9).

$$W_{Fracture}^{Pre-peak} = \int_{0}^{Dis.\ at\ Peak\ load}(P.dx) \quad 3.7$$

$$W_{Fracture}^{Post-peak} = \int_{Dis.\ at\ peak\ load}^{Dis.\ at\ test\ termination}(P.dx) \quad 3.8$$

$$W_{Fracture}^{Total} = W_{Fracture}^{Pre-peak} + W_{Fracture}^{Post-peak} \quad 3.9$$

where $W_{Fracture}^{Pre-peak}$ is the pre-peak work of fracture (J), $W_{Fracture}^{Post-peak}$ is the post-peak work of fracture (J), $W_{Fracture}^{Total}$ is the total work of fracture (J), P is the applied load (KN), and X is the vertical actuator displacement (mm).

### *3.5.5. Fracture energy*

The fracture energy is defined as the amount of energy required to generate a new unit fracture surface in the specimen [13]. It is a normalization of the fracture work by the cracking face area. The crack face area for SC specimen is the ligament length ($L_{lig}$) (radius [r] - notch depth [a]) multiplied by specimen thickness (t) as presented in Equation 3.10 [14].

For circular or IDT specimen, the cracking face area is the specimen thickness (t) multiplied by specimen diameter (D) as presented in Equation 3.11 [15]. Similar to the fracture work, three fracture energy indicators have been identified: pre-peak fracture energy ($G_{Fracture}^{Pre-peak}$), post-peak fracture energy ($G_{Fracture}^{Post-peak}$) and total fracture energy ($G_{Fracture}^{Total}$). The pre-peak fracture energy is the consumed energy in crack initiation phase (Equation 3.12). The post-peak fracture energy is the consumed energy in the crack propagation phase (Equation 3.13). The fracture energy is the energy consumed in the crack initiation and propagation phases (Equation 3.14). Previous studies demonstrated that the total fracture energy is sensitive to the change in air void content, binder PG, and binder content [16]. The fracture energy decreases with the decrease in air void content and the increase in binder content. Also, it increases with the increase in binder PG (i.e., stiffness) until a limit before it decreases [16].

$$SC_{crack\ face\ area} = (\mathrm{r} - \mathrm{a}) \times \mathrm{t} \quad 3.10$$

$$IDT_{crack\ face\ area} = D \times \mathrm{t} \quad 3.11$$

$$G_{Fracture}^{Pre-peak} = \frac{W_{Fracture}^{Pre-Peak}}{crack\ face\ area} \quad 3.12$$

$$G_{Fracture}^{Post-Peak} = \frac{W_{Fracture}^{Post-Peak}}{crack\ face\ area} \quad 3.13$$

$$G_{Fracture}^{Total} = \frac{W_{Fracture}^{Total}}{crack\ face\ area} \quad 3.14$$

where $SC_{cracking\ face\ area}$is the crack face area for SC specimen (mm$^2$), r is the specimen radius (mm), a is the specimen notch depth (mm), t is the specimen thickness (mm), $IDT_{crack\ face\ area}$ is the crack face area for the circular specimen (mm$^2$), $G_{Fracture}^{Total}$ is the total fracture energy (J/m$^2$), $G_{Fracture}^{Pre-peak}$ is the pre-peak fracture energy (J/m$^2$), $G_{Fracture}^{Post-peak}$ is the post-peak fracture energy (J/m$^2$),$W_{Fracture}^{Pre-peak}$ is the pre-peak work of fracture (J), $W_{Fracture}^{Post-peak}$ is the post-peak work of fracture (J), and $W_{Fracture}^{Total}$ is the total work of fracture (J).

*3.5.6. Flexibility Index (FI)*

Al-Qadi et al. (2015) introduced and proposed the FI as a normalization of the fracture energy with respect to the post-peak slope using a SCB test as presented in Equation 3.15 [14]. The post-peak slope is the slope of the descending part of the load-displacement curve which describes mixture's flexibility or brittleness (Figure 3.1) [13,14,16,17]. Higher flexibility index indicates better mix flexibility and slower crack propagation; therefore, the mix is expected to exhibit better resistance to cracking. Al-Qadi et al. (2015) defined the post-peak slope as the tangent slope at the inflection point ($m_{Inflection}$) in the descending part of the load-displacement curve as presented in Equation 3.16. AASHTO TP 124 uses the FI as a performance indicator to assess asphalt mix resistance to cracking.

Several research studies investigated FI as a cracking resistance indicator. Al-Qadi et al (2015) found that the FI to have a good correlation with the observed field cracking performance of the accelerated pavement test sections [14]. Hans et al. (2017) found that FI is sensitive to the change in binder PG, RAP content, and aging conditions [18]. West et al. (2018) showed that FI has a strong direct Pearson correlation coefficient (R > +0.8) with Texas- and NCAT-overlay tests (OTs) [4]. Also, it was found to have a fair direct correlation (R of 0.3) with $J_c$ but FI results showed better statistical mixture grouping as compared to $J_c$ results. Kaseer et al. (2018) found that FI is sensitive to the change in binder grade, aging conditions, and RAP/RAS content, specimen thickness, and air void content [19]. Chen and Solaimanian (2018) demonstrated that FI is sensitive to binder content, binder PG, and air void content [16]. Kim et al. (2018) found that FI to increase with binder content and decrease with NMAS and notch depth [20]. In the meantime, several studies documented some limitations of FI at specific testing conditions [16,19,20]. For example, the FI showed an unexpected trend with the change in air void content and specimen thickness. The FI increased with the increase in air void content and decreased with the increases in specimen thickness. In addition, the FI was found to be highly affected by the post-peak slope [16,19,21]. An adjustment approach was proposed to normalize the FI with respect to air void content and sample thickness as presented in Equations 3.17 to 3.19 [14,19,22,23].

$$\mathrm{FI} = 0.01 * \frac{G_{Fracture}^{Total}}{\left|m_{\mathrm{Inflection}}^{Post-peak}\right|} \quad 3.15$$

$$m_{\mathrm{Inflection}}^{Post-peak} = \frac{dy}{dx}[P = f(x)], \text{ when } \frac{dy^2}{dx^2}[P = f(x)] = 0, \quad 3.16$$

$$\mathrm{FI}_{50} = \mathrm{FI}_{\mathrm{t}} \times \frac{\mathrm{t}}{50} = 0.01 * \frac{G_{Fracture}^{Total}}{\left|m_{\mathrm{Inflection}}^{Post-peak}\right|} \times \frac{\mathrm{t}}{50} \quad 3.17$$

$$FI_{7\%} = FI_{AV} \times \frac{7\%}{\mathrm{AV}\%} \quad 3.18$$

$$FI_{7\%} = FI_{AV} \times \frac{0.0651}{\mathrm{AV}\text{-}AV^2} \quad 3.19$$

where FI is the Flexibility Index, $G_{Fracture}^{Total}$ is the total fracture energy (J/m$^2$), $m_{\mathrm{Inflection}}^{Post-peak}$ is the post-peak slope at the inflection point, t is the specimen thickness (mm), $\mathrm{FI}_{50}$ is the adjusted flexibility index at a specimen thickness of 50 mm, $\mathrm{FI}_{\mathrm{t}}$ is the flexibility index at specimen thickness t, $FI_{7\%}$ is the adjusted flexibility index at air void content of 7%, $FI_{AV}$ is the flexibility index at air voids of AV. AV% is the specimen air void content.

### *3.5.7. Indirect Tensile Asphalt Cracking Test (IDEAL-Cracking Test Index [IDEAL-CT$_{Index}$])*

Zhou et al. (2017) proposed a new cracking performance index called IDEAL-CT$_{\mathrm{Index}}$, which is a normalization of the fracture energy with respect to the post-peak slope and strain tolerance using the IDT specimen (Equation 3.20) [15]. The post-peak slope is determined as the tangent slope at 75% of the peak load for the post-peak curve ($m_{75\%}^{Postpeak}$) as presented in Equation 3.21. The strain tolerance ($\varepsilon_{\mathrm{v}}^{tolerance}$) is defined as the vertical strain until 75% of peak load (Equation 3.22). Higher IDEAL-CT$_{\mathrm{Index}}$ demonstrates better resistance to cracking. A number of studies evaluated the IDEAL-CT$_{\mathrm{Index}}$ as a cracking resistance indicator. Zhou et al (2017) found that IDEAL-CT$_{\mathrm{Index}}$ to capture the change in RAP content, binder type, binder content, aging, and air void content [15]. However, the results had unexpected trends with air void content similar to FI, where IDEAL-CT$_{\mathrm{Index}}$ increased with the increase in air void content. The IDEAL-CT$_{\mathrm{Index}}$ showed a strong correlation with field cracking performance ($R^2$ = 0.87). Dong and Charmot (2019) found that the IDEAL-CT$_{\mathrm{Index}}$ to increase with emulsion content and decrease with the decrease in binder content [24]. Bennert et. al. (2018) evaluated IDEAL-CT$_{\mathrm{Index}}$ as a quality control parameter in New Jersey

[25]. They found good correlation between IDEAL-$CT_{Index}$ and OT test; however, the IDEAL-$CT_{Index}$ had lower variability in test results as compared to the OT. ASTM D8225 uses the IDEAL-$CT_{Index}$ as a performance indicator to assess asphalt mixes resistance to cracking.

$$\text{IDEAL} - CT_{Index} = \frac{G_{Fracture}^{Total}}{\left|m_{75\%}^{Postpeak}\right|} \times \frac{t}{62} \times \varepsilon_v{}^{tolerance} \quad 3.20$$

$$m_{75\%}^{Post-peak} = \left|\frac{P_{85\%}-P_{65\%}}{L_{85}\%-L_{65\%}}\right|, \quad 3.21$$

$$\varepsilon_v{}^{tolerance} = \frac{L_{75\%}^{Postpeak}}{D} \quad 3.22$$

where $\text{IDEAL} - CT_{Index}$ is the IDEAL-Cracking test index indicator, $G_{Fracture}^{Total}$ is the total fracture energy (J/m$^2$), $m_{75\%}^{Postpeak}$ is the post-peak slope at 75% of the peak load, $\varepsilon_v{}^{tolerance}$ is the strain tolerance, t is the specimen thickness (mm), $L_{75\%}^{Postpeak}$ is the displacement at 75% of peak-load at post-peak curve, $P_{65\%}$ and $P_{85\%}$, is the post-peak load at 65% and 85% of the peak load (KN) respectively, $L_{65\%}$ and $L_{85\%}$, is the displacement at 65% and 85% of the peak load (KN) respectively, and D is the specimen diameter (mm).

### *3.5.8. Cracking Resistance Index (CRI)*

The Cracking Resistance Index (CRI) is a normalization of the fracture energy with respect to the peak load (Equation 3.23). Kaseer et al. (2018) proposed the CRI to overcome the limitations of the FI (e.g., high variability, difficult computation process, and brittle mixes assessments [no post-peak data]) [19]. Higher CRI values demonstrate better resistance to cracking. Kaseer et al (2018) reported that CRI is sensitive to the change in binder PG, aging conditions, RAP/RAS content, specimen thickness, and air voids content [19]. They found a strong correlation between CRI and FI ($R^2 > 0.90$); however, the CRI had lower variability, simple calculation procedures, and could differentiate between more mixes with different performance (Tukey's groups) compared to FI. Kaseer et al (2018) proposed Equations 3.24 and 3.25 to normalize CRI with respect to air void content and specimen thickness [19].

$$CRI = \frac{G_{Fracture}^{Total}}{P_{Peak}} \quad 3.23$$

$$CRI_{50} = CRI_t \times \frac{t}{50} \quad 3.24$$

$$CRI_{7\%} = CRI_{AV} \times \frac{7\%}{\text{AV}\%} \quad 3.25$$

where $CRI$ is the Cracking Resistance Index performance indicator, $G_{Fracture}^{Total}$ is the total fracture energy (J/m$^2$), CRI$_{50}$ is the CRI value at 50 mm thickness, $G_{Fracture}^{Total}$ is the total fracture energy (J/m$^2$), t is the specimen thickness (mm), AV% is the specimen air void content, CRI$_{50}$ is the adjusted CRI at specimen thickness of 50 mm, $CRI_{7\%}$ is the adjusted CRI at specimen air voids of 7%, $CRI_{AV}$ is the CRI at air voids AV. And AV% is the specimen air void content

*3.5.9. Nflex factor (Nflex)*

West et al. (2017) proposed the Nflex indicator as a normalization of the mixture toughness with respect to the post-peak slope using the IDT test (Equation 3.26) [12]. The post-peak slope was determined as the tangent slope at the post-peak inflection point ($m_{\text{inflection}}^{Postpeak}$) under the stress-strain curve (Equation 3.27). Toughness was calculated as the area until the post-peak inflection point (Equation 3.28). The stress and strain were calculated using Equations 3.2 and 3.29 respectively. They studied the correlation between Nflex and observed field cracking performance of eight accelerated loading facility test sections. The results showed a reasonable correlation between Nflex and the observed field cracking performance ($R^2$ = 0.55). Such correlation was improved ($R^2$ of 0.67) when the observed field cracking performance was adjusted using surface layer thickness and base layer modulus. Yin et al. (2018) found that the Nflex had insignificant statistical sensitivity to binder PG and binder content and a significant sensitivity to RAP content and test temperature [26]. They reported that considering a constant Poisson's ratio may provide an inaccurate determination of Nflex [26]. Yin et al. (2018) found that the measured Poisson's ratio had a significant dependency on specimen air void content and test temperature. They recommended to estimate the Poisson's ratio using the secant approach as shown in Equation 3.30. This approach requires measuring the horizontal and vertical deformation during the IDT test which adds more complexity to the test setup and data analysis.

$$N_{flex} = \frac{\text{Toughness}}{m} \quad 3.26$$

$$m_{inflection}^{Postpeak} = \frac{dy}{dx}[\sigma = f(\varepsilon_i)], \text{ when } \frac{dy^2}{dx^2}[P = f(\varepsilon_i)] = 0 \quad 3.27$$

$$\text{Toughness} = \int_0^{\text{Strain at } m_{inflection}^{Postpeak}} (\sigma . d\varepsilon) \quad 3.28$$

$$\varepsilon_i = \frac{L_i \times \mu}{D} \quad 3.29$$

$$\mu = 0.15 + \frac{0.35}{1 + e^{(a+bS_c)}} \quad 3.30$$

where $N_{flex}$ is the Nflex factor, $m_{inflection}^{Postpeak}$ is the tangent slope at post peak inflection point (kPa/ %), $\sigma_i$ is the estimated tensile stress at load i (kPa) (Equation 3.2), $\varepsilon_i$ is the estimated tensile strain at load i (%), toughness is the area under stress-strain curve until post peak inflection point, $L_i$ is the vertical deformation at load i (m), D is the specimen diameter (m), $\mu$ is the Poisson's ratio, a and b are the regression fitting coefficients, and $S_c$ is the secant modulus defined as the ratio of peak load to displacement at peak load.

### *3.5.10. Critical strain energy release rate ($J_C$)*

$J_c$ is defined as "a path independent integration of strain energy density, traction, and displacement along an arbitrary contour path around the crack" [27]. It describes the change in strain energy per unit depth with specimen notch depth (dU/da) ( Equation 3.31) [27]. The strain energy to failure (U) is determined as the pre-peak work of fracture ($W_{Fracture}^{Pre-peak}$) as presented in Equation 3.32. The variation of strain energy with notch depth (dU/da) is normalized by the specimen thickness (t). The $J_c$ can be determined using two or three-notch depths. Elseifi et al (2005) suggested using three notch depths for better determination of $J_c$ [28]. Several researchers evaluated the use of $J_c$ as a performance indicator. Bayomy et al. (2006) found that $J_c$ to increase with binder content and the percentage of rough and angular aggregates and decrease with the increase in the percentage of flat and elongated aggregates in the mix. In addition, the $J_c$ decreases for finer aggregate gradation [27]. Cao et al. (2018) found that $J_c$ to decrease with RAP content [29]. Mohammad et al. (2012) found good correlation between $J_c$ and field cracking performance [30]. Louisiana Department of Transportation and Development (LaDOTD) requires that mixes should have minimum $J_c$ of

0.5 kJ/m$^2$ and 0.6 kJ/m$^2$ for Level 1 and Level 2 mix design, respectively [31]. ASTM D8044 uses $J_c$ as a performance indicator to assess asphalt mixes resistance to cracking.

$$J_c = -\left(\frac{1}{t}\right)\frac{dU}{da} \quad 3.31$$

$$W_{Fracture}^{Pre-peak} = \int_0^{Dis.\ at\ Peak\ load}(P.dx) \quad 3.32$$

where $J_c$ is the strain energy release rate (kJ/m$^2$), U is the strain energy to failure (kJ), t is the specimen thickness (mm), a is the specimen notch depth (mm), du/da is the variation of strain energy with notch depth (kJ/mm), $W_{Fracture}^{Pre-peak}$ is the pre-peak work of fracture (J), P is the applied load (KN), x is the vertical actuator displacement (mm)

*3.5.11. Weibull Cracking Resistance Index (Weibull$_{CRI}$)*

Alkuime et al. (2019) introduced and proposed the Weibull Cracking Resistance Index (Weibull$_{CRI}$) as a performance indicator presented in Equation 3.33 [32]. Alkuime et al. (2019) found that among all previous indicators, Weibull$_{CRI}$ was the only indicator that can interpret the overall load-displacement curve shape rather than using a limited number of curve elements (i.e., area under the curve, peak load, peak slope, etc.). Weibull$_{CRI}$ was evaluated for 16 asphalt mixes with different characteristics. They reported that Weibull$_{CRI}$ was sensitive to binder grade, binder content and could distinguish among mixes with different resistance to cracking the of Weibull$_{CRI}$ had low variability. In addition, another study by the authors found that good correlation between Weibull$_{CRI}$ and the dynamic cracking tests compared to other monotonic performance indicators [33].

$$Weibull_{CRI} = \left(\frac{\eta}{\beta}\right) \times log[A] \quad 3.33$$

where $\beta$ is the shape parameter (Weibull slope), $\eta$ is the scale parameter, and $A$ is the fitting constant equals to the area under the load-displacement curve.

## 3.6. Laboratory Experimental Program

One of the objectives of this study was to perform a laboratory evaluation for intermediate temperature cracking testing standards and performance indicators. To fulfill this objective,

an extensive laboratory testing plan was developed as shown in Figure 3.2. The plan included testing 16 asphalt mixes using the four testing methods (i.e., AASHTO TP 124, ASTM D6931, ASTM D8044, and ASTM D8225). In this study, the standard tests requirements were followed as specified with some modification including specimen size and testing temperature. These requirements were unified for all testing standards to remove its effects on the evaluation results. The prepared specimens (IDT and SC) had a thickness of 50 mm and a diameter of 150 mm. Also, all test specimens were tested using a Materials Testing System (MTS) at a fixed intermediate temperature of 25 °C. A total of 240 specimens were prepared, tested and analyzed. In addition, the researchers selected and evaluated 12 performance indicators. Table 3.2 presents the evaluated performance indicators, data sources, and symbols. $G_{fracture}$, CRI, and FI were calculated for two standards to be able to evaluate the data source (e.g., data variability). Test asphalt mixes included six Laboratory-Mixed Laboratory-Compacted (LMLC) mixes and 10 Plant-Mixed Laboratory-Compacted mixes. The LMLC mixes were prepared in the laboratory (

Table **3.3**), while PMLC materials were collected from new paving projects in Idaho (Table 3.4). Details on mix properties and specimen preparation procedures are provided in Alkuime et al. (2019) [32]. The goal of evaluating the LMLC mixes was to examine the sensitivity of various testing standards and performance indicators to the variation in binder content and binder PG. The LMLC specimens were prepared using two binder grades (i.e., PG 70-28 and PG 58-34) and three binder contents (i.e., OBC, OBC-0.75%, and OBC+0.75%). The goal of evaluating the PMLC mixes was to examine the sensitivity of various performance indicators to the composition of the PMLC mixes. In addition, the results of both LMLC and PMLC were used to examine the variability and correlation between various performance indicators.

Table **3.3** and Table 3.4 summarize the LMLC and PMLC mix properties, respectively. The test specimens were compacted using Superpave gyratory compactor at 7% ± 0.5% air voids.

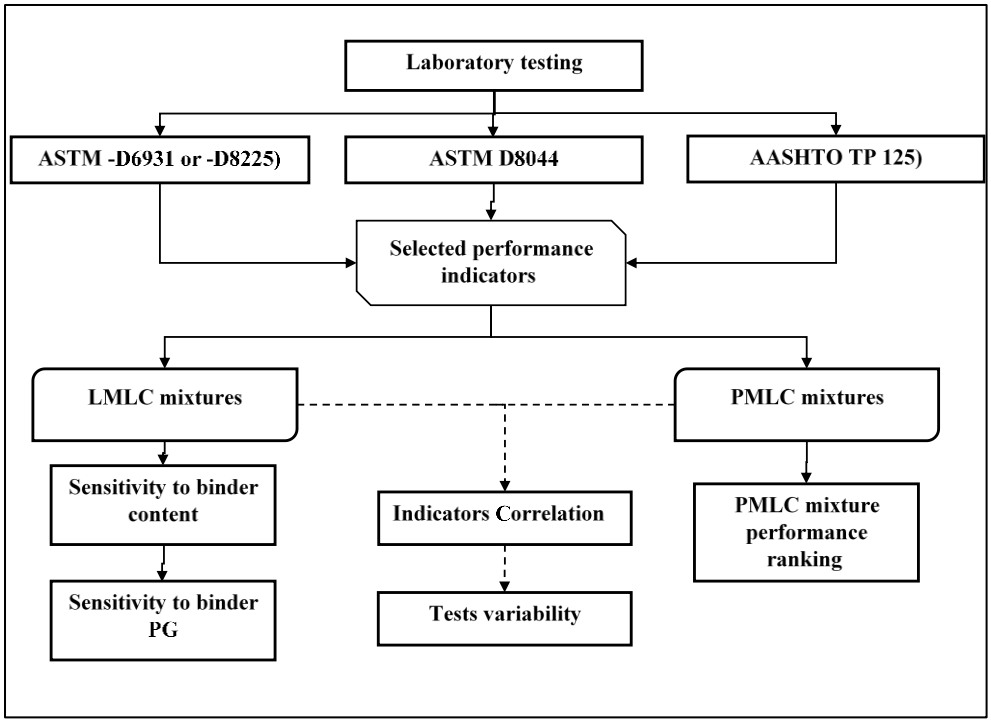


**Figure 3.2**. Laboratory testing plan

**Table 3.2** Selected performance indicator and test data source

| # | Symbol | Testing standards | Performance Indicator Concept |
|---|---|---|---|
| 1 | $G_{fracture}$ (IDT) | ASTM -D6931 and D8225 | Total Fracture Energy |
| 2 | $G_{fracture}$ (SCB-FI) | AASHTO TP 124 | Total Fracture Energy |
| 3 | CRI (IDT) | ASTM -D6931 and D8225 | Cracking Resistance Index |
| 4 | CRI (SCB-FI) | AASHTO TP 124 | Cracking Resistance Index |
| 5 | FI (IDT) | ASTM -D6931 and D8225 | Flexibility Index |
| 6 | FI (SCB-FI) | AASHTO TP 124 | Flexibility Index |
| 7 | $IDEAL\text{-}CT_{Index}$ | ASTM -D6931 and D8225 | $IDEAL\text{-}CT_{Index}$ |
| 8 | Nflex factor | ASTM -D6931 and D8225 | Nflex factor |
| 9 | $IDT_{Strength}$ | ASTM -D6931 and D8225 | $IDT_{Strength}$ |
| 10 | $IDT_{Modulus}$ | ASTM -D6931 and D8225 | $IDT_{Modulus}$ |
| 11 | $J_c$ | ASTM D8044 | Strain energy release rate |
| 12 | $Weibull_{CRI}$(IDT) | ASTM -D6931 and D8225 | $Weibull_{CRI}$ |

**Table 3.3** LMLC asphalt mixture characteristics [32]

| Mixture ID | Mix Type | NMAS | Binder Type | Binder Content |
|---|---|---|---|---|
| PG 70-4.25% | SP3 | 12.5mm | PG 70-28 | 4.25% |
| PG 70-5.00% | | | PG 70-28 | 5.00% |
| PG 70-5.75% | | | PG 70-28 | 5.75% |
| PG 58-4.25% | | | PG 58-34 | 4.25% |
| PG 58-5.00% | | | PG 58-34 | 5.00% |
| PG 58-5.75% | | | PG 58-34 | 5.75% |

**Table 3.4** PMLC asphalt mixture characteristics [32]

| # | District | Project ID | Mix Type | Specified Binder PG | Virgin Binder PG | Binder content Pb% | Recycle Binder Replacement (RBR) | NMAS |
|---|---|---|---|---|---|---|---|---|
| 1 | 1 | D1L1 | SP5 | 64-28 | 58-34 | 5.30% | 30% | 12.5 |
| 2 | 2 | D2L1 | SP3 | 70-28 | 64-34 | 5.70% | 50% | 12.5 |
| 3 | | D2L2 | SP3 | 64-28 | 58-34 | 5.70% | 30% | 12.5 |
| 4 | 3 | D3L1 | SP3 | 70-28 | 52-34 | 5.20% | 50% | 12.5 |
| 5 | | D3L2 | SP3 | 70-28 | 64-34 | 5.20% | 30% | 12.5 |
| 6 | | D3L3 | SP3 | 64-28 | 58-34 | 5.30% | 30% | 12.5 |
| 7 | | D3L4 | SP3 | 70-28 | 64-34 | 5.30% | 30% | 12.5 |
| 8 | | D3L5 | SP5 | 76-28 | 70-34 | 5.30% | 30% | 12.5 |
| 9 | 5 | D5L1 | SP5 | 70-28 | 70-28 | 4.80% | 30% | 19.0 |
| 10 | | D5L2 | SP5 | 70-28 | 64-34 | 5.10% | 30% | 19.0 |
| 11 | 6 | D6L1 | SP5 | 64-34 | 64-34 | 5.40% | 0% | 12.5 |

## 3.7. Analysis of Results and Discussion

### *3.7.1. The Relation Between the Load-Displacement Curve Shape and the Composition of Asphalt Mixes*

The monotonic tests collect similar data including time, load, and vertical actuator displacement, which is used to establish the load-displacement curve. In its core concept, the monotonic tests assume that the shape of the load-displacement curve represents the mix resistance to cracking. The variation in mix resistance to cracking can be evaluated using the variation in the shape of the load-displacement curve. The shape of the load-displacement curve varies with the change in the mix properties, which indicates improving or declining in mixture cracking resistance.

In this study, the researchers examined the effect of mix properties on the load-displacement curves for LMLC mixes. The variation in the shape of the load-displacement curve with binder content and binder PG are shown in Figure 3.3 and Figure 3.4, respectively. It should be noted that the SCB-$J_c$ is conducted with specimens that have three notch depths (i.e., 38.4 mm, 31.8 mm, and 25.4 mm). In Figure 3.3 and Figure 3.4, the load-displacement curve at 25.4 mm notch depth for the SCB- $J_c$ was shown; however, the $J_c$ test was conducted at the three designated notch depths.

Figure 3.3 illustrates that as the binder content increases, the curve peak load, the pre- and the post-peak slope decrease, and the terminal displacement increases. Such variation in the shape of the load-displacement curve indicates improved resistance to cracking. Figure 3.4 illustrates that the pre-peak slope, the curve peak load, and the post-peak slope of the load-displacement curve for mixes prepared with stiffer binder (PG 70-28) are higher compared to mixes prepared with the softer binder (PG 58-34). Such changes demonstrate declining in the cracking resistance. Also, it was observed that the load-displacement of various monotonic tests (e.g., IDT, SCB-FI, and SCB-$J_c$) were sensitive to the variation in mix composition (i.e., binder content and binder grade). A similar conclusion can be observed used the data published in the literature [14,19].

Figure 3.5 demonstrates the variation in the load-displacement curve with RAP materials using data published by [14,19]. Figure 3.5 illustrates that as the percent of RAP materials increases, the curve peak load, the pre- and the post-peak slope increases and the terminal displacement decreases. Such variation in the shape of the load-displacement curve indicates reduced resistance to cracking. This conclusion is in good agreement with the expected effects of RAP materials in mix resistance to cracking.

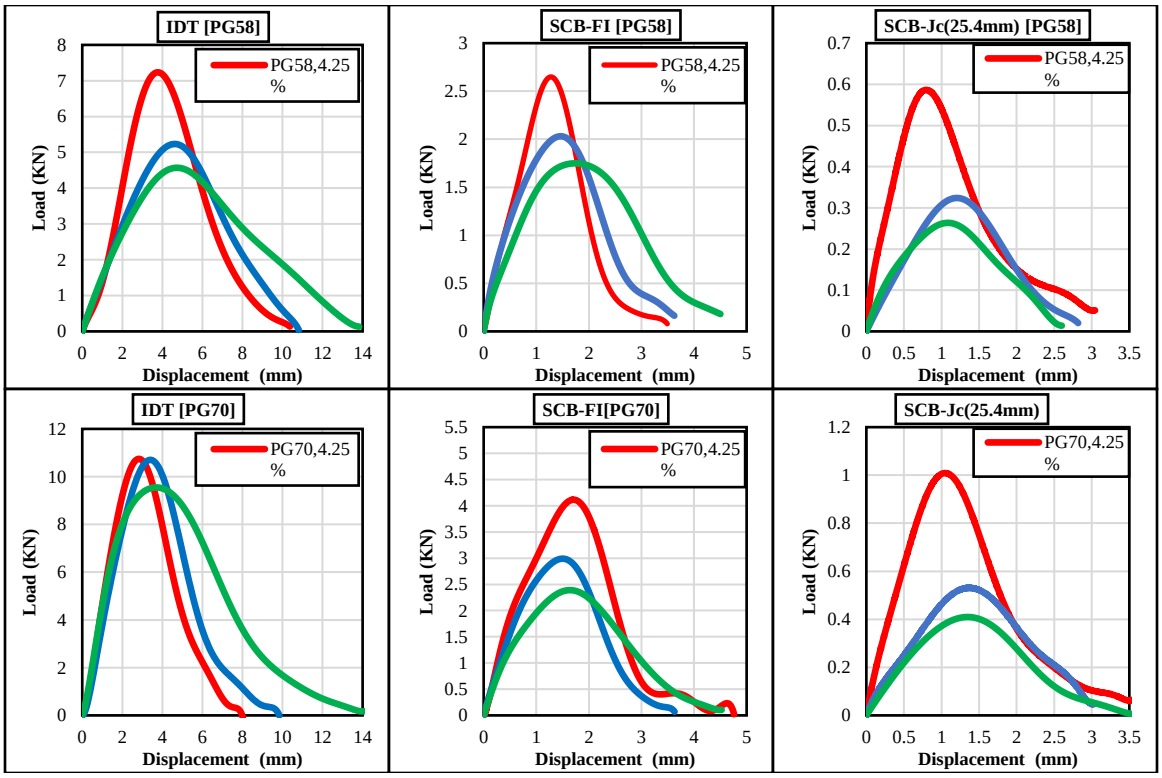


**Figure 3.3.** Monotonic tests load-displacement curve at different binder contents

*3.7.2. The Sensitivity of Monotonic Performance Indicators to Binder Content and Binder Grade*

The LMLC specimens were used to study the sensitivity of the selected performance indicators to the variation in binder content and binder PG. Figure 3.6 illustrates an example of analysis results for the average total fracture energy calculated from the IDT test ($G_{fracture}$ [IDT]). The error bars represent ± one standard deviation from the average value. Sensitivity to binder content was evaluated using a statistical ANOVA and Tukey's Honestly Significant Difference (Tukey's HSD) at each binder PG (three binder content groups at each binder PG). Sensitivity for binder PG was evaluated using a statistical t-test at each binder content (two binder PG groups at each binder content). Both tests (Tukey's HSD and t-test) were performed at 95% confidence interval (i.e., $\alpha = 0.05$). The statistical analysis results are included in the form of letters or numbers at the bottom of each bar. Mixes that do not share the same letter/number are significantly different in terms of their fracture energy.

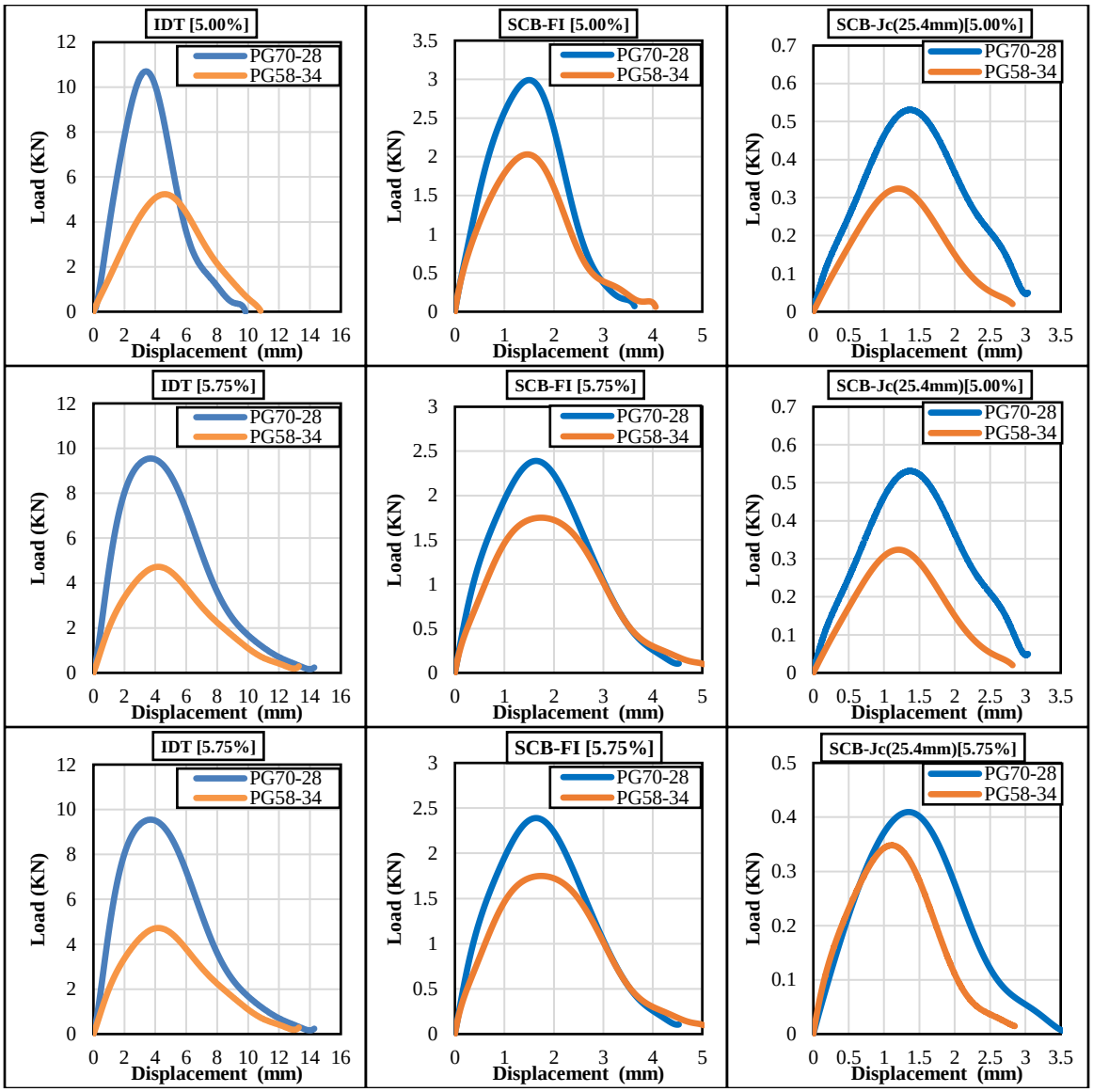


**Figure 3.4.** Monotonic tests load-displacement curve at binder PG and contents

The $G_{fracture}$ (IDT) results showed a low variability (COV = 11%). In addition, the $G_{fracture}$ (IDT) was sensitive to the variation in binder PG and binder content. The mixes prepared with the PG 70-28 binder had higher $G_{fracture}$ (IDT) when compared to mixes prepared with the PG 58-34 binder for a given binder content. Higher fracture energy is associated with better resistance to cracking [14]. Meanwhile, one can expect that a softer binder (e.g., PG 58-34) would provide better cracking resistance when compared to a stiffer binder (e.g., PG 70-28). A significant difference in $G_{fracture}$ (IDT) was found at all binder contents ($p$-value <0.05). Figure 3.6 shows that $G_{fracture}$ (IDT) increases with binder content. Mixes prepared with PG 70-28 binder were more sensitive to the change in binder content as

compared mixes prepared with PG 58-34 binder. The PG 70-28 mixes showed a statistically significant difference ($p$-value < 0.05) between mixes prepared at 4.25% and 5.75% binder content. Meanwhile, there was no statistically significant difference between mixes with different binder contents for the PG 58-34 binder ($p$-value > 0.05).

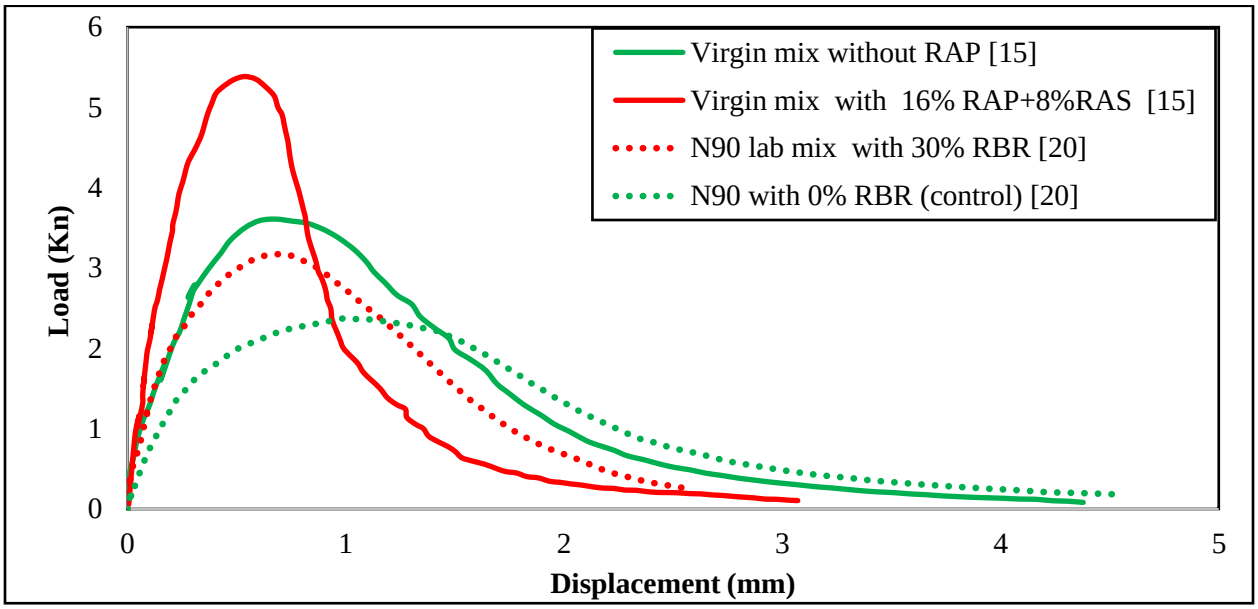


**Figure 3.5.** Monotonic tests load-displacement curve at different RAP content using data published in [14,19]

The research team repeated the analysis for the other selected monotonic indicators as presented in Appendix B. Table 3.5 summarizes the results of the analysis for all 12 selected performance indicators. Details on $Weibull_{CRI}$ results were provided by Alkuime et al. (2019a) [32]. The results of $G_{fracture}$ (IDT), $G_{fracture}$ (SCB-FI), $IDT_{strength}$, $IDT_{Modulus}$, and $J_c$ indicate that mixes with PG 70-28 binder are expected to provide better resistance to cracking when compared to mixes prepared with PG 58-34 binder. Other parameters (i.e., CRI [IDT], CRI [SCB-FI], FI [IDT], FI [SCB-FI], IDEAL-$CT_{Index}$, Nflex factor) showed that mixes with PG 58-34 binder are expected to provide better resistance to cracking when compared to mixes prepared with PG 70-28 binder. The results of $Weibull_{CRI}$(IDT) showed that mixes prepared with the PG 58-34 binder at 5.0 % binder provided better resistance to cracking when compared to mixes prepared with PG 70-24 binder at the same binder content. However, mixes prepared with PG 70-24 binder at 4.25% and 5.75% binder content had higher $Weibull_{CRI}$(IDT) when compared to mixes prepared with PG 58-34 binder at the same

binder content. Alkuime et al. (2019a) showed that $Weibull_{CRI}$ calculated from SCB test data (i.e., AASHTO TP 124) was capable to differentiate between binder grades [32].

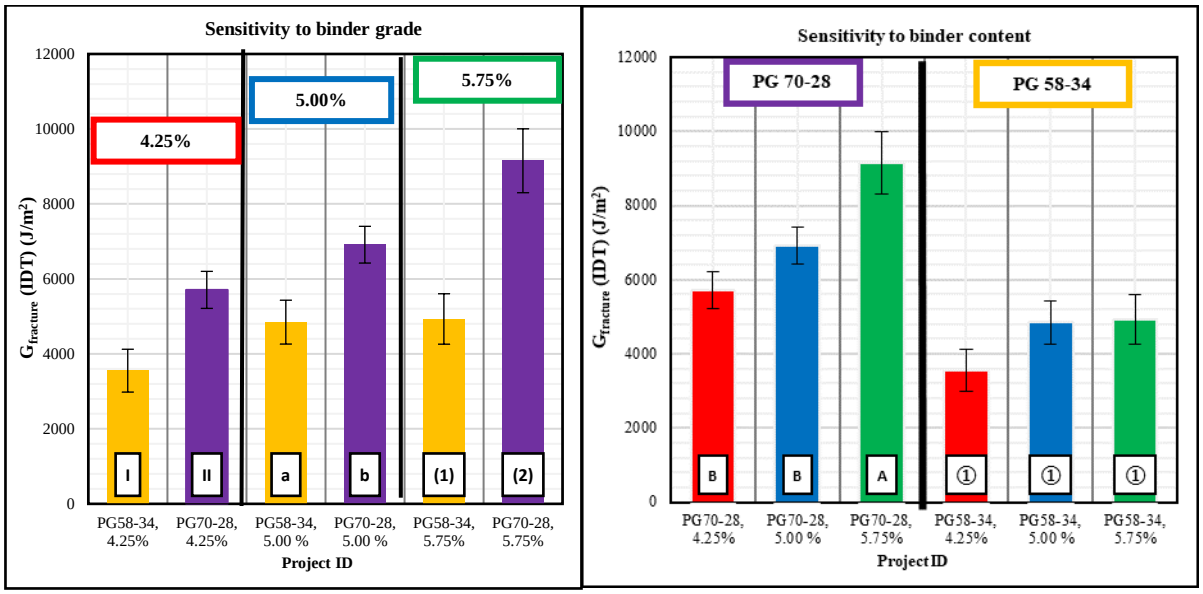


**Figure 3.6.** Sensitivity of total fracture energy calculated from the IDT test to the binder PG and binder content

Several performance indicators including CRI (IDT), CRI (SCB-FI), FI (IDT), FI (SCB-FI), $IDEAL\text{-}CT_{Index}$, Nflex factor, and $Weibull_{CRI}$ showed that cracking resistance is improved with the increase in binder content for the same binder PG (i.e., PG 70-28 and PG 58-34 ) as expected. Other performance indicators including $G_{fracture}$ (IDT), $G_{fracture}$ (SCB-FI), $IDT_{strength}$, $IDTModulus$, and $J_c$ showed mixed trends with increasing the binder content. The $G_{fracture}$ (SCB-FI) and $IDT_{strength}$ results showed an insignificant statistical difference at various binder contents. It should be noted that the sensitivity analysis was conducted on the LMLC mixes that were prepared using only two binders at three different binder contents. Investigation of additional mixes with various properties including mix design is recommended.

**Table 3.5** The sensitivity of monotonic performance indicators to binder content and binder PG

| Performance indicator | Parameter | | | |
|---|---|---|---|---|
| | Binder PG (using softer binder) | | Binder content (increasing binder content) | |
| | Trend | Statistically Significant? | Trend | Statistically Significant? |
| $G_{fracture}$ (IDT) | ↙ | ✓ | ⇳ | ⇔ |
| $G_{fracture}$ (SCB-FI) | ↙ | × | ⇳ | × |
| CRI (IDT) | ↗ | × | ↗ | ⇔ |
| CRI (SCB-FI) | ↗ | ⇔ | ↗ | ⇔ |
| FI (IDT) | ↗ | × | ↗ | ⇔ |
| FI (SCB-FI) | ↗ | ✓ | ↗ | ⇔ |
| IDEAL-$CT_{Index}$ | ↗ | × | ↗ | ⇔ |
| Nflex factor | ↗ | × | ↗ | ⇔ |
| $IDT_{strength}$ | ↙ | ✓ | ↙ | × |
| $IDT_{Modulus}$ | ↙ | ⇔ | ⇳ | ⇔ |
| $J_c$ | ↙ | N/A | ⇳ | N/A |
| $Weibull_{CRI}$(IDT) | ↗ | ⇔ | ↗ | ⇔ |

↙ indicates worse cracking resistance.
↗ indicates better cracking resistance.
⇳ shows both trends.
✓ test results are statistically different (e.g., binder content and grade).
× test results are not statistically different (e.g., binder content and grade).
⇔ Results showed statistically significant/insignificant difference at comparison levels (e.g., binder content and PG).Note: $J_c$ indicator had only one value for each mix, thus ANOVA and Tukey's HSD tests could not be performed for this parameter.

### *3.7.3. Cracking Performance Evaluation of PMLC Mixes Using Load-Displacement Curve*

The resistance of asphalt mixes to cracking depends on material proportions and properties. Mix characteristics can improve or reduce the resistance to cracking. For instance, mix resistance to cracking is declined with lower binder content, stiffer binder PG, aged binder, high air void content, a high percent of RBR, larger NMAS, or lower aggregate angularity [34–37]. In this study, 10 PMLC mixes were evaluated using all the selected 12 performance indicators. Results were used to compare the performance indicator ranking and variability. In addition, a set of comparison of resistance to cracking ranking between performance indicators ranking and the expected ranking based on PMLC mix composition was performed. In this approach, a set of mixes that have similar materials properties except one

or two were compared. Six different comparisons were studied based on PMLC mix properties as summarized in Table 3.6.

First, mix resistance to cracking was compared based on the variation in the load-displacement curve. Figure 3.7 shows the load-displacement curve from the IDT test for the selected comparison in Table 6. Figure 3.7-A shows that the load-displacement curves for D2L2 and D6L1 mixes had a higher area under the curve, less steep pre-peak and post-peak slopes, and higher termination displacement compared to the load-displacement of D3L1 mix. The variations in load-displacement curve shape are associated with improved or better resistance to cracking, therefore D2L2 and D6L1 mixes are expected to have better resistance to cracking when compared to D3L1 mix resistance to cracking. Figure 3.7-B and Figure 3.7-C show that the load-displacement curve for D1L1 had higher curve peak, the area under the curve, less steep pre-peak and post-peak slopes, higher termination displacement as compared to the load-displacement curves of D3L3 and D3L5 mixes. Figure 3.7-D shows that the load-displacement curves for D2L1 mix had higher curve peak, the area under the curve, less steep pre-peak and post-peak slopes, higher termination displacement as compared to the load-displacement curve of D3L1 mix. Figure 3.7-E shows that the load-displacement curves for D2L1 and D2L2 mixes had a similar curve peak, pre-peak slope, but D2L2 mix curve had a less steep post-peak slope and higher termination displacement as compared to D2L1 curve. These results demonstrate that there is good agreement between the findings of mix resistance to cracking comparison based on the shape of the load-displacement curve and based on mix composition (Table 3.4).

Also, Figure 3.7 shows the limitation of using specific curve elements (i.e., curve peak, the area under the curve, etc.) to evaluate the cracking resistance. For instance, Figure 3.7-E shows that the load-displacement curves for D2L1 and D2L2 mixes had a relatively similar curve peak and area under the curve, therefore performance indicators using these basic elements such as $G_{fracture}$ [IDT], CRI [IDT], or $IDT_{Strength}$ may provide an inaccurate ranking of mix cracking resistance. Among all proposed indicators, $Weibull_{CRI}$ is the only indicators can describe the entire variation in the load-displacement curve.

*3.7.4. The Sensitivity of Monotonic Performance Indicators to PMLC mixes*

Figure 3.8 shows the average total fracture energy calculated from the IDT test ($G_{fracture}$ [IDT]). The $G_{fracture}$ (IDT) ranged from 5300 J/m$^2$ to 7540 J/m$^2$ with a standard deviation (SD) between 694 J/m$^2$ and 1214 J/m$^2$. Higher total fracture energy is associated with better resistance cracking [38]. The $G_{fracture}$ (IDT) had low variability (COV = 10%). ANOVA test indicated a statistically significant difference in the test results ($p$-value < 0.05). Tukey's HSD test classified the mixes into four performance groups; A (higher $G_{fracture}$ [IDT]), B, C, and D (lower $G_{fracture}$ [IDT]). The $G_{fracture}$ (IDT) results were not consistent with expected cracking resistance based on mix composition (Table 3.6).

The research team repeated the analysis for the other 11 performance indicators as summarized in Table 3.7. Details on $Weibull_{CRI}$ results were provided by Alkuime et al. (2019a) [32]. The results of performance indicators including $G_{fracture}$ (SCB-FI), CRI (IDT), FI (IDT), Nflex factor, and $Weibull_{CRI}$ (IDT) were consistent with the expected resistance to cracking based on mix composition (Table 3.6). Other indicators provided limited agreements with the expected mix ranking. $J_c$ indicators results had the lowest number of agreements (two comparisons) with the expected ranking. Also, the test data source was found to affect the results of some performance indicators. For example, CRI calculated from the IDT test (CRI [IDT]) was able to provide accurate estimation for all comparisons (six comparisons), while the results of CRI calculated from SCB (CRI [SCB-FI]) test provided a good assessment with three comparisons.

**Table 3.6** Estimated mix cracking resistance based on its composition

| # | Mix | Similarity | Differences | Expected cracking performance |
|---|---|---|---|---|
| 1 | D2L2 and D6L1 | -- | -- | ***Either D2L2 or D6L1 to have the best resistance to cracking*** D6L1 has no recycled materials (RBR =0%), second highest binder content (5.40%), softer specified binder PG (PG 64-34), good mix type (SP5), and smallest NMAS (12.5mm). D2L2 has the highest binder content (5.70%), and softer virgin binder content (PG58-34), smallest NMAS (12.5 mm). |
| 2 | D3L1 | -- | -- | ***D3L1 to have the poorest resistance to cracking*** D3L1 mix has the highest RBR content (50%), third lowest binder content (5.20%) and stiffer binder PG (PG 70-28). |
| 3 | D1L1 and D3L3. | Specified binder PG (PG 64-28), virgin binder PG (PG 58-34), binder content (5.30%), RBR content (30%), and NMAS (12.5) | Mix type (D1L1 has SP5 mix while D3L3 has SP3 mix ) | ***D1L1 to have better resistance to cracking than D3L3*** SP5 mixes are designed for higher traffic as compared to SP3, therefore D1L1 is expected to have better resistance to cracking. |
| 4 | D1L1 and D3L5. | Mix type (SP5), binder content (5.30%), RBR content (30%), and NMAS (12.5 mm), | Specified binder PG (D1L1 has PG 64-28 while D3L5 has PG 76-28) and Virgin binder PG (D1L1 has PG 58-34 while D3L5 has PG 70-34 ) | ***D1L1 to have better resistance to cracking than D3L5*** D1L1 has a softer specified and virgin binder PG than D3L5 which is expected to have better cracking performance |
| 5 | D2L1 and D3L1 | Mix type (SP3), specified binder PG (PG 70-28), RBR content (50%), and NMAS (12.5 mm | Virgin binder PG (D2L1 has PG 64-34 while D3L1 has PG 52-34) and Binder content (D2L1 has 5.7 % binder content while D3L1 has 5.2% ) | ***D2L1 to have better resistance to cracking than D3L1*** D2L1 has a higher binder content (5.7%) compared to D3L1 (5.20 %), which is expected to have better performance. |
| 6 | D2L2 and D2L1 | Mix type (SP3), binder content (5.7%) and NMAS (12.5 mm) | RBR content ( D2L2 has 30% RBR% while D2L1 has 50% ), specified binder PG ( D2L2 has PG 64-28 while D2L1 has PG70-28 ) and virgin binder PG ( D2L2 has PG 58-34 while D2L1 has PG 64-34 ) | ***D2L2 to have better resistance to cracking than D2L1*** D2L2 has lower RBR content (30%) and softer specified binder PG (PG 64-28), virgin binder PG (PG 58-34) compared to D2L1 (RBR [50 %], specified binder PG [PG 70-28], and virgin binder PG [PG 64-34]), which is expected to have better resistance to cracking |

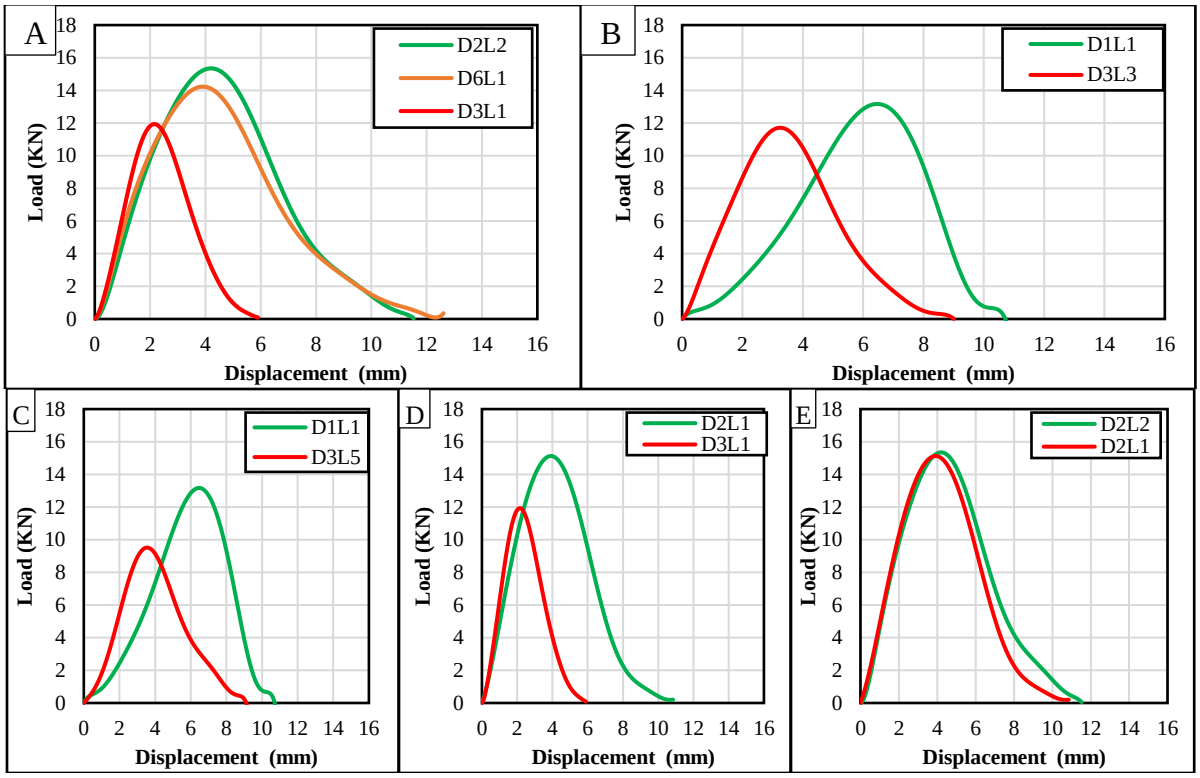


**Figure 3.7** The changes in Load-displacement curve from the IDT test for different PMLC mixes

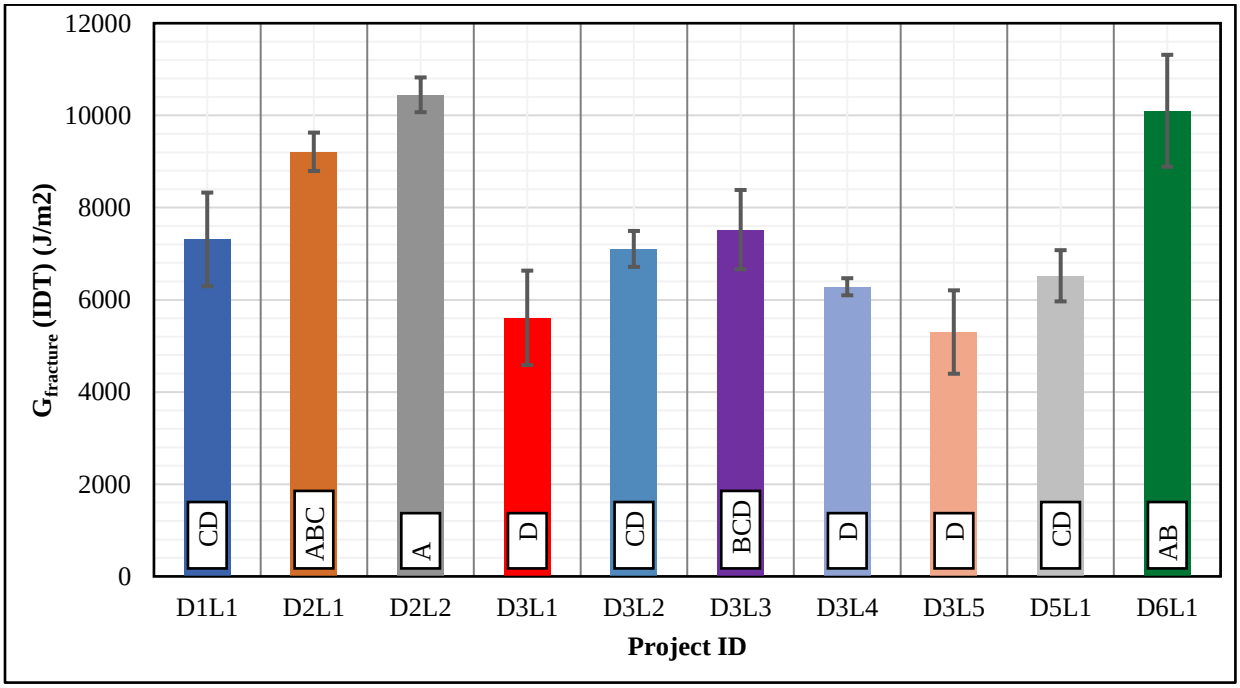


**Figure 3.8** Total fracture energy calculated from the IDT test for the PMLC mixes

**Table 3.7** Sensitivity of monotonic performance indicators to PMLC mixe ranking

| Performance indicators | PMLC comparison | | | | | |
|---|---|---|---|---|---|---|
| | D2L2 and D6L1 to have the best resistance to cracking | D3L1 to have the worst resistance to cracking | D1L1 to have better resistance to cracking than D3L3 | D1L1 to have better resistance to cracking than D3L5 | D2L1 to have better resistance to cracking than D3L1 | D2L2 to have better resistance to cracking than D2L1 |
| $G_{fracture}$ (IDT) | ✓ | ✗ | ✗ | ✓ | ✓ | ✓ |
| $G_{fracture}$ (SCB-FI) | ✓ | ✓ | ✓ | ✓ | ✓ | ✓ |
| CRI (IDT) | ✓ | ✓ | ✓ | ✓ | ✓ | ✓ |
| CRI (SCB-FI) | ✗ | ✗ | ✗ | ✓ | ✓ | ✓ |
| FI (IDT) | ✓ | ✓ | ✓ | ✓ | ✓ | ✓ |
| FI (SCB-FI) | ✗ | ✗ | ✗ | ✓ | ✓ | ✓ |
| IDEAL-$CT_{Index}$ | ✗ | ✓ | ✓ | ✓ | ✓ | ✓ |
| Nflex factor | ✓ | ✓ | ✓ | ✓ | ✓ | ✓ |
| $IDT_{strength}$ | ✗ | ✗ | ✗ | ✓ | ✓ | ✗ |
| $IDT_{Modulus}$ | ✗ | ✗ | ✓ | ✓ | ✗ | ✓ |
| $J_c$ | ✗ | ✗ | ✗ | ✗ | ✓ | ✓ |
| $Weibull_{CRI}$(IDT) | ✓ | ✓ | ✓ | ✓ | ✓ | ✓ |

✓ indicates agreement between indicator ranking and the expected ranking.

✗ indicates disagreement between indicator ranking and the expected ranking.

### *3.7.5. Variability in The Results of Various Monotonic Performance Indicators*

Higher variability in the results of performance indicators indicates reduced accuracy and confidence in the predicted cracking resistance. In general, the variability of monotonic tests (i.e. IDT, SCB-FI, and SCB-$J_c$) are low to moderate variability when compared to the repeated load cracking tests (i.e. Overlay Tester [OT]). Several statistical measures are used to measure the data variability such as range, standard deviation, variance, interquartile range, and coefficient of variation (COV). In this study, the COV was used to assess the variability of the various performance indicators and tests. COV is the normalization of the standard deviation by the average value [39]. COV is a unitless measure, thus it can be used to compare the variability of selected indicators. COV ranges from 0% to 100%, where lower COV indicates less variability in the test results.

Figure 3.9 shows the average, median, and range of the COV for various performance indicators calculated from the respective monotonic tests for all test mixes (i.e., LMLC and PMLC). The indicators were classified into three categories based on their average COV; 1) low variability (average COV <10%), 2) moderate variability (15% < average COV < 30%), and 3) high variability (average COV > %30%). The results demonstrate that the WeibullCRI had the lowest average COV (7.4%) and the median value (6.4%) and CRI had the narrowest range (2.4%-13.8%). The FI calculated from the SCB-FI test (FI [SCB-FI]) had the highest average COV (25.8%). Performance indicators with low variability (COV <10%) included $Weibull_{CRI}$, $IDT_{strength}$, and CRI (IDT). Other indicators had a moderate variability (15% < average COV < 35%). Also, it was observed that performance indicators calculated from the IDT test data exhibited a lower variability as compared to the variability of indicators calculated from the SCB test data. $G_{fracture}$ (IDT) had an average COV of 10.3% while Gfracture (SCB-FI) had an average COV of 14.2%. FI (IDT) had an average COV of 19%, while FI (SCB-FI) had an average COV of 25.8%. CRI (IDT) had an average COV of 8.7%, while CRI (SCB-FI) had an average COV of 11.3%.

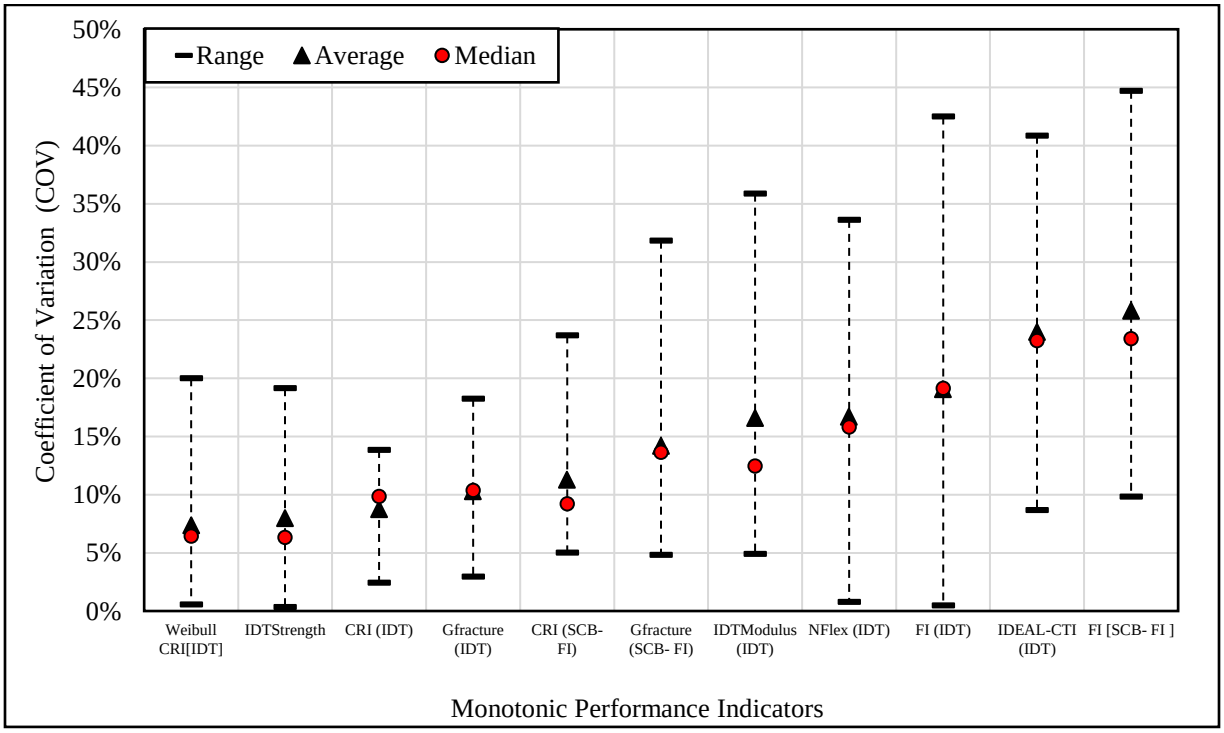


**Figure 3.9.** COV average, median, and range for different performance indicators using LMLC and PMLC data

### *3.7.6. Correlation Between Monotonic Performance Indicators*

This section studied the type and strength of the correlation between various performance indicators. The correlation is defined as "*a measure of association between two variables that expresses the degree to which the two variables are rectilinearly related*" [39]. Two statistical tools were used to examine the correlation between the monotonic performance indicator; the Pearson product-moment correlation coefficient (r) and the Spearman rank correlation coefficient ($r_s$). The Pearson coefficient examines the linear relationship between two performance indicators [39]. The Spearman rank coefficient is a particular case of the Pearson coefficient where it examines the agreement of mix resistance to cracking ranking between two performance indicators [39]. The coefficients (r and $r_s$) range between -1 and +1. The coefficient magnitude indicates the relationship strength; the higher the value, the better the correlation. The coefficient sign indicates the relationship type, where a positive sign indicates a direct relationship and a negative sign indicates an inverse relationship [39]. The coefficients were computed using Minitab statistical analysis software.

Table 3.8 presents the computed Pearson coefficients. All coefficients had a direct (positive sign) correlation with each other except with $IDT_{Modulus}$. Performance indicators from different tests (i.e., IDT or SCB) showed excellent or good correlation. There was a strong correlation between $G_{fracture}$ (IDT) and $G_{fracture}$ (SCB-FI) (r = 0.912). There was a good correlation between CRI (IDT) and CRI (SCB-FI), FI (IDT) and FI (SCB-FI) with r = 0.774, 0.742, and 0.713, respectively. $J_c$ and $IDT_{strength}$ did not correlate well or had no correlation at all with other indicators. Conversely, the $Weibull_{CRI}$ correlated with more indicators than any other performance indicators. The $Weibull_{CRI}$ had a strong correlation with CRI (IDT) (r = 0.941), FI (IDT) (r = 0.950), $IDEAL\text{-}CT_{Index}$ (r = 0.922), and Nflex factor (r = 0.922). Also, the $Weibull_{CRI}$ had good correlation with $G_{fracture}$ (IDT) (r =0.767), $G_{fracture}$ (SCB-FI) (r = 0.784) and fair correlation with and $J_c$ (r = 0.634), FI (SCB-FI) (r = 0.516), and $IDT_{Modulus}$ (r = -0.498). The good correlation between $Weibull_{CRI}$ and most of the performance indicators is attributed to its calculation concept. Each indicator uses one or more elements of the load-displacement curve, while $Weibull_{CRI}$ describes the entire load-displacement curve thus it correlates with more indicators.

Understanding the correlation between indicators is needed; however, it is important to examine how various performance indicators rank the same mixes in terms of cracking resistance. Table 3.9 presents the computed Spearman correlation coefficients. The $Weibull_{CRI}$ had an excellent agreement ($r_s > 0.9$) with CRI (IDT), FI (IDT), and Nflex factor. Also, it had good ranking agreement ($0.7< r_s > 0.9$) with $G_{fracture}$ (IDT), $G_{fracture}$ (SCB-FI), CRI (SCB-FI), and IDEAL-$CT_{Index}$. The CRI (IDT) had an excellent ranking agreement with FI (IDT) ($r_s = 0.975$) and perfect agreement ($r_s$ of 1) with Nflex factor. $J_c$ had fair to poor ranking agreement with all indicators. $IDT_{Modulus}$ ranking had an inverse ranking with other indicators. The Pearson and Spearman correlation results clearly demonstrate the advantages of using $Weibull_{CRI}$ over other parameters. $Weibull_{CRI}$ had better ranking agreement and correlation with more indicators than any other performance indicators.

### *3.7.7. Selection Recommendation of Performance Indicators*

Various performance indicators calculated from monotonic test output (i.e., load-displacement curve) are used in the literature to evaluate the resistance of asphalt mixes to cracking. This study examined 12 different performance indicators and identified the most promising performance indicators based on several criteria including the sensitivity to performance indicators to mix compositions (i.e., binder content and binder grade), PMLC mixes ranking, indicator variability, and indicator statistically significant groups (Tukey's HSD).

Table 3.10 summarizes the finding of the comparisons of the selected performance indicators. Among all of these indicators, CRI (IDT), FI (IDT), Nflex factor, $Weibull_{CRI}$(IDT) were able to provide a good estimation of mix ranking and sensitivity to binder content and binder PG. CRI (IDT) and $Weibull_{CRI}$(IDT) had the highest number of Tukey's HSD groups (4 groups), thus it would provide a better statistically significant difference between mixes as compared to other indicators. Meanwhile, $Weibull_{CRI}$(IDT) had the lowest average variability, which provides more repeatable results. In addition, previous research by the authors showed the $Weibull_{CRI}$(IDT) to have better correlation with dynamic cracking assessment tests compared to other performance indicators [40]. Therefore, the

$Weibull_{CRI}$(IDT) is proposed and recommended as a performance indicator to assess the resistance of asphalt mixes to cracking.

**Table 3.8** Pearson coefficient (r) for monotonic performance indicators

| Pearson *coefficient | $Weibull_{CRI}$ | $G_{fracture}$ (IDT) | $G_{fracture}$ (SCB-FI) | CRI (IDT) | CRI (SCB-FI) | FI (IDT) | FI (SCB-FI) | IDEAL-$CT_{Index}$ | Nflex factor | $IDT_{strength}$ | $IDT_{Modulus}$ | J c |
|---|---|---|---|---|---|---|---|---|---|---|---|---|
| $Weibull_{CRI}$ | 1 | | | | | | | | | | | |
| $G_{fracture}$ (IDT) | 0.767[2] | 1 | | | | | | | | | | |
| $G_{fracture}$ (SCB-FI) | 0.784 | 0.912 | 1 | | | | | | | | | |
| CRI (IDT) | 0.941[1] | 0.805 | 0.810 | 1 | | | | | | | | |
| CRI (SCB-FI) | 0.626 | 0.426 | 0.507 | 0.774 | 1 | | | | | | | |
| FI (IDT) | 0.950 | 0.742 | 0.738 | 0.975 | 0.760 | 1 | | | | | | |
| FI (SCB-FI) | 0.516 | 0.342 | 0.409 | 0.713 | 0.952 | 0.673 | 1 | | | | | |
| IDEAL-$CT_{Index}$ | 0.922 | 0.756 | 0.700 | 0.878 | 0.685 | 0.902 | 0.562 | 1 | | | | |
| Nflex factor | 0.962 | 0.830 | 0.807 | 0.981 | 0.674 | 0.977 | 0.606 | 0.911 | 1 | | | |
| $IDT_{strength}$ | 0.199 | 0.758 | 0.617 | 0.231 | -0.110 | 0.147 | -0.178 | 0.257 | 0.281 | 1 | | |
| $IDT_{Modulus}$ | -0.4984[4] | -0.093 | -0.101[4] | -0.572[3] | -0.731 | -0.586 | -0.801 | -0.576 | -0.538 | 0.471 | 1 | |
| Jc | 0.634 | 0.476 | 0.560 | 0.668 | 0.499 | 0.628 | 0.384 | 0.433 | 0.601 | 0.054 | -0.228 | 1 |

[1] Green cells indicate excellent correlation ($r \geq 0.9$),[2] orange cells indicate good correlation ($0.7 < r < 0.9$),[3] yellow cells indicate fair correlation ($0.5 < r \leq 0.7$), white cells indicate poor correlation ($0.1 < r \leq .5$), and [4] red cells indicate no correlation

**Table 3.9** Spearman coefficient ($r_s$) for monotonic performance indicators

| Spearman Coefficient | $Weibull_{CRI}$ | $G_{fracture}$ (IDT) | $G_{fracture}$ (SCB-FI) | CRI (IDT) | CRI (SCB-FI) | FI (IDT) | FI (SCB-FI) | IDEAL-$CT_{Index}$ | Nflex factor | $IDT_{strength}$ | $IDT_{Modulus}$ | $J_c$ |
|---|---|---|---|---|---|---|---|---|---|---|---|---|
| $Weibull_{CRI}$ | 1 | | | | | | | | | | | |
| $G_{fracture}$ (IDT) | 0.697[2] | 1 | | | | | | | | | | |
| $G_{fracture}$ (SCB-FI) | 0.733 | 0.745 | 1 | | | | | | | | | |
| CRI (IDT) | 0.964[1] | 0.794 | 0.806 | 1 | | | | | | | | |
| CRI (SCB-FI) | 0.721 | 0.564[3] | 0.576 | 0.818 | 1 | | | | | | | |
| FI (IDT) | 0.927 | 0.745 | 0.758 | 0.964 | 0.891 | 1 | | | | | | |
| FI (SCB-FI) | 0.442[4] | 0.418 | 0.273 | 0.576 | 0.879 | 0.624 | 1 | | | | | |
| IDEAL-$CT_{Index}$ | 0.842 | 0.770 | 0.661 | 0.879 | 0.709 | 0.891 | 0.515 | 1 | | | | |
| Nflex factor | 0.964 | 0.794 | 0.806 | 1.000 | 0.818 | 0.964 | 0.576 | 0.879 | 1 | | | |
| $IDT_{strength}$ | 0.139 | 0.685 | 0.479 | 0.212 | -0.091[5] | 0.115 | -0.176 | 0.152 | 0.212 | 1 | | |
| $IDT_{Modulus}$ | -0.515 | -0.236 | -0.115 | -0.576 | -0.758 | -0.600 | -0.830 | -0.612 | -0.576 | 0.442 | 1 | |
| $J_c$ | 0.491 | 0.309 | 0.539 | 0.503 | 0.345 | 0.442 | 0.127 | 0.285 | 0.503 | 0.103 | -0.103 | 1 |

[1] Green cells indicate excellent correlation ($r_s \geq 0.9$),[2] orange cells indicate good correlation ($0.7 < r_s < 0.9$),[3] yellow cells indicate fair correlation ($0.5 < r_s \leq 0.7$) white cells indicate poor correlation ($0.1 < r_s \leq .5$) and [4] red cells indicate no correlation

**Table 3.10**. Monotonic performance indicators comparison summary

| performance indicator | LMLC mixes | | PMLC mixes | | | | | | | PMLC and LMLC mixes |
|---|---|---|---|---|---|---|---|---|---|---|
| | Binder PG | Binder Content | D2L2 and D6L1 to have the best cracking resistance | D3L1 to have the worst cracking resistance | D1L1 to have better-cracking resistance than D3L3 | D1L1 to have better-cracking resistance than D3L5 | D2L1 to have better-cracking resistance than D3L1 | D2L2 to have better-cracking resistance than D2L1 | Number of Tukey Groups (PMLC) | Variability |
| Gfracture (IDT) | ↙ | ⇳ | ✓ | ✗ | ✗ | ✓ | ✓ | ✓ | 4 | Moderate |
| Gfracture (SCB-FI) | ↙ | ⇳ | ✓ | ✓ | ✓ | ✓ | ✓ | ✓ | 4 | Moderate |
| CRI (IDT) | ↗ | ↗ | ✓ | ✓ | ✓ | ✓ | ✓ | ✓ | 4 | low |
| CRI (SCB-FI) | ↗ | ↗ | ✗ | ✗ | ✗ | ✓ | ✓ | ✓ | 3 | Moderate |
| FI (IDT) | ↗ | ↗ | ✓ | ✓ | ✓ | ✓ | ✓ | ✓ | 2 | Moderate |
| FI (SCB-FI) | ↗ | ↗ | ✗ | ✗ | ✗ | ✓ | ✓ | ✓ | 2 | Highest |
| IDEAL-CTIndex | ↗ | ↗ | ✗ | ✓ | ✓ | ✓ | ✓ | ✓ | 2 | Moderate |
| Nflex factor | ↗ | ↗ | ✓ | ✓ | ✓ | ✓ | ✓ | ✓ | 2 | Moderate |
| IDTstrength | ↙ | ↙ | ✗ | ✗ | ✗ | ✓ | ✓ | ✗ | 2 | low |
| IDTModulus | ↙ | ⇳ | ✗ | ✗ | ✓ | ✓ | ✗ | ✓ | 1 | Moderate |
| Jc | ↙ | ⇳ | ✗ | ✗ | ✗ | ✗ | ✓ | ✓ | NA | NA |
| WeibullCRI (IDT) | ↗ | ↗ | ✓ | ✓ | ✓ | ✓ | ✓ | ✓ | 4 | Lowest |

↙ indicates worse cracking resistance, ↗ indicates better cracking resistance, ⇳ shows both trends, ✓ indicates agreements between indicator ranking and the expected ranking, ✗ indicates disagreements between indicator ranking and the expected ranking.

*3.7.8. Summary and Conclusions*

The main objective of this study was to review test methods used to evaluate the cracking resistance of asphalt mixtures and identify the appropriate performance indicators to interpret the monotonic cracking test data. The authors performed a comprehensive review of current performance tests and their indicators. The research involved extensive laboratory experimental program. A total number of 12 performance indicators were evaluated and compared in different aspects including sensitivity to mix compositions, variability, statistically grouping was well as performance ranking and the correlation between various performance indicators. The main findings of this study can be summarized as followed:

- Different performance indicators were proposed in the literature to analyze the load-displacement curve of monotonic tests. $G_{fracture,}$ $IDT_{strength}$, $IDT_{Modulus}$, and $J_c$, CRI, FI, IDEAL-$CT_{Index}$, Nflex factor, and $Weibull_{CRI}$ indicators were found to be the most promising indicators.

- Several performance indicators including CRI (IDT), CRI (SCB-FI), FI (IDT), FI (SCB-FI), IDEAL-$CT_{Index}$, Nflex factor, and $Weibull_{CRI}$ showed that the cracking resistance is improved with the increase in binder content. Other performance indicators including $G_{fracture}$ (IDT), $G_{fracture}$ (SCB-FI), $IDT_{strength}$, $IDT_{Modulus}$, and $J_c$ showed mixed trends with increased binder content.

- The results of $G_{fracture}$ (IDT), $G_{fracture}$ (SCB-FI), $IDT_{strength}$, $IDT_{Modulus}$, and $J_c$ indicate that mixes with PG 70-28 binder are expected to provide better cracking resistance when compared to mixes prepared with PG 58-34 binder. Other parameters (e.g., CRI (IDT), CRI (SCB-FI), FI (IDT), FI (SCB-FI), IDEAL-$CT_{Index}$, Nflex factor) showed that mixes with PG 58-34 binder are expected to provide better cracking resistance when compared to mixes prepared with PG 70-28 binder.

- There was good agreement between mix cracking resistance based on the shape of the load-displacement curve and mix composition

- The $Weibull_{CRI}$ had the lowest average COV (7.4%) with a median value of 6.4%. The FI calculated from the SCB-FI test had the highest average COV (25.8%). Performance indicators with low variability (COV <10%) included $Weibull_{CRI,}$ $IDT_{strength,}$ and CRI (IDT). Other indicators had a moderate variability (15% < average COV < 35%). Also, it was observed that performance indicators calculated from the IDT test data exhibited a lower variability compared to the variability of indicators calculated from the SCB test data.

- All indicators had a positive Pearson's coefficients correlation with each other except with $IDT_{Modulus}$. Performance indicators from different tests (i.e., IDT or SCB) showed excellent or good correlation. There was a strong correlation between $G_{fracture}$ (IDT) and $G_{fracture}$ (SCB-FI) (r = 0.912). There was a good correlation between CRI (IDT) and CRI (SCB-FI), FI (IDT) and FI (SCB-FI) with r = 0.774, 0.742, and 0.713, respectively. $J_c$ and $IDT_{strength}$ did not correlate well or had no correlation at all with other indicators. Also, Spearman correlation coefficients comparison showed that $Weibull_{CRI}$ had excellent agreement ($r_s$ > 0.9) with CRI (IDT), FI (IDT), and Nflex factor. Also, it had good ranking agreement (0.7< $r_s$ > 0.9) with $G_{fracture}$ (IDT), $G_{fracture}$ (SCB-FI), CRI (SCB-FI), and IDEAL-$CT_{Index}$. The CRI (IDT) had an excellent ranking agreement with FI (IDT) ($r_s$ = 0.975) and perfect agreement ($r_s$ of 1) with Nflex factor. $J_c$ had fair to poor ranking agreement with all indicators. $IDT_{Modulus}$ ranking had an inverse ranking with the other indicators.

- Among all examined indicators, CRI (IDT), FI (IDT), Nflex factor, $Weibull_{CRI}$(IDT) were able to provide a reasonable cracking resistance assessment to expected one and were sensitive to binder content and binder PG. CRI (IDT) and $Weibull_{CRI}$(IDT) had the highest number of Tukey's HSD groups (4 groups), However, $Weibull_{CRI}$(IDT) had the lowest variability, which offers more repeatable results. Based on the results of this study, the $Weibull_{CRI}$ is recommended to evaluate the cracking resistance of asphalt mixtures. Each indicator uses one or more elements of the load-displacement curve, while $Weibull_{CRI}$ describes the entire load-displacement curve.

### 3.8. References

[1] J.S. Miller, W.Y. Bellinger, Distress identification manual for the long-term pavement performance program, Publication NO FHWA-RD-03-031. FHWA, U.S. Department of Transportation. (2003) 129. doi:FHWA-RD-03-031.

[2] A. Braham, B.S. Underwood, State of the art and practice in fatigue cracking evaluation of asphalt concrete pavements, 2016. http://asphalttechnology.org/downloads/Fatigue_Cracking_of_Asphalt_Pavements_2017_06.pdf.

[3] M. Kim, L.N. Mohammad, M. a. Elseifi, Characterization of fracture properties of asphalt mixtures as measured by semicircular bend test and indirect tension test, Transportation Research Record: Journal of the Transportation Research Board. 2296 (2012) 115–124. doi:10.3141/2296-12.

[4] R. West, D. Timm, B. Powell, M. Heitzman, N. Tran, C. Rodezno, D. Watson, F. Leiva, A. Vargas, NCAT draft Report 18-04 PHASE VI (2012-2015) NCAT test track findings, 2018.

[5] R.C. West, C. Rodenzo, F. Leiva, F. Yin, Development of a framework for balanced mix design, NCHRP project 20-07/task 406, 2018. http://apps.trb.org/cmsfeed/TRBNetProjectDisplay.asp?ProjectID=4324.

[6] W.G. Buttlar, R. Roque, N. Kim, Accurate asphalt mixture tensile strength, in: Proceedings of the Materials Engineering Conference, 1996.

[7] AASHTO, Standard method of test for determining the creep compliance and strength of hot mix asphalt (HMA) using the indirect tensile test device AASHT322-07:, Washington D.C., 2011.

[8] A.A.A. Molenaar, A. Scarpas, X. Liu, S.M.J.G. Erkens, Semi-circular bending test; simple but useful, Asphalt Paving Technology: Association of Asphalt Paving Technologists. (2002). https://trid.trb.org/view.aspx?id=698764.

[9] L. Huang, K. Cao, M. Zeng, Evaluation of semicircular bending test for determining tensile strength and stiffness modulus of asphalt mixtures, Journal of Testing and Evaluation. 37 (2009) 122–128.

[10] R. Hofman, B. Oosterbaan, S.M.J.G. Erkens, J. Van der Kooij, Semi-circular bending test to assess the resistance against crack growth, 6th International Rilem Symposium. (2003) 257–263.

[11] R.C. West, A. Copeland, High RAP asphalt pavements: Japan practice-lessons learned, National Asphalt Pavement Association. 139 (2015) 62.

[12] R.C. West, C. Van Winkle, S. Maghsoodloo, S. Dixon, Relationships between simple asphalt mixture cracking tests using ndesign specimens and fatigue cracking at FHWA's accelerated loading facility, Road Materials and Pavement Design. 86 (2017) 579–602. doi:10.1080/14680629.2017.1389083.

[13] Y. Zhu, E. V. Dave, R. Rahbar-Rastegar, J.S. Daniel, A. Zofka, Comprehensive evaluation of low temperature fracture indices for asphalt mixtures, Asphalt Paving Technology: Association of Asphalt Paving Technologists-Proceedings of the Technical Sessions. 86 (2017) 629–658. doi:10.1080/14680629.20l7.1389085.

[14] I. Al-Qadi, H. Ozer, J. Lambros, A. El Khatib, D. Singhvi, Testing protocols to ensure performance of high asphalt binder replacement mixes using RAP and RAS, Urbana, IL: Illinois Center for Transportation, Illinois Dept. of Transportation. (2015).

[15] F. Zhou, S. Im, L. Sun, T. Scullion, Development of an IDEAL cracking test for asphalt mix design and QC/QA, Asphalt Paving Technology: Association of Asphalt Paving Technologists-Proceedings of the Technical Sessions. 86 (2017) 549–577.

[16] X. Chen, M. Solaimanian, Simple indexes to identify fatigue performance of asphalt concrete, Journal of Testing and Evaluation. 48 (2018) 20170722. doi:10.1520/JTE20170722.

[17] H. Ozer, I.L. Al-Qadi, J. Lambros, A. El-Khatib, P. Singhvi, B. Doll, Development of the fracture-based flexibility index for asphalt concrete cracking potential using modified semi-circle bending test parameters, Construction and Building Materials. 115 (2016) 390–401. doi:10.1016/j.conbuildmat.2016.03.144.

[18] A. Hanz, E. Dukatz, G. Reinke, Use of performance-based testing for high RAP mix design and production monitoring, Road Materials and Pavement Design. 0629 (2017). doi:10.1080/14680629.2016.1266766.

[19] F. Kaseer, F. Yin, E. Arámbula-Mercado, A.E. Martin, J.S. Daniel, S. Salari, Development of an index to evaluate the cracking potential of asphalt mixtures using the semi-circular bending test, Construction and Building Materials. 167 (2018) 286–298. doi:10.1016/j.conbuildmat.2018.02.014.

[20] S.S. Kim, J.J. Yang, R.A. Etheridge, Effects of mix design variables on flexibility index of asphalt concrete mixtures, International Journal of Pavement Engineering. 0 (2018) 1–6. doi:10.1080/10298436.2018.1538514.

[21] J. Rivera-Perez, H. Ozer, I.L. Al-Qadi, Impact of specimen configuration and characteristics on illinois flexibility index, Transportation Research Record. 2672 (2018) 383–393. doi:10.1177/0361198118792114.

[22] M. Barry, An analysis of impact factors on the Illinois Flexibility Index test, University of Illinois at Urbana-Champaign, 2016.

[23] J. Rivera-Perez, Effects of speciemn geometry and test configuration on the fracture process zone for asphalt materials, University of Illinois at Urbana-Champaign, 2017.

[24] W. Dong, S. Charmot, Proposed tests for cold recycling balanced mixture design with measured impact of varying emulsion and cement contents, Journal of Materials in Civil Engineering. 2 (2019) 1–8. doi:10.1061/(ASCE)MT.1943-5533.0002611.

[25] T. Bennert, E. Haas, E. Wass, Indirect Tensile Test (IDT) to determine asphalt mixture performance indicators during quality control testing in New Jersey, Transportation Research Record. 2672 (2018) 394–403. doi:10.1177/0361198118793276.

[26] F. Yin, J. Garita, A. Taylor, R. West, Refining the indirect tensile (IDT) Nflex Factor test to evaluate cracking resistance of asphalt mixtures for mix design and quality assurance, Construction and Building Materials. 172 (2018) 396–405. doi:10.1016/j.conbuildmat.2018.03.251.

[27] F. Bayomy, A. abdo Ahmad, M. Ann Mull, Evaluation of hot mix asphalt ( HMA ) fracture resistance using the critical strain energy release rate, 2006.

[28] M.A. Elseifi, L.N. Mohammad, H. Ying, S.C. Iii, Modeling and evaluation of the cracking resistance of asphalt mixtures using the semi-circular bending test at intermediate temperatures, X (2005) 1–23.

[29] W. Cao, L. Mohammad, M. Elseifi, S.B. Cooper, S. Saadeh, Fatigue performance prediction of asphalt pavement based on semicircular bending test at intermediate temperature, Journal of Materials in Civil Engineering. 30 (2018) 1–8. doi:10.1061/(ASCE)MT.1943-5533.0002448.

[30] L. Mohammad, M. Kim, M. Elseifi, Characterization of asphalt mixture's fracture resistance using the Semi-Circular Bending (SCB) test, 7th RILEM International Conference on Cracking in Pavements SE - 1. 4 (2012) 1–10. doi:10.1007/978-94-007-4566-7_1.

[31] Louisiana Department of Transportation and Development (LaDOT), Louisiana Standard Specification for Roads and Bridges, 2016.

[32] H. Alkuime, E. Kassem, F. Bayomy, Development of a new performance indicator to evaluate the resistance of asphalt mixes to intermediate temperature cracking., Journal of Transportation Engineering, Part B: Pavements. (2019).

[33] H. Alkuime, E. Kassem, F. Bayomy, Development of performance-engineered mix design (PEMD) specifications for intermediate temperature monotonic cracking assessment tests and performance indicators, Road Materials and Pavement Design. (2019).

[34] M. Zaumanis, L.D. Poulikakos, M.N. Partl, Performance-based design of asphalt mixtures and review of key parameters, Materials and Design. 141 (2018) 185–201. doi:10.1016/j.matdes.2017.12.035.

[35] R. AWu, J. Harvey, J. Buscheck, A. Mateos, Mechanistic-Empirical (ME) design: mix design guidance for use with asphalt concrete performance-related specifications, 2018.

[36] L. Barros, Influence of mix design parameters on performance of balanced asphalt concrete, University of Texas at El Paso, 2018.

[37] F. Bayomy, A.A. Abdo, Performance evaluation of Idaho HMA mixes using gyratory stability, University of Idaho , Idaho Transportation Department, Idaho. (2007).

[38] I. Al-Qadi, H. Ozer, J. Lambros, A. El Khatib, D. Singhvi, Testing Protocols to Ensure Performance of High Asphalt Binder Replacement Mixes Using RAP and RAS, 2020.

[39] N.J. Salkind, Encyclopedia of research design, 2010.

[40] H. Alkuime, E. Kassem, F.M. Bayomy, R. Nielsen, Development and evaluation of Multi-Stage Semi-circle bending Dynamic (MSSD) test to assess the cracking resistance of asphalt mixes., Construction and Building Materials. (2019).

# Chapter 4: Development and Evaluation of Multi-Stage Semi-Circle Bending Dynamic (MSSD) Test to Assess the Cracking Resistance of Asphalt Mixes

Hamza Alkuime[1]; Emad Kassem[1]; Fouad M.S. Bayomy[1] and Richard J. Nielsen[1]

(Submitted to Journal of Road Materials and Pavement Design)

## 4.1. Abstract

This study aimed to develop, evaluate, and validate a new cyclic cracking assessment test that has advantages over the available monotonic and dynamic cracking assessment tests. Also, it addresses the major concerns related to the implementation of the Balanced Mix Design (BMD) such as long specimen preparation and testing time and the validity of cracking performance assessment tests. The laboratory evaluation findings showed that the proposed test and derived performance indicators were sensitive to the composition of mixes, had variability lower than other dynamic tests and similar to the one obtained from the monotonic performance indicators. In addition, it correlated well with the observed field cracking performance of sixteen field projects. The derived indicators were able to distinguish between different field cracking performance groups and develop a pass/fail performance cracking assessment threshold.

Keywords: asphalt mix racking resistance; balanced mixed design; semi-circular bending; performance-engineered mix design, fatigue crack intermediate temperature cracking

## 4.2. Introduction

Fatigue cracking is one of the main distresses that requires attention in pavement design and evaluation along with other pavement distresses including rutting and moisture damage. A recent national survey showed that 40 state Departments of Transportations (DOTs) are

[1] Department of Civil and Environmental Engineering, University of Idaho, Moscow, ID 83844 USA.

planning to consider use of performance tests at the mix design level to assess the resistance of asphalt mixes to fatigue cracking and rutting as a part of a balanced mix design (BMD) approach [1]. Nowadays, more focus is placed on asphalt mix performance assessment tests. A new approach to design asphalt mixes called Performance-Engineered Mix Design (PEMD) or Balanced Mix Design (BMD) is being developed. This system is defined as "*Asphalt mix design using performance tests on appropriately conditioned specimens that address multiple modes of distress taking into consideration mix aging, traffic, climate and location within the pavement structure*" [2]. The BMD system depends on performance assessment tests to ensure that mixes will have sufficient resistance to specific distress during its service life. Therefore, the success of BMD depends on selecting the appropriate performance assessment tests.

This paper focuses on the Fatigue cracking performance assessment tests. Monotonic tests apply the load at a constant displacement rate, while dynamic tests apply a cyclic small repeated load. The monotonic tests require less testing time, simpler specimen geometry, inexpensive testing setup and is simple to perform compared to the dynamic tests. However, since fatigue cracking in asphalt mixes is initiated and propagated due to repeated traffic loading, dynamic tests better represent the fatigue damage under repeated traffic loads.

Several dynamic loading performance assessment tests have been proposed such as the four-point Bending Beam Fatigue (BBF), uniaxial fatigue test, trapezoidal test, overlay tester, and the dogbone tester [3]. In addition, some of these tests have been standardized such as AASHTO T 321 "*Standard Method of Test for Determining the Fatigue Life of Compacted Asphalt Mixtures Subjected to Repeated Flexural Bending*", AASHTO TP 107 "*Standard Method of Test for Determining the Damage Characteristic Curve and Failure Criterion Using the Asphalt Mixture Performance Tester (AMPT) Cyclic Fatigue Test* ". Also, several theories were proposed to develop performance indicators using test results such as continuum damage method, energy and energy-inspired methods, and general fatigue approach, and fracture methods) [3].

State DOTs show a national interest in implementing the BMD or performance assessment tests. In the same national survey, 29 state DOTs are interested in implementing the BMD, while six state DOTs are currently implementing it [1]. In case of fatigue cracking performance assessment tests, 40 state DOTs are interested in implementing the fatigue cracking assessment tests [1]. The survey showed that the state DOTs and contractors have several concerns about implementing the BMD method and the major concerns are related to the performance assessment tests. The state DOTs and contractors are concerned about the validity of the current performance tests including 1) correlation with the observed field performance 2) the developing of pass/fail performance thresholds, and 3) the variability of the results. In addition, the second major concern was about the long testing time and the specimen preparation time.

The current fatigue intermediate temperature cracking (monotonic and dynamic) performance assessment tests have either of the two concerns. It was reported that some monotonic performance indicators to provide illogical trends with the change in air void content or specimen thickness, where higher air void content or specimen thickness results in improved cracking resistance which is misleading [4–7]. Therefore, this limitation is expected to affect the laboratory results of the extracted field cores since it has different air void content and thickness. Also, in a previous study by the authors, ten performance indicators (e.g., total fracture energy [$G_{fracture}$], indirect tensile modulus [$IDT_{Modulus}$], indirect tensile asphalt cracking test IDEAL-$CT_{Index}$ ], cracking resistance index [CRI], flexibility index [FI], Nflex factor [Nflex], critical strain energy release rate [$J_C$], and Weibull cracking resistance index [$Weibull_{CRI}$ ]) obtained from four standardized monotonic testing standards (i.e., AASHTO TP 124, ASTM D6931, ASTM D8044, and ASTM D8225) did not correlate well with the observed field cracking performance of seventeen field projects [8]. The study showed that the monotonic tests provided an illogical trend with the variation in specimen air void content and thickness, which affected the laboratory evaluation results. Therefore, it was not possible to develop a performance threshold for these indicators based on a direct correlation with the observed field performance. On the other hand, dynamic performance assessment tests have several limitations such as requiring a long testing time or having an

unknown testing completion time. In addition, complex specimen shapes (e.g., beam, trapezoidal, cylinder) complicate or prevent the ability to evaluate the extracted field cores in the laboratory. Thus, the correlation between the laboratory evaluation results and the field core cannot be studied. Therefore, there is a need to develop a new fatigue cracking assessment test to overcome these limitations.

### 4.3. Study Objectives

The main objective of this study was to develop and evaluate a new intermediate temperature cracking assessment test that have advantages over the current monotonic and dynamic cracking assessment tests and address the major concerns of state DOTs and contractors to ensure successful implementation of BMD. To achieve the objective of this study, the developed test and its performance indicators are sought to:

- utilize cyclic dynamic loads to better simulate the fatigue cracking in the field,
- complete within a reasonable time (i.e., maximum 9 hours),
- use simple testing equipment similar to that used in the monotonic tests,
- require simple specimen geometry,
- can be conducted on extracted cores from field projects, and
- use simple and efficient performance indicators to interpret the change in cracking resistance.

It is also sought to develop test performance indicators that shall:

- be sensitive to the composition of different asphalt mixes,
- have low variability,

- correlate well with the observed field performance of field projects (i.e., distinguish between the good and poor field performance), and
- have the ability to develop pass/fail performance assessment thresholds for BMD implementation.

This study developed a new test called Multi-Stage Semi-circle bending Dynamic (MSSD) test to evaluate asphalt mixes resistance to intermediate temperature cracking. The MSSD test simulates the cyclic loading (dynamic) in reasonable testing time, has a fixed loading sequence that works for mixes with different characteristics (e.g., mix composition, percent air void content, thickness, etc.) and utilizes the same testing equipment and specimen geometry used in monotonic tests. Table 4.1 summarizes the advantages of the MSSD test compared to monotonic tests and other dynamic tests (i.e., BBF). The MSSD and BBF apply cyclic loading, while monotonic tests apply constant loading. The dynamic tests simulate the fatigue cracking development and propagation while monotonic tests use performance indicators to describe mix cracking performance. Monotonic tests require a short testing time (< 30 minutes), while BBF testing times varies from a few hours to several days [9]. The MSSD requires shorter testing times (maximum of 9 hours) regardless of mix characteristics. In addition, the MSSD uses a Semi-Circle (SC) test specimen which is easy to prepare in the laboratory as compared to the beams used in the BBF test.

## 4.4. MSSD Development

### *4.4.1. Test Conditions*

The MSSD test uses a SC test specimen with a radius of 75 mm and a notch depth of 15 ±1 mm. The thickness of the laboratory prepared specimens is 50 mm, while the thickness of the extracted field cores can vary between 25 mm to 50 mm depending on the lift thickness. Figure 4.1 shows a schematic of the test setup. The support span of the test fixture is 120 mm. The test is performed at 25°C and can be conducted using the Asphalt Mixture Performance Test (AMPT) machine or other servohydraulic testing system (e.g., Universal

Testing Machine [UTM], or Material Testing System [MTS]). In this study, an AMPT was used (Figure 4.2). The AMPT is available in typical materials and pavement laboratory and is simple to operate and use compared to other systems, and cheaper than the advanced systems such as MTS.

**Table 4.1.** Comparison between monotonic, bending beam fatigue, and MSSD tests.

| Criteria | Monotonic tests (e.g., SCB, IDT) | MSSD | Bending Beam Fatigue |
|---|---|---|---|
| Loading | Constant displacement rate | Repeated load | Repeated load |
| Testing time | 1-2 hour | < 9 hours | 30 minutes-several days |
| Specimen preparation | Easy | Easy | Difficult |
| Specimen geometry | Semi-circular and circular | Semi-circular | Beam |
| Evaluation of field cores | Yes | Yes | No |
| Testing system complexity | Simple | Simple | Complex |
| Equipment cost | Low (< $20,000) | Intermediate (< $80,000) | High (> $200,000) |

*4.4.2. Theory and Concept*

For a notched test specimen (e.g., Semi-Circular [SC]), the magnitude of stress at the notch tip is a function of specimen geometry and applied loading [10]. In Linear Elastic Fracture Mechanics (LEFM), the Stress Intensity Factor (SIF or K) describes the stress state at the notch tip after accounting for the effect of loading and geometry [10]. The SIF increases with an increase in the applied load until reaching a critical value (defined as fracture toughness [$K_{IC}$]), which is associated with crack initiation [11]. The fracture toughness is computed at the critical load which is assumed to be the peak load [11]. The MSSD applies a series of compressive loads to a SC test specimen with one notch (i.e., 15 mm notch depth) that produces a predetermined SIF. Figure 4.3 shows a flow chart that was developed in this study to select the applied loads at various loading stages. The researchers used the monotonic test data of 106 SC specimens that were tested in accordance with AASHTO TP124 to select the

appropriate loading level for MSSD dynamic tests. The test specimens were obtained from 17 different field projects, 10 Plant Mixed-Laboratory Compacted (PMLC) mixes and six Laboratory Prepared-Laboratory Compacted (LMLC) mixes. More details about the properties of the evaluated mixes and laboratory evaluation results were provided in previous studies by the authors [8,12,13]. The same PMLC mixes and field projects were evaluated in this study using the MSSD test. More discussion on mix properties is provided in the next sections.

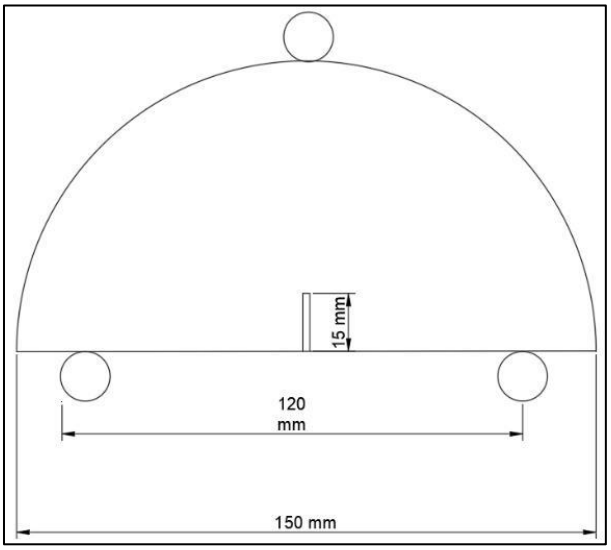


**Figure 4.1**. Schematic MSSD test specimen and fixture

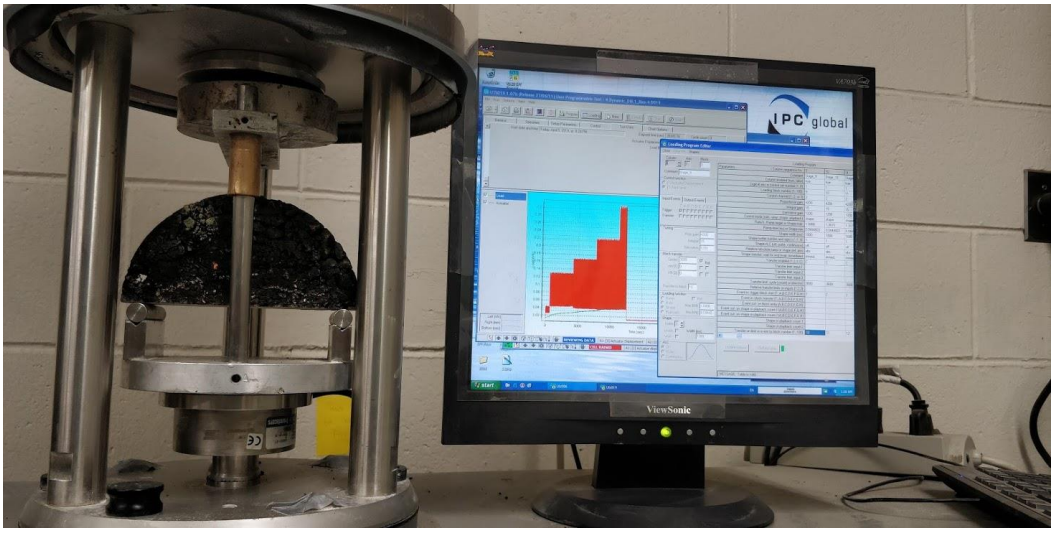


**Figure 4.2.** MSSD test fixture inside the AMPT chamber

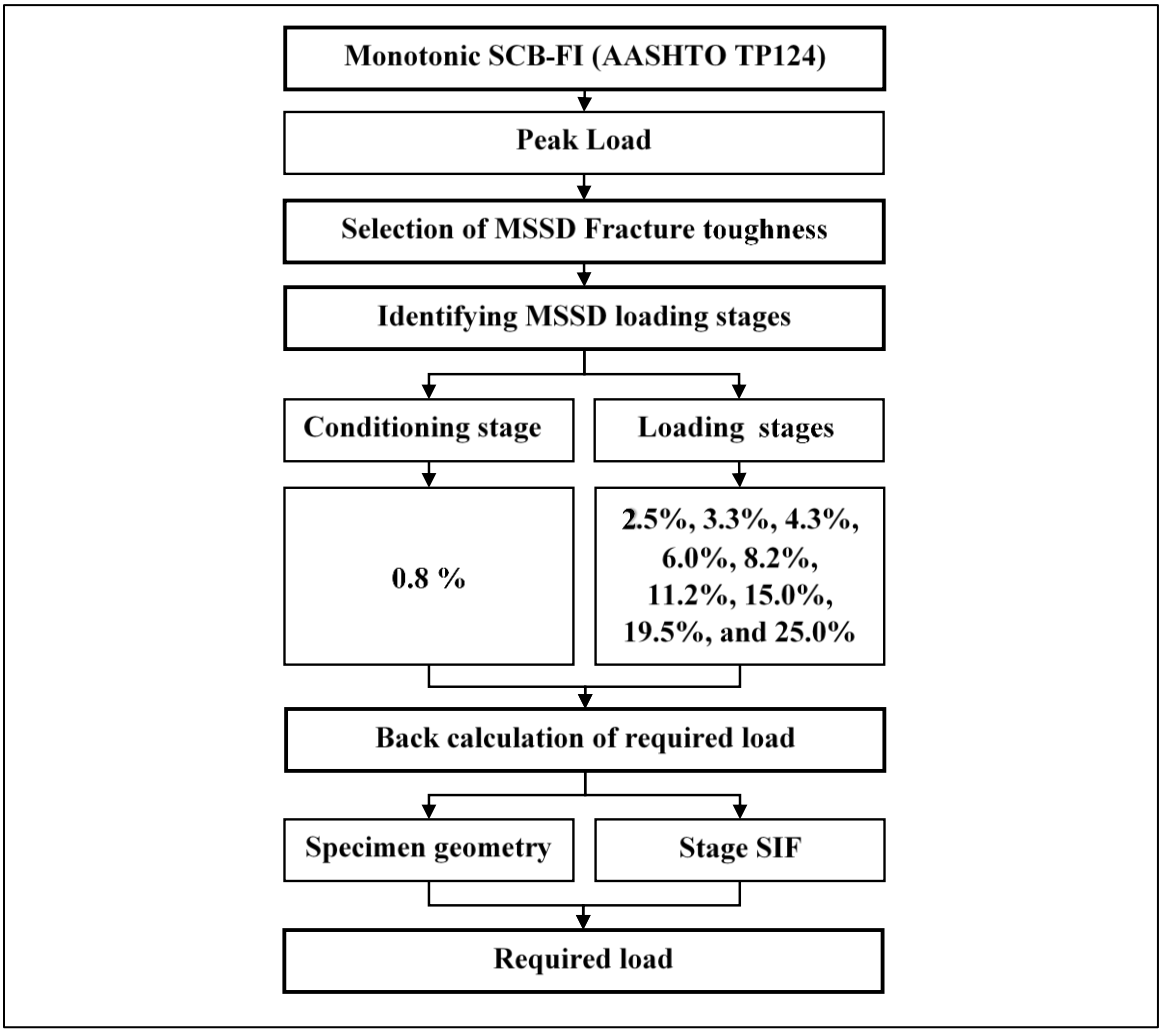


**Figure 4.3.** Flow chart for MSSD testing stage identification procedures

The fracture toughness of each test specimen was computed using a model developed by Lim et al. (1993) as presented in Equation 4.1 [14]. This model is used in AASHTO TP105 and several research studies to estimate the fracture toughness of asphalt mixes [11,15–19].

$$\frac{\mathrm{K\,I}}{(\sigma\sqrt{\pi a})} = Y_{1_{(\frac{S_0}{r})}} + \frac{\Delta S_0}{r}\mathrm{B} \qquad \text{for } 0.5 \leq \frac{S_a}{r} \geq 0.8 \qquad 4.1$$

$$Y_{1_{(\frac{S_0}{r})}} = C_1\text{-}C_2\left(\frac{a}{r}\right) + C_3 exp\left(C_4\left(\frac{a}{r}\right)\right), \qquad 4.2$$

$$\frac{\Delta S_0}{r} = \frac{S_a - S_0}{r} \quad 4.3$$

$$\sigma = \frac{P}{D \times t}; \quad 4.4$$

$$B = 6.55676 + 16.64035\left(\frac{a}{r}\right)^{2.5} + 27.97042\left(\frac{a}{r}\right)^{6.5} + 215.0839\left(\frac{a}{r}\right)^{16} \quad (\text{for } 0.03 \leq \frac{a}{r} \geq 0.8) \quad 4.5$$

where $K_I$ is the stress intensity factor for mode I loading (N/mm $^{3/2}$), $\frac{S_a}{r}$ is the ratio of support span ($S_a$) to specimen radius (r), $\frac{S_0}{r}$ is the ratio of support span ($S_0$ ) to specimen radius (r) used by Lim et al (1993) study (including: 0.5, 0.61, 0.67, and 0.8), $\frac{\Delta S_0}{r}$ is the ratio between $\frac{S_a}{r}$ and $\frac{S_0}{r}$ , σ is the tensile stress, P is the load (kN), t is the specimen thickness (mm), D is the specimen diameter (mm), $Y_{1_{(\frac{S_0}{r})}}$ is the normalized SIF at predetermined ($S_0$/r) ratio, $C_1$, $C_2$, $C_3$, $C_4$ are regression constants, and a is the specimen notch depth (mm).

Figure 4.4 shows the computed fracture toughness ($K_{IC}$) for the test specimens from the monotonic loading test (AASHTO TP124). Field projects had an average $K_{IC}$ of 21.49 N/mm$^{3/2}$ and ranged between 8.72 N/mm$^{3/2}$ and 37.91 N/mm$^{3/2}$. PMLC mixes had an average $K_{IC}$ of 19.62 N/mm$^{3/2}$ and ranged between 9.75 N/mm$^{3/2}$ and 34.68 N/mm$^{3/2}$. LMLC mixes had an average $K_{IC}$ of 10.61 N/mm$^{3/2}$ and ranged between 5.01 N/mm$^{3/2}$ and 23.80 N/mm$^{3/2}$. The field projects had the highest $K_{IC}$ when compared to PMLC or LMLC mixes. The researchers believe that this is attributed to the aging effect since field cores mixes are often stiffer compared to PMLC or LMLC mixes. All mixes had $K_{IC}$ between 5.01 N/mm$^{3/2}$ and 37.91 N/mm$^{3/2}$ as shown in Figure 4.4. An appropriate $K_{IC}$ for the dynamic test should be selected to avoid premature failure or extended testing time. The research team selected a fracture toughness of 24 N/mm$^{3/2}$ for this purpose after several testing trials.

The MSSD applies a series of compressive loads that produce a predetermined series of SIFs in the SC test specimen. The research team selected ten predetermined SIFs associated with ten loading stages, including one conditioning stage (Stage-0) and nine loading stages (Stage-1 to Stage-9). Each loading stage applies a continuous haversine loading wave with a frequency of 1Hz (Figure 4.5). Each wave resulted in a change in SIF (ΔK) of $K_{max}$-$K_{min}$ where $K_{max}$ is the SIF associated with maximum applied load and $K_{min}$ is the stress intensity factor associated with the setting load (Figure 4.5). In the MSSD test, the $K_{min}$ and $K_{max}$ were predetermined for each loading stage. $K_{min}$ of 0.12 N/mm$^{3/2}$ was selected for the conditioning stage and 0.20 N/mm$^{3/2}$ for all remaining testing stages (i.e., Stage-1 to Stage-9). $K_{max}$ was determined as a percent of the MSSD fracture toughness value (i.e., 24 N/mm$^{3/2}$). Figure 4.6 shows the selected percent for each loading stage. Figure 4.7 shows $K_{min}$, $K_{max}$, and ΔK for each loading stage of the nine stages of the test. These stress intensity values in addition to specimen geometry were used to calculate the required compressive applied loads using Equation 4.9 (Figure 4.3).

$$K_{IC} = \left(Y_{1_{(0.8)}}\right) \times \left(\sigma_{max}\sqrt{\pi a}\right) \; ; \qquad 4.6$$

$$Y_{1_{(0.8)}} = 4.782\text{-}1.219\left(\frac{a}{r}\right) + 0.063exp\left(7.045\left(\frac{a}{r}\right)\right) \qquad 4.7$$

$$\sigma_{max} = \frac{P_{max}}{D \times t} \qquad 4.8$$

$$P_{stage-i} = \left[\frac{24 \times (\%K_{IC\,stage-i})}{\left(Y_{1_{(0.8)}}\right) \times \left(\sqrt{\pi a}\right)}\right] \times (D \times t) \qquad 4.9$$

where $K_{IC}$ is the fracture toughness ( N/mm$^{3/2}$ ), $P_{stage-i}$ is the required load for stage-i, $\%K_{ICU}$ is the percentage of fracture toughness for stage-i (N/mm$^{3/2}$), $\sigma_{max}$ is the maximum tensile stress (N/mm$^2$), $P_{max}$ is the maximum load (N), t is the specimen thickness (mm), D is the specimen diameter (mm).

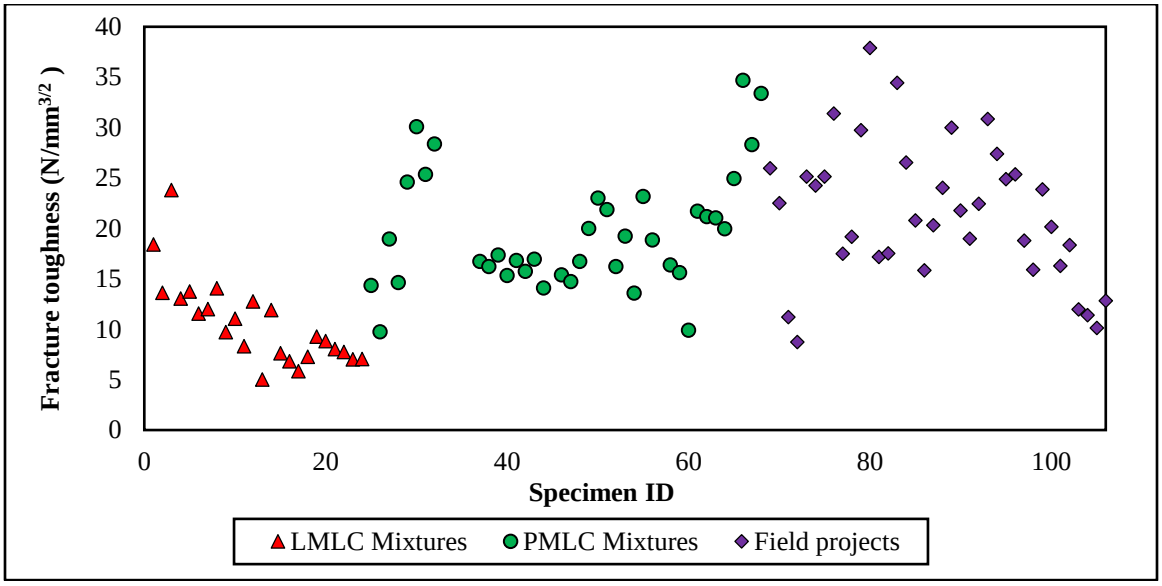


**Figure 4.4.** Computed fracture toughness for monotonic SCB specimens

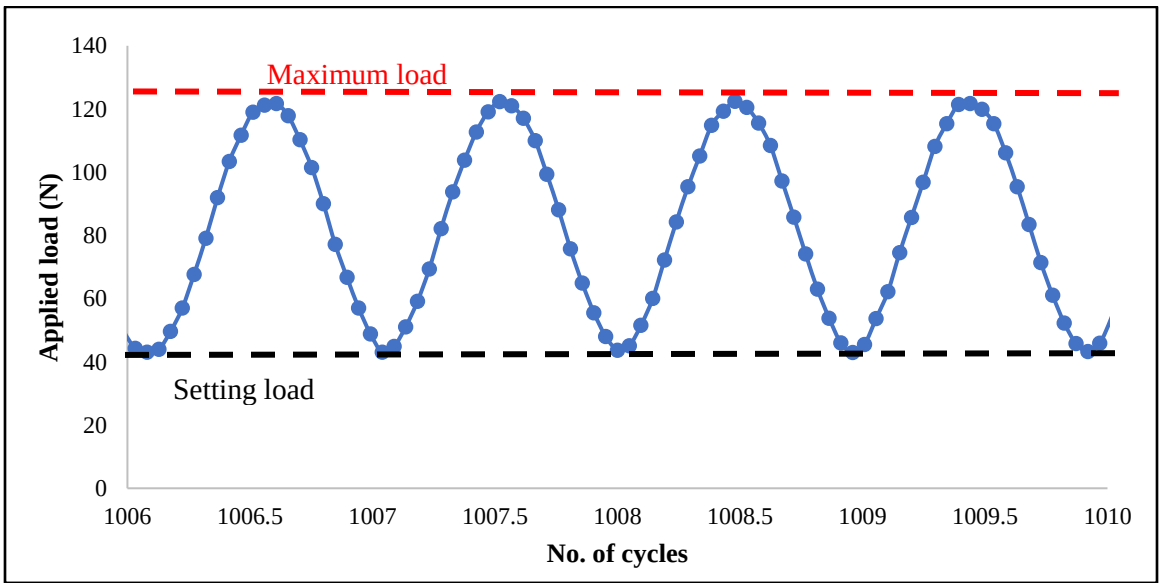


**Figure 4.5.** MSSD continuous haversine loading wave

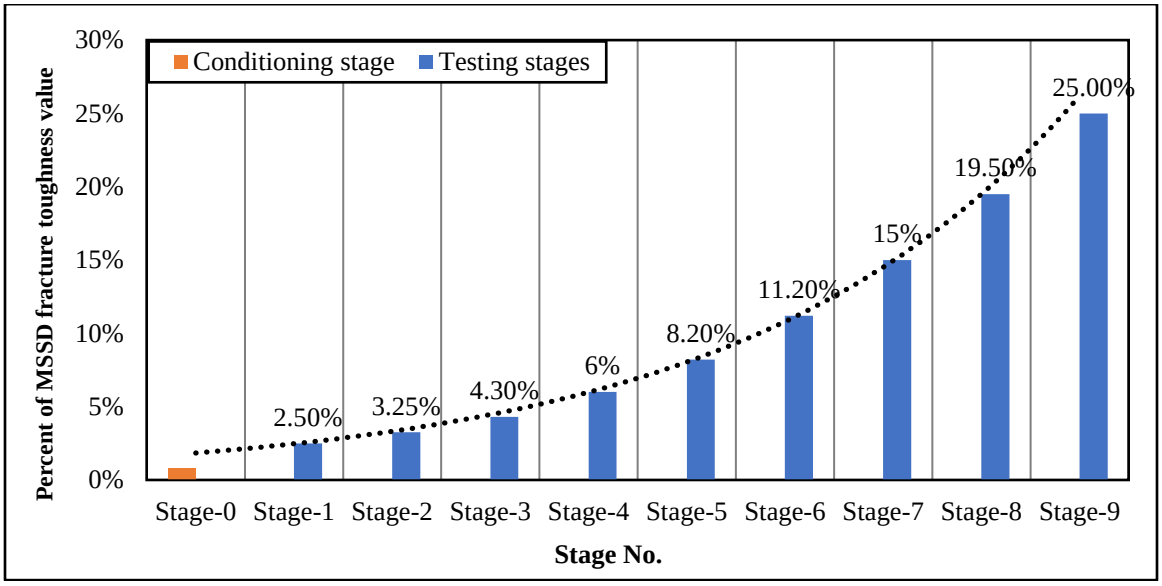


**Figure 4.6.** Selected Kmax value for each loading stage

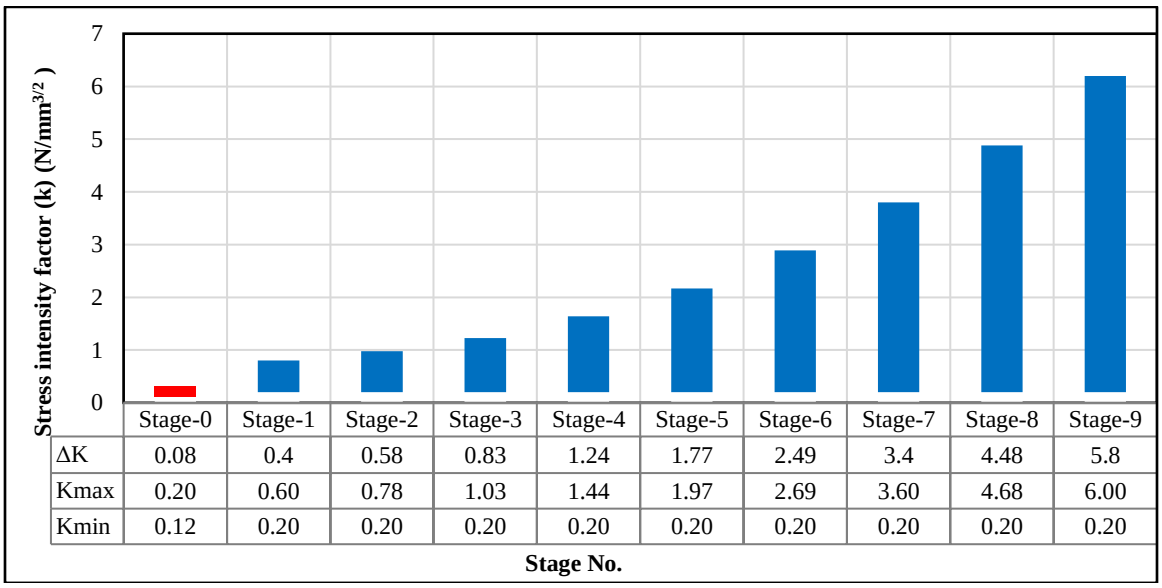


| | Stage-0 | Stage-1 | Stage-2 | Stage-3 | Stage-4 | Stage-5 | Stage-6 | Stage-7 | Stage-8 | Stage-9 |
|---|---|---|---|---|---|---|---|---|---|---|
| ΔK | 0.08 | 0.4 | 0.58 | 0.83 | 1.24 | 1.77 | 2.49 | 3.4 | 4.48 | 5.8 |
| Kmax | 0.20 | 0.60 | 0.78 | 1.03 | 1.44 | 1.97 | 2.69 | 3.60 | 4.68 | 6.00 |
| Kmin | 0.12 | 0.20 | 0.20 | 0.20 | 0.20 | 0.20 | 0.20 | 0.20 | 0.20 | 0.20 |

**Figure 4.7.** ΔK, Kmax, and Kmin for each loading stage

*4.4.3. MSSD Test Outputs and Performance Indicators*

Figure 4.8 shows the collected data in the MSSD test, including the applied load, the actuator vertical displacement, and the number of loading cycles. The data are recorded at a rate of 20 Hz during the test. A total number of 600 cycles are applied in the conditioning stage (i.e., Stage-0). The maximum SIF ($K_{max}$) increases after the completion of each loading stage

(Figure 4.8), while the same minimum SIF ($K_{min}$) is maintained (0.20 N/mm$^{3/2}$) for all the stages (i.e., Stage-0 to Stage-9) as shown Figure 4.6. The rate of change in the vertical displacement with the loading cycles followed the S-shape curve as shown in Figure 4.9. The S-shape curve is divided into three phases: I, II, and III. Phase I showed a high rate of vertical displacement per cycle. It is usually completed within the first testing stage (Stage-1). Upon its completion, the displacement rate is decreased, which identifies the start of phase II. In this phase, the displacement rate started at a slower rate compared to phase I but increased after the completion of each loading stage. The displacement rate increment follows an exponential trend line similar to the trend exponential trend line of the applied load (Figure 4.6). Phase III shows a significant rapid increase in the displacement rate until the specimen fails (straight vertical line).

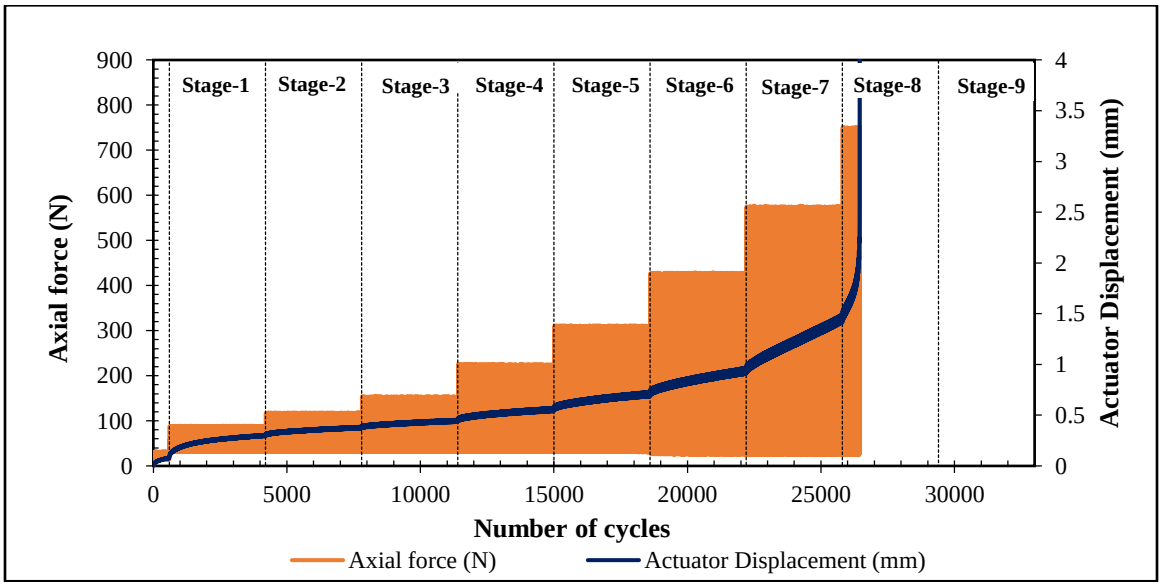


**Figure 4.8.** MSSD test typical output

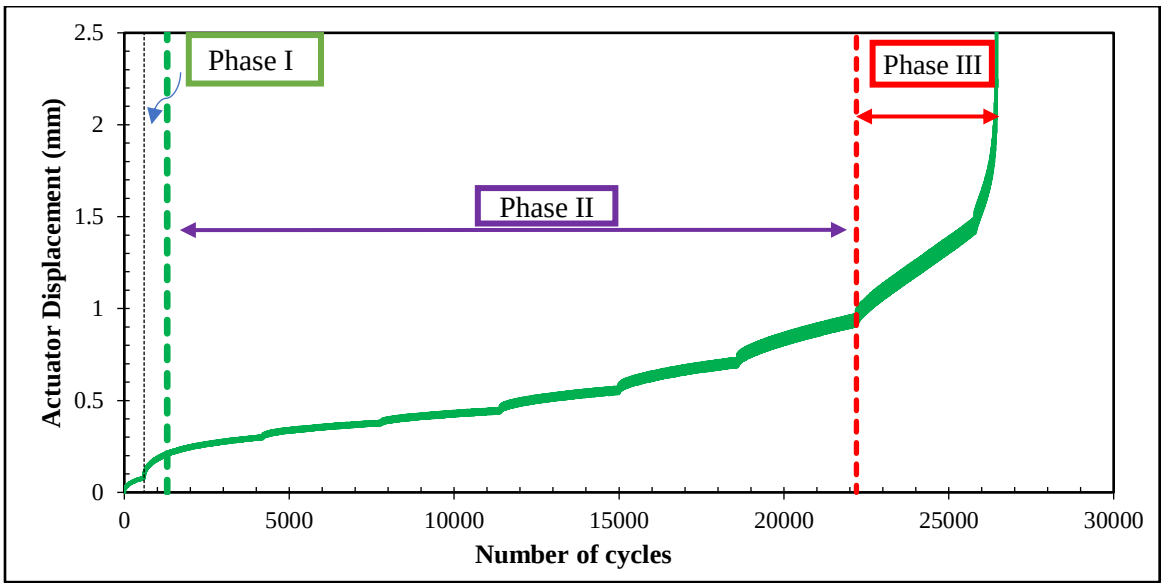


**Figure 4.9.** Typical vertical displacement S-shaped curve and Inflection points

The derivation of the MSSD performance indicators was inspired by the well-known Paris' law parameters. Paris' law describes the relation between crack growth rate and change in SIF (ΔK) (Equation 4.10) [20]. Measuring the crack length is not a simple task. It requires complex and costly equipment (e.g., Digital Image Correlation) and difficult analyses (e.g., image processing), which reduce the practicality of the test for use by state DOTs or contractors on a daily basis for implementing the BMD. Therefore, to simplify the MSSD test, the vertical actuator displacement was used as an alternative to the true crack length. An analogous formula to Paris' law was used to describe the relationship between the rate of change of the vertical actuator displacement and the change in SIF (ΔK) as presented in Equation 4.11. It should be noted that Equation 4.11 does not represent Paris' Law. The MSSD performance indicators (H and z) can be determined by performing the following steps:

(1) plot the vertical actuator displacement ($v$) versus the number of loading cycles ($N$) (Figure 4.10),

(2) fit the curve from Step No. 1 with a 6th-degree polynomial function (Figure 4.10)

(3) determine the rate of change in vertical actuator displacement with the number of cycles ($\frac{dv}{dN}$) at the end of each testing stage and the failure cycle,

(4) determine the change in SIF (ΔK) for each testing stage (Figure 4.10),

(5) plot ΔK versus the associated $\frac{dv}{dN}$ on a log-log scale (Figure 4.11), and

(6) determine the MSSD performance indicators (H and z) by fitting the data using a power function.

$$\frac{da}{dN} = A\,(\Delta K)^n \qquad 4.10$$

$$\frac{dv}{dN} = H\,(\Delta K)^z \qquad 4.11$$

where *a* is the crack length (mm), v is the vertical actuator displacement (mm), N is the number of load cycles (Cycle), *da*/*dN* is the crack growth rate (mm/cycle), *dv*/*dN* is the rate of vertical actuator displacement to the number of cycles, ΔK is the mode I SIF range ($K_{max}$ - $K_{min}$), *A* and *n* are the fitting constants for Paris' law, and *H* and *z* are the fitting constants for the MSSD model.

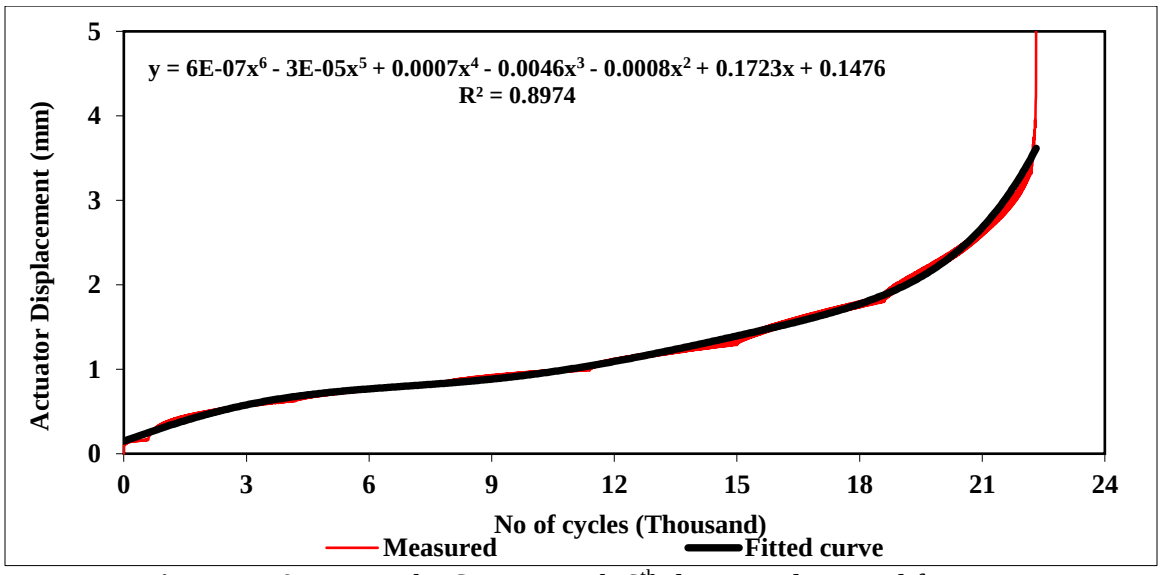


**Figure 4.10.** Fitting the S-curve with 6th-degree polynomial function

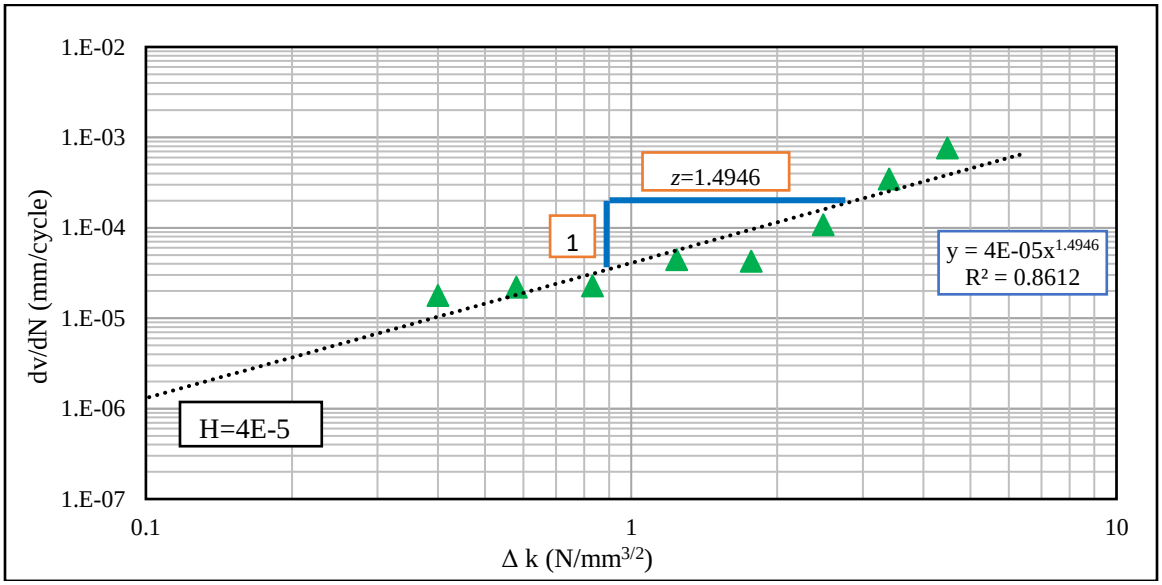


**Figure 4.11.** Determination of MSSD performance indicators

Equation 4.10 can be rearranged and presented in Equation 4.12. The value of log *H* represents the intercept, while the *z* value represents the slope. The intercept (log *H*) reflects the initial rate of displacement per cycle, while the slope (z) reflects the increment in the displacement rate with the change in SIF. The higher slope indicates a faster rate of damage. A higher slope is associated with a lower absolute intercept (Abs [log *H*]). Therefore, mixes with a lower slope (z) and higher Abs (log *H)* would exhibit higher resistance to cracking.

Previous research reported a good correlation between the Paris' law parameters (*A* and *n*) as shown in Equation 4.13 [21,22]. A similar relationship between MSSD performance indicators (*H* and *z*,) presented in Equation 4.14 is validated in the next section.

$$log(\frac{dv}{dN}) = log\ H + z\ log\ \Delta K \quad (4.12)$$

$$n = C_1\ Log\ A + C_2 \quad (4.13)$$

$$z = C_3\ Log\ H + C_4 \quad (4.14)$$

where, $C_1$ , $C_2$, $C_3$, and $C_4$ are linear regression fitting constants.

### 4.5. Experimental Evaluation

The research team designed and conducted an experimental testing program to evaluate the MSSD performance indicators (i.e., *z* and Abs [log *H*]) from different aspects as shown in Figure 4.12. The laboratory evaluation results of PMLC mixes were used to evaluate the sensitivity of MSSD performance indicators to the composition of PMLC mixes. The laboratory evaluation results of the extracted field cores were used to study the correlation between the laboratory results and the observed field cracking resistance and to develop performance threshold to assess asphalt mix resistance to cracking. The developed performance thresholds were used to evaluate the estimated resistance to cracking of PMLC mixes. In addition, the PMLC and field cores results were used to propose and validate a simpler approach to develop initial performance thresholds. Also, the laboratory evaluation results of both field projects and PMLC mixes were used to study the variability and the correlation of MSSD performance indicators. A total of 26 asphalt mixes that include 10 PMLC mixes and 16 field projects were evaluated in this study. The following sections provide information about the testing mixes.

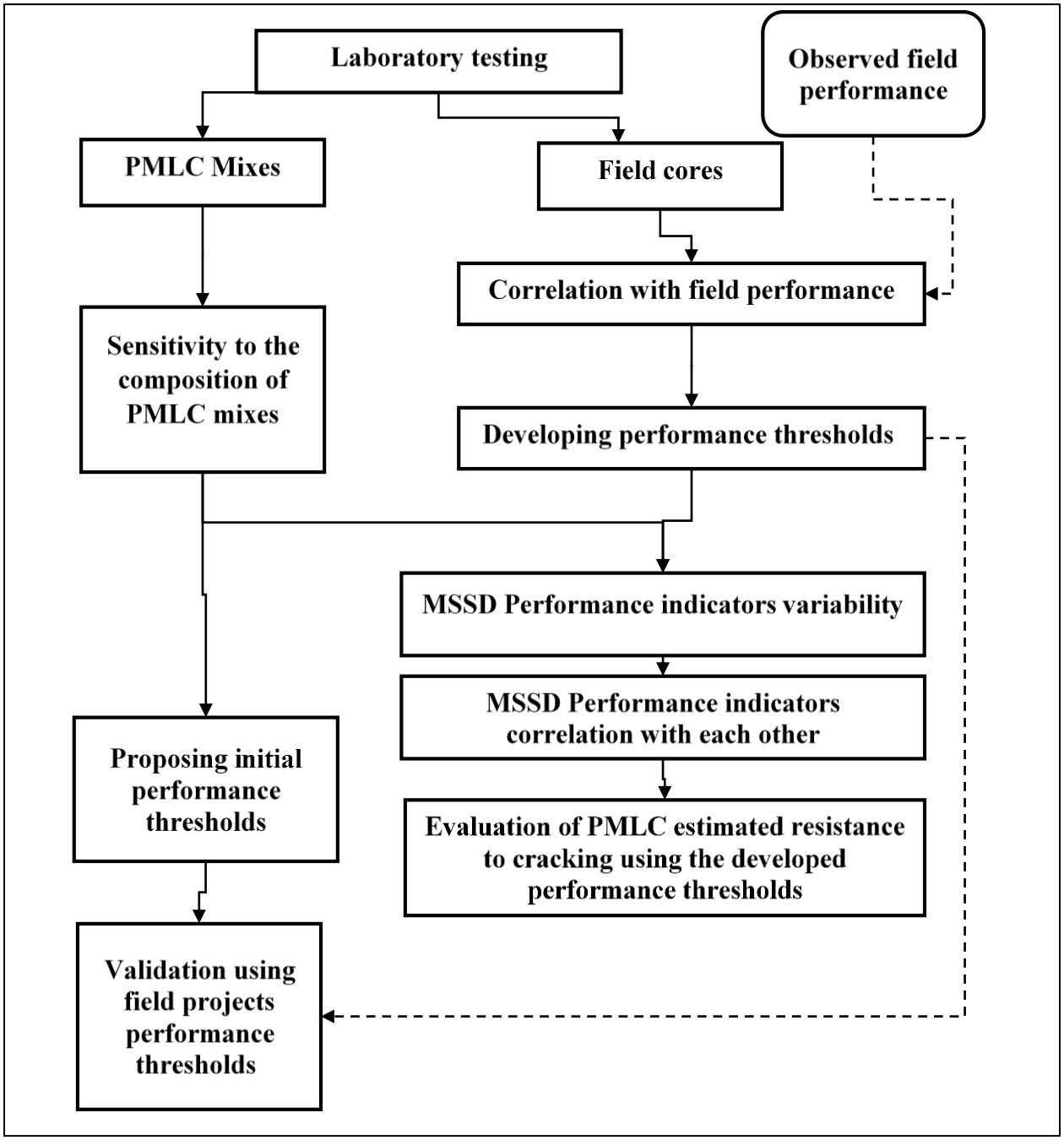


**Figure 4.12.** Study experimental plan

### *4.5.1. Asphalt Mixes Properties*

#### *4.5.1.1. PMLC Mixes*

In this study, 10 PMLC mixes were collected from new field projects in Idaho. Table 4.2 provides information about these field projects (e.g., project ID, date of construction, location, etc.). Table 4.3 summarizes various properties (e.g., mix type, specified binder PG, virgin binder PG, and binder content [Pb] percent) of the PMLC mixes. Further information about PMLC mixes is provided by Alkuime et al. (2019) [13]. The laboratory testing results of the PMLC mixes were used to evaluate the sensitivity of the MSSD performance indicators (i.e., *z* and Abs [log *H*]) to the composition of PMLC mixes, indicators variability, and to evaluate a simpler approach method to propose initial performance thresholds.

**Table 4.2.** PMLC project information

| # | District | Project ID | Construction year | Project Key No. (KN) | Location |
|---|---|---|---|---|---|
| 1 | 1 | D1L1 | 2017 | 19002 | I-90, Northwest Blvd to Sherman Ave. CDA & US-95, Cocolalla CR Br, Bonner CO |
| 2 | 2 | D2L1 | 2017 | 19187 | US-12. Arrow Br to Big canyon creek Br |
| 3 | | D2L2 | 2018 | 19640 | TOP of Bear CR. TO Pine CR, Latah CO |
| 4 | 3 | D3L1 | 2017 | 13463 | SH-44./JCT I84 to star |
| 5 | | D3L2 | 2017 | 19412 | US20. Borchers Ln to locust grove |
| 6 | | D3L3 | 2017 | 13924 | SH-67. MP0 TO JCT 51,EKLMORE CO |
| 7 | | D3L4 | 2017 | 13935 | FY16 Capital maintenance ACHD |
| 8 | | D3L5 | 2017 | 18723 | I-84, Cleft to MP90, Elmore co |
| 9 | 5 | D5L1 | 2017 | 13103 | I-15. Sands RD upass to IC #89, Bingham co |
| 10 | 6 | D6L1 | 2017 | 19543 | Spalding br. To US 12/SH-3 |

**Table 4.3.** Properties of received PMLC materials [13]

| # | District | Project ID | Mix Type | Specified binder PG | Virgin binder PG | Pb% | Recycle Binder Replacement (RBR%) | NMAS |
|---|---|---|---|---|---|---|---|---|
| 1 | 1 | D1L1 | SP5 | 64-28 | 58-34 | 5.30% | 30% | 12.5 |
| 2 | 2 | D2L1 | SP3 | 70-28 | 64-34 | 5.70% | 50% | 12.5 |
| 3 | | D2L2 | SP3 | 64-28 | 58-34 | 5.70% | 30% | 12.5 |
| 4 | 3 | D3L1 | SP3 | 70-28 | 52-34 | 5.20% | 50% | 12.5 |
| 5 | | D3L2 | SP3 | 70-28 | 64-34 | 5.20% | 30% | 12.5 |
| 6 | | D3L3 | SP3 | 64-28 | 58-34 | 5.30% | 30% | 12.5 |
| 7 | | D3L4 | SP3 | 70-28 | 64-34 | 5.30% | 30% | 12.5 |
| 8 | | D3L5 | SP5 | 76-28 | 70-34 | 5.30% | 30% | 12.5 |
| 9 | 5 | D5L1 | SP5 | 70-28 | 70-28 | 4.80% | 30% | 19.0 |
| 10 | 6 | D6L1 | SP5 | 64-34 | 64-34 | 5.40% | 0% | 12.5 |

#### *4.5.1.2. Field Projects*

The research team obtained field cores from various test sections across Idaho. The cores were extracted from sites identified by Idaho Transportation Department (ITD) material engineers. The researchers prepared a survey that was sent to the material engineers. The material engineers identified field test sections (projects) with different cracking performance (e.g., good, fair, and poor). In addition, they provided information about the mix design, binder PG, and the age of the identified sections. A total number of 16 test sections were identified and field cores were obtained from these sections. In addition, ITD engineers provided the relevant information including section location (route name, beginning Mile Post [MP] and end MP), construction year, and mix JMFs (if available). Table 4.4 presents the location of the test sections, while Table 4.5 summarizes the properties of asphalt mixes for each section.

### *4.5.2. Test Specimen Preparation*

PMLC specimens have a 50 mm thickness, 150 mm diameter, and 15 mm notch depth. The PMLC mixes were collected from new field projects constructed in 2017 and 2018. These

test specimens were compacted using a Superpave gyratory compactor to achieve a target air void content of 7 ± 0.5% as per AASHTO T 312 [23]. The field cores were extracted from the test sections using a 150-mm coring bit. The cores were extracted from the shoulder of test sections or between the wheel path in cases where the road had no shoulder. Upon extraction of the field cores by ITD crews, the cores were labeled and shipped to the laboratory. It should be noted that any surface treatment (e.g., seal coat) was trimmed and excluded. The researchers measured the bulk specific gravity ($G_{mb}$) in accordance with ASTM 2726 [24] for the test specimens after cutting to the required thickness. The theoretical maximum specific gravity ($G_{mm}$) was obtained from the provided mix Job Mix Formula (JMF) for different projects. In cases where the JMF was not available, the researchers measured the $G_{mm}$ according to ASTM D 6857 [25].

**Table 4.4** .Location of selected field projects

| # | District | Project ID | Route | Beginning MP | End MP | Construction Year |
|---|---|---|---|---|---|---|
| 1 | D2 | D2C4 | US95 | 366.6 | 373.2 | 2007 |
| 2 | | D2C5 | US95 | 242 | 251.1 | 2010 |
| 3 | | D2C6 | US95 | 222.4 | 223.3 | 2007 |
| 4 | | D2C7 | SH6 | 100 | 104 | 2007 |
| 5 | | D2C8 | US-95 | 233.5 | 239 | 2006 |
| 6 | | D2C9 | SH162 | 8 | 13 | 2007 |
| 7 | | D2C10 | SH13 | 11.2 | 25.4 | 2007 |
| 8 | | D2C11 | US12 | 90.7 | 111.4 | 2009 |
| 9 | | D2C12 | US95 | 267.6 | 271.5 | 2007 |
| 10 | | D2C13 | SH6 | 7.3 | 13.52 | 2010 |
| 11 | D3 | D3C3 | SH55 | 44.7 | 51.7 | 2009 |
| 12 | | D3C4 | SH44 | 19.4 | 21.8 | 2009 |
| 13 | | D3C5 | SH44 | 14.3 | 16.2 | 2013 |
| 14 | D5 | D5C2 | US30 | 405.5 | 413.1 | 2016 |
| 15 | D6 | D6C1 | US-26 | 338.5 | 342 | 2010 |
| 16 | | D6C2 | US-20/26/93 | 225 | 227 | 2006 |

**Table 4.5.** Mix properties of selected field projects

| # | *Project ID | Mix type | NMAS | OBC % | RBR% | Design PG |
|---|---|---|---|---|---|---|
| 1 | D2C4 | Hveem | 19 | ** | ** | 58-28 |
| 2 | D2C5 | SP4 | 19 | 5.29% | 17.00% | 64-28 |
| 3 | D2C6 | SP3 | ** | ** | ** | 70-22 |
| 4 | D2C7 | SP2 | ** | ** | ** | 58-28 |
| 5 | D2C8 | SP3 | 19 | 5.00% | 0.00% | 70-28 |
| 6 | D2C9 | SP3 | 12.5 | ** | ** | 58-28 |
| 7 | D2C10 | SP3 | 12.5 | 5.27% | 0.00% | 64-28 |
| 8 | D2C11 | SP3 | 12.5 | ** | ** | 58-28 |
| 9 | D2C12 | SP3 | 12.5 | 5.53% | 0.00% | 64-28 |
| 10 | D2C13 | SP3 | 12.5 | 6.35% | 17.00% | 58-28 |
| 11 | D3C3 | SP4 | 12.5 | 5.49% | 11.50% | 64-28 |
| 12 | D3C4 | SP4 | 12.5 | 5.56% | 9.00% | 64-28 |
| 13 | D3C5 | SP4 | 19 | 4.72% | 28.40% | 64-28 |
| 14 | D5C2 | SP3 | ** | 5.00% | 62.2% | 64-34 |
| 15 | D6C1 | SP4 | 19 | 5.29% | 17.00% | 64-34 |
| 16 | D6C2 | Hveem | ** | ** | ** | 64-34 |

* Missing information

## 4.6. Analysis and Discussion of Test Results

The laboratory evaluation for field projects and PMLC mix is described in this section.

### *4.6.1. Field projects*

#### *4.6.1.1. Cracking Performance Evaluation of Field Projects Mixes Using the MSSD Test*

Figure 4.13 shows the rate of the change in the vertical actuator displacement with the number of cycles ($\frac{dv}{dN}$) versus the change in SIF (ΔK) for 16 field projects. The change in $\frac{dv}{dN}$ increased with the increase in ΔK. Mixes with higher $\frac{dv}{dN}$ failed faster compared to mixes with lower $\frac{dv}{dN}$. Figure 4.14 shows an example of asphalt mixes with good observed field cracking resistance (D2C8) and poor observed field cracking resistance (D5C2). The D2C8 mix had a lower initial $\frac{dv}{dN}$ of 1.45 E-5 mm/cycle, while the D5C2 mix had a higher initial $\frac{dv}{dN}$ of 1.15 E-4 mm/cycle. The D2C8 mix failed within the 8$^{th}$ loading state (Stage-8 [ΔK = 4.48 N/mm$^{3/2}$]), while D5C2 failed in the third loading state (Stage-3 [ΔK = 0.832 N/mm$^{3/2}$]). The

MSSD performance indicators (i.e., *H* and *z*) for the field cores were obtained by fitting the data with a power function (Figure 4.14). The power function fitted the test data with a coefficient of determination ($R^2$) of 0.94 for the D5C2 mix and 0.90 for the D2C8 mix. The D2C8 mix had a smaller slope (*z*) of 1.66 compared to the D5C2 mix (*z* = 4.87). The smaller slope indicates a slower rate of damage, therefore the D2C8 mix has better cracking resistance when compared to the D5C2 cracking resistance. These findings are consistent with the observed cracking resistance in the field where the D2C8 mix showed good cracking resistance while D5C2 showed poor cracking performance. This example demonstrates that the MSSD performance indicators were able to differentiate between mixes with good and poor observed field cracking resistance.

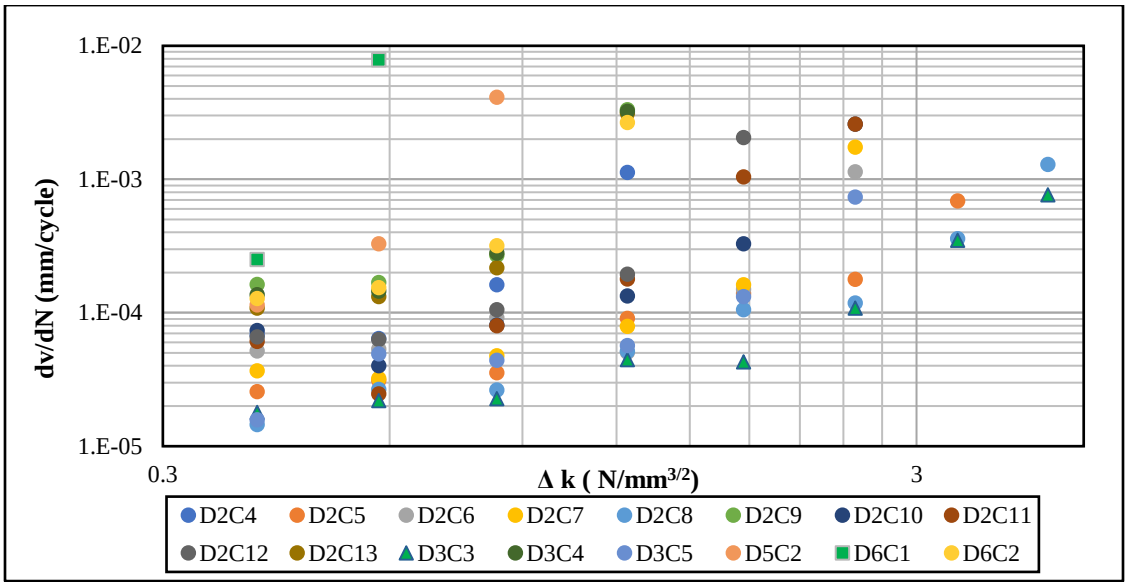


**Figure 4.13.** The variation in the rate of change of vertical actuator displacement and number of cycles versus the change in SIF (ΔK) for all field projects

Figure 4.15 shows the slope (*z*) performance indicator for all field projects (a total of 16 projects). Two SC specimens were tested from each project. The field projects had an average slope between 1.21 and 3.90 with a standard deviation between 0.02 and 0.97. The results showed a moderate variability (average COV of 15.1%). Analysis of variance (ANOVA) results of the slope performance indicator showed a statistically significant (*p*-value < 0.05) difference between the cracking resistance of the various field projects.

Tukey's Honestly Significant Difference (Tukey's HSD) categorized the field projects into two groups (i.e., A and B). Mix D2C8 had the lowest slope value of 1.21, while Mix D5C2 had the highest slope value of 3.90.

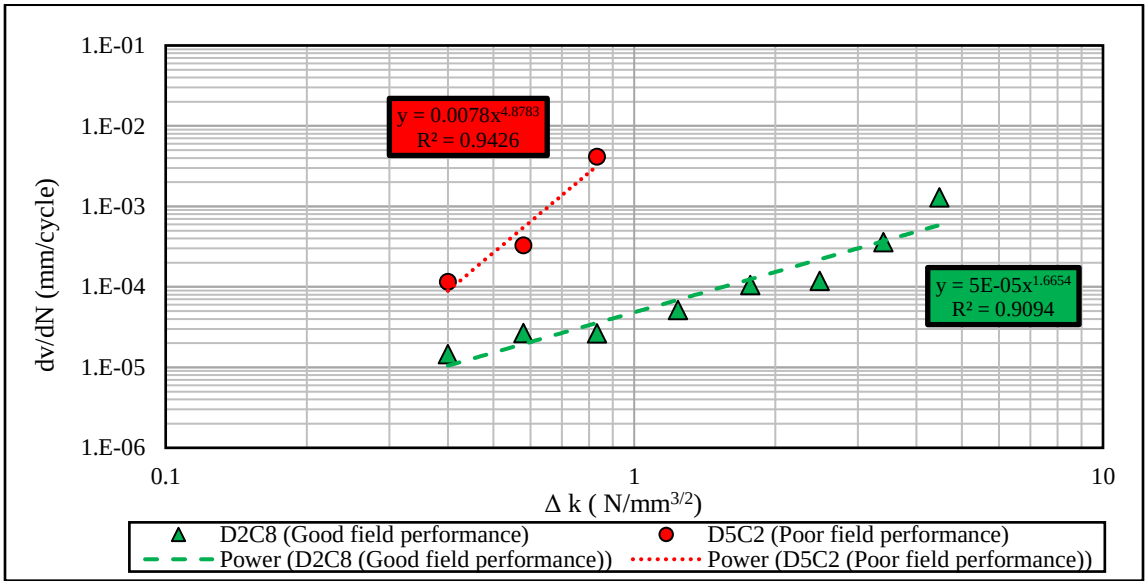


**Figure 4.14.** Example of MSSD performance indicators (H and z) for mixes with good and poor observed field cracking resistance.

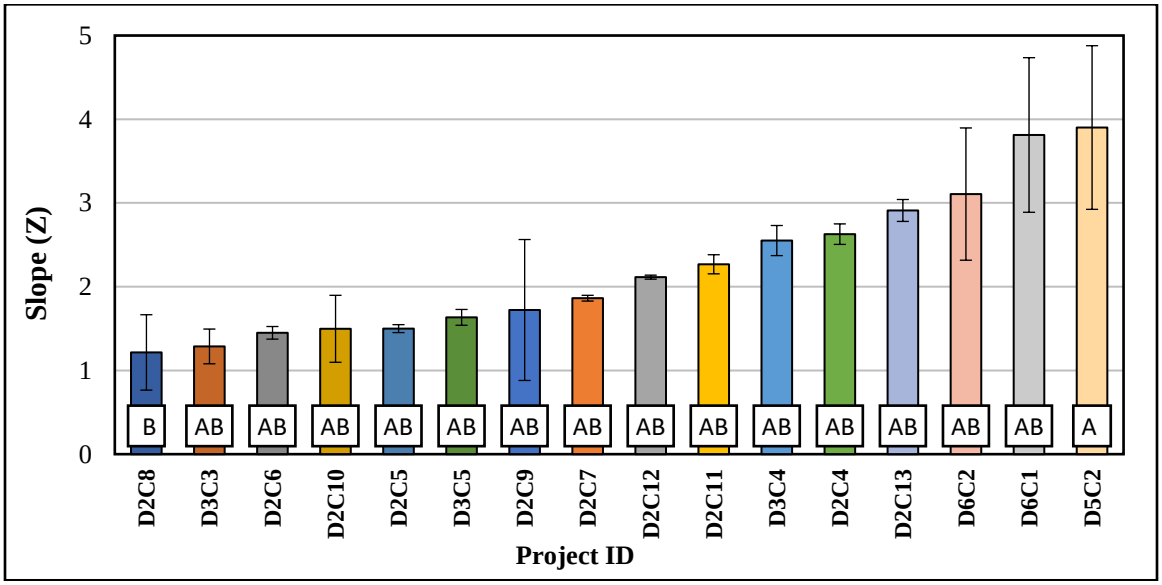


**Figure 4.15.** MSSD Slope (z) performance indicator results and proposed performance thresholds for field projects

Figure 4.16 shows the absolute intercept (Abs [log *H*]) performance indicator calculated from the MSSD test. The field projects had average values between 1.92 and 4.26 with standard deviations between 0.0 and 0.472. This performance indicator had a low variability (average COV of 4.4 %). ANOVA results of the absolute intercept performance indicator showed a statistically significant difference between the results ($p$-value < 0.05). Tukey's HSD test categorized field projects into five groups; A, B, C, D, and E. The absolute intercept (Abs [log *H*]) performance indicator was able to differentiate between field projects with different cracking performance (Figure 4.16). In general, mixes with higher Abs (log *H*) showed better cracking resistance compared to mixes with lower Abs (log *H*).

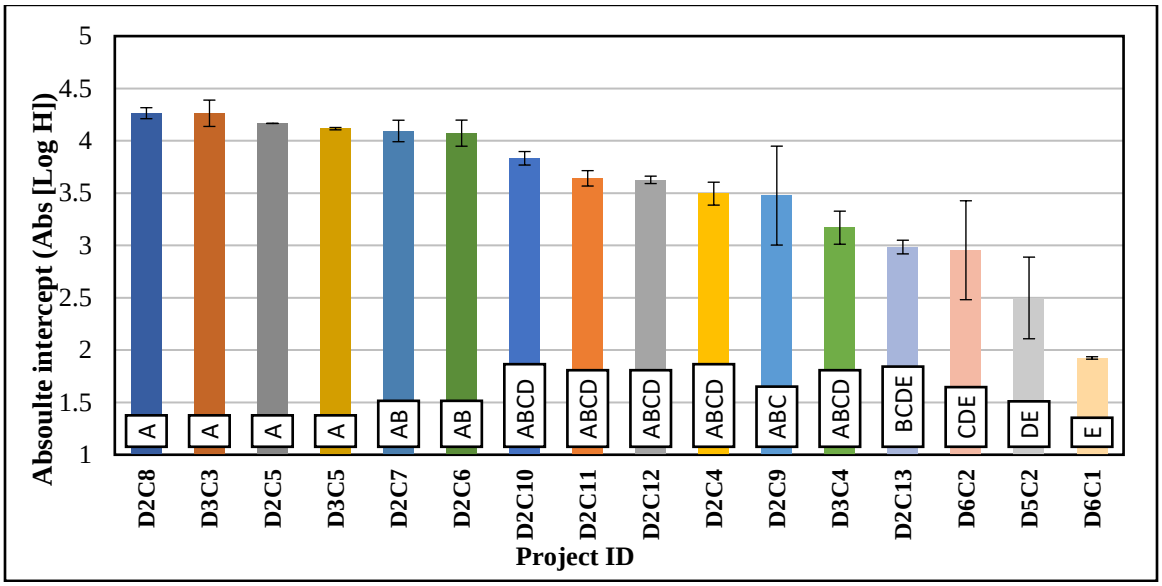


**Figure 4.16.** MSSD absolute intercept (Abs [Log H]) performance indicator and proposed performance thresholds for field projects

### *4.6.2. Developing Performance Thresholds for MSSD Performance Indicators*

The performance thresholds are defined as " pre-determined thresholds/limits that need to be achieved for a given performance indicator obtained from a given performance assessment test to assess mix resistance to a specific distress" [8]. The performance thresholds are the tools used within the performance-engineered mix design or BMD to distinguish between good or poor performance mixes. Therefore, developing proper performance thresholds is the key to the success of the BMD. The performance thresholds are often developed on the basis

of the correlation between the laboratory evaluation results and the observed field cracking resistance for the same mixes. More details about the available approaches to develop performance thresholds were provided in a previous study by the authors [8]. This section correlates the laboratory results of the 16 field projects and the observed field cracking resistance to develop proper performance thresholds for the MSSD performance indicators.

#### *4.6.2.1. Observed Field Cracking Resistance of Field Projects*

ITD performs an annual field pavement surface evaluation [26]. Two evaluation methods are used: windshield surveys and profiler vehicle surveys. Windshield survey involves visual inspection of pavement surfaces while driving on the road. The asset management engineer is often the one who performs this evaluation. The Cracking Index (CI) is used to describe the cracking distresses. The CI ranges between 0 and 5, where 5 indicates excellent performance (no cracks) and 0 indicates severely cracked surfaces. Pavement engineers use these classifications to determine the need for maintenance and rehabilitation treatments.

Recently, ITD has started using the profiler vehicle to conduct the pavement distress surveys that can replace the windshield surveys. This profiler is equipped with advanced equipment (e.g., high definition cameras, road profiler, GPS, and laser-based crack measurement [27]. The profiler scans the pavement surface and collects information related to several performance measures including rut depth, crack detection, roughness index, and longitudinal and transverse profile and it stores video logs of the pavement surface. This system determines the crack types (i.e., transverse, longitudinal, fatigue) and severity.

The automated crack detection and classification system within the profiler vehicle is used to determine the overall condition index (OCI) for the tested pavements [26,28]. However, the OCI data were limited to the last four years. The history of cracking performance is needed to understand the performance decay (decrease in OCI) of test sections over time. The OCI is highly influenced by surface treatments (mostly seal coat). Such treatments improve the OCI since they seal the cracks at the surface. Thus, there is a need for cracking performance over time to determine if higher OCI and CI are related to

better mix resistance to cracking or it is caused by the applied preservation treatment. The current practice at ITD is to apply a surface treatment as soon as needed, especially for commerce routes (sections with more than 300 Commercial Average Annual Daily Traffic [CAADT]). For this reason, the team considered and used the CI to describe the performance of various field projects.

The researchers examined the CI history for all test sections and considered the lowest CI in their analysis. Field cracking resistance was classified into three groups after combining the CI and the subjective evaluation provided by ITD material engineers including test sections with good cracking resistance ($4.5 \leq CI \leq 5$), test sections with fair cracking resistance ($3.5 \leq CI < 4.5$), and test sections with poor to very poor cracking resistance ($CI < 3.5$). Figure 4.17 shows a graphical representation of the cracking resistance for all studied test sections. Sections with good cracking resistance are presented in green bars, sections with fair cracking resistance are presented in yellow bars, and sections with poor cracking resistance are presented in red bars. Only two projects were found to have poor cracking resistance (i.e., D2C13 and D5C2), while seven and eight projects showed fair and good cracking resistance, respectively.

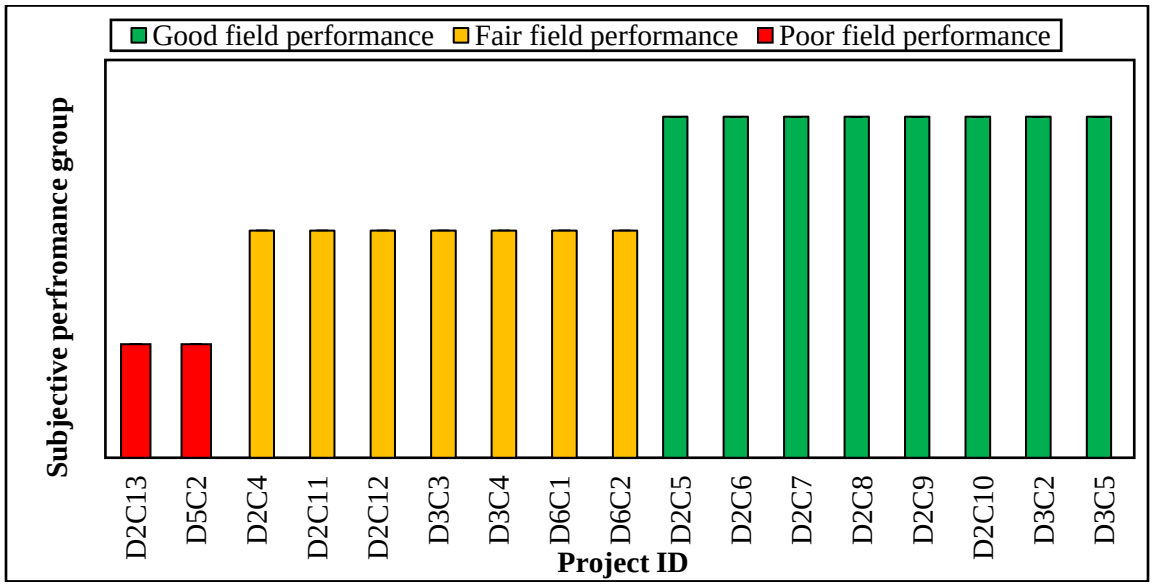


**Figure 4.17.** Subjective cracking performance evaluation for all field test projects

#### *4.6.2.2. Correlation Between the Laboratory Results and the Observed Field Performance*

Figure 4.18 and Figure 4.19 present the correlation between the slope (*z*) and Abs (log *H*), respectively with the observed field cracking resistance groups (i.e., good, fair, and poor cracking resistance). Field projects with good observed field cracking resistance are presented in green bars, while projects with fair and poor observed field cracking resistance are presented in yellow and red bars.

It can be observed from Figure 4.18 and Figure 4.19 that the MSSD performance indicators (i.e., *z*) and Abs [log *H*]) were well correlated with the observed field cracking resistance. This characteristic gives the MSSD performance indicators an advantage over monotonic performance indicators. In a previous study by the authors, the monotonic performance indicators (i.e., $G_{fracture,}$ $IDT_{Modulus}$, $IDEAL\text{-}CT_{Index}$, CRI, FI, $J_C$, and $Weibull_{CRI}$) were not well correlated with the observed field cracking resistance for the same field projects used in this study [8]. The monotonic performance indicators provided illogical trends with the variation in air void content or thickness, which affected the laboratory evaluation results of field cores. Therefore, it was not possible to develop a performance threshold for these indicators based on the direct correlation with the observed field performance. Rather, the MSSD results were used to develop performance thresholds for these monotonic performance indicators. More details about this approach are provided by Alkuime et al. (2019) [8].

The correlation results presented in Figure 4.18 demonstrate that mixes with lower slope (*z*) showed better cracking resistance compared to mixes with higher slope (*z*). Also, Figure 4.18 illustrates that field projects with good observed field cracking resistance had a slope less than 1.9, projects with poor observed field cracking resistance had a slope higher than 2.9, while projects with fair observed field cracking resistance had a slope between 1.9 and 2.9. Tukey's HSD results showed a statistically significant difference between good and fair/poor observed field cracking resistance groups and a statistically insignificant difference between fair and poor observed field cracking resistance groups.

The correlation results presented in Figure 4.19 demonstrate that mixes with higher Abs (log *H*) showed better cracking resistance compared to mixes with lower Abs (log *H*). Also, Figure 4.19 illustrates that projects with good cracking resistance had an absolute intercept (Abs [log *H*]) higher than 3.6, projects with fair cracking resistance had an absolute intercept (Abs [log *H*]) between 3.0 and 3.6, while projects with poor cracking resistance had an absolute intercept (Abs [log *H*]) less than 3.0. Similar to the slope (*z*) performance indicator, the ANOVA results indicated a statistically significant difference between cracking resistance groups (*p*-value < 0.05) based on the Abs (log *H*) performance indicator. Tukey's HSD results showed a statistically significant difference between good cracking resistance group and fair/poor groups, while there was a statistically insignificant difference between fair and poor cracking resistance groups.

#### *4.6.2.3. Development of Performance Thresholds for MSSD Performance Indicators*

Figure 4.18 and Figure 4.19 present the developed performance thresholds for the slope (*z*) and Abs (log *H*), respectively. Three thresholds were proposed for each performance indicator to distinguish between the different cracking resistance groups (i.e., good, fair, and poor). As can be observed in Figure 4.18 and Figure 4.19, mixes with good observed field cracking resistance (green bars) had slopes (*z*) ($z \leq 1.9$) and Abs (log *H*) > 3.6. Therefore, these values were used to distinguish mixes with good estimated field resistance to cracking. Also, it can be observed that mixes with fair observed field cracking resistance (yellow bars) had slopes (*z*) ($1.9 < z \leq 2$) and ($3.0 <$ Abs [log *H*] $\leq 3.60$). Therefore, these values were used to identify mixes with fair estimated field resistance to cracking. In addition, mixes with poor observed field cracking resistance (red bars) had slopes (*z*) ($z > 2.9$) and Abs (log *H*) < 3.0. Therefore, these values were proposed to identify mixes with poor field resistance to cracking. Based on these results, the research team proposed three thresholds to distinguish between mixes; good cracking resistance ($z \leq 1.9$) or (Abs [log *H*]>3.60), fair cracking resistance ($1.9 < z \leq 2.9$) or ($3.0 <$ Abs [log *H*] $\leq 3.60$), and poor cracking resistance ($z > 2.9$) or (abs [log H] < 3.0).

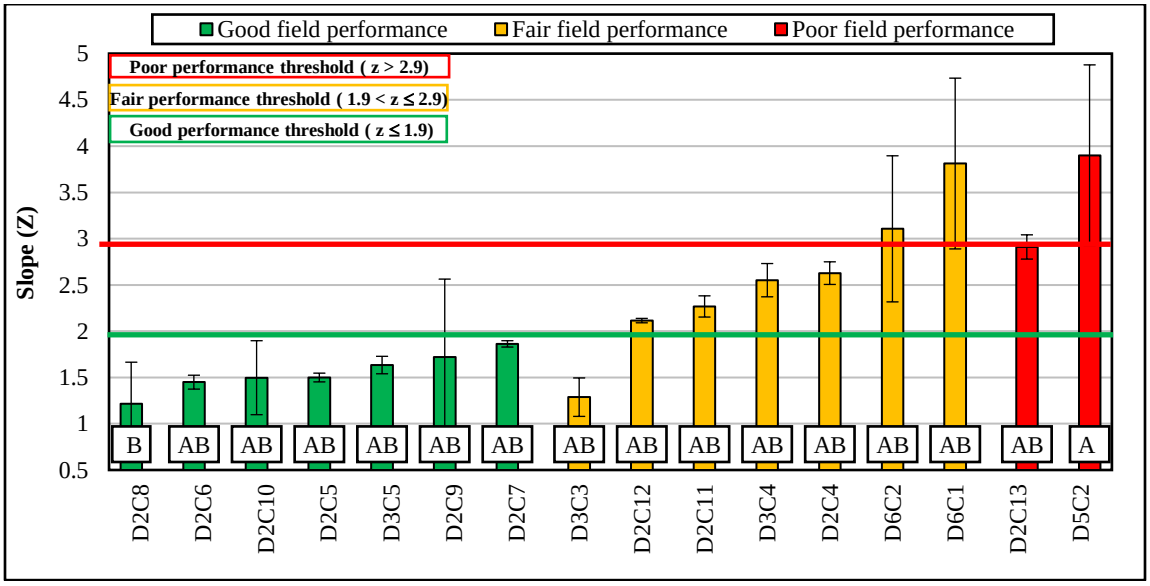


**Figure 4.18.** Correlation between the Slope (z) performance indicator with the observed field cracking resistance and developing the performance thresholds

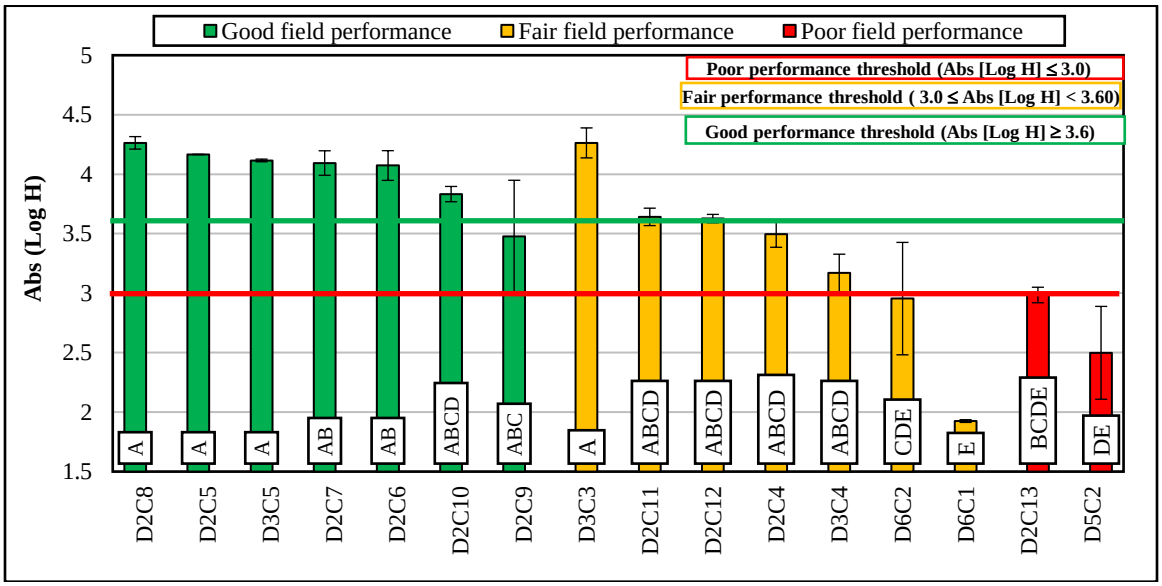


**Figure 4.19.** Correlation between the Abs (Log *H*) performance indicator with the observed field cracking resistance and developing the performance thresholds using field projects results

#### *4.6.2.4. Cracking Performance Evaluation of PMLC Mixes Using MSSD Test*

##### *4.6.2.4.1. PMLC Mixes*

Figure 4.20 shows the change in the vertical actuator displacement with the number of cycles ($\frac{dv}{dN}$) versus the change in SIF (ΔK) for all PMLC mixes. The computed MSSD performance indicators (*z* and Abs [log *H*]) were obtained by fitting the data with a power function. The $R^2$ for the power functions ranged between 0.661 and 0.926.

Figure 4.21 shows the slope (*z*) performance indicator for PMLC mixes. Four SC specimens were tested for each mix type. The slopes ranged between 1.20 and 4.25 with standard deviations (SD) between 0.10 and 1.40. The slope results had a moderate variability (average coefficient of variation [COV] of 25 %). Analysis of variance (ANOVA) results showed a statistically significant difference between mixes cracking resistance (*p*-value < 0.05). Tukey's HSD categorized mix cracking resistance into two groups; A and B. Similarly, Figure 4.22 shows the Abs (log *H*) performance indicator results for PMLC mixes. The Abs (log *H*) ranged between 1.94 and 4.43 with SD between 0.03 and 0.98. Also, the Abs (log *H*) results showed low variability (average COV of 11 %). ANOVA results showed a statistically significant difference between mix cracking resistance (*p*-value <0.05). Tukey's HSD categorized the PMLC mixes into two groups; A and B.

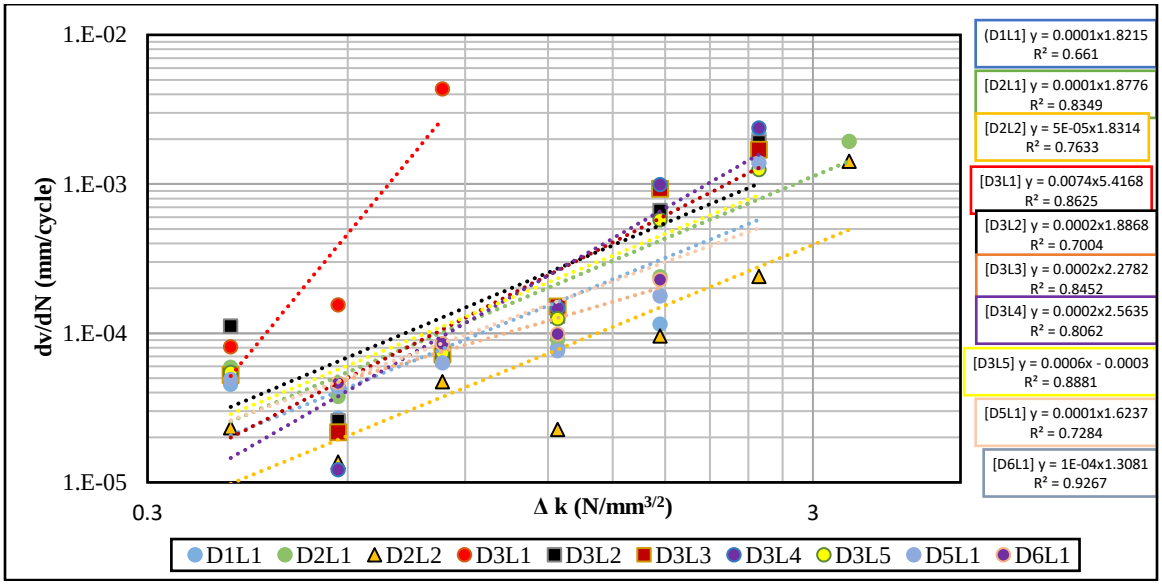


**Figure 4.20**. Determination of MSSD performance indicators (z and Abs [log H]) for PMLC mixes

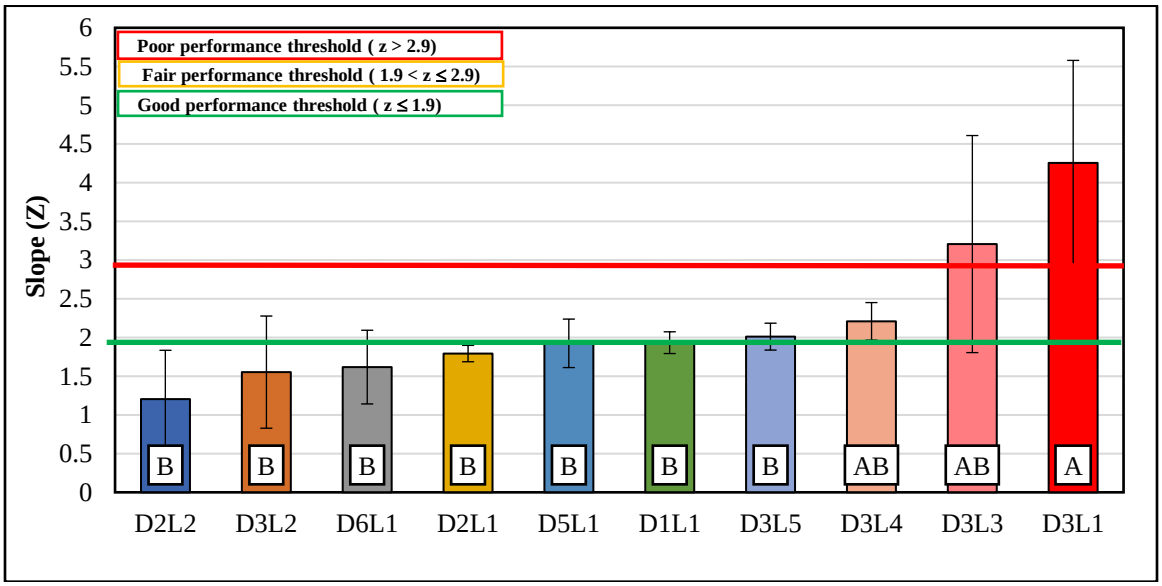


**Figure 4.21**. MSSD slope (z) performance indicator for PMLC mixes

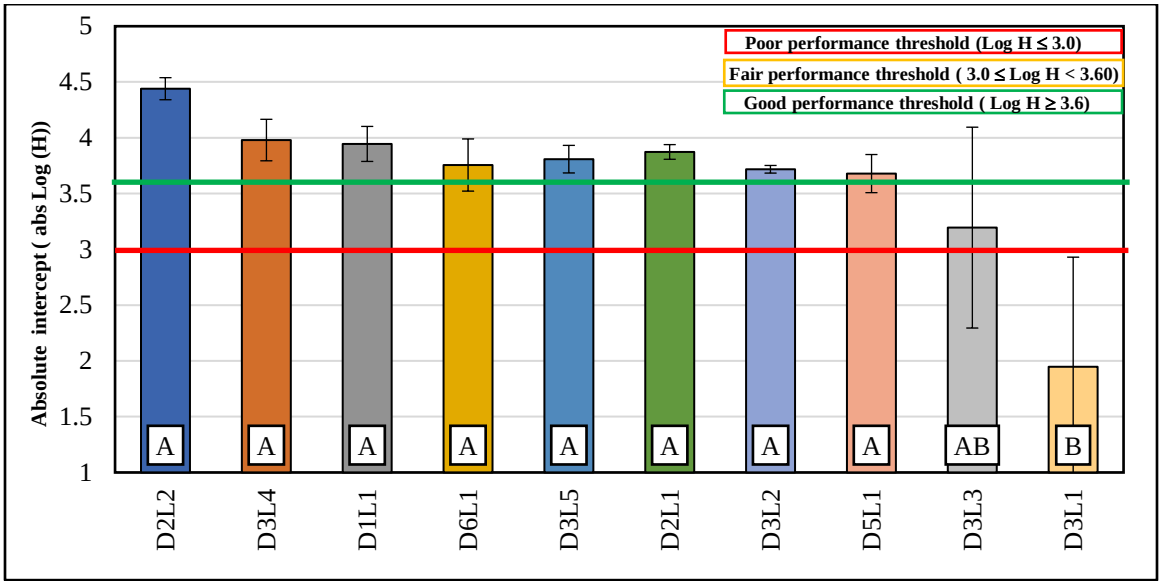


**Figure 4.22.** MSSD Abs (Log H) performance indicator for PMLC mixes

The composition of asphalt mixes affects their cracking resistance. In a previous study by Alkuime et al. (2019) [12] examined the effect of mix composition of PMLC mixes on estimated resistance to cracking determined using the monotonic tests (e.g., ITD, SCB-FI, SCB-$J_c$, etc.). In this study, a similar approach was performed and the results of the MSSD test were related to PMLC mix compositions as presented in Table 4.3. Mix D2L2 had the lowest MSSD slope (1.20) which indicates the best cracking resistance, while mix D3L1 had the highest slope (4.25) (i.e., a higher rate of damage) which demonstrates poor cracking resistance. Mix D2L2 had the highest binder content (5.70%), softer virgin binder PG (PG 58-34), and small NMAS (12.5 mm), therefore it is expected to provide better resistance to cracking compared to other mixes. Mix D3L1 had the highest RBR content (50%) and stiffer specified binder PG (PG 70-28). The use of higher RBR content with relatively stiffer binder may have reduced the resistance of mix D3L1 to cracking.

Also, based on the MSSD slope results, mix D1L1 is expected to provide better resistance to cracking compared to mix D3L3. Both mixes have the same RBR content (30%), binder content (5.30%), NMAS (12.5 mm), specified binder PG (PG 64-28), and softer virgin binder PG (PG 58-34), but the D1L1 mix is SP5 while D3L3 mix type is SP3.

SP5 mixes are designed for higher traffic levels according to ITD specifications [29], therefore they are expected to provide better cracking resistance.

The results also demonstrated that mix D1L1 is expected to provide better resistance to cracking when compared to mix D3L5. Both mixes (i.e., D1L1 and D3L5) have the same RBR content (30%), binder content (5.3%), NMAS (12.5 mm) and mix type (SP5), but mix D1L1 has softer specified binder PG (PG 64-28) and softer virgin binder PG (PG 58-34) while D3L5 has stiffer specified binder PG (PG 76-28) and virgin binder PG (PG 70-34). The use of a softer binder in mix D1L1 may improve its cracking resistance compared to mix D3L5.

Mix D2L1 was found also to provide better resistance to cracking when compared to mix D3L1. Both mixes have the same RBR content (50%), specified binder PG (PG 70-28), NMAS (12.5), and mix type (SP3), but D2L1 has relatively higher binder content (5.7%) compared to mix D3L1 (5.20%); therefore the higher binder content could improve the cracking resistance of D2L1 compared to D3L1.

Furthermore, the results demonstrated that mix D2L2 exhibited better resistance to cracking compared to mix D2L1. Both mixes had the same NMAS (12.5), mix type (SP3), and binder content (5.7%), but mix D2L2 had a lower RBR content (30%) and softer specified binder PG (PG 64-28) and virgin binder grade PG (PG 58-34) compared to mix D2L1 which had RBR of 50%, specified binder grade PG of 70-28, and virgin binder PG of 64-34. It is believed that the softer binder and low RBR content improved the cracking resistance of D2L2 compared to D2L1. Similar to the slope ($z$) performance indicator, the absolute intercept performance indicator (Abs [log $H$]) (Fig. 17) had good agreement with mix composition as discussed above.

#### *4.6.2.5. Evaluation of PMLC Estimated Resistance to Cracking using the Developed Performance Thresholds*

The previous section developed performance thresholds for MSSD performance indicators based on the correlation between the laboratory results of field cores and the observed field cracking resistance. Three thresholds to distinguish between mixes; good cracking resistance ($z \leq 1.9$) or (Abs [log $H$] > 3.60), fair cracking resistance ($1.9 < z \leq 2.9$) or ($3.0 <$ Abs [log $H$] $\leq 3.60$), and poor cracking resistance ($z > 2.9$) or (abs [log H] < 3.0). These thresholds can be used to identify mixes with different expected cracking resistance in the field.

Figure 4.21 and Figure 4.22 present the estimated field resistance to cracking of PMLC mixes for the slope ($z$) and Abs (log $H$), respectively. Based on the slope ($z$) performance thresholds, mixes D2L2, D3L2, D6L1, and D2L1 are expected to have good field cracking resistance. Mixes D5L1, D1L1, D3L5, and D3L4 are expected to have fair field cracking resistance, while mixes D3L3 and D3L1 are expected to have poor field cracking resistance (Figure 4.21).

The Abs (log $H$) performance thresholds suggest that mixes D2L2, D3L4, D1L1, D6L1, D3L5, D2L1, and D3L2 are expected to have good field cracking resistance in the field. Mix D3L2 are expected to have fair field cracking resistance, while mixes D3L1 are expected to have poor field cracking resistance (Figure 4.22). Also, the thresholds are in agreement with the estimated performance using the composition of PMLC mixes. The performance thresholds for both indicators estimated that mix D2L2 should exhibit good field cracking resistance, while mix D3L1 should exhibit poor field cracking resistance. These results are in agreement with the estimated performance based on the composition of these mixes.

### *4.6.3. Field Projects and PMLC Mixes*

#### *4.6.3.1. Correlation Between MSSD Performance Indicators*

Previous research reported that the Paris' law parameters (i.e., *n* and *A*) are correlated [21,22] and a direct linear correlation was reported between *n* and Log (*A*) (Equation 4.13). Similarly, the authors evaluated the correlation between MSSD performance indicators (*z* and Abs [log *H*]). Figure 4.23 shows the correlation between these two performance indicators for the PMLC mixes and field projects. The results demonstrate that there is a direct relationship between both performance indicators. Field projects had a coefficient of determination ($R^2$) of 0.80, while $R^2 = 0.75$ for PMLC mixes. These relationships indicate that higher slopes are associated with lower values of Abs (log *H)*. A similar relationship was reported by Rooijen and Bondt (2008) for Paris' law parameters computed using the dynamic SCB (Equation 4.15) [30]. Rooijen and Bondt's (2008) model provided strong correlation ($R^2 = 1.0$).

$$Log\ A = -1.4397 \times n - 2.5273 \qquad 4.15$$

where *A* and *n* are the Paris law parameters

#### *4.6.3.2. MSSD Performance Indicators Variability*

The slope (*z*) determined from PMLC mixes had an average COV of 24%, median of 23%, and a range between 5.9% and 47%, while the slope (*z*) determined from field projects had an average COV of 15%, median of 6.5%, and a range between 1.1% and 49%. The Abs (log *H*) determined from PMLC mixes had an average COV of 9.6% , median of 4.3%, and a range between 0.9% and 49%, while the Abs (log *H*) determined from field projects had an average COV of 4.4%, median of 2.4%, and a range between 0% and 16%. The Abs (log *H*) results showed low variability (average COV < 10%), while the slope (*z*) results showed moderate variability (15% < average COV < 35%) for both field cores and PMLC mixes. In general, the dynamic tests have high variability; however, the variability of MSSD performance indicators are still better than other dynamic assessment tests. For example, the BBF test has

a COV between 40% and 50% while the overlay tester has a COV between 30% and 50% [1]. In addition, the MSSD performance indicators have comparable variability to that of monotonic performance indicators. The variability of several monotonic performance indicators was evaluated in a previous study by the authors, [12]. The analysis demonstrated $Weibull_{CRI,}$ $IDT_{strength,}$ and CRI (IDT) had low variability (i.e. average COV <10%), while other monotonic indicators (e.g., FI (SCB-FI), $G_{fracture,}$ IDEAL-$CT_{Index}$, and Nflex, etc.) had moderate variability (i.e, 15% < average COV < 30%).

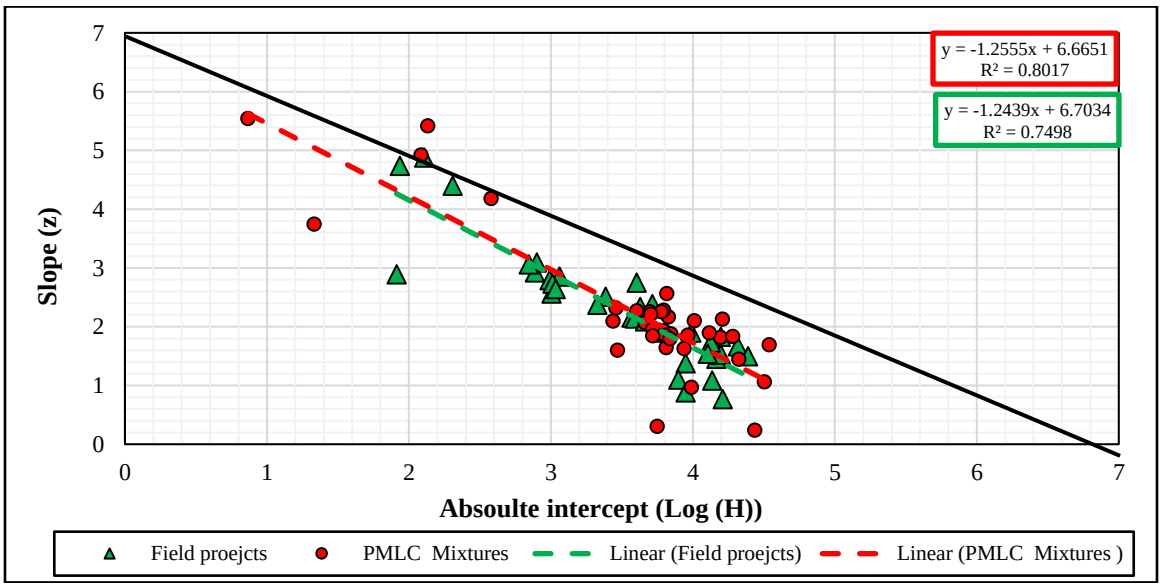


**Figure 4.23**. Correlation between MSSD test performance indicators (z and abs [log H]) for both field and PMLC mixes

*4.6.4. Simple Approach to Develop Performance Thresholds*

The pass/fail performance thresholds for performance assessment indicators are often developed on the basis of the direct correlation between the laboratory results and the observed field cracking performance of the same mix. However, extracting field cores is difficult and costly. Therefore, previous research proposed alternative approaches for initial performance thresholds. Diefenderfer and Bowers (2019) proposed three methods (i.e., Method 1, Method 2, and Method 3) to set initial performance thresholds based on statistical analysis of PMLC mixes [31]. Method 1 assumes that the studied PMLC mixes have an

acceptable field cracking resistance; therefore, the threshold is specified to allow all the evaluated mixes to pass. Method 2 assumes that the average cracking resistance of the studied PMLC mixes is minimally acceptable; therefore, the threshold is specified as the average value of these mixes. Method 3 assumes that using the average value alone to specify a performance threshold may not be sufficient; therefore, the threshold is specified as the average value ± one standard deviation. Further details on these methods are provided in [13,31]. In this section, the authors evaluated the applicability of such methods to set initial performance thresholds for PMLC mixes.

#### *4.6.4.1. Initial Performance Thresholds Using PMLC Mixes*

Figure 4.24 and Figure 4.25 present initial proposed thresholds for the slope (*z*) and Abs (log *H*) performance indicators using Methods 1, 2, and 3. The maximum slope (*z*) thresholds are set at 4.25, 2.17, and 3.00 using Methods 1, 2, and 3, respectively. The minimum Abs (log *H*) thresholds are set at 1.95, 3.60, and 3.00 using Methods 1, 2, and 3, respectively to ensure adequate resistance to cracking. It can be observed that the Method 1 thresholds (maximum slope (*z*) of 4.2, and minimum Abs (log *H*) of 2.0) are more conservative compared to thresholds proposed using Methods 2 and 3. Method 1 thresholds aim to maintain the same cracking resistance level for future produced mixes to prevent any decline in mix cracking resistance resulting from design and/or production issues (e.g., adding more RAP materials than an allowable percent). The second method (Method 2) specified the thresholds at a maximum slope of 2.17 or minimum Abs (log *H*) of 3.6. These thresholds decrease the chance of accepting mixes with poor resistance to cracking, but it may also eliminate mixes with good cracking resistance due to the test or indicator variability. The third method (Method 3) is proposed to overcome the limitations of Method 2 by including the standard deviation to the specified thresholds to account for the test variability and reduce the chance of rejecting mixes with good cracking resistance.

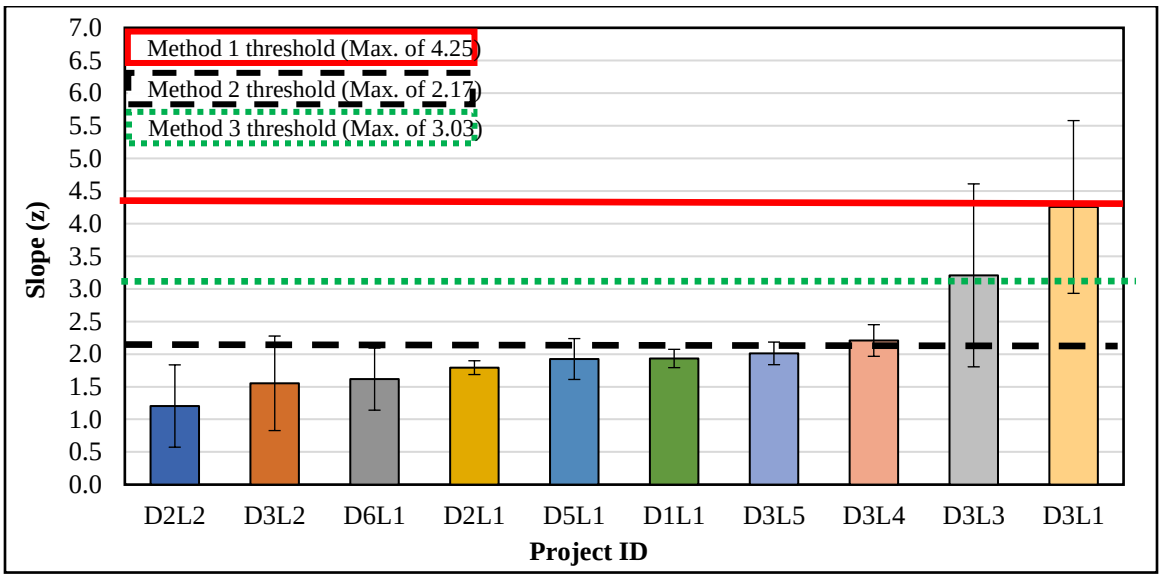


**Figure 4.24.** Initial estimation of cracking resistance for slope (z) performance indicator using PMLC mixes laboratory results

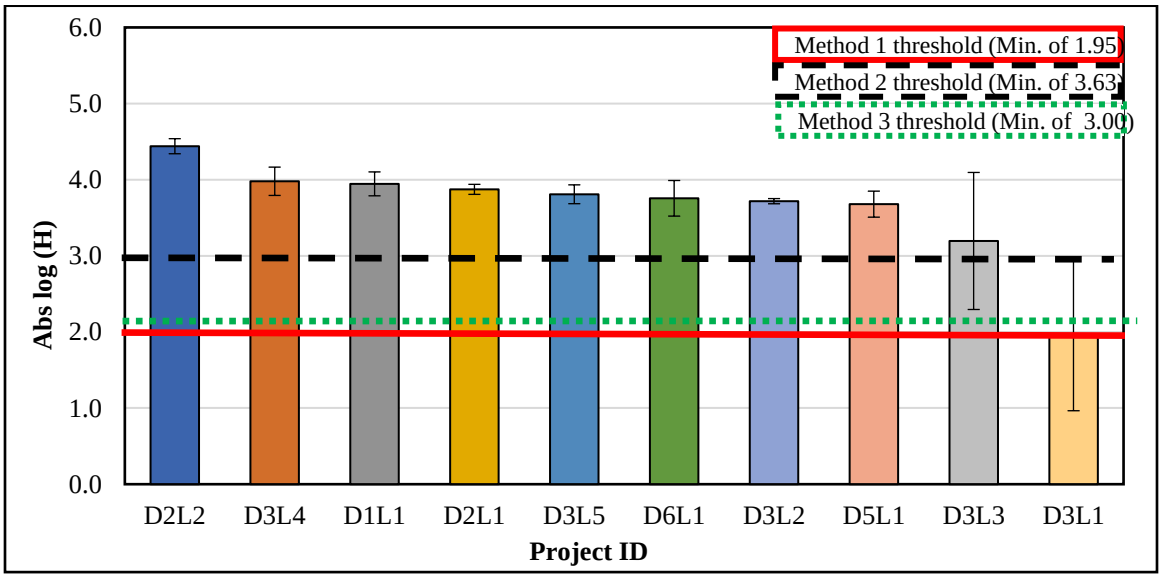


**Figure 4.25**. Initial estimation of cracking resistance for Abs (log H) performance indicator using PMLC mixes laboratory results

The initial performance thresholds were developed based on a statistical analysis of the laboratory results for the PMLC mixes. However, the field performance of the PMLC mixes is not known yet since they were collected from new paving projects. Thus, the researchers verified these initial thresholds using the developed performance thresholds from the correlation between field cores and the observed field cracking resistance (Figure 4.18

and Figure 4.19). Table 4.6 summarizes the proposed initial thresholds using the PMLC mixes and the developed performance threshold using the field projects (Figure 4.18 and Figure 4.19) for each cracking resistance group (i.e., good, fair, and poor). The proposed initial thresholds using the PMLC mixes can only differentiate between mixes with good and poor cracking resistance, while the proposed thresholds using field projects can differentiate between good, fair, and poor cracking resistance groups.

The results of various thresholds summarized in Table 4.6 demonstrate that Method 2 provided a comparable threshold for the slope (*z*) performance indicator (maximum of 2.17) compared to thresholds based on field performance (1.9) while Methods 1 and 3 provided relatively higher thresholds (i.e., 4.25 and 3.0, respectively). The results also showed that Method 2 provided the same value (i.e., minimum of 3.6) of the Abs (log *H*) performance indicator compared to proposed thresholds based on field performance. These findings demonstrate that Method 2 can be used by transportation agencies to initially estimate proposed cracking thresholds using PMLC mixes if field performance is not yet known.

**Table 4.6.** Summary of proposed performance thresholds

| MSSD indicators | Performance group categories | | | | | | | | | | | |
|---|---|---|---|---|---|---|---|---|---|---|---|---|
| | Good | | | | Fair | | | | Poor | | | |
| | PMLC mixes | | | Field projects | PMLC mixes | | | Field projects | PMLC mixes | | | Field projects |
| | Method number | | | | Method number | | | | Method number | | | |
| | 1 | 2 | 3 | | 1 | 2 | 3 | | 1 | 2 | 3 | |
| Slope (z) | <4.25 | <2.17 | <3.00 | <1.9 | NA | NA | NA | 1.9 < z ≤ 2.9 | ≥4.25 | ≥2.17 | ≥3.00 | > 2.9 |
| Abs (log *H*) | >1.95 | >3.60 | >3.00 | ≥ 3.6 | NA | NA | NA | 3.0 ≤ Abs (log *H*) < 3.60 | ≤1.95 | ≤3.60 | ≤3.00 | ≤ 3.0 |

## 4.7. Conclusions

This study presented the development of a new dynamic test called Multi-Stage Semi-circle bending Dynamic (MSSD) test. The MSSD has advantages over the available monotonic and dynamic cracking assessment tests and addresses the major concerns to implement the Balanced Mix Design (BMD) (i.e., performance test validity, specimen preparation, and testing time). The developed MSSD test simulates the repeated loading (dynamic) in a reasonable testing time (less than 9 hours per test regardless of mix type), has a fixed loading sequence that works for mixes with different characteristics (e.g., mix composition, percent air void content, thickness, etc.) and utilizes testing equipment and specimen geometry similar to that used in monotonic tests.

The MSSD test uses a SC test specimen with a radius of 75 mm and a notch depth of 15 ±1 mm. The thickness of the laboratory compacted specimens is 50 mm, while the thickness of field cores can vary between 25 mm to 50 mm depending on the lift thickness. Two performance indicators were proposed to analyze the MSSD data including the slope (z) and Abs (log *H*). The intercept (log *H*) reflects the initial rate of displacement per cycle, while the slope (*z*) reflects the increment in the displacement rate with the change in SIF. The higher slope indicates a faster rate of damage. A higher slope is associated with a lower absolute intercept (Abs [log *H*]). Therefore, mixes with a lower slope (z) and higher Abs (log *H)* would exhibit higher resistance to cracking.

The study performed an experimental evaluation for MSSD performance indicators using 26 different mix types including 10 PMLC mixes and 16 field projects. The findings showed that the MSSD performance indicators were able to differentiate between mixes with good and poor observed field cracking resistance. The study compared the laboratory results with the field cracking performance in order to develop proper performance thresholds for the MSSD performance indicators. The correlation results showed that the MSSD performance indicators (i.e., *z*) and Abs [log *H*]) were well correlated with the observed cracking performance in the field. The results demonstrate that mixes with lower slope (*z*) and higher Abs (log *H*) showed better cracking resistance compared to mixes with higher

slope (*z*) and lower Abs (log *H*). The research team proposed three thresholds to distinguish between mixes; good cracking resistance ($z \leq 1.9$) or (Abs [log *H*] > 3.60), fair cracking resistance ($1.9 < z \leq 2.9$) or ($3.0 <$ Abs [log *H*] $\leq 3.60$), and poor cracking resistance ($z > 2.9$) or (abs [log H] <3.0). These performance thresholds were used to estimate the field resistance to cracking of PMLC mixes. The results demonstrated that there was a good agreement between expected cracking performance and mix composition.

The results of the PMLC and field projects showed that there is a direct relationship between both performance indicators (i.e, slope [*z*] and abs [log H]). Field project had a coefficient of determination ($R^2$) of 0.80, while it was 0.75 for PMLC mixes. Also, the results indicated that the Abs (log *H*) had low variability (average COV <10%), while the slope (*z*) had moderate variability (15% < average COV < 35%) for both field cores and PMLC mixes. Overall, the MSSD performance indicators had lower variability compared to other dynamic tests and comparable variability to that of monotonic performance indicators.

Finally, this study evaluated an alternative approach to develop initial performance thresholds using the statistical analysis of the laboratory results for the PMLC mixes. The findings demonstrate that Method 2 can be used by transportation agencies to initially estimate proposed cracking thresholds using PMLC mixes if field performance is not yet known.

### 4.8. References

[1] R.C. West, C. Rodenzo, F. Leiva, F. Yin, Development of a framework for balanced mix design, NCHRP project 20-07/task 406, 2018. http://apps.trb.org/cmsfeed/TRBNetProjectDisplay.asp?ProjectID=4324.

[2] S. Buchanan, Balanced Mix Design Task Force Update of Activities, Presented at Asphalt Mixture Expert Task Group(ETG) Meeting. (2016).

[3] A. Braham, B.S. Underwood, State of the art and practice in fatigue cracking evaluation of asphalt concrete pavements, 2016. http://asphalttechnology.org/downloads/Fatigue_Cracking_of_Asphalt_Pavements_2017_06.pdf.

[4] I. Al-Qadi, H. Ozer, J. Lambros, A. El Khatib, D. Singhvi, Testing Protocols to Ensure Performance of High Asphalt Binder Replacement Mixes Using RAP and RAS (Report No. R27-128), Urbana, IL: Illinois Center for Transportation, Illinois Dept. of Transportation. (2015).

[5] M. Barry, An analysis of impact factors on the Illinois flexibility index test, University of Illinois at Urbana-Champaign, 2016.

[6] J. Rivera-Perez, Effects of speciemn geometry and test configuration on the fracture process zone for asphalt materials, University of Illinois at Urbana-Champaign, 2017.

[7] F. Kaseer, F. Yin, E. Arámbula-Mercado, A.E. Martin, J.S. Daniel, S. Salari, Development of an index to evaluate the cracking potential of asphalt mixtures using the semi-circular bending test, Construction and Building Materials. 167 (2018) 286–298. doi:10.1016/j.conbuildmat.2018.02.014.

[8] H. Alkuime, E. Kassem, F. Bayomy, Development of performance-engineered mix design (PEMD) specifications for intermediate temperature monotonic cracking assessment tests and performance indicators, Road Materials and Pavement Design. (2019).

[9] F. Zhou, D. Newcomb, C. Gurganus, S. Banihashemrad, M. Sakhaeifar, E.S. Park, R.L. Lytton, Field Validation of Laboratory Tests to Assess Cracking Resistance of Asphalt Mixtures: An Experimental Design, 2016. doi:10.17226/23608.

[10] S.K. Maiti, Fracture Mechanics: Fundamentals and Applications, Cambridge University Press, Delhi, India, 2015.

[11] AASHTO TP 105, Determining the Fracture Energy of Asphalt Mixtures Using the Semicircular Bend Geometry ( SCB ), American Association of State Highway and Transportation Officials. (2013).

[12] H. Alkuime, F. Tousif, E. Kassem, F. Bayomy, Review and evaluation of intermediate temperature cracking testing standards and performance indicators for asphalt mixes., Construction and Building Materials. (2019).

[13] H. Alkuime, E. Kassem, F. Bayomy, Development of a new performance indicator to evaluate the resistance of asphalt mixes to intermediate temperature cracking., Journal of Transportation Engineering, Part B: Pavements. (2019).

[14] I.L. Lim, I.W. Johnston, S.K. Choi, Stress intensity factors for semi-circular specimens under three-point bending, Engineering Fracture Mechanics. 44 (1993) 363–382. doi:10.1016/0013-7944(93)90030-V.

[15] M.M. Hassan, H.A. Khalid, Fracture Characteristics of Asphalt Bottom Ash Aggregate, (2005) 1–8. doi:10.3141/2180-01.

[16] I. Artamendi, H.A. Khalid, A comparison between beam and semi-circular bending fracture tests for asphalt, Road Materials and Pavement Design. 7 (2006) 163–180. doi:10.1080/14680629.2006.9690063.

[17] K.P. Biligiri, S. Said, H. Hakim, Asphalt mixtures'crack propagation assessment using semi -circular bending tests, Chinese Society of Pavement Engineering. 5 (2012) 209–217.

[18] M. Pszczola, C. Szydlowski, Influence of bitumen type and asphalt mixture composition on low-temperature strength properties according to various test methods, Materials. 11 (2018) 1–18. doi:10.3390/ma11112118.

[19] H.A. Khalid, O.K. Monney, Moisture damage potential of cold asphalt, International Journal of Pavement Engineering. 10 (2009) 311–318.

[20] P. Paris, A. Director, F. Erdogan, A Critical Analysis of Crack Propagation Laws, Journal of Basic Engineering. 85 (1963) 528–533.

[21] O.G. Bilir, Crack propagation in a commercial steel, International Journal of Fracture. 80 (1988) 73–80.

[22] Ö.G. Bilir, The relationship between the parameters and of Paris' law for fatigue crack growth in a SAE 1010 steel, Engineering Fracture Mechanics Vol. 36 (1990) 361–364.

[23] AASHTO T 312, Standard method for preparing and determining the density of hot mix asphalt (HMA ) specimens by means of the SHRP gyratory compactor ( AASHTO T312), Washington D.C., 2015.

[24] ASTM D2726, Standard test method for bulk specific gravity and density of non-absorptive compacted bituminous mixtures, 2005. doi:10.1520/D2726.

[25] ASTM D6857 / D6857M, Standard Test Method for Maximum Specific Gravity and Density of Asphalt Mixtures Using Automatic Vacuum Sealing Method, 2018.

[26] J. Poorbaugh, Idaho Transportation System Pavement Performance-2017 Report, (2017).

[27] PathWay Services Incorporated Companies, Pavement profiler information- the PathRunner, (2019). http://www.pathwayservices.com/equipment-1/.

[28] Kercher Engineering, Agile assets pavement management system engineering configuration, 2015.

[29] Idaho Transportation Department (ITD), Standard specification for highway construction, 2017.

[30] R.C. Van Rooijen, A.H. De Bondt, Crack propagation performance evaluation of asphaltic mixes using a new procedure based on cyclic semi-circular bending tests, (2008) 437–450.

[31] S.D. Diefenderfer, B.F. Bowers, Initial approach to performance (balanced) mix design : the Virginia experience, Transportation Research Board. (2019). doi:10.1177/0361198118823732.

# Chapter 5: Evaluation and Development of Performance-Engineered Specifications for Monotonic Loading Cracking Performance Assessment Tests

Hamza Alkuime[1]; Emad Kassem[1]; Fouad M.S. Bayomy[1] and Richard J. Nielsen[1]

(To be submitted to Journal of Testing and evaluation)

## 5.1. Abstract

This study investigated the validity of various monotonic cracking performance assessment tests and indicators to describe the expected cracking performance in the field. A total number of 17 field test projects with known field cracking performance were selected and evaluated. Field cores were extracted from these projects and a comprehensive laboratory testing program was carried out. The authors conducted four monotonic standard tests and calculated 12 performance indicators. The study findings showed that there was no direct correlation between the results of the monotonic tests and field performance. The air void content and thickness are believed to influence the results of the monotonic tests and indicators. Therefore, this study proposed an alternative approach to develop performance specifications for the monotonic tests indirectly using a correlation between dynamic testing and both various monotonic tests and field performance. The results demonstrated that such approach to be effective. The Weibull Cracking Resistance Index ($Weibull_{CRI}$) determined from Indirect Tension Test (IDT) test is recommended as a performance indicator to assess cracking resistance of asphalt mixes. Three pass/fail cracking performance assessment thresholds were proposed for $Weibull_{CRI}$ to distinguish between asphalt mixes with good, fair, and poor cracking resistance.

Keywords: balanced mixed design; performance indicators, semi-circular bending; indirect tension test; cracking resistance; performance-engineered Mix Design

[1] Department of Civil and Environmental Engineering, University of Idaho, Moscow, ID 83844 USA.

## 5.2. Introduction

The Superpave design system was developed to produce asphalt mixes with the desired performance. The design of asphalt mixes uses the available materials and account for environmental conditions, traffic level, structure, and reliability factors [1]. The design of asphalt mixtures is often conducted to meet the volumetric requirements without assessing the performance [2]. Cracking and rutting are observed in pavements designed in accordance with Superpave. In fact, pavement cracking was reported as the main concern for state Departments of Transportations (DOTs) [3].

Recently, a new asphalt mix design approach called Performance-Engineered Mix Design (PEMD) or Balanced Mix Design (BMD) has been proposed [4]. The PEMD incorporates asphalt mix performance assessment tests and thresholds (i.e., PEMD specifications) to design asphalt mix with sufficient resistance to specific distresses [3]. A recent national survey demonstrated that several state DOTs are interested in implementing PEMD, but they have some concerns. These concerns are related to the validity of the proposed performance assessment tests including 1) sensitivity to mix composition, 2) variability of test results, 3) statistical mix performance grouping, 4) ability to correlate with the observed field performance, and 5) ability to develop PEMD specifications (i.e., pass/fail performance assessment thresholds) [3].

Several research studies examined the correlation between specific monotonic performance indicators and the observed field cracking performance. Zhou et al. (2017) studied the correlation between indirect tensile asphalt cracking test (IDEAL-$CT_{Index}$ ) and the observed field cracking performance of eight Accelerated Loading Facilities (ALF) test sections [5]. The study findings showed that IDEAL-$CT_{Index}$ had an excellent correlation (coefficient of determination [$R^2$] of 0.87) with the number of passes to the appearance of the first crack. Mohammad et al. (2017) investigated the correlation between critical strain energy release rate ($J_C$) with the observed field performance of nine test sections in Louisiana Department of Transportation (LADOT) [6]. The findings demonstrated that $J_C$ had a good correlation ($R^2$ of 0.73) with the cracking index obtained from the Pavement Management System (PMS) used in LADOT.

In addition, Al-Qadi et al. (2015) investigated the correlation between flexibility index determined from SCB test (FI [SCB]) and the subjective field performance of 18 field test sections in Illinois [7]. The results showed that FI(SCB) was able to differentiate between field test sections with different performance (i.e., good, fair, and bad cracking performance). In addition, West et al. (2017) examined the correlation between Cantabro loss (%), modified overlay cycles to failure (OT), $J_C$, indirect tensile strength ($IDT_{Strength}$), indirect tensile modulus ($IDT_{Modulus}$) (or Japan IDT coefficient), and Nflex with the observed field cracking performance of eight ALF test sections [8]. The results showed a reasonable correlation between these indicators and the observed and adjusted number of passes to reach 240 in of cracking in the selected sections. Cantabro loss (%), modified OT, $J_C$, $IDT_{Strength}$, $IDT_{Modulus}$, Nflex had $R^2$ of 0.54, 0.41, 0.05, 0.18, 0.33, and 0.55 with the observed performance, respectively and 0.59, 0.47, 0.23, 0.34, 0.47, and 0.67 with the adjusted observed performance, respectively.

Sreedhar et al. (2018) examined the correlation between the total fracture energy determined from SCB test ($G_{fracture}$ [SCB)]) and FI(SCB) at three different notch depths (25.4, 31.75, and 38.1 mm), $IDT_{Strength}$, flexibility index determined from IDT test (FI [IDT]), and fatigue life from Bending Beam Fatigue (BBF) with the observed field performance of four field test sections in Oregon [9]. The cracking performance for the selected sections was represented using a subjective evaluation (i.e., cracked and no crack) obtained from PMS used in ODOT, where two sections were cracked, and two sections were not cracked. The findings showed that $G_{fracture}$ (SCB) and Fatigue life (BBF) were not able to differentiate between different subjective performance groups, while FI(SCB), FI(IDT), and $IDT_{Strength}$ were able to differentiate between sections with different performance.

Recent studies by the authors investigated the validity of various monotonic cracking tests and performance indicators (i.e., four testing standards and 12 performance indicators) [10,11] (Chapter 2 and Chapter 3). These studies addressed various concerns including sensitivity to mix composition, statistical grouping of mix cracking performance, correlation between various performance indicators, and variability in test results using laboratory-prepared asphalt mixtures. However, there is a need to evaluate the correlation of various test

methods and indicators to field performance and develop PEMD specifications (i.e., pass/fail performance assessment thresholds).

## 5.3. Study Objectives

The main goal of this study is to investigate the validity of various monotonic cracking tests and performance indicators to describe the observed cracking performance in the field. This is one of the main concerns raised by several state DOTs that need to be addressed before PEMD implementation (as discussed in Chapter 1). The main objectives of this study are:

- Examine the ability of various monotonic cracking tests and performance indicators to correlate with the observed field cracking performance.
- Identify and select the appropriate monotonic cracking tests and performance indicators to evaluate the resistance of asphalt mixes to cracking.
- Develop appropriate cracking performance thresholds for various monotonic tests.

### Experimental Plan

In this study, a total number of 17 field projects with known field cracking performance were identified. Project selection was performed with help from Idaho Transportation Department (ITD) Materials Engineers. These projected were distributed across the state of Idaho. Table 5.1 presents information about the locations and mix properties of the selected field projects. The selected projects have different mix properties (e.g., mix design, binder content, etc.) and field performance. In this paper, field projects are referred to as DxCy hereafter, where D refers to district, x refers to district number (i.e, 1 to 6), C refers to core, and y refers to the project number. For example, D2C4 refers to field project number four obtained from district two in the state of Idaho.

A number of approaches were used in the literature to describe the field cracking performance including 1) cracking measurements (e.g., fatigue cracking area, number of traffic passes to achieve specific cracking area, etc. [5,12]), 2) numerical field performance indicator derived from Pavement Management Systems (PMS) data (e.g., Cracking Index

[CI] range between 0 and 100, where 0 indicates poor cracking performance and 100 indicates good cracking performance [13]), 3) subjective performance grouping derived from PMS data (e.g., good, fair, poor, and very poor field cracking groups [7]), and 4) subjective evaluation (e.g., cracked and uncracked field projects [9]).

In this study, the authors examined the available approaches to describe the field cracking performance of the selected field projects. ITD performs annual field evaluation to identify the existing pavement distress within their road network [14]. Two types of field surveys are used; windshield survey and profiler vehicle survey. The windshield survey incorporates numerical field performance indicator and subjective performance grouping, while the profiler survey incorporates cracking measurements, numerical field performance indicators and subjective performance grouping to describe the observed field cracking performance.

The collected cracking measurements and numerical field performance indicator were not useful to assess the performance of the selected field projects. The data was available for the period 2013 to 2017 only, but the study included field projects with age more than 4 years (e.g., D2C4). Therefore, the subjective performance grouping was used to describe the cracking performance of the selected field projects.

Table 5.1 presents the subjective performance grouping of the selected field projects. The evaluation demonstrated that eight field projects had good cracking resistance (e.g., D2C5, D2C6, D2C7, D2C8, D2C9, D2C10, D3C2, and D3C5), seven field projects had fair cracking resistance (e.g., D2C4, D2C11, D2C12, D3C3, D3C4, D6C1, and D6C2), and two field projects with poor cracking resistance (e.g., D2C13 and D5C2). None of these sections had any structural deficiency based on the collected information from ITD Material Engineers.

**Laboratory Evaluation**

Previous studies by the authors reviewed and evaluate various monotonic testing standards and promising performance indicators (Chapter 2 and Chapter 3) [10,11]. The studies evaluated four testing standards including ASTM D6931, ASTM D8044, ASTM D8225, and

AASHTO TP 124 and 12 performance indicators (i.e., total fracture energy determined from IDT test [$G_{fracture}$ {IDT}], total fracture energy determined from SCB test [$G_{fracture}${SCB}], cracking resistance index determined from IDT test [CRI {IDT}], cracking resistance index determined from SCB test [CRI {SCB}], flexibility index determined from IDT test [FI {IDT}], flexibility index determined from SCB test [FI {SCB}], indirect tensile strength [$IDT_{Strength}$], indirect tensile modulus [$IDT_{Modulus}$], indirect tensile asphalt cracking test [IDEAL-$CT_{Index}$ ], Nflex factor [Nflex], critical strain energy release rate [$J_C$], and Weibull cracking resistance index [$Weibull_{CRI}$ ]) were evaluated. Table 5.2 summarizes the concept and the formula used to evaluate the resistance of asphalt mixes to cracking.

In this study, the same monotonic cracking performance testing standards and indicators were used to assess the cracking resistance of cores extracted from the selected field projects. The field cores were 150 mm in diameter and had varied thicknesses. These cores were extracted from the shoulder or between the wheel path if there is no shoulder. In the laboratory, the top layer of the cores was trimmed to the required thickness (e.g., 50 mm for Indirect tension test [IDT]), if needed. Prior to testing, the thickness and air void content of the trimmed field cores were measured. The extracted field cores had a wide range of air void content and thicknesses (Figure 5.1). The air void content was between 2.85% to 9.78% with a Standard Deviation (SD) between 0.16 % and 4.25% (Figure 5.1-A) while the thickness varied between 40.6 mm and 54.4 mm with an SD between 0.2 mm and 1.23 mm (Figure 5.1-B).

**Table 5.1.** Identified field projects [15]

| # | District | Project ID | Location | | | | Mix properties | | | Observed field cracking performance group |
|---|---|---|---|---|---|---|---|---|---|---|
| | | | Route | Beginning MP | End MP | Construction Year | Mix type | NMAS | OBC % | |
| 1 | D2 | D2C4 | US95 | 366.6 | 373.2 | 2007 | Hveem | 19 | ** | Fair |
| 2 | | D2C5 | US95 | 242 | 251.1 | 2010 | SP4 | 19 | 5.29% | Good |
| 3 | | D2C6 | US95 | 222.4 | 223.3 | 2007 | SP3 | ** | ** | Good |
| 4 | | D2C7 | SH6 | 100 | 104 | 2007 | SP2 | ** | ** | Good |
| 5 | | D2C8 | US-95 | 233.5 | 239 | 2006 | SP3 | 19 | 5.00% | Good |
| 6 | | D2C9 | SH162 | 8 | 13 | 2007 | SP3 | 12.5 | ** | Good |
| 7 | | D2C10 | SH13 | 11.2 | 25.4 | 2007 | SP3 | 12.5 | 5.27% | Good |
| 8 | | D2C11 | US12 | 90.7 | 111.4 | 2009 | SP3 | 12.5 | ** | Fair |
| 9 | | D2C12 | US95 | 267.6 | 271.5 | 2007 | SP3 | 12.5 | 5.53% | Fair |
| 10 | | D2C13 | SH6 | 7.3 | 13.52 | 2010 | SP3 | 12.5 | 6.35% | Poor |
| 11 | D3 | D3C2 | US20/26 | 42.6 | 44 | 2016 | SP3 | 12.5 | 5.20% | Good |
| 12 | | D3C3 | SH55 | 44.7 | 51.7 | 2009 | SP4 | 12.5 | 5.49% | Fair |
| 13 | | D3C4 | SH44 | 19.4 | 21.8 | 2009 | SP4 | 12.5 | 5.56% | Fair |
| 14 | | D3C5 | SH44 | 14.3 | 16.2 | 2013 | SP4 | 19 | 4.72% | Good |
| 15 | D5 | D5C2 | US30 | 405.5 | 413.1 | 2016 | SP3 | ** | 5.00% | Poor |
| 16 | D6 | D6C1 | US-26 | 338.5 | 342 | 2010 | SP4 | 19 | 5.29% | Fair |
| 17 | | D6C2 | US-20/26/93 | 225 | 227 | 2006 | Hveem | ** | ** | Fair |

** Missing information

**Table 5.2.** Intermediate temperature cracking most promising performance indicators and its associate testing standards [11].

| # | Symbol | Testing standards | Performance Indicator Concept | Formula |
|---|---|---|---|---|
| 1 | $G_{fracture}$ (IDT) | ASTM -D6931 and D8225 | Total Fracture Energy | $G_{Fracture}^{Total} = \frac{W_{Fracture}^{Total}}{crack\ face\ area}$ |
| 2 | $G_{fracture}$ (SCB-FI) | AASHTO TP 124 | | |
| 3 | CRI (IDT) | ASTM -D6931 and D8225 | Cracking Resistance Index | $CRI = \frac{G_{Fracture}^{Total}}{P_{Peak}}$ |
| 4 | CRI (SCB-FI) | AASHTO TP 124 | | |
| 5 | FI (IDT) | ASTM -D6931 and D8225 | Flexibility Index | $FI = 0.01 * \frac{G_{Fracture}^{Total}}{\lvert m_{Inflection}^{Post-peak} \rvert}$ |
| 6 | FI (SCB-FI) | AASHTO TP 124 | | |
| 7 | IDEAL-$CT_{Index}$ | ASTM -D6931 and D8225 | IDEAL-$CT_{Index}$ | $IDEAL - CT_{Index} = \frac{G_{Fracture}^{Total}}{\lvert m_{75\%}^{Postpeak}) \rvert} \times \frac{t}{62} \times \varepsilon_v^{tolerance}$ |
| 8 | Nflex factor | ASTM -D6931 and D8225 | Nflex factor | $N_{flex} = \frac{Toughness}{m_{inflection}^{Postpeak}}$ |
| 9 | $IDT_{Strength}$ | ASTM -D6931 and D8225 | $IDT_{Strength}$ | $\sigma_{tesnile}^{IDT} = \frac{2000xP_{Peak}}{\pi \times t \times D}$ |
| 10 | $IDT_{Modulus}$ | ASTM -D6931 and D8225 | $IDT_{Modulus}$ | $IDT_{modulus} = \frac{\sigma_{Tensile}^{IDT}}{L_{Peak\ load}}$ |
| 11 | $J_c$ | ASTM D8044 | Strain energy release rate | $J_c = -\left(\frac{1}{t}\right)\frac{dU}{da}$ |
| 12 | $Weibull_{CRI}$(IDT) | ASTM -D6931 and D8225 | $Weibull_{CRI}$ | $Weibull_{CRI} = \left(\frac{\eta}{\beta}\right) \times log[A]$ |

where $crack\ face\ area$ is the crack face area for testing specimen ($mm^2$), $G_{Fracture}^{Total}$ is the total fracture energy ($J/m^2$), $W_{Fracture}^{Total}$ is the total work of fracture (J), $CRI$ is the Cracking Resistance Index performance indicator, $P_{Peak}$ is the peak load, FI is the Flexibility Index, $m_{\text{Inflection}}^{Post-peak}$ is the post-peak slope at the inflection point, IDEAL $-$ $CT_{\ Index}$ is the IDEAL-Cracking test index indicator, $m_{75\%}^{Postpeak}$ is the post-peak slope at 75% of the peak load, ${\varepsilon_v}^{tolerance}$ is the strain tolerance, t is the specimen thickness (mm), $L_{75\%}^{Postpeak}$ is the displacement at 75% of peak-load at post-peak curve, $P_{65\%}$ and $P_{85\%}$, is the post-peak load at 65% and 85% of the peak load (KN), respectively, $L_{65\%}$ and $L_{85\%,}$ is the displacement at 65% and 85% of the peak load (KN) respectively, and D is the specimen diameter (mm), $N_{flex}$ is the Nflex factor, $m_{\text{inflection}}^{Postpeak}$ is the tangent slope at post-peak inflection point (kPa/ %) calculated from stress-strain curve, toughness is the area under stress-strain curve until post-peak inflection point, ${\sigma_{tesnile}}^{IDT}$ is the tensile strength (kPa) determined from IDT test, D is the specimen diameter (mm), $IDT_{Modulus}$ is the ratio of the tensile strength to the displacement at the peak load (MPa), and $L_{Peak\ load}$ is the displacement at the peak load (mm), $J_c$ is the strain energy release rate ($kJ/m^2$), U is the strain energy to failure (kJ), t is the specimen thickness (mm), a is the specimen notch depth (mm), du/da is the variation of strain energy with notch depth (kJ/mm), $\beta$ is the shape parameter (Weibull slope), $\eta$ is the scale parameter, and *A* is the fitting constant equals to the area under the load-displacement curve

## 5.4. Results and Discussion

### *5.4.1. Correlation Between Laboratory Performance Indicators and Field Cracking Performance*

Figure 5.2 presents direct correlations between the laboratory testing results of various monotonic performance indicators and subjective cracking performance grouping of the selected field projects. In this figure, the performance groups were represented using bar colors. Field projects with good, fair, and poor observed field cracking resistance were represented in green, yellow, and red bars, respectively. In addition, the mean values of various performance indicators were also provided in Figure 5.2. The error bars represent ± one standard deviation (SD) from the mean value. Appendix C provides the correlation between all monotonic indicators and field performance.

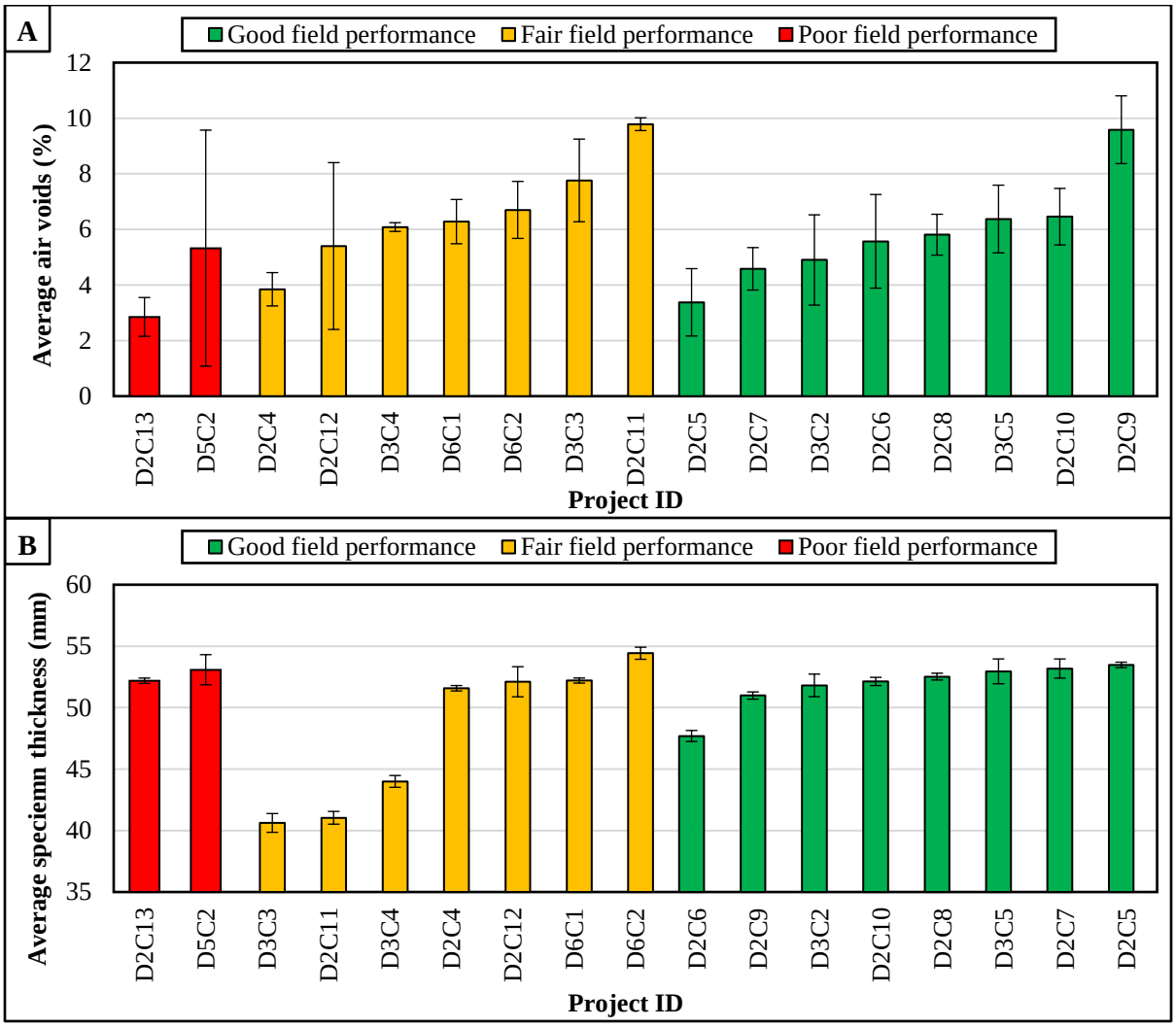


**Figure 5.1.** Measured (A) average Air void content, (B) average thickness for the extracted field cores

It can be observed from Figure 5.2 that none of these indicators was able to distinguish between project groups with different field cracking performance (i.e., good, fair, and poor). The laboratory testing results are overlapping; thus, it was not possible to identify the appropriate cut-off value to propose the performance thresholds.

In a previous study by the authors, the mechanistic (cyclic) fatigue cracking assessment test (i.e., Multi-Stage Semi-circle bending Dynamic [MSSD]) was able to distinguish between the same subjective field performance groups for the same selected field projects [15] (Chapter 4). The findings showed that MSSD performance indicators (i.e., slope [*z*] and Absolute intercept [Abs {log H}]) were able to distinguish between project groups with different field cracking performance (i.e., good, fair, and poor) and to develop pass/fail

performance thresholds. On the other hand, other studies by the authors reported that the same selected monotonic cracking resistance indicators provided proper cracking assessment using laboratory-prepared specimens [10,11] (Chapter 2 and Chapter 3). In light of previous results and findings, the authors believed that the monotonic performance assessment tests and indicators lack the ability to assess mix resistance to cracking using the extracted field cores due to effect of air voids and thicknesses of field cores.

Several research studies reported that variable air void content or thickness could provide misleading test results for several monotonic indicators (i.e., FI [SCB-FI] and CRI[SCB-FI]) [16–19]. The results demonstrated illogical variation in mix resistance to cracking with the variation in specimen air voids and thickness (i.e., higher air void content and thickness provides better resistance to cracking). These results explain the overlapping in the testing results of the extracted field cores (Figure 5.2) since the field cores had a wide range of air void content (2.85% - 9.78%) and specimen thickness (40.6 mm – 54.4 mm) as can be observed in Figure 5.1.

Previous studies by the authors addressed the fundamental meaning of the variation in the outputs of monotonic tests (i.e., load-displacement curve) in terms of the change in mix resistance to cracking [10,11] (Chapter 2 and Chapter 3). It was reported that the increase in the curve peak load, the pre- and the post-peak slope and the decrease in the terminal displacement of the load-displacement curve indicate declining in mix resistance to cracking.

These findings were used to evaluate the variation in the load-displacement curve with the change in specimen air void content and thickness. Figure 5.3-A and Figure 5.3-B show an example to illustrate the variation in the load-displacement curve due to the change in specimen air void content and thickness, respectively for semi-circle specimen using published data by Rivera (2017) [19].

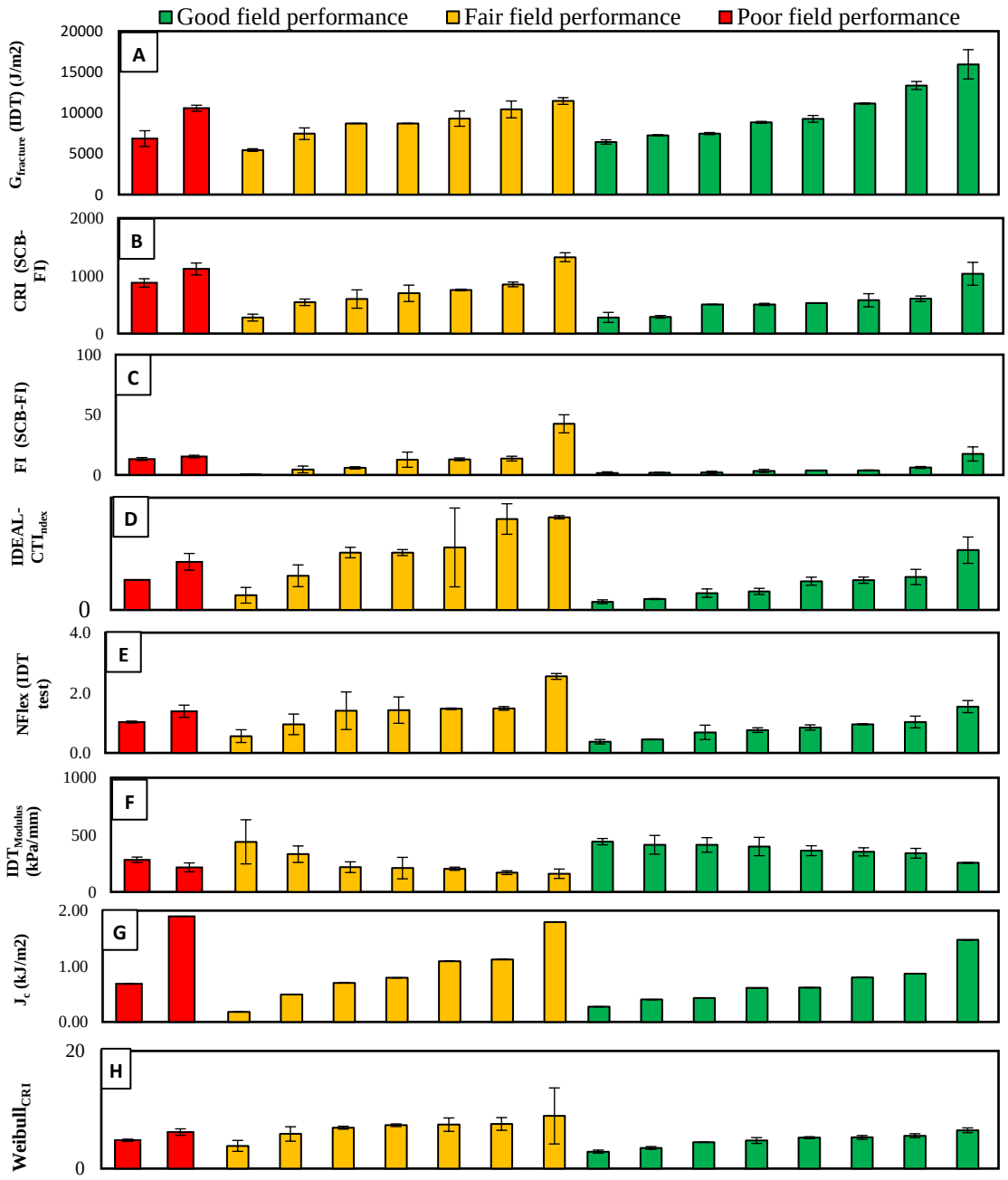


**Figure 5.2.** Correlation between subjective performance groups and (A) $G_{fracture}$ [IDT]), (B) CRI(SCB-FI), (C) FI (SCB-FI), (D) IDEAL-$CT_{Index}$, (E) Nflex, (F) $IDT_{Modulus}$, (G) $J_c$, and (H) $Weibull_{CRI}$

Figure 5.3-A shows the load-displacement curve for various air voids (i.e., 2%, 4%, 6%, 8%, and 10%). The curve peak, post-peak slope, pre-peak slope decreased, while the failure (termination) displacement increased as air voids decreased. Such changes indicate an overall declining in mix resistance to cracking. In other words, the variation in curve shape

with air void content exhibits improved cracking resistance which is not true based on our knowledge of the effects of air void on mix cracking resistance. The air void content plays an important role in the performance of asphalt mixes including the resistance to cracking. Linden et al. (1989) reported that a 1 % increment above the target air void content (i.e., 7 % initial air voids) resulted in a reduction of 10% in pavement life [20]. Tran et al. (2016) reported that a reduction of 1% in air void content improved the cracking resistance between 8.2% and 43.8% [21]. In addition, Kassem et al. (2011) reported that air void content distribution affected fatigue cracking resistance [22].

A similar conclusion was observed for the variation in specimen thickness (Figure 5.3-B). The curve peak, post-peak slope, and pre-peak slope increased with the increase in specimen thickness, which indicates overall positive effects on mix resistance to cracking. However, the performance indicators should be able to normalize the results based on specimen thickness. In light of this discussion, it can be concluded that these limitations are related to the outputs of the monotonic tests and are not related to a specific performance indicator.

### *5.4.2. Approaches to Enhance/Correct the Correlation Between Laboratory Performance Indicators and Field Cracking Performance*

The effect of these two factors (i.e., specimen air void content and thickness) on the testing results of the monotonic cracking performance indicators is critical when assessing field cores. The extracted field cores from different field projects are expected to have variable air void content and thickness, thus these factors may mislead the interpretation of the test outputs and provide an improper assessment. Therefore, a suitable approach(s) is needed to correct the data for each factor (i.e., air void content and thickness) to be able to correlate with the observed field cracking and develop performance thresholds. However, it is important to understand the type of correction approach needed for each factor (i.e., specimen air void and thickness), otherwise, it may worsen the correlation rather than enhancing it.

The variation in the thickness of the extracted field cores is related to different structure designs for each field project, but it is not related to the properties of the mixes.

Therefore, incorporating specimen thickness in the results of laboratory testing is not needed and shall be eliminated under the assumption that all field projects have adequate structural design. On the other hand, the variation in the air void content of the extracted field cores is related to different compaction efforts when constructing the section or traffic application during the section service life or both. However, the traffic effects can be eliminated (or reduced) by extracting the field cores from the road shoulders or between the wheel paths. The air void content is one of the key parameters that control the performance of the placed mix in the field, thus it shall be considered in the laboratory testing results. Therefore, the propose correction approach shall be able to eliminate the effects of specimen thickness and correct the variation trend line in testing results with specimen air void content.

Several approaches were proposed to normalize the laboratory testing results to a reference specimen thickness (i.e., 50 mm) as presented in Equations 5.1-5.3 [17–19]. Similarly, several approaches were also proposed to normalize the laboratory testing results to a reference specimen air void content (i.e., 7% or 6.5%) as presented in Equations 4 - 6 [17,18].

$$FI_{50} = FI_t \times \frac{t}{50} \quad \text{5.1 [17,18]}$$

$$CRI_{50} = CRI_t \times \frac{t}{50} \quad \text{5.2 [17]}$$

$$\text{IDEAL} - CT_{Index} = \frac{G_{Fracture}^{Total}}{\left| m_{75\%}^{Postpeak} \right|} \times \varepsilon_v{}^{tolerance} \times \frac{t}{62} \quad \text{5.3 [5]}$$

$$FI_{7\%} = FI_{AV} \times \frac{7\%}{AV\%} \quad \text{5.4 [17]}$$

$$FI_{7\%} = FI_{AV} \times \frac{0.0651}{AV\text{-}AV^2} \quad \text{5.5 [18]}$$

$$CRI_{7\%} = CRI_{AV} \times \frac{7\%}{AV\%} \quad \text{5.6 [17]}$$

where $FI_{50}$ is the adjusted flexibility index at a specimen thickness of 50 mm, $FI_t$ is the flexibility index at specimen thickness t, $CRI_{50}$ is the adjusted cracking resistance index at a

specimen thickness of 50 mm, $CRI_t$ is the cracking resistance index at specimen thickness t, IDEAL $-$ $CT_{Index}$ is the IDEAL-Cracking test index indicator, $m_{75\%}^{Postpeak}$ is the post-peak slope at 75% of the peak load, $\varepsilon_v{}^{tolerance}$ is the strain tolerance, t is the specimen thickness (mm), $L_{75\%}^{Postpeak}$ is the displacement at 75% of peak-load at post-peak curve, $P_{65\%}$ and $P_{85\%}$, is the post-peak load at 65% and 85% of the peak load (KN), respectively, $L_{65\%}$ and $L_{85\%}$, is the displacement at 65% and 85% of the peak load (KN) respectively, D is the specimen diameter (mm), $FI_{7\%}$ is the adjusted flexibility index at air void content of 7%, $FI_{AV}$ is the flexibility index at air voids of AV. AV% is the specimen air void content, $CRI_{7\%}$ is the adjusted CRI at specimen air voids of 7%, $CRI_{AV}$ is the CRI at air voids AV and AV% is the specimen air void content.

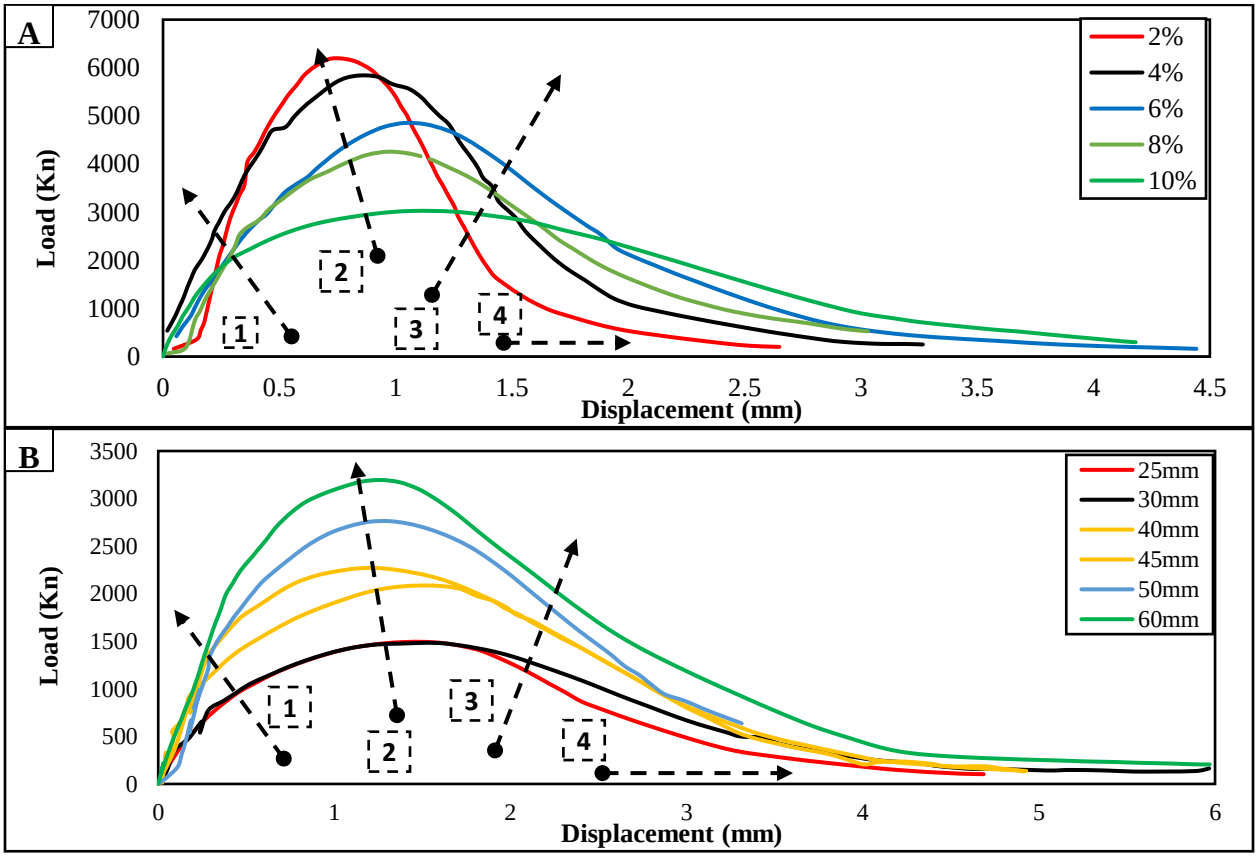


**Figure 5.3.** The variation in the load-displacement curve of SCB test with A) specimen air void content and B) specimen thickness; (1) increasing pre-peak slope, (2) increasing peak, (3) increasing post-peak slope, and (4) decreasing failure displacement using data published in Rivera (2017) [19]

In this study, the authors combined the proposed correction approaches as presented in Equation 5.7 to examine the correlation between the corrected laboratory testing results

and the subjective field performance groups. Figure 5.4 summarizes the correlation results of the selected indicators. Appendix C provides the corrected correlation between all monotonic indicators and field performance.

It can be observed that none of these indicators was able to correlate with the observed field cracking performance (or distinguish between different field performance groups) after the correction (Figure 5.4). The laboratory testing results are overlapping; thus, it was not possible to identify the appropriate cut-off value to propose the performance thresholds.

It should be noted that the proposed approaches were not always effective [17]. Kaseer et al (2018) found that the CRI (SCB) and FI(SCB) were still affected after correcting for air void contents. Perez. et al. (2018) indicated that the correction factor was to be applied when the air void content was less than 8% [23]. They observed that when the test specimen had air void contents higher than 8%, the SCB-FI test could not be considered as a fracture test.

$$X_{Corrected} = \mathrm{X} \times \frac{7\%}{\mathrm{AV}\%} \times \frac{\mathrm{t}}{50} \qquad 5.7$$

where AV% is the specimen air void content, X is the computed performance indicator, $X_{Corrected}$ .

*5.4.3. An Alternative Proposed Approach*

As discussed in the previous section, the available approaches to correct the laboratory testing results of the monotonic performance indicators for the extracted field cores had limited efficiency to enhance/correct the correlation between the laboratory testing results and the observed field cracking. In this study, the authors propose a new alternative approach to develop appropriate performance thresholds for monotonic performance indicators. The approach develops the thresholds indirectly using a correlation between dynamic testing and both field performance and various monotonic tests. First, they correlated field performance with a cyclic cracking assessment test called MSSD. Then, they used the correlation between

MSSD and various monotonic performance indicators and transferred the thresholds of the MSSD test to the monotonic performance indicators.

The approach consists of two main phases; Phase 1 and Phase 2. Phase 1 requires the selection of an appropriate cyclic cracking assessment test that is able to distinguish between different performance groups (i.e., good, fair, and poor performance groups). In addition, it requires developing performance thresholds for the performance indicators of the selected dynamic test using field cores. Phase 2 requires examining the correlation between the laboratory testing results of the dynamic performance indicators (Phase 1) and the monotonic performance indicators using laboratory-prepared specimens, thus the developed performance thresholds of the dynamic performance indicator are transferred to the monotonic performance indicators.

In this study, the MSSD cracking assessment test, which was developed by the authors [15] (Chapter 4), was selected as the mechanistic test for Phase 1. The MSSD performance indicators (i.e., slope [$z$] and Absolute intercept [Abs {log $H$}]) were able to correlate with the cracking performance in the field (i.e., good, fair, and poor) [15]. The authors proposed three performance thresholds were developed for each of MSSD performance indicators to distinguish between mixes with different performance group including; mixes with good estimated resistance to cracking to have ($z \leq 1.9$) or (Abs [log $H$]>3.60), mixes with fair estimated resistance to cracking to have ($1.9 < z \leq 2.9$) or ($3.0 <$ Abs [log $H$] $\leq 3.60$), and mixes with poor estimated resistance to cracking to have ($z > 2.9$) or (abs [log H] < 3.0).

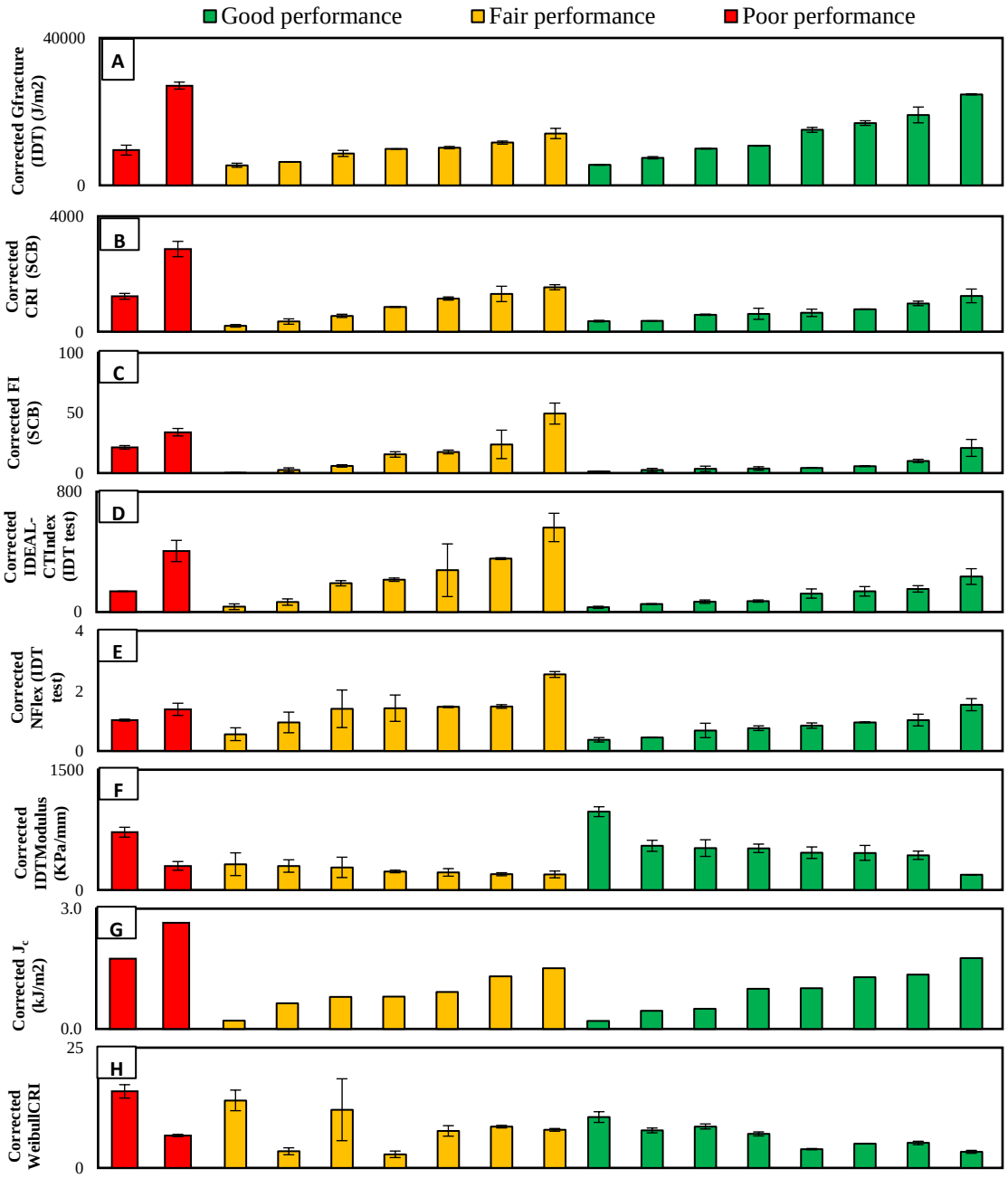


**Figure 5.4.** Correlation observed field project performance with corrected (A) $G_{fracture}$ [IDT]), (B) CRI(SCB-FI), (C) FI (SCB-FI), (D) IDEAL-$CT_{Index}$, (E) Nflex, (F) $IDT_{Modulus}$, (G) $J_c$, and (H) $Weibull_{CRI}$

In addition, the MSSD test and monotonic tests (Table 5.2) were performed using laboratory-prepared specimens prepared from 10 currently produced asphalt mixes in the state of Idaho (i.e., Plant-prepared-Laboratory Compacted [PMLC] mixes). Table 5.3 presents the properties of the selected PMLC mixes. The materials were collected from new paving projects and shipped to the laboratory. The specimens were prepared with a fixed air

void content range of 7% ± 0.5 and specimen thickness of 50 mm to eliminates the effect of these variables on the results of the monotonic tests, thus leading to better performance evaluation.

Figure 5.5-A illustrates an example of the correlation between MSSD performance indicators (i.e., slope [*z*] and Absolute intercept [Abs {log *H*}]) and $Weibull_{CRI}$ performance indicator calculated using the IDT test. The correlation between $Weibull_{CRI}$ performance indicator and MSSD slope (*z*) parameters provided $R^2$ of 0.81 and 0.51 for the MSSD absolute intercept [Abs (log *H*)]) parameters. Such correlations can be described using an exponential function (Equation 5.8). The $Weibull_{CRI}$ decreases with the slope while it increases with the absolute intercept. Both trend lines agree with the definition of each parameter/indicator. Higher $Weibull_{CRI}$, lower slope, and higher absolute intercept indicate better resistance to cracking [10,15] (Chapter 2 and Chapter 4).

**Table 5.3**. Properties of received PMLC materials

| # | District | Project ID | Mix Type | Specified Binder PG | Virgin Binder PG | Binder content Pb% | RAP % | NMAS |
|---|---|---|---|---|---|---|---|---|
| 1 | 1 | D1L1 | SP5 | 64-28 | 58-34 | 5.30% | 30% | 12.5 |
| 2 | 2 | D2L1 | SP3 | 70-28 | 64-34 | 5.70% | 50% | 12.5 |
| 3 | | D2L2 | SP3 | 64-28 | 58-34 | 5.70% | 30% | 12.5 |
| 4 | 3 | D3L1 | SP3 | 70-28 | 52-34 | 5.20% | 50% | 12.5 |
| 5 | | D3L2 | SP3 | 70-28 | 64-34 | 5.20% | 30% | 12.5 |
| 6 | | D3L3 | SP3 | 64-28 | 58-34 | 5.30% | 30% | 12.5 |
| 7 | | D3L4 | SP3 | 70-28 | 64-34 | 5.30% | 30% | 12.5 |
| 8 | | D3L5 | SP5 | 76-28 | 70-34 | 5.30% | 30% | 12.5 |
| 9 | 5 | D5L1 | SP5 | 70-28 | 70-28 | 4.80% | 30% | 19.0 |
| 10 | 6 | D6L1 | SP5 | 64-34 | 64-34 | 5.40% | 0% | 12.5 |

Since the slope provided a better correlation with $Weibull_{CRI}$, the next step was to transfer the MSSD performance thresholds to the $Weibull_{CRI}$ as illustrated in (Figure 5.5-B). The slope (*z*) parameter proposed three cracking resistance thresholds; good cracking resistance ($z \leq 1.9$), fair cracking resistance ($1.9 < z \leq 2.9$), and poor cracking resistance ($z > 2.9$). These thresholds were transferred to $Weibull_{CRI}$ using the correlation function between $Weibull_{CRI}$ and *z* performance indicators (Figure 5.5-B) [15]. Three thresholds for $Weibull_{CRI}$ were proposed, good cracking resistance group ($Weibull_{CRI} > 4.7$), fair cracking resistance group ($3.57 < Weibull_{CRI} \leq 4.7$), and poor cracking resistance group ($Weibull_{CRI} < 3.57$).

$$Y = B_1 \times e^{B_2 X} \quad 5.8$$

where $Y$ is MSSD indicators (slope, or absolute intercept), X is monotonic performance indicators, and $B_1$ and $B_2$ are exponential fitting constants

The same above procedures were repeated and followed with all other monotonic performance indicators (Table 5.2). Table 5.2 summarizes the correlation coefficients ($B_1$ and $B_2$), coefficient of determination ($R^2$), and the proposed thresholds for other monotonic performance indicators. Appendix D provides the correlation between MSSD indicators with all the monotonic indicators.

The results of Table 5.2 demonstrated that all monotonic indicators had better correlation (higher $R^2$) with the slope ($z$) as compared to the absolute intercept parameter. The best correlation was found between the slope ($z$) and $Weibull_{CRI}$ ($R^2$ of 0.8). Good correlations were found between the slope ($z$) and Nflex factor, CRI (IDT), FI (IDT), $IDEAL\text{-}CT_{Index}$, and $G_{fracture}$ (SCB-FI) with $R^2$ values of 0.62, 0.59, 0.57, 0.55, and 0.55, respectively. Fair correlations were found between the slope ($z$) and $J_c$ and $G_{fracture}$ (IDT), and with $R^2$ values of 0.46 and 0.38, respectively. Poor correlations were found between the slope ($z$) and CRI (SCB-FI), FI (SCB-FI), and $IDT_{Modulus}$ with $R^2$ values of 0.18, 0.13, and 0.10, respectively. No correlation was found between the slope ($z$) and $IDT_{strength}$ ($R^2$ of 0.01). Monotonic performance thresholds were proposed for $Weibull_{CRI}$, Nflex factor, CRI (IDT), FI (IDT), $IDEAL\text{-}CT_{Index}$, $G_{fracture}$ (SCB-FI), and $J_c$ and provided in Table 5.2.

The authors also compared the proposed performance thresholds for the selected monotonic cracking performance indicators with the thresholds proposed in the literature as available. West et al. (2017) recommended Nflex factor as a performance cracking indicator and specified a minimum threshold of 0.8 to have good cracking resistance [8]. This study proposed a threshold for Nflex of 0.7 for good cracking resistance which is close to the threshold recommended by West et al. (2017) [8]. Sreedhar et al. (2018) data showed that the FI (IDT) value of 27 was able to differentiate between cracked and uncracked mixes [9]. This study proposed a threshold of 22.6 for FI (IDT) for good cracking performance. Diefenderfer and Bowers (2019) proposed the $IDEAL\text{-}CT_{Index}$ to evaluate the cracking resistance of asphalt mixes and proposed a minimum threshold of 80 as initial performance criteria for Virginia

Department of Transportation (VDOT) [24]. This study proposed a threshold of 73.7 for IDEAL-$CT_{Index}$ to ensure good cracking resistance. Also, LADOT uses $J_c$ as a cracking resistance indicator and requires a minimum $J_c$ of 0.5 kJ/m$^2$ and 0.6 kJ/m$^2$ for Level-1 and Level-2 mix design, respectively [25]. In this study, a value of 0.6 for $J_c$ was established to ensure good resistance to cracking.

In general, the proposed performance thresholds were comparable to the ones proposed by other researchers for the respective indicators. These findings support the approach followed by the authors to determine the corresponding performance thresholds for selected monotonic tests to the ones developed using the MSSD test.

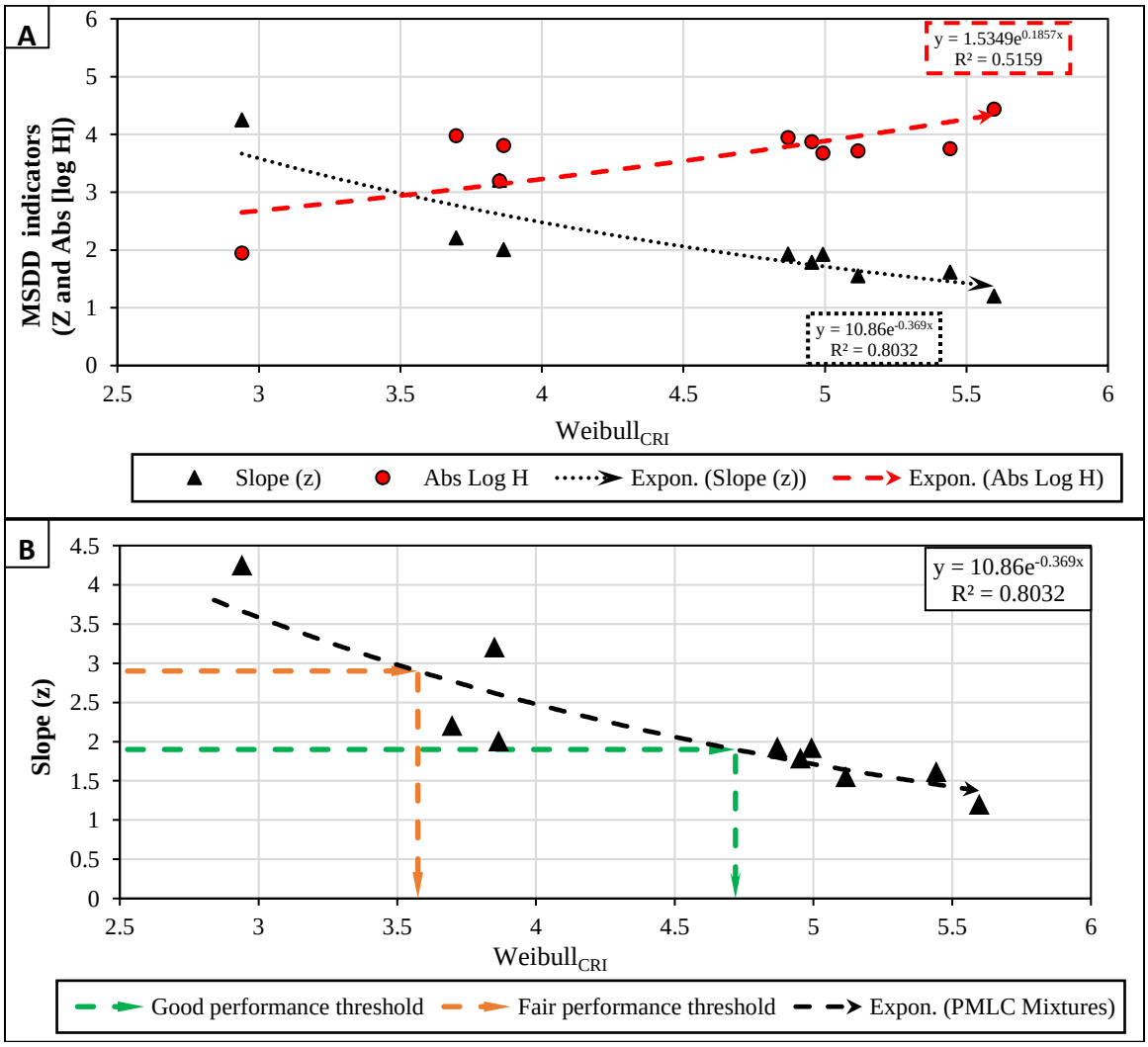


**Figure 5.5.** (A) Correlation between MSSD parameters (slope, and absolute intercept) and $Weibull_{CRI,}$(B) Proposed $Weibull_{CRI}$ performance thresholds based on the MSSD slope (*z*) parameter

**Table 5.4.** Correlation results between MSSD parameters and monotonic cracking resistance indicators

| Monotonic indicators | MSSD Indicators | | | | | | | | | Proposed thresholds in the literature | |
|---|---|---|---|---|---|---|---|---|---|---|---|
| | Slope ($z$) parameter | | | | | Absolute intercept value (Abs [Log H]) | | | | | |
| | Exponential Fitting | | | Proposed threshold (Minimum of) | | Exponential Fitting | | | Proposed threshold (Minimum of) | Threshold s | Ref. |
| | $B_1$ | $B_2$ | $R^2$ | Fair | Good | $B_1$ | $B_2$ | $R^2$ | | | |
| $G_{fracture}$ (IDT) | 5.18 | -1.24 E-4 | 0.38[3] | ---- | ---- | 2.22 | 5.85E-5 | 0.21 | - | | |
| $G_{fracture}$ (SCB-FI) | 7.08 | -5.77E-4 | 0.55[2] | 1546 | 2280 | 1.7 | 3.3E-4 | 0.46 | - | | |
| CRI (IDT) | 11.0 | -2.86E-3 | 0.59 | 466 | 614 | 1.56 | 1.3E-3 | 0.35 | - | | |
| CRI (SCB-FI) | 4.94 | -1.86E-3 | 0.18 | ---- | ---- | 2.02 | 1.07E-3 | 0.19 | - | | |
| FI (IDT) | 4.46 | -3.79E-2 | 0.57 | 11.4 | 22.6 | 2.48 | 1.74E-2 | 0.33 | - | 27 | [9] |
| FI (SCB-FI) | 2.80 | -6.68E-2 | 0.10 | ---- | ---- | 2.95 | 3.91E-2 | 0.09 | - | | |
| IDEAL-$CT_{Index}$ | 3.67 | -8.94E-3 | 0.55 | 26.4 | 73.7 | 2.70 | 4.16E-3 | 0.32 | - | 80 | [24] |
| Nflex factor | 4.60 | -1.21 | 0.62 | 0.40 | 0.70 | 2.49 | 0.533 | 0.30 | - | 0.8 | [8] |
| $IDT_{strength}$ | 2.85 | -3.23E-4 | 0.01[4] | ---- | ---- | 3.15 | 1.1E-4 | 0.00 | - | | |
| $IDT_{Modulus}$ | 0.68 | 3.47E-3 | 0.13 | ---- | ---- | 4.19 | -1.0E-3 | 0.03 | - | | |
| $J_c$ (kJ/m$^2$) | 3.60 | -1.03 | 0.46 | 0.20 | 0.60 | 2.57 | 0.588 | 0.37 | - | 0.5 and 0.6 | [6,25] |
| $Weibull_{CRI}$ | 10.8 | -0.36 | 0.8[1] | 3.6 | 4.7 | 1.53 | 0.18 | 0.51 | - | | |

[1] Green cell indicate good correlation ($R^2 \geq 0.80$),[2] yellow cells indicate fair correlation ($0.5 < r_s \leq 0.7$), [3] white cells indicate poor correlation ($0.1 < r_s \leq .5$), and [4] red cells indicate no correlation

## 5.5. Examine the Cracking Resistance of Currently Produced Asphalt Mixes in Idaho

The developed performance thresholds (i.e., good and fair performance thresholds) were used to assess the cracking resistance of 10 currently produced asphalt mixes in Idaho (Table 5.3). Table 5.5 presents the expected cracking resistance of the evaluated PMLC using the developed performance thresholds for monotonic (Table 5.2) and dynamic (i.e., slope [*z*] and Absolute intercept [Abs {log *H*}]) assessment performance indicators. It can be seen that all indicators demonstrated that D6L1 to have good resistance to cracking while D3L1 to have poor resistance to cracking. In addition, most of the performance indicators, except $J_c$ and $G_{fracture}$ (SCB-FI), indicated that D2L2, D3L2, and D5L1 to have good cracking resistance. Other mixes are expected to exhibit good or fair performance. Among all indicators, $Weibull_{CRI}$ assessment was similar to the MSSD performance assessment. In general, the currently produced mixes in the state of Idaho are expected to have good/fair resistance to cracking. Further monitoring of these sections is required.

**Table 5.5.** Estimated cracking resistance of currently produced mixes in the state of Idaho using the developed performance thresholds for monotonic and cyclic assessment tests

| Project ID | Estimated resistance to cracking | | | | | | | | |
|---|---|---|---|---|---|---|---|---|---|
| | Monotonic performance indicators | | | | | | | MSSD performance indicators | |
| | $J_c$ | $G_{fracture}$ (SCB-FI) | CRI (IDT) | FI (IDT) | IDEAL-$CT_{Index}$ | Nflex factor | $Weibull_{CRI}$ (IDT) | Slope (Z) | Abs log (H) |
| D6L1 | Good | Good | Good | Good | Good | Good | Good | Good | Good |
| D2L2 | Fair | Good | Good | Good | Good | Good | Good | Good | Good |
| D3L2 | Good | Fair | Good | Good | Good | Good | Good | Good | Good |
| D5L1 | Fair | Fair | Good | Good | Good | Good | Good | Good | Good |
| D2L1 | Fair | Good | Fair | Fair | Fair | Good | Good | Good | Good |
| D1L1 | Fair | Fair | Fair | Fair | Good | Fair | Good | Good | Good |
| D3L5 | Fair | Fair | Poor | Fair | Fair | Poor | Good | Good | Good |
| D3L4 | Fair | Fair | Fair | Fair | Fair | Fair | Fair | Good | Good |
| D3L1 | Poor | Poor | Poor | Poor | Fair | Poor | Poor | Poor | Poor |

## 5.6. Selection Recommendation of the Best Monotonic Performance Assessment Test(s) and Indicator(s) to Assess Asphalt Mix Resistance to Cracking

Among all the monotonic performance indicators, the $Weibull_{CRI}$ determined from IDT test had the best correlation with MSSD slope parameter ($R^2$ of 0.8), which is expected to provide more reliable performance thresholds. The authors recommend the selection of IDT and $Weibull_{CRI}$ as monotonic performance assessment test and indicator, respectively to assess cracking resistance of asphalt mixes. $Weibull_{CRI}$ indicator had the best correlation with MSSD indicators ($R^2$ of 0.8). Also, it was found by the authors to have the lowest variability in the test results, was sensitive to the variation in mix properties (e.g., binder content and PG), had good statistical grouping of mix properties, and was able to describe the entire load-displacement curve rather [10,11] (Chapter 2 and Chapter 4).

## 5.7. Conclusions and Recommendations

This research aimed to investigate the validity of the monotonic cracking resistance assessment tests and performance indicators in terms of ability to correlate with the observed field cracking and to develop pass/fail performance assessment thresholds in order to advance the implementation of PEMD or monotonic cracking performance assessment tests. A total number of 17 field test projects with known observed field cracking performance were selected across the state of Idaho. The laboratory evaluation included four monotonic cracking tests and 12 performance indicators. Based on the findings of this study, the following conclusions can be summarized:

- None of the monotonic cracking resistance indicators was able to provide direct correlation with the observed cracking performance in the field or to distinguish between field cores with good, fair, and poor performance.

- It was found that the monotonic performance assessment tests and indicators have shortcomings when they are calculated for field cores. The air voids and thickness have significant effects on the results of the monotonic cracking test. In addition, the proposed correction approaches in the literature to account for different air voids and thicknesses have limitations and are not effective.

- The study proposed an alternative approach to develop appropriate performance thresholds for monotonic performance indicators. Such an approach was found to be very helpful in developing performance thresholds for monotonic tests. In addition, it was found that the proposed performance thresholds of monotonic tests using the new approach were comparable to the ones proposed by other researchers.

- Among all monotonic performance indicators, the $Weibull_{CRI}$ was found to have the best correlation with the MSSD slope performance indicator ($R^2$ of 0.8), which is expected to provide more reliable performance thresholds. The authors recommend the selection of IDT and $Weibull_{CRI}$ as monotonic performance assessment test and indicator, respectively to assess the resistance of asphalt mixes to cracking. Three thresholds for $Weibull_{CRI}$ were proposed, good cracking resistance ($Weibull_{CRI} > 4.7$), fair cracking resistance ($3.57 < Weibull_{CRI} \leq 4.7$), and poor cracking resistance ($Weibull_{CRI} < 3.57$).

- The study further used the developed performance thresholds to assess the cracking resistance of currently produced mixes in Idaho. The results showed that these mixes are expected to show good to fair cracking performance in the field.

## 5.8. References

[1] R. Cominsky, G. a Huber, T.W. Kennedy, M. Anderson, The Superpave Mix Design Manual for New Construction and Overlays, Publication NO SHRP-S-407 Strategic Highway Research Program, U.S. (1994) 184.

[2] S. Buchanan, Balanced Mix Design (BMD) for Asphalt Mixtures, Presented at Econd Strategic Highway Research Program (SHRP2). (2016).

[3] R.C. West, C. Rodenzo, F. Leiva, F. Yin, Development of a framework for balanced mix design, NCHRP project 20-07/task 406, 2018. http://apps.trb.org/cmsfeed/TRBNetProjectDisplay.asp?ProjectID=4324.

[4] S. Buchanan, R.F. Bonaquist, J. Bukowski, C. Abadie, FHWA Asphalt Mixture Expert Task Group annual meeting, 2015.

[5] F. Zhou, S. Im, L. Sun, T. Scullion, Development of an IDEAL cracking test for asphalt mix design and QC/QA, Asphalt Paving Technology: Association of Asphalt Paving Technologists-Proceedings of the Technical Sessions. 86 (2017) 549–577. doi:10.1080/14680629.2017.1389082.

[6] L. Mohammad, S.B. Cooper, D. Ph, Balanced Mix Design for Asphalt Mixtures 3 - Part Webinar Series Part 3 : A case study of BMD implementation in Louisiana , Lessons learned Durability, in: Balanced Mix Design for Asphalt Mixtures Webinar, 2017.

[7] I. Al-Qadi, H. Ozer, J. Lambros, D. Lippert, A. El Khatib, T. Khan, P. Singh, J.J. Rivera-Perez, Testing protocols to ensure performance of high asphalt binder replacement mixes using RAP and RAS, 2015.

[8] R.C. West, C. Van Winkle, S. Maghsoodloo, S. Dixon, Relationships between simple asphalt mixture cracking tests using ndesign specimens and fatigue cracking at FHWA's accelerated loading facility, Road Materials and Pavement Design. 86 (2017) 579–602. doi:10.1080/14680629.2017.1389083.

[9] S. Sreedhar, E. Coleri, S.S. Haddadi, Selection of a performance test to assess the cracking resistance of asphalt concrete materials, Construction and Building Materials. 179 (2018) 285–293. doi:10.1016/j.conbuildmat.2018.05.258.

[10] H. Alkuime, E. Kassem, F. Bayomy, Development of a new performance indicator to evaluate the resistance of asphalt mixes to intermediate temperature cracking., Journal of Transportation Engineering, Part B: Pavements. (2019).

[11] H. Alkuime, F. Tousif, E. Kassem, F. Bayomy, Review and evaluation of intermediate temperature cracking testing standards and performance indicators for asphalt mixes., Construction and Building Materials. (2019).

[12] M. Kim, L.N. Mohammad, M. a. Elseifi, Characterization of fracture properties of asphalt mixtures as measured by semicircular bend test and indirect tension test, Transportation Research Record: Journal of the Transportation Research Board. 2296 (2012) 115–124. doi:10.3141/2296-12.

[13] L. Mohammad, M. Kim, H. Challa, Development of performance-based specifications for Louisiana asphalt mixtures, 2016. http://www.ltrc.lsu.edu/downloads.html.

[14] J. Poorbaugh, Idaho Transportation System Pavement Performance-2017 Report, (2017).

[15] H. Alkuime, E. Kassem, F.M. Bayomy, R. Nielsen, Development and evaluation of Multi-Stage Semi-circle bending Dynamic (MSSD) test to assess the cracking resistance of asphalt mixes., Construction and Building Materials. (2019).

[16] I. Al-Qadi, H. Ozer, J. Lambros, A. El Khatib, D. Singhvi, Testing Protocols to Ensure Performance of High Asphalt Binder Replacement Mixes Using RAP and RAS (Report No. R27-128), Urbana, IL: Illinois Center for Transportation, Illinois Dept. of Transportation. (2015).

[17] F. Kaseer, F. Yin, E. Arámbula-Mercado, A.E. Martin, J.S. Daniel, S. Salari, Development of an index to evaluate the cracking potential of asphalt mixtures using the semi-circular bending test, Construction and Building Materials. 167 (2018) 286–298. doi:10.1016/j.conbuildmat.2018.02.014.

[18] M. Barry, An analysis of impact factors on the Illinois flexibility index test, University of Illinois at Urbana-Champaign, 2016.

[19] J. Rivera-Perez, Effects of speciemn geometry and test configuration on the fracture process zone for asphalt materials, University of Illinois at Urbana-Champaign, 2017.

[20] R.N. Linden, J. Mahoney, N.C. Jackson, Effect of Compaction on Asphalt Concrete Performance, Transportation Research Board. (1989).

[21] N. Tran, P. Turner, J. Shambley, Enhanced compaction to improve durability and extend pavement service life : a literature review (NCAT Report 16-02R), 2016.

[22] E. Kassem, E. Masad, R. Lytton, A. Chowdhury, Influence of Air Voids on Mechanical Properties of Asphalt Mixtures Influence of Air Voids on Mechanical Properties of Asphalt Mixtures, Road Materials and Pavement Design. (2011) 37–41.

[23] J. Rivera-Perez, H. Ozer, I.L. Al-Qadi, Impact of specimen configuration and characteristics on illinois flexibility index, Transportation Research Record. 2672 (2018) 383–393. doi:10.1177/0361198118792114.

[24] S.D. Diefenderfer, B.F. Bowers, Initial approach to performance (balanced) mix design : the Virginia experience, Transportation Research Board. (2019). doi:10.1177/0361198118823732.

[25] Louisiana Department of Transportation and Development (LaDOT), Louisiana Standard Specification for Roads and Bridges, 2016.

# Chapter 6: Comprehensive Evaluation of Wheel-Tracking Rutting Performance Assessment Tests

Hamza Alkuime[1]; Emad Kassem[1];

(Submitted to International Journal of Pavement Research and Technology)

## 6.1. Abstract

This study aimed to advance the implementation of the most promising wheel-tracking rutting assessment tests in the newly proposed Balanced Mixed Design (BMD) (or Performance-Engineered Mix Design method [PEMD]). In order to achieve this goal, the study examined the validity of two rutting assessment tests (i.e. Hamburg Wheel Tracking test [HWTT], and Asphalt Pavement Analyzer [APA] rut test) and three performance indicators (i.e., HWTT rut depth after 15,000 passes [$HWTT_{15000}$], HWTT rut depth at 20,000 passes [$HWTT_{20000}$], and APA rut depth after 8,000 cycles [$APA_{8000}$]). A total number of 33 asphalt mixes including six Laboratory Mixed-Laboratory Compacted (LMLC), 10 Plant Mixed-Laboratory Compacted (PMLC), and 17 field projects were evaluated in this study. The results demonstrated that HWTT and APA rut test rutting performance indicators were sensitive to the variation in binder content and binder PG. Also, $APA_{8000}$ results had low/moderate variability, while $HWTT_{15000}$ and $HWTT_{20000}$ had moderate variability in test results. In addition, HWTT and APA rut test performance indicators were correlated with the rutting performance in the field. Several pass/fail performance assessment thresholds were proposed including maximum rut depth of 5 mm, 10 mm, and 12.5 mm for $APA_{8000}$, $HWTT_{15000}$, $HWTT_{20000}$, respectively. Also, the results showed that both HWTT and APA rut test to provide similar rutting assessment for the evaluated mixes. The study recommended using HWTT over APA rut test since HWTT can also assess asphalt mix moisture damage resistance. In addition, it is recommended to use $HWTT_{15000}$ over $HWTT_{20000}$ as a performance indicator, since it requires less testing time.

[1] Department of Civil and Environmental Engineering, University of Idaho, Moscow, ID 83844 USA.

## 6.2. Introduction

Although the main focus of the Superpave design system was to improve the rutting resistance of asphalt mixes, rutting is still considered major pavement distress in the United States [1]. Recently, a new design approach called Balanced Mix Design (BMD) or Performance-Engineered Mix Design (PEMD) is proposed to improve the resistance of asphalt mix to various distresses such as rutting and cracking. This design approach incorporates asphalt performance assessment test(s) to address specific pavement distress(s) during mix design and/or production process. A recent national survey showed that state Departments of Transportation (DOTs) are either currently implementing or interested in implementing PEMD approach. Also, state DOTs identified rutting as the second major pavement distress to be addressed using PEMD approach [1].

Several performance assessment tests are used to assess asphalt mix resistance to rutting. These tests have different approaches to simulate the rutting in the laboratory including repeated axial load tests (i.e., flow number [AASHTO T 378]), repeated shear load (i.e., Superpave shear tester [AASHTO T320]), or wheel-tracking load tests (i.e., Hamburg Wheel Tracking Test [HWTT] [AASHTO T324], and Asphalt Pavement Analyzer [APA] rut test [AASHTO T340]).

The wheel-tracking rutting assessment tests have better potential to assess asphalt mix resistance to rutting more than other rutting assessment tests. The survey showed that most state DOTs and contractors selected either HWTT or APA rut test to assess asphalt mix resistance to rutting [1]. In fact, currently, 21 state DOTs use either HWTT or APA rut test in their mix design specifications [1].

The same survey demonstrated that various state DOTs and contractors have concerns about the validity of available performance assessment tests (i.e., cracking and rutting). These concerns include 1) sensitivity of tests results to the variations in mix compositions (e.g, binder content), 2) variability of test results, 3) correlation between the laboratory testing results and observed field performance and ability to distinguish between different performance groups, and 4) ability to develop PEMD specifications (i.e., pass/fail performance assessment thresholds). Therefore, this study aimed to address the above

concerns through a comprehensive evaluation of two commonly used rutting resistance assessment tests (i.e., HWTT and APA rut test).

## 6.3. Study Objectives

This study aims to advance the implementation of PEMD through a comprehensive evaluation of two commonly used rutting resistance assessment tests (i.e., HWTT and APA rut test). The main objectives of this study are as follows:

- Review and document the requirements and performance indicators of both HWTT [AASHTO T324] and APA rut test [AASHTO T340].
- Evaluate the sensitivity of HWTT and APA rut test and their performance indicators to mix composition (i.e., variation in binder content and binder PG), the variability of test results, statistical grouping for mixes rutting performance, and correlation between both tests.
- Examine the correlation between the laboratory results and field rutting performance.
- Propose performance thresholds to ensure adequate rutting resistance for PEMD implementation.

## 6.4. Review Testing Standards

Both testing standards (i.e., HWTT and APA rut test) have standardized and non-standardized testing requirements. This section discusses the test requirements and documents the similarities and differences between each testing standards.

### *6.4.1. Standardized Testing Requirements*

Table 6.1 summarizes the test conditions and specimen geometry for both HWTT and APA rut test. In both tests, the test specimen is subjected to accelerated reciprocating wheel loading. HWTT loading wheels apply a 705 N load directly on the specimen surface at a rate of 52 pass/minute. The loading wheels of the APA rut test apply 578 N load on pressurized rubber hoses that have a constant pressure of 690 kPa at a rate of 60 cycle/minute. HWTT

requires conditioning the test specimens in a water bath for 30 to 60 minutes at a temperature specified by each agency, while APA rut test requires conditioning the specimen in air bath for six to 24 hours at a temperature equals to the high end of performance grade of the used binder. The HWTT can be used to assess moisture susceptibility in addition to rutting since the test specimen is conditioned in a water bath.

Both tests are performed on a cylindrical specimen that is 150 mm in diameter and 60 mm or 75 mm thickness for HWTT and APA rut test, respectively. In addition, HWTT can be run on slab specimens that have 320 mm length, 260 mm width and thickness from 38 mm to 100 mm. Meanwhile, the cylindrical specimens are commonly used since they require less preparation time and field cores can be tested. Both tests can evaluate four or six cylindrical specimens at once depending on the capability of the testing machine (e.g., Asphalt Pavement Analyzer [APA] uses three wheels, while Asphalt Pavement Analyzer-Junior [APA JR.] uses two-wheels). Extracted circular field cores can be evaluated and plastering materials are used if the field cores have a thickness less than the height of the testing mold.

Both tests collect the rut depth measurements (i.e., deformation) with the number of loading cycles or passes. Figure 6.1 shows typical cycle-deformation curves for HWTT and APA rut test. Rut depth measurements are collected at 11 and five locations along each wheel path for HWTT and APA rut test, respectively. HWTT test data follow an S-curve shape, where three phases can be identified; primary (pre-consolidation), secondary, and tertiary [2]. The primary phase shows a high deformation rate per pass due to initial specimen consolidation. This stage is usually completed within the first 1,000 cycles [2]. In the secondary phase, the deformation continues to increase but at a smaller constant rate (creep slope). The deformation in the secondary phase is due to plastic flow. The tertiary phase exhibits a rapid increase in the rate of deformation (stripping slope). The deformation in the tertiary phase could be due to both rutting plastic flow and moisture damage. In the APA rut test, there are only two phases; primary (pre-consolidation) and secondary phase.

**Table 6.1** Selected testing protocols for rutting assessments [16,22]

| Test | | HWTT | APA rut test |
|---|---|---|---|
| Testing Standards | | AASHTO T 324 | AASHTO T 340 |
| Specimen shape | | Cylindrical or slabs | Cylindrical or slabs |
| Number of specimens per test | | 4 | 4 or 6 |
| Specimen Diameter (mm) | | 150 | |
| Specimen thickness (mm) | Lab prepared | 60 | 75 |
| | Field Projects | Minimum of 38 | Minimum of 50 |
| Test temperature (°C) | | Specified temperature by the agency | High binder PG |
| Specimen conditioning | | Water bath | Air bath |
| Conditioning time (hour) | | 1 | 6 – 24 |
| Testing time (hour) | | ≈10 | ≈ 2 |
| Wheel type | | Solid steel | Concave wheel |
| Wheel speed (Pass/minute) | | 52 | 50 ± 5 |
| Load (N) | | 705 ± 4.5 | 578 |
| Number of data collection locations | | 11 locations | 5 locations |
| Test output | | Cycle-deformation curve | Cycle-deformation curve |
| Distress assessed | | Rutting and moisture damage | Rutting |
| Test termination | | 20,000 cycle or specified rut depth (i.e. 12.5 mm) | 8,000 cycle |

### *6.4.2. Non-Standardized Items*

Although most of the testing requirements have been standardized for both tests, there are some items that were not standardized and often specified by each agency. This section discusses these items and the current and preferred practice used by different transportation agencies for each item.

#### *6.4.2.1. Test termination point*

The test termination point is a prespecified limit to stop the test. The APA rut test is terminated after 8,000 cycles, while HWTT is terminated either after a specified number of passes or measured rut depth as specified by each agency. For instance, state DOTs in Utah and Washington specify the termination point as a maximum rut depth of 10 mm, while state DOTs in Texas, Illinois, Oklahoma, Massachusetts, and California specify the termination point as a maximum rut depth of 12.5 mm. On the other hand, state DOTs in Colorado and

Louisiana DOT specify the termination point as a maximum number of passes of 10,000 and 20,000, respectively. Table 6.2 and Table 6.3 summarize the termination point specified by different State DOTs [3,4,13–15,5–12].

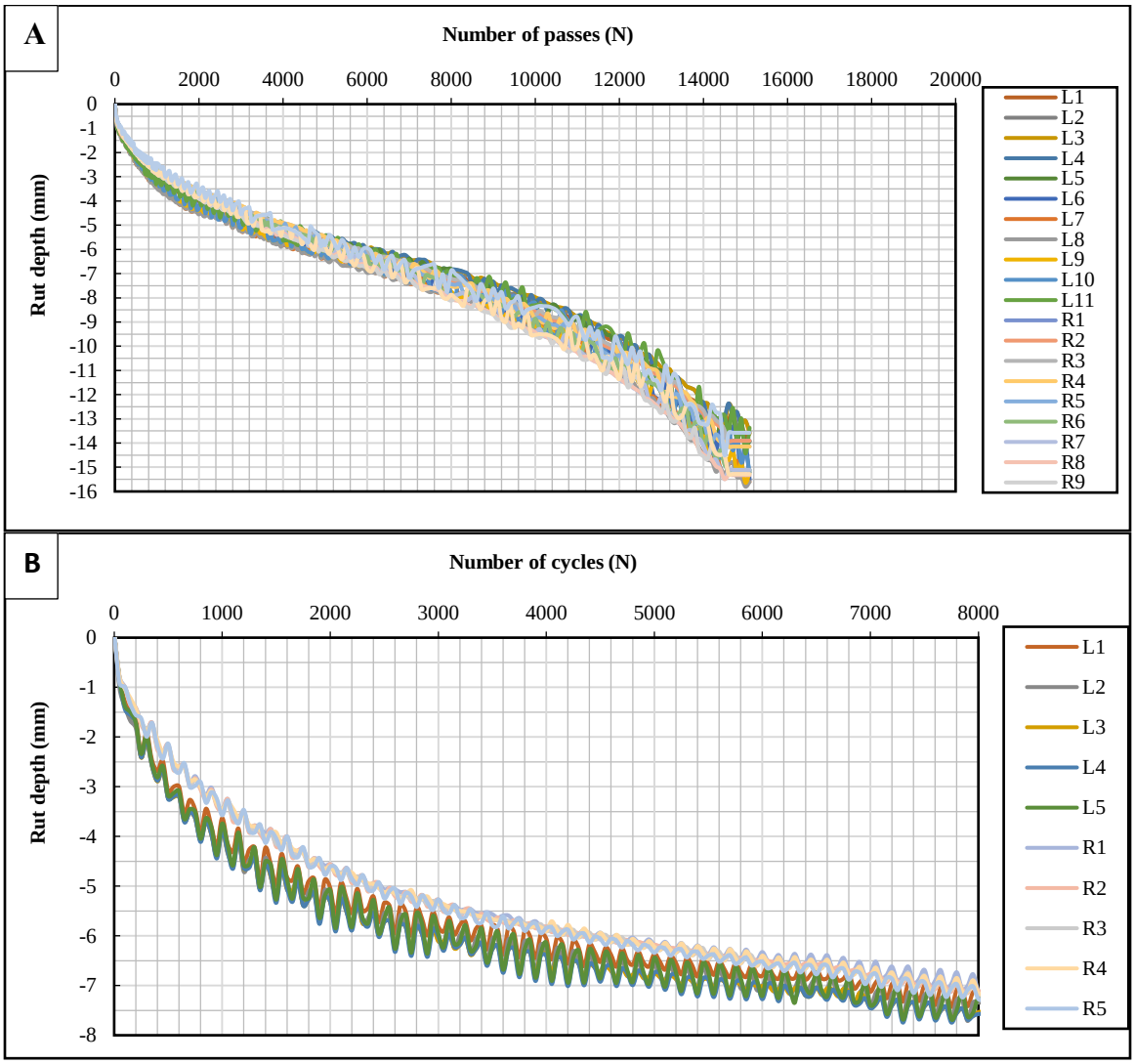


**Figure 6.1**. Cycle-deformation curves for A) HWTT and B) APA rut test, respectively

**Table 6.2.** HWTT rutting performance thresholds [3,4,13–15,5–12]

| Threshold type | Specified criteria | State | Test Temp. (°C) | Additional Distinguish criteria (i.e., binder PG, traffic level. | | | Limits |
|---|---|---|---|---|---|---|---|
| Minimum number of passes at specified rut depth | 10.0 mm | Utah | | *Binder PG* | | | |
| | | | 46 | PG 58-xx | | | 20,000 |
| | | | 50 | PG 64-xx | | | 20,000 |
| | | | 54 | PG 70-xx | | | 20,000 |
| | | Washington | 50 | *Traffic level ESAL's [millions])* | | | |
| | | | | < 0.3 | | | 10,000 |
| | | | | 0.3 to 3 | | | 12,500 |
| | | | | ≥3 | | | 15,000 |
| | 12.5 mm | Texas | | *Binder PG* | | | |
| | | | | PG 64-xx or lower | | | 10,000 |
| | | | | PG 70-xx | | | 15,000 |
| | | | | PG 76-xx or higher | | | 20,000 |
| | | Illinois | | *Binder PG* | | | |
| | | | | PG 58-xx | | | 5,000 |
| | | | | PG 64-xx | | | 7,500 |
| | | | | PG 70-xx | | | 15,000 |
| | | | | PG 76-xx or higher | | | 20,000 |
| | | Oklahoma | | *Binder PG* | | | |
| | | | | PG 64-xx | | | 10,000 |
| | | | | PG 70-xx | | | 15,000 |
| | | | | PG 76-xx | | | 20,00 |
| | | Massachusetts | | *Traffic level* | | | |
| | | | | 1 | | | 10,000 |
| | | | | 2 and 3 | | | 15,000 |
| | | California | | *Binder PG* | | | |
| | | | 45 | PG 58-xx | | | 10,000 |
| | | | 50 | PG 64-xx | | | 15,000 |
| | | | 55 | PG 70-xx | | | 20,000 |
| | | | | PG 76-xx or higher | | | 25,000 |
| | 13 mm | Montana | | *Binder PG* | | *Mix type* | |
| | | | 44 | PG 58-28 | | Plant mix | 10,000 |
| | | | | | | Mix design | 15,000 |
| | | | 50 | PG 64-22 and PG 64-28 | | Plant mix | 10,000 |
| | | | | | | Mix design | 15,000 |
| | | | 56 | PG 70-28 | | Plant mix | 10,000 |
| | | | | | | Mix design | 15,000 |
| | At the inflection point | California | | *Binder PG* | | | |
| | | | 45 | PG 58-xx | | | 10,000 |
| | | | 50 | PG 64-xx | | | 10,000 |
| | | | 55 | PG 70-xx | | | 12,500 |
| | | | | PG 76-xx or higher | | | 15,000 |
| | | IOWA | | *Binder PG* | | *Traffic* | |
| | | | 40 | PG 52-xx and PG 58-xx | | Small | 10,000 |
| | | | | | | High and very high | 14,000 |
| | | | 50 | All other binder PG | | Small | 10,000 |
| | | | | | | High and very high | 14,000 |
| | | | | | | High and very high | 14,000 |
| Maximum rut depth at specified number of cycles | 10,000 | Colorado | | *Binder PG* | | | |
| | | | 45 | PG 58-xx | | | 4 mm |
| | | | 50 | PG 64-xx | | | |
| | | | 55 | PG 70-xx or PG 76-xx | | | |
| | 20,000 | Louisiana | 50 | *NMAS(mm)* | *Mix type* | *Traffic level* | |
| | | | | 12.5 | Incidental paving | A | 10 |
| | | | | 25.0 | ATB | 1 | 10 |
| | | | | 12.5 | Wearing course | 1 | 10 |
| | | | | | | 2 | 6 |
| | | | | 19.0 | Wearing course | 2 | 6 |
| | | | | | Binder course | 1 | 10 |
| | | | | | | 2 | 6 |
| | | | | 25.0 | Binder course | 1 | 10 |
| | | | | | | 2 | 6 |
| | | | | | Base course | 1 | 12 |

**Table 6.3** APA rut pass/fail performance thresholds [23,24,33–39,25–32]

| Threshold type | Test Temp. (°C) | State DOT | Additional Distinguish criteria (i.e., binder PG, traffic level. etc.) | | | Limits (Max. rut depth [mm]) |
|---|---|---|---|---|---|---|
| Maximum rut depth at specified at 8,000 loading cycles | Binder High PG Temp. | Idaho | All mixes (SP3, SP5) | | | 5.0 |
| | | Alabama | SMA mixes and HMA with traffic ESALs between 1.0E7 and 3.0E7 | | | 4.5 |
| | | North Carolina | Binder PG | Mix type | Design traffic (xE6) | |
| | | | PG 64-22 | S4.75A | <1 | 11.5 |
| | | | | SF9.5A | <1 | 11.5 |
| | | | | S9.5B | 0.3-3 | 9.5 |
| | | | PG 70-22 | S9.5C | 3-30 | 6.5 |
| | | | PG 76-22 | S9.5D | >30 | 4.5 |
| | | South Dakota | Mix type (Design gyration) | | | |
| | | | Q1 (40) | | | 8.0 |
| | | | Q2 (50) | | | 7.0 |
| | | | Q3 (60) | | | 6.0 |
| | | | Q4 (70) and Q5 (80) | | | 5.0 |
| | 40 | Alaska | All mixes | | | 3.0 |
| | 49 | Virginia | Mix designation | | | |
| | | | A | | | 7.0 |
| | | | D | | | 5.5 |
| | | | E | | | 3.5 |
| | | Georgia | 19.0 mm and 25.0 mm NMAS mixes | | | 5.0 |
| | | Ohio | Non-polymer mixes | | | 5.0 |
| | 54.4 | | Surface mixes | | | 5.0 |
| | | | High-stress mixes | | | 3.0 |
| | 64 | | BDWASC5 | | | 4.0 |
| | | Georgia | NMAS | Mix type | | |
| | | | 4.75 | NA | | 8.0 |
| | | | 9.50 | Type I | | |
| | | | 9.50 | Type II | | 6.0 |
| | | | 12.5 | NA | | 5.0 |
| | | Arkansas | Mix design gyration | | | |
| | | | 75 and 115 | | | 8.0 |
| | | | 160 | | | 5.0 |
| | | | 205 | | | 5.0 |
| | | Oregon | Binder PF | Mix type | | |
| | | | PG 58-xx | Level 3 | | 6.0 |
| | | | PG 64-xx | Level 3 | | 6.0 |
| | | | | Level 4 | | 5.0 |
| | | | PG 70-xx | Level 3 | | 5.0 |
| | | | | Level 4 | | 4.0 |
| | | South Carolina | Binder PG | Course type (Application | | |
| | | | PG 76-22 | surface course (interstate /intersections) and intermediate course (intersection) | | 3.0 |
| | | | PG 64-22 | surface course (high and low volume primary) and intermediate course (interstate / high volume primary) | | 5.0 |
| | | NJDOT | Mix type (production phase or binder PG) | | | |
| | | | High-performance thin overlay (mix design) and high RAP mixes (PG 76-22) | | | 4.0 |
| | | | High-performance thin overlay (mix production) and bituminous rich-base course | | | 5.0 |
| | | | Bituminous rich intermediate course (mix design) | | | 6.0 |
| | | | Bituminous rich intermediate course (mix production) and high RAP mixes (PG 64-22) | | | 7.0 |
| | | | Bridge deck waterproofing asphalt surface course | | | 3.0 |

#### *6.4.2.2. Performance* Indicators

Several rutting performance indicators are proposed to analyze the rut depth plot (change of rut depth with the number of passes or cycles). The performance indicators of the APA rut test consider the overall average rut depth after 8,000 cycles, while the performance indicators of HWTT consider the rut depth at specified number of passes (e.g., 20,000 passes) or the number of passes at a specified rut depth (e.g., 12.5 mm). In addition, it may include the creep slope, strip slope and stripping inflection point. The creep slope is the slope of the secondary stage of the S-curve shape, while the strip slope is the slope of the tertiary stage of the S-curve. The stripping inflection point is the intercepting point between the creep and strip slops.

Most state DOTs either use a maximum rut depth at a specific number of passes/cycles or a minimum number of cycles at a specified rut depth. For example, Idaho Transportation Department (ITD) specifies a maximum rut depth of 5 mm at 8,000 cycles in the APA rut test, while Utah DOT specifies a minimum number of passes of 20,000 at 10 mm rut depth in the HWTT test. Table 6.2 and Table 6.3 summarize the selected performance indicators selected by various state DOTs [3,4,13–15,5–12].

#### *6.4.2.3. Test Temperature*

Each of APA rut test and HWTT is performed at different test temperature. According to AASHTO T340 (APA rut test), “The test temperature shall be set to the high temperature of the standard Superpave performance-grade (PG) binder identified by the specifying agency for the project for which the HMA is intended. For circumstances where the high-temperature binder grade has been increased, the APA test temperature will remain at the standard PG binder high temperature”. While according to AASHTO T324-16 (HWTT) “The specimen is submerged in a temperature-controlled water bath at a temperature specified by the agency”. The APA rut test (AASHTO T340) is performed at a temperature equals to the high end of utilized binder PG, while the HWTT (AASHTO T324) is performed at a specified fixed temperature that is often selected by each agency regardless of mix properties (i.e., binder PG).

Currently, there are 11, and ten state DOTs use the HWTT and APA rut test, respectively as presented in Table 6.2 and Table 6.3. Most of the state DOTs that use the HWTT specify a fixed single test temperature irrespective of the binder PG (e.g., state DOTs in Washington, Texas, Illinois, Oklahoma, and Massachusetts conduct the test at 50 °C). While, some state DOTs specify different temperatures based on binder PG (e.g., Utah DOT conduct the test at 46 °C for PG 58-xx, and at 50 °C for PG 64-xx, and at 54 °C for PG 70-xx).

Most of the state DOTs that use APA rut test specify a fixed test temperature rather than specifying a test temperature equivalent to the high binder PG as required by AASHTO 340 (Table 6.2 and Table 6.3). State DOTs in Alaska, Virginia, Georgia, Ohio, Arkansas, Oregon, South Carolina, and New Jersey specify a fixed temperature, while state DOTs in Idaho, Alabama, North Carolina, and South Dakota specify a test temperature equivalent to the high binder PG in accordance to AASHTO 340. It can be concluded that most state DOTs prefer to conduct either HWTT or APA rut test at a fixed test temperature rather than a test temperature equivalent to the high binder PG.

#### *6.4.2.4. Performance Thresholds*

The HWTT performance threshold is specified as either a minimum number of passes at a specified rut depth or a maximum rut depth at a specified number of cycles, while the APA rut test performance threshold is specified as maximum rut depth at 8,000 loading cycles. Several state DOTs use additional classification criteria (e.g., binder PG, traffic level, etc.) to add more detailed limits. For instance, Washington State DOT specifies a minimum number of passes at maximum rut depth of 10 mm based on the traffic levels (i.e, 10,000 passes for 0.3 million ESALs, 12,500 passes for 0.3 to 3 million ESALs, and 15,000 pass for 0.3 to 3 million ESALs). Table 6.2 and summarize the performance assessment thresholds specified by various State DOTs [3,4,13–15,5–12].

## 6.5. Experimental Testing Plan

In order to achieve the objectives of this study, the authors designed and conducted a comprehensive experimental testing plan (Figure 6.2). The HWTT and APA rut test were

conducted on laboratory-prepared specimens and extracted field cores. The testing program included six Laboratory Mixed-Laboratory Compacted (LMLC), 10 Plant Mixed-Laboratory Compacted (PMLC) mixes, in addition to field cores extracted from 17 field pavement projects with known field rutting performance. Table 6.4 summarizes the main characteristics of these test mixtures. This section discusses the properties of the test mixtures.

### *6.5.1. Laboratory Mixed-Laboratory Compacted (LMLC) mixes*

Six LMLC mixes were prepared to examine the sensitivity of HWTT and APA rut tests and their performance indicators to mix composition (e.g., variation in binder PG and content), test variability, and the correlation between APA rut test and HWTT rut results. LMLC mixes were prepared using two binder PG (i.e., PG 58-34 and PG 70-28) and three binder contents (Optimum Binder Content [OBC] [i.e., 4.25%], OBC-0.75% [i.e., 5.00%], and OBC+0.75% [i.e., 5.75%]). Other mix properties were kept constant for all test mixes (Table 6.4). LMLC mixes are referred to as PGXX-YY% where PGXX refers to high-temperature binder PG and YY% refers to binder content. For example, PG58-5.00% means mix was prepared with binder PG of 58-34 and binder content of 5.00%.

### *6.5.2. Plant Mixed-Laboratory Compacted (PMLC) mixes*

The research also evaluated 10 PMLC mixes obtained from new paving projects in the state of Idaho. Loose materials were sampled and delivered in boxes to the laboratory. Details on mix properties are provided in Table 6.4 and Table 6.3 The testing results of PMLC mixes were used to 1) identify any concerns related to the rutting performance and moisture damage of asphalt mixes currently produced in the state of Idaho, 2) evaluate indicators statistical grouping for mixes rutting performance, 3) examine tests and indicators variability, and 4) study the correlation between rutting performance indicators of the HWTT and APA rut test. PMLC mixes are referred to as DxLy, where “x” refers to district and “y” refers to the project number. For example, D2L1 means project number one that obtained from district two in the state of Idaho.

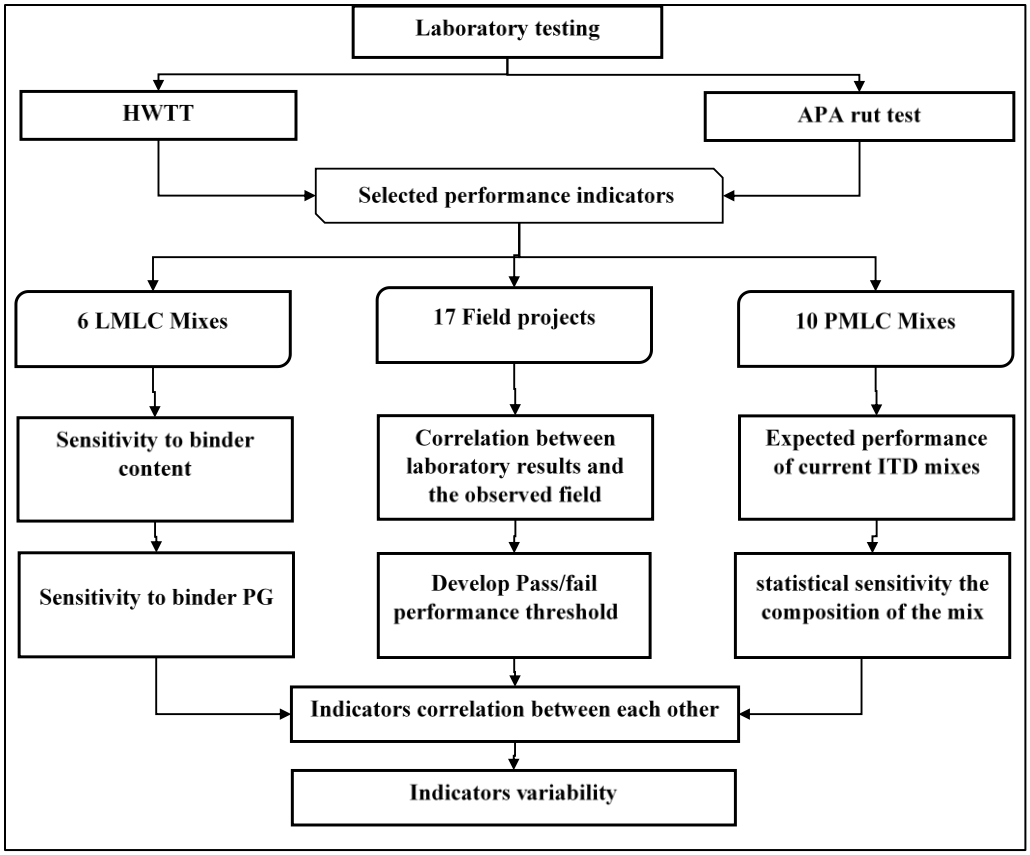


**Figure 6.2**. Study experimental design

*6.5.3. Field Projects*

The field cores were extracted from sites identified by ITD Material Engineers based on a survey that was sent to them. In their responses, they identified field projects with different performance (e.g., good, fair, and poor) to rutting. A total number of 17 field projects were identified. ITD Material Engineers provided relevant information about the field projects (e.g., construction year, mix design, binder PG, and age) as presented in Table 6.4.

The field cores were extracted using a 150-mm coring bit from the shoulder of the test sections or between the wheel path if the road had no shoulder. Upon receiving the cores, the top layer was cut to the target thickness (60 mm and 75 mm for HWTT and APA rut test [Table *6.1*]). However, some field cores were plastered as recommended in AASHTO T340 and T324 to meet the required thickness for those thin cores (less than 60 mm and 75 mm for HWTT and APA rut test (Table 6.1). Figure 6.3 illustrates the procedures followed to prepare HWTT test specimens.

**Table 6.4** Properties of evaluated asphalt mixes

| # | Type | Project ID | Mix properties | | | | | |
|---|---|---|---|---|---|---|---|---|
| | | | Construction Year | Mix type | NMAS | OBC % | RBR% | Design Binder PG |
| 1 | LMLC | PG 70-4.25% | - | SP3 | 12.5 | 4.25% | 0 % | 70-28 |
| 2 | | PG 70-5.00% | - | SP3 | 12.5 | 5.00% | 0 % | 70-28 |
| 3 | | PG 70-5.75% | - | SP3 | 12.5 | 5.75% | 0 % | 70-28 |
| 4 | | PG 58-4.25% | - | SP3 | 12.5 | 4.25% | 0 % | 58-34 |
| 5 | | PG 58-5.00% | - | SP3 | 12.5 | 5.00% | 0 % | 58-34 |
| 6 | | PG 58-5.75% | - | SP3 | 12.5 | 5.75% | 0 % | 58-34 |
| 7 | PMLC | D1L1 | 2017 | SP5 | 12.5 | 5.30% | 30% | 64-28 |
| 8 | | D2L1 | 2017 | SP3 | 12.5 | 5.70% | 50% | 70-28 |
| 9 | | D2L2 | 2018 | SP3 | 12.5 | 5.70% | 30% | 64-28 |
| 10 | | D3L1 | 2017 | SP3 | 12.5 | 5.20% | 50% | 70-28 |
| 11 | | D3L2 | 2017 | SP3 | 12.5 | 5.20% | 30% | 70-28 |
| 12 | | D3L3 | 2017 | SP3 | 12.5 | 5.30% | 30% | 64-28 |
| 13 | | D3L4 | 2017 | SP3 | 12.5 | 5.30% | 30% | 70-28 |
| 14 | | D3L5 | 2017 | SP5 | 12.5 | 5.30% | 30% | 76-28 |
| 15 | | D5L1 | 2017 | SP5 | 19.0 | 4.80% | 30% | 70-28 |
| 16 | | D6L1 | 2017 | SP5 | 12.5 | 5.40% | 0% | 64-34 |
| 17 | Field projects | D2C4 | 2007 | Hveem | 19 | ** | ** | 58-28 |
| 18 | | D2C5 | 2010 | SP4 | 19 | 5.29% | 17.00% | 64-28 |
| 19 | | D2C6 | 2007 | SP3 | ** | ** | ** | 70-22 |
| 20 | | D2C7 | 2007 | SP2 | ** | ** | ** | 58-28 |
| 21 | | D2C8 | 2006 | SP3 | 19 | 5.00% | 0.00% | 70-28 |
| 22 | | D2C9 | 2007 | SP3 | 12.5 | ** | ** | 58-28 |
| 23 | | D2C10 | 2007 | SP3 | 12.5 | 5.27% | 0.00% | 64-28 |
| 24 | | D2C11 | 2009 | SP3 | 12.5 | ** | ** | 58-28 |
| 25 | | D2C12 | 2007 | SP3 | 12.5 | 5.53% | 0.00% | 64-28 |
| 26 | | D2C13 | 2010 | SP3 | 12.5 | 6.35% | 17.00% | 58-28 |
| 27 | | D3C2 | 2016 | SP3 | 12.5 | 5.20% | 50.00% | 76-28 |
| 28 | | D3C3 | 2009 | SP4 | 12.5 | 5.49% | 11.50% | 64-28 |
| 29 | | D3C4 | 2009 | SP4 | 12.5 | 5.56% | 9.00% | 64-28 |
| 30 | | D3C5 | 2013 | SP4 | 19 | 4.72% | 28.40% | 64-28 |
| 31 | | D5C2 | 2016 | SP3 | ** | 5.00% | 62.2% | 64-34 |
| 32 | | D6C1 | 2010 | SP4 | 19 | 5.29% | 17.00% | 64-34 |
| 33 | | D6C2 | 2006 | Hveem | ** | ** | ** | 64-34 |

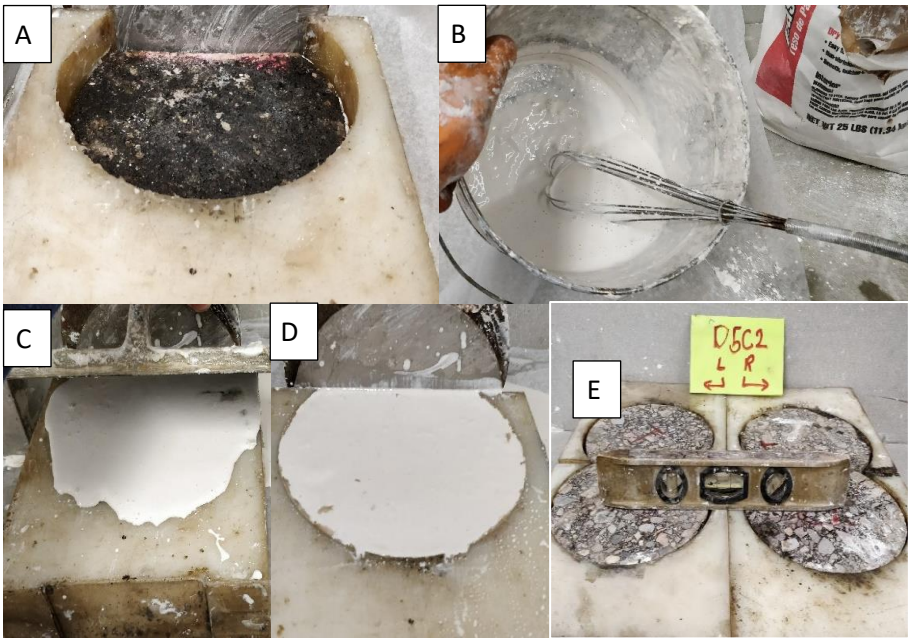


**Figure 6.3.** Hamburg test specimen preparation; a) placing the specimen in the casting mold, b) mixing the plastering materials, c) filling the gap with plastering materials and smoothing the surface, d) the bottom surface after plastering, e) levelling the Hamburg test specimens.

## 6.6. Rutting Performance Evaluation

The authors conducted accelerated rutting tests (i.e., APA and HWTT) in the laboratory to assess the performance of LMLC, PMLC, and field cores. In addition, they collected information about the rutting performance of the selected field projects. This section discusses the selected laboratory testing conditions and performance indicators, and the collected observed field rutting evaluation data.

### *6.6.1. Laboratory Rutting Evaluation*

In this study, both tests were performed using the Asphalt Pavement Analyzer-Junior (APA Jr.) device. The testing temperature for the HWTT was fixed at 50 °C for various asphalt mixes, while it varies based on the higher PG temperature for the APA rut test. The HWTT test was terminated either after 20,000 passes or 12.5 mm measured rut depth was achieved, while the APA rut test was terminated after 8,000 cycles. The rut depth (deformation) was collected at 11 and 5 locations along each wheel for HWTT and APA rut test, respectively. The average rut depth of all locations was reported for both tests as recommended by

AASHTO T324 and AASHTO T340 [16]. Other testing standards requirements were followed as specified.

Three different rutting performance assessment indicators were considered including the HWTT rut depth after 15,000 passes ($HWTT_{15000}$), the HWTT rut depth at 20,000 passes ($HWTT_{20000}$), and the APA rut depth after 8,000 cycles ($APA_{8000}$). In addition, mixes moisture susceptibility was evaluate using HWTT testing results.

### *6.6.2. Field Rutting Evaluation*

ITD performs an annual field pavement surface evaluation [17]. Two evaluation methods are often used; windshield survey and profiler vehicle survey. Windshield survey involves visual inspection of the pavement surface while driving on the road. The profiler survey incorporates scanning the pavement surface using the profiler vehicle and collects information related to several performance measures [18]. In this study, the authors collected information about the rutting performance such as video logs collected by the profiler vehicle and Agile Assets Transportation Asset Management System (TAMS database) managed by ITD [17].

Since the application of surface treatments improves the surface conditions, the rutting measurements over time are needed to accurately evaluate the performance of the field projects. However, the rutting measurements were available for the last four years from the video logs only. Therefore, the rutting measurements calculated from the video logs (limited to only four years) were not sufficient. Instead, the authors used the TAMS to obtain rutting measurements over time. The maximum rut depth was considered and used in evaluating the field performance of the field projects.

ITD classified routes rutting performance into four groups including good, fair, poor, and very poor. The route classification depends on the measured rut depth and route functional class (e.g., interstate and arterials or collectors). Projects with good rutting have rut depth between 0 and 6.09 mm for interstate and arterials routes and between 0 and 12.44 for collectors routes. Projects with fair rutting performance have rut depth between 6.09 and 12.44 mm for interstate and arterials routes and between 12.44 and 25.14 for collectors.

Projects with poor rutting performance have rut depth between 12.44 and 18.79 mm for interstate and arterials routes and between 25.44 and 37.8 for collectors. Projects with very poor have rut depth more than 19.05 mm for interstate routes and arterials and more than 38.1 for collectors.

The measured field rut depth for all selected test sections in this study is presented in Figure 6.4. The rut depth was between 2.80 mm and 8.64 mm. The green bars in Figure 6.4 indicate projects with good rutting resistance while yellow bars indicate projects with fair rutting resistance. The test sections were classified into two groups based on ITD's rutting criteria. Eleven projects had good rutting resistance, while six projects showed fair rutting resistance. None of the projects showed poor rutting resistance in the field. This evaluation was used to study the correlation between laboratory results and the observed field rutting, and to develop rutting pass/fail performance thresholds for the selected indicators.

## 6.7. Analysis and discussion

Figure 6.5 through Figure 6.7 show the analysis results for all selected performance indicators. In these figures, the error bars represent ± one Standard Deviation (SD) from the mean value. Also, statistical analyses of mixes rutting performance were performed. The t-test, One-Way Analysis of Variance (ANOVA), and Tukey's Honestly Significant Difference (Tukey' HSD) tests were used to examine the statistical sensitivity of performance indicators to mix composition at 95% confidence interval. Tukey's HSD groups were represented in the form of numbers or letters at the bottom of each bar. Mixes share the same letter/number were not significantly different in terms of their resistance to rutting.

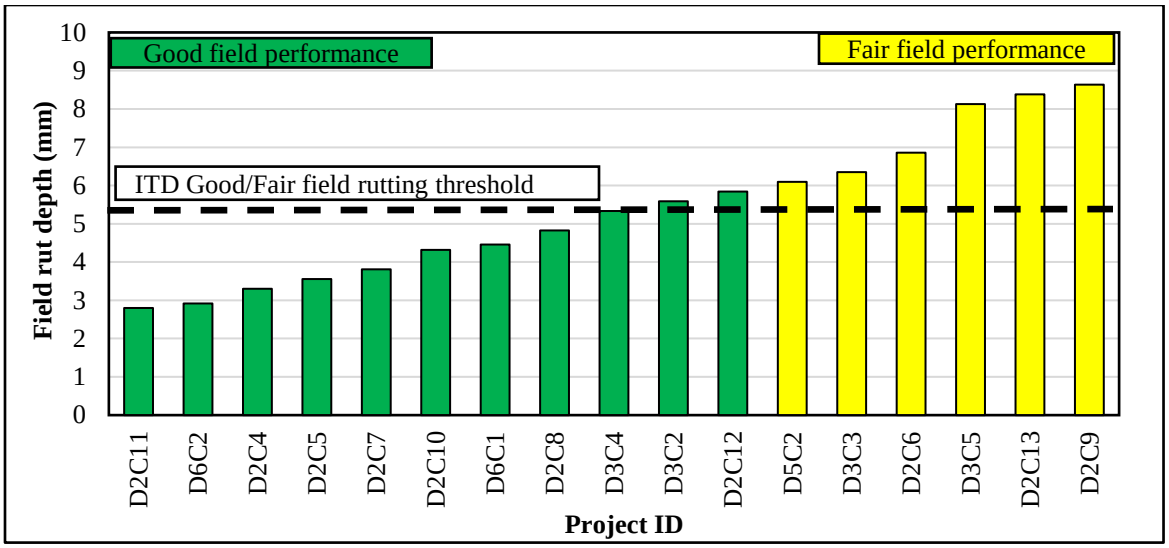


**Figure 6.4.** Field rut depth measurements for selected locations

*6.7.1. Rutting Evaluation of LMLC Mixes*

Six LMLC mixes were prepared to examine the sensitivity of HWTT and APA rut tests and their performance indicators to the variation in binder PG and content. Figure 6.5-A and Figure 6.5-B present the sensitivity of $HWTT_{15000}$ and $HWTT_{20000}$ performance indicators to the variation in binder content and binder PG, respectively. Mixes prepared with the PG 70-28 binder exhibited less rutting when compared to the ones prepared with the PG 58-34 binder. The difference was statistically significant ($p$-value < 0.05) at all studied binder contents. The results also demonstrated that the rut depth increased with the increase in binder content for both binders' types. However, for both binders, the difference in rut depth was only statistically significant between either 4.25% and 5.75% and between 5.00% and 5.75% binder contents, while it was not statistically significant between 4.25% and 5.00%.

Figure 6.5-C presents the $APA_{8000}$ performance indicator results for the LMLC mixes. The mixes prepared with the PG 70-28 binder were tested at 70 °C, while the mixes prepared with the PG 58-34 binder were tested at 58 °C in accordance with AASHTO T340 test procedure. Mixes with the PG 70-28 binder experienced higher rut depth compared to mixes with the PG 58-34 at the corresponding binder content and the difference was statistically significant ($p$-value <0.05) at the corresponding binder content. Asphalt mixes prepared with stiffer binders are expected to show higher resistance to rutting compared to mixes with softer binders if both are tested at the same temperature. However, since the test was

conducted at a higher PG temperature in accordance with AASHTO T340, mixes tested at a higher temperature experienced higher rutting compared to those tested at a lower temperature.

The results also showed that the $APA_{8000}$ rutting increased with the binder content for both binders (i.e., PG 70-28 and PG 58-34). The results of PG 70-28 binder had a significant statistical difference between 4.25 % and 5.75 % binder content. Meanwhile, there was a statistically significant difference between mixtures prepared at different binder contents for PG 58-34 binder.

### *6.7.2. Rutting Evaluation of PMLC Mixes*

Figure 6.6-A, Figure 6.6-B, and Figure 6.6-C show the laboratory testing results for the PMLC mixes for $HWTT_{15000}$, $HWTT_{20000}$, and $APA_{8000,}$ respectively. $HWTT_{15000}$ results had an average rut depth between 1.62 mm and 4.84 mm, with standard deviation (SD) between 0.05 mm and 0.81 mm (Figure 6.6-A). The results showed that D3L3 and D3L4 had higher rut depth compared to other mixes, while D2L1 had the lowest rut depth. $HWTT_{20000}$ results had an average rut depth between 1.74 mm and 5.09 mm and SD between 0.04 mm and 0.85 mm (Figure 6.6-B). $APA_{8000}$ results had an average rut depth between 1.67 mm and 4.36 mm and SD between 0.01 mm and 0.69 mm (Figure 6.6-C). The results showed that both mixes D3L3 and D5L1 had the highest rut depth, while mixture D2L1 had the lowest rut depth.

### *6.7.3. Rutting Evaluation of Field Projects*

Figure 6.7-A, Figure 6.7-B, and Figure 6.7-C show the laboratory testing results for $HWTT_{15000}$ and $HWTT_{20000}$, and $APA_{8000,}$ respectively. $HWTT_{15000}$ results had an average rut depth between 2.63 mm and 14.39 mm with SD between 0.28 mm and 4.57 mm (Figure 6.7-A). $HWTT_{20000}$ results had an average rut depth between 2.82 mm and 14.39 mm with an SD between 0.21 mm and 4.05 mm (Figure 6.7-B). Figure 6.7-C shows field cores testing results for $APA_{8000}$ performance indicator. Due to the limited number of field cores obtained from some of the field projects, only 12 field projects were tested using the APA rut test. $APA_{8000}$ results had an average rut depth between 1.86 mm and 7.15 mm with a standard deviation between 0.03 mm and 0.63 mm. Cores extracted from D5C2 project had a higher rut depth

(7.15 mm) while cores from D2C6 project had the lowest rutting depth (1.86 mm) when compared to other projects.

### *6.7.4. Moisture Susceptibility Evaluation of LMLC Mixes, PMLC Mixes, and Field Projects*

The water bath conditioning included in the HWTT can provide the ability to assess the moisture susceptibility in addition to rutting, which is considered an advantage over the APA rut test. In this research, the field cores, PMLC mixes, and LMLC mixes resistance to moisture damage were also assessed using the HWTT performance indicators.

The HWTT results showed that only two field projects (i.e., D5C2 and D2C11) out of the 17 evaluated projects that were tested exhibited signs of moisture damage. D5C2 project exceeded the HWTT test termination rut depth (14.39 mm after 15,000 cycles) as shown in Figure 6.8-A. D2C11 project showed inconsistent results, the left wheel specimens exhibited good rutting resistance (average rut depth of 5.2 mm at 20,000 cycles) while the right wheel had poor rutting resistance and moisture damage (average rut depth of 12.42 at 14,800 cycles) (Figure 6.8-B). This could be contributed to different air void content between the left and right wheel specimens, but the researchers were not able to conduct additional tests for this field project due to the limited number of field cores.

In addition, the HWTT performance indicators were used to assess PMLC mixes resistance to moisture damage. The laboratory evaluation results demonstrated that none of the PMLC mixes showed signs of moisture damage. It should be noted that the current ITD specifications require the use of anti-strip agents or additives as a percent of the binder by weight (minimum of 0.5%) [19,20].The current practice of Idaho Department of Transportation (ITD) involves performing the immersion compression. In this test, the index of retained strength is utilized as performance indicator to assess asphalt mix resistance to moisture susceptibility. ITD specifies a minimum retained strength of 85%. It was found that all mixes satisfied the threshold requirements per current ITD specifications. Similarly, none of the LMLC mixes exhibited any sign of moisture damage although anti strip additives were not used.

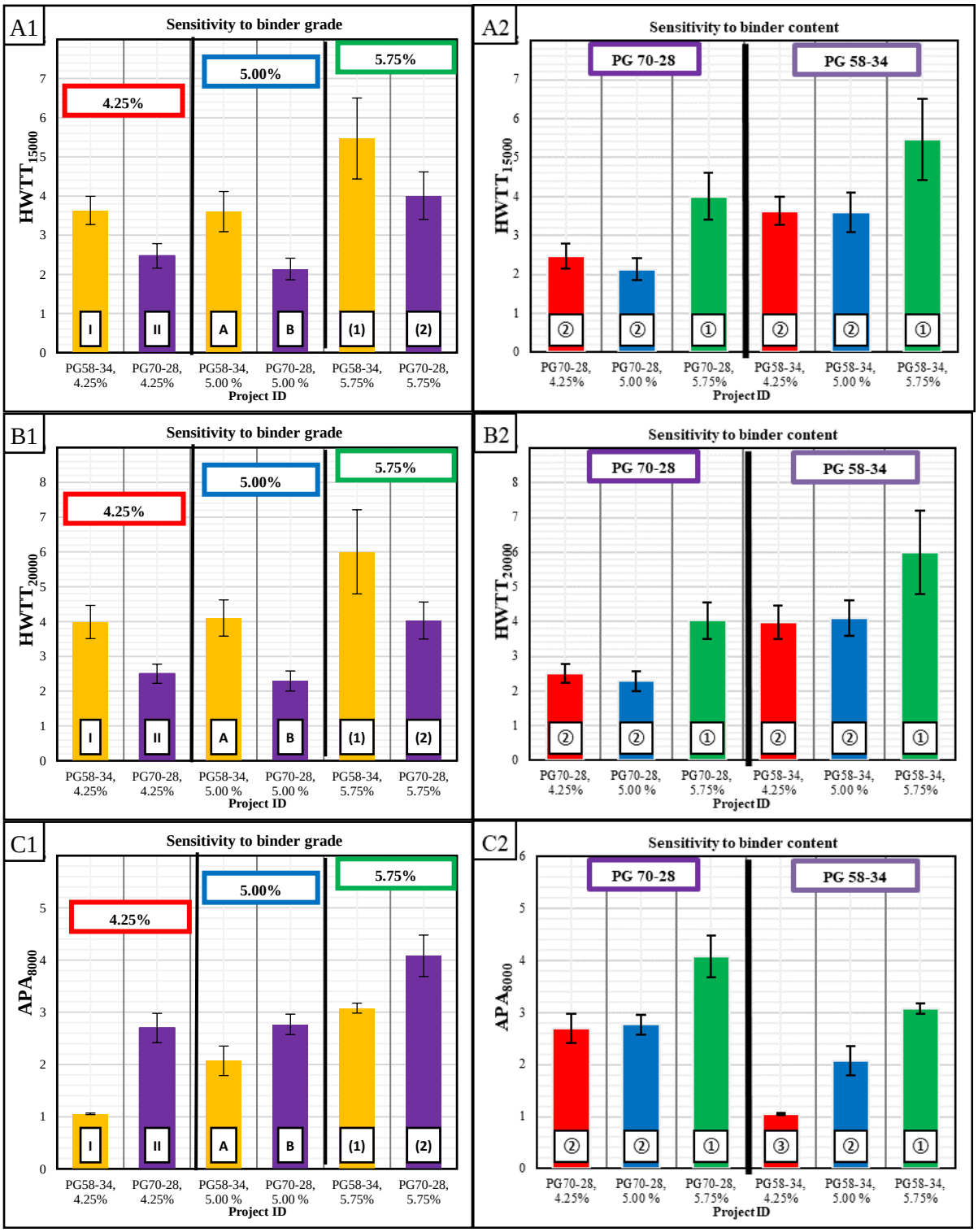


Figure 6.5. Sensitivity to binder PG A1) $HWTT_{15000}$, B1) $HWTT_{20000}$, and C1) $APA_{8000}$ and sensitivity to binder content A2) $HWTT_{15000}$, B2) $HWTT_{20000}$, and C2) $APA_{8000}$

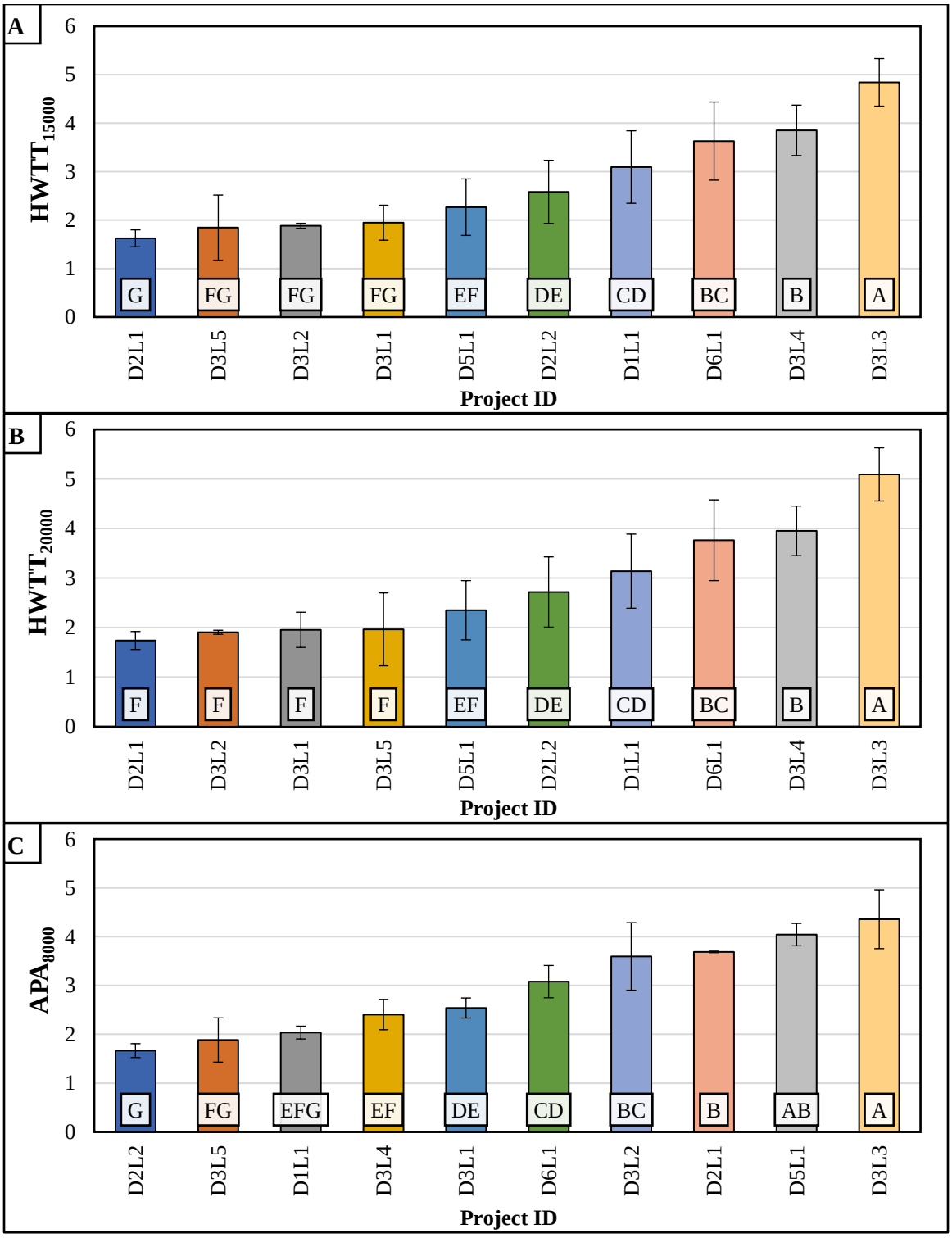


**Figure 6.6.** PMLC mixes results for performance A) $HWTT_{15000}$, B) $HWTT_{20000}$, and C) $APA_{8000}$

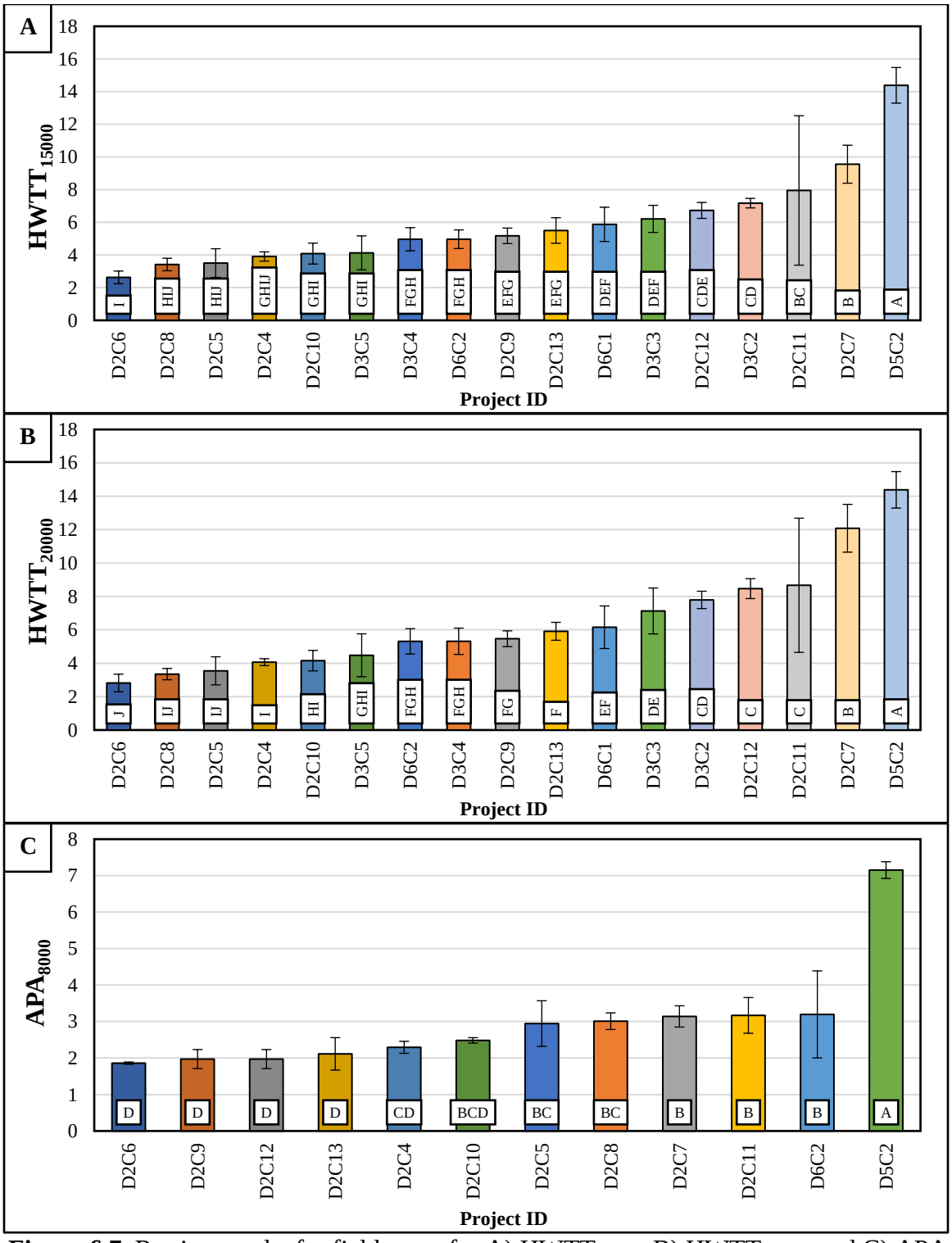


**Figure 6.7.** Rutting results for field cores for A) $HWTT_{15000}$, B) $HWTT_{20000}$, and C) $APA_{8000}$

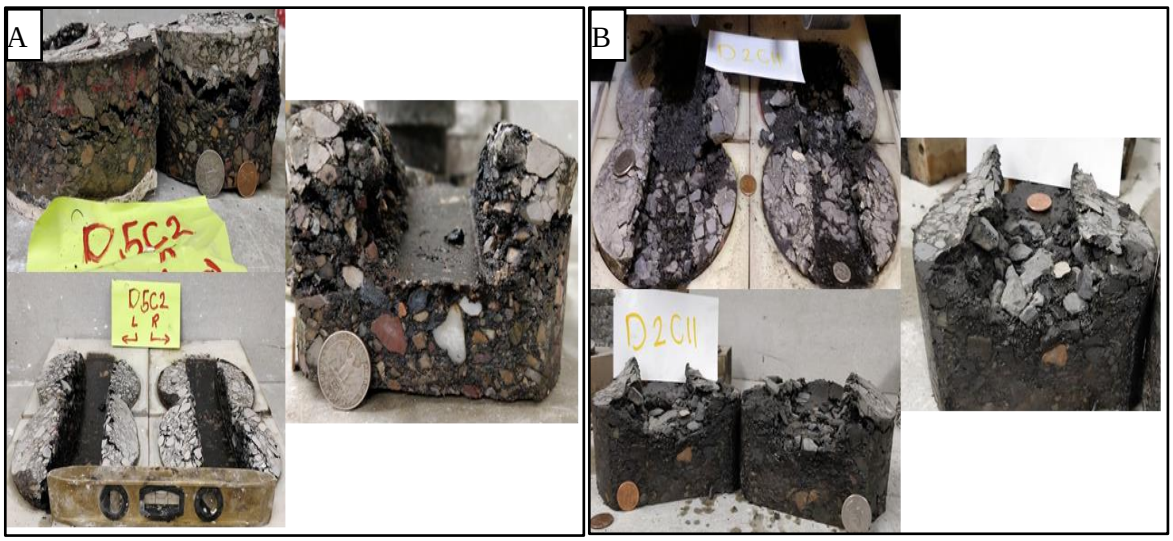


**Figure 6.8.** Moisture damage in A) D5C2 field project and B) D2C11 field project

*6.7.5. Indicators Statistical Grouping of Mix Resistance to Cracking*

Figure 6.6 and Figure 6.7 present the statistical analysis for PMLC mixes and field projects, respectively. Turkey's HSD statistical groups were represented in the form of numbers or letters at the bottom of each bar for all studied mixes. Mixes share the same letter/number were not significantly different in terms of their resistance to rutting.

It can be observed that $HWTT_{15000}$, $HWTT_{20000}$, and $APA_{8000}$ classified PMLC mixes into seven, six, and seven Tukey's HSD groups, respectively (Figure 6.6). In addition, $HWTT_{15000}$ and $HWTT_{20000}$ result classified field projects into ten Tukey's HSD groups, while $APA_{8000}$ results classified field projects into four groups (Figure 6.7). The field projects results demonstrated that $HWTT_{15000}$, $HWTT_{20000}$ had better statistical grouping of mix rutting resistance for field project mixes as compared to $APA_{8000}$. However, this comparison was eliminated since only 12 field projects were tested using the APA rut test, while 17 projects were tested using HWTT.

The Indicators with a higher number of Turkey's HSD statistical groups would provide a better comparison between mixes resistance to rutting. The analysis results demonstrated that $HWTT_{15000}$, $HWTT_{20000}$, and $APA_{8000}$ had a similar statistical grouping of mix rutting resistance.

### *6.7.6. Indicators Variability*

In this study, the variability of HWTT and APA rut test performance indicators (i.e., $APA_{8000}$, $HWTT_{15000}$, and $HWTT_{20000}$) were examined using the Coefficient of Variation (COV). Figure 6.9-A, Figure 6.9-B, and Figure 6.9-C show the testing results variability of $HWTT_{15000}$, $HWTT_{20000}$, and $APA_{8000}$, respectively for all studied mixes (i.e., field cores, PMLC mixes, and LMLC mixes). Indicators were categories based on their average COV into three groups including low variability (average COV <10%), moderate variability (15% < average COV < 30%), and high variability (average COV > %30%).

The $HWTT_{15000}$ and $HWTT_{20000}$ results had average COV values of 14%, 19%, and 16% for LMLC, PMLC, and field projects, respectively. Also, the $HWTT_{15000}$ results had a COV range between 10% and 19% for LMLC mixes, 3% and 36% for PMLC mixes, and 4% to 58% for field projects. The $HWTT_{20000}$ results had a COV range between 11% to 20 % for LMLC mixes, 2% to 37% for PMLC mixes, and 5% to 46% for field projects. It can be observed that there was no major difference between HWTT performance indicators (i.e., $HWTT_{15000}$ and $HWTT_{20000}$) in terms of testing results variability. The $APA_{8000}$ results had average COV of 8%, 11%, and 13% for LMLC, PMLC, and field projects, respectively. Also, the $APA_{8000}$ results had a COV range between 1% to 14% for LMLC mixes, 0% to 24% for PMLC mixes, and 2% to 37% for field projects.

The $APA_{8000}$ results exhibited lower variability compared to $HWTT_{15000}$ and $HWTT_{20000}$ results. The $APA_{8000}$ results had low to moderate variability, while $HWTT_{15000}$ and $HWTT_{20000}$ had moderate variability. It should be noted that the mix type may affect test variability. Overall the LMLC mixes had less variability in the test results compared to field cores. This could be contributed to different air void distribution and content of the extracted cores.

### *6.7.7. Correlation Between Rutting Performance Assessment Tests and Indicators*

The correlation between $HWTT_{15000}$ and $HWTT_{20000}$, and $APA_{8000}$ were evaluated using LMLC, PMLC, and field projects results as presented in Figure 6.10. There was an excellent correlation between HWTT performance indicators (i.e., $HWTT_{15000}$ and $HWTT_{20000}$). Field

projects had a coefficient of determination ($R^2$) of 0.9, PMLC mixes had $R^2$ of 0.98, while LMLC mixes had $R^2$ of 0.99. In addition, Spearman rank correlation coefficient ($r_s$) was also evaluated. This coefficient was used to study the ranking correlation (from best to worst in terms of rutting resistance) between both rutting indicators (e.g., $HWTT_{15000}$ and $HWTT_{20000}$). An excellent ranking agreement was found between HWTT performance indicators (i.e., $HWTT_{15000}$ and $HWTT_{20000}$) ($r_s = 0.98$) was found. These results demonstrate that the two HWTT rutting performance indicators ($HWTT_{15000}$ and $HWTT_{20000}$) are highly correlated and thus using one or the other would be sufficient. Since the $HWTT_{15000}$ requires a smaller number of load passes which would reduce the HWTT testing time, it is recommended over $HWTT_{20000}$.

Figure 6.10-A and Figure 6.10-B show the correlation between $APA_{8000}$ and both $HWTT_{15000}$ and $HWTT_{20000}$, respectively. The results showed no correlation between HWTT and APA rut test performance indicators. The correlation between $HWTT_{15000}$ vs. $APA_{8000}$ had $R^2$ of 0.35, 0.03, and 0.66 for LMLC mixes, PMLC mixes, and field projects, respectively. The correlation between $HWTT_{20000}$ vs. $APA_{8000}$ had $R^2$ of 0.04, 0.006, and 0.49 for LMLC mixes, PMLC mixes, and field projects, respectively. The coefficient of determination ($R^2$) based on laboratory testing results of field cores were affected by the testing results of D5C2 field project. The correlation between $HWTT_{15000}$ vs. $APA_{8000}$ and $HWTT_{20000}$ vs. $APA_{8000}$ had $R^2$ of 0.11, and 0.08 after excluding D5C2 project from the analysis. The $APA_{8000}$ was also found to have a poor ranking agreement with both $HWTT_{15000}$ and $HWTT_{20000}$ rutting indicators ($R_s = 0.14$ and 0.10 with $HWTT_{15000}$ and $HWTT_{20000}$, respectively).

The HWTT and APA rut tests evaluate the resistance of asphalt mixes under different testing temperatures and conditions. For instance, the HWTT test was performed at 50 °C, while the APA rut test was performed at the high binder performance grade. Since the viscosity of asphalt binder changes with the testing temperature, it is expected that asphalt mixes provide different performance. In addition, the HWTT test is conducted in wet conditions, while the APA rut test is conducted in dry conditions.

### *6.7.8. Correlation Between Laboratory and Field Rutting Measurements And Proposing Pass/Fail Rutting Performance Thresholds*

Figure 6.11-A, Figure 6.11-B, and Figure 6.11-C show the measured rut depth in the field against the rut depth measured in the laboratory for $HWTT_{15000}$, $HWTT_{20000}$, and $APA_{8000,}$ respectively. The figures were divided into three shaded areas include green, yellow, and red. The green area represents projects with good resistance to rutting, the yellow area represents projects with fair resistance to rutting, while the red area represents projects with poor to very poor resistance to rutting.

All field projects had either good rutting resistance (field rut depth < 6.09 mm) or fair rutting resistance (field rut depth < 12.44 mm) according to ITD criteria. Field results demonstrated that 11 mixes had good resistance to rutting and six had fair rutting resistance. None of the field projects exhibited poor or very poor resistance to rutting.

The laboratory and field results were in good agreement in terms of assessment of rutting resistance. None of them showed potential rutting problems. In general, the Superpave mix design tends to produce dry mixes that provide good resistance to rutting. Based on the correlation between the laboratory testing results of the extracted field cores and the measured field rutting, in addition to the findings of literature review (Table 6.2 and Table 6.3), the authors proposed performance thresholds to ensure that asphalt mixes have good/fair rutting performance and to eliminate the ones with poor resistance to rutting. A maximum rut depth of 10 mm for $HWTT_{15000}$ (Figure 6.11-A), 12.5 mm for $HWTT_{20000}$ (Figure 6.11-B), and 5 mm for $APA_{8000}$ (Figure 6.11-C) were proposed as pass/fail performance assessment thresholds. These thresholds can differentiate between mixes with good/fair from those that may exhibit poor resistance to rutting in the field.

Similar thresholds are adopted by several transportation agencies. For example, Washington Department of Transportation (WSDOT) specifies a maximum rut depth of 10 mm for $HWTT_{15000}$ (for mixes designed for more than 3 million ESAL's tested at 50 °C without any sign on moisture damage) [21]. Louisiana Department of Transportation (LADOT) specifies a maximum rut depth of 10 mm rut depth for $HWTT_{20000}$ for wearing course tested at 50 °C [7].

Similarly, other state DOTs adopted different thresholds for $APA_{8000}$. Alabama Department of Transportation (ALDOT) specifies a minimum value of 4.5 mm after 8000 cycles for "E" mixes ($1E10^7$ < ESALs < $3E10^7$). Also, Virginia Department of Transportation (VDOT) specifies minimum values of 3.5 mm, 5.5 mm, and 7 mm for mixture designation A, D, and E, respectively after 8000 load cycles.

### *6.7.9. Implementation of the Developed Performance Assessment Thresholds*

Figure 6.12-A, Figure 6.12-B, and Figure 6.12-C show the implementation of the proposed thresholds to assess the rutting resistance of LMLC and PMLC mixes for $HWTT_{15000}$, $HWTT_{20000}$, and $APA_{8000}$, respectively. It can be observed that all LMLC and PMLC mixes satisfied the specified performance thresholds. These results demonstrated that the PMLC mixes are expected to exhibit good rutting performance if proper field construction and compaction are achieved and the required density is met.

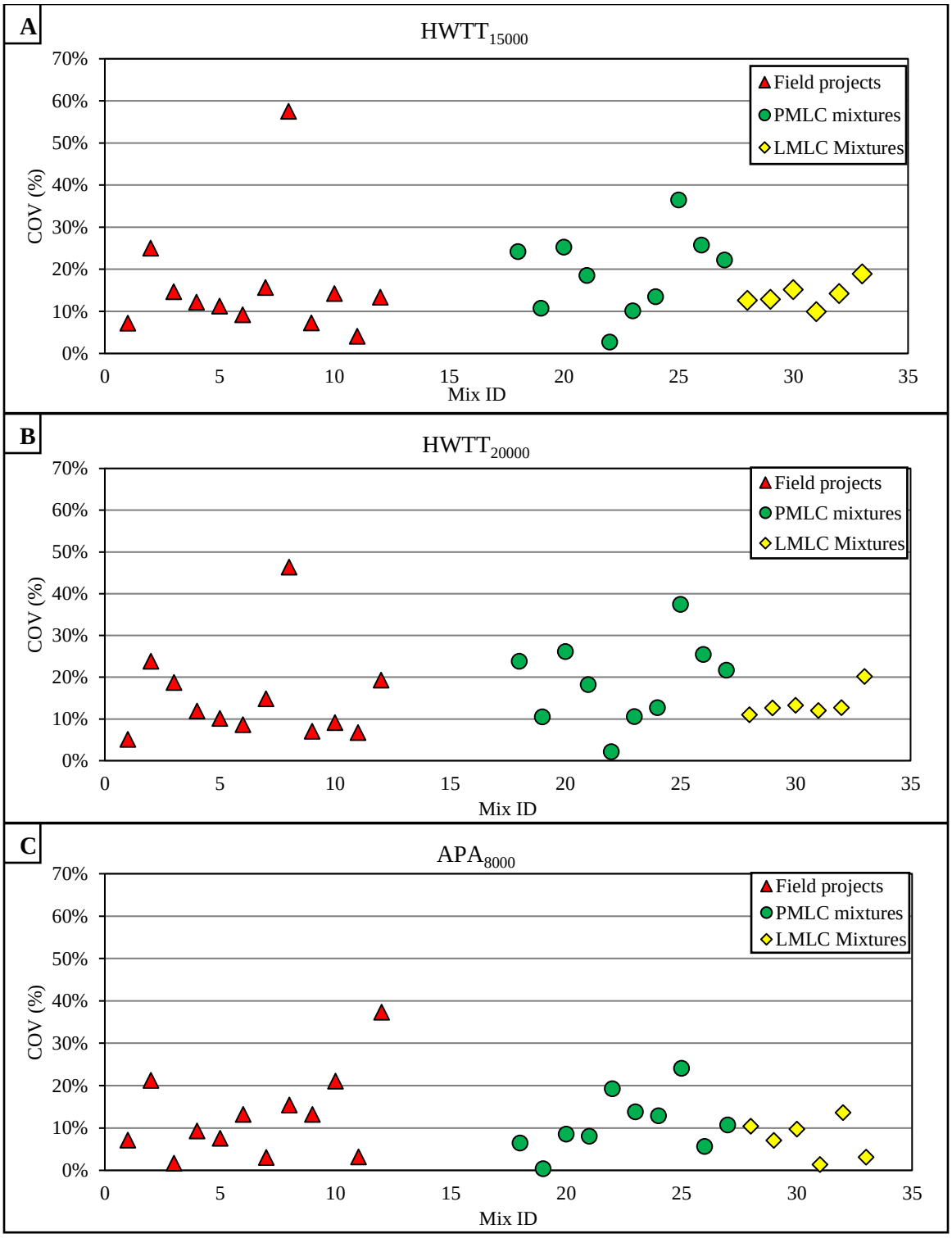


**Figure 6.9.** Testing results variability for all mixes (LMLC, PMLC, and field cores) for A) $HWTT_{15000}$, B) $HWTT_{20000}$, and C) $APA_{8000}$

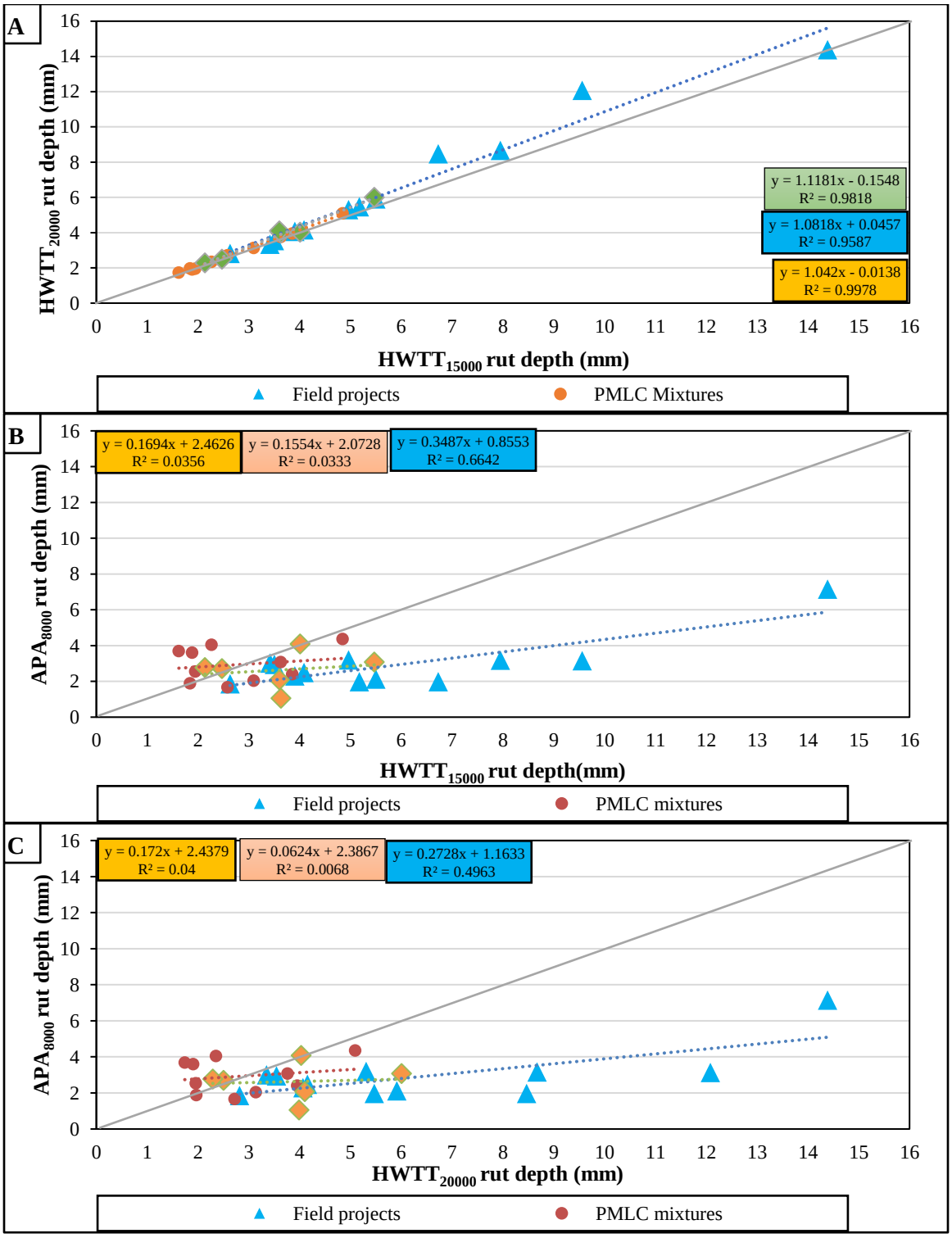


**Figure 6.10**. Correlation between A) $HWTT_{15000}$ and $HWTT_{20000}$, B) $HWTT_{15000}$ and $APA_{8000}$, $HWTT_{20000}$ and $APA_{8000}$ indicators

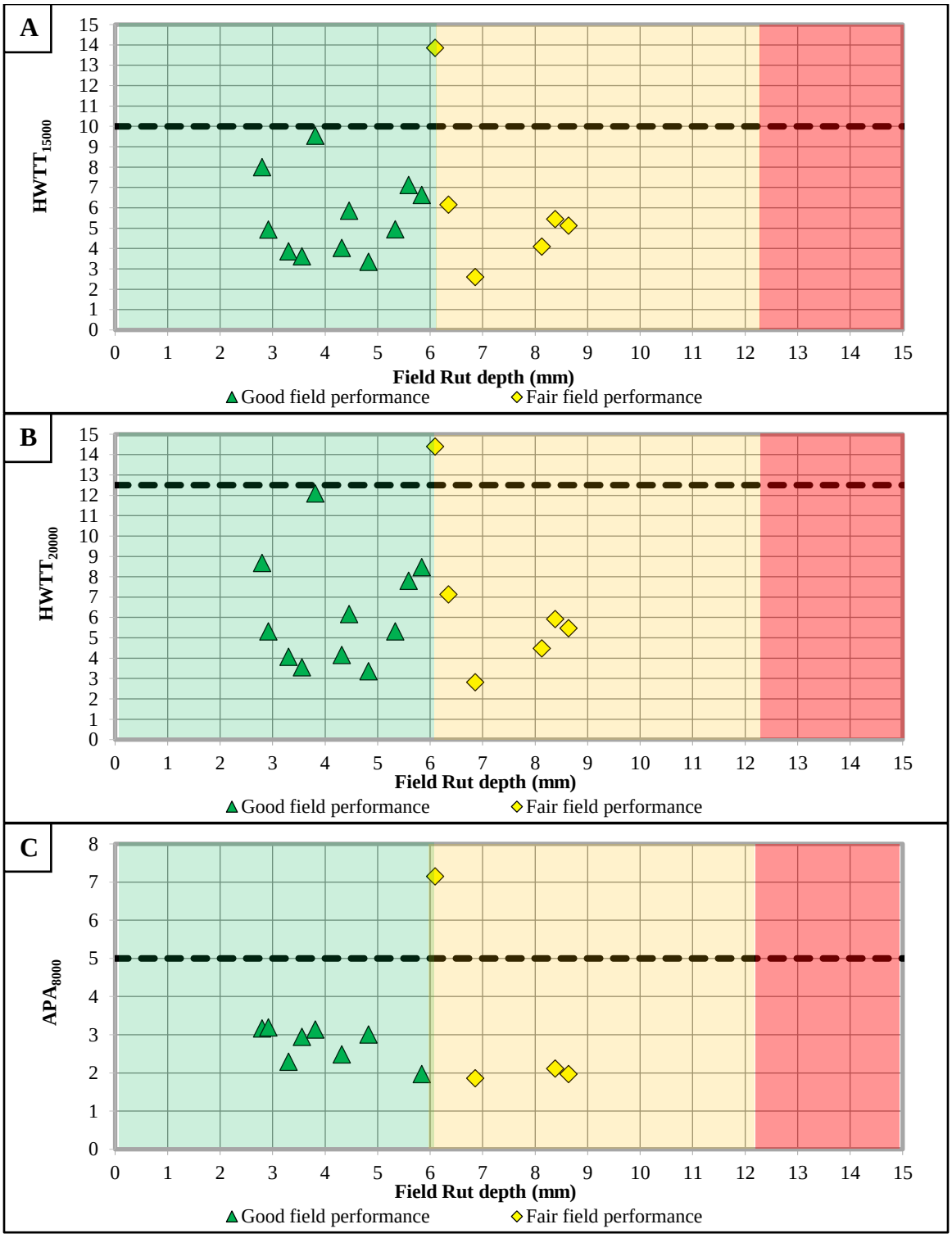


**Figure 6.11**. Laboratory versus field performance A) $HWTT_{15000}$, B) $HWTT_{20000}$, and C) $APA_{8000}$

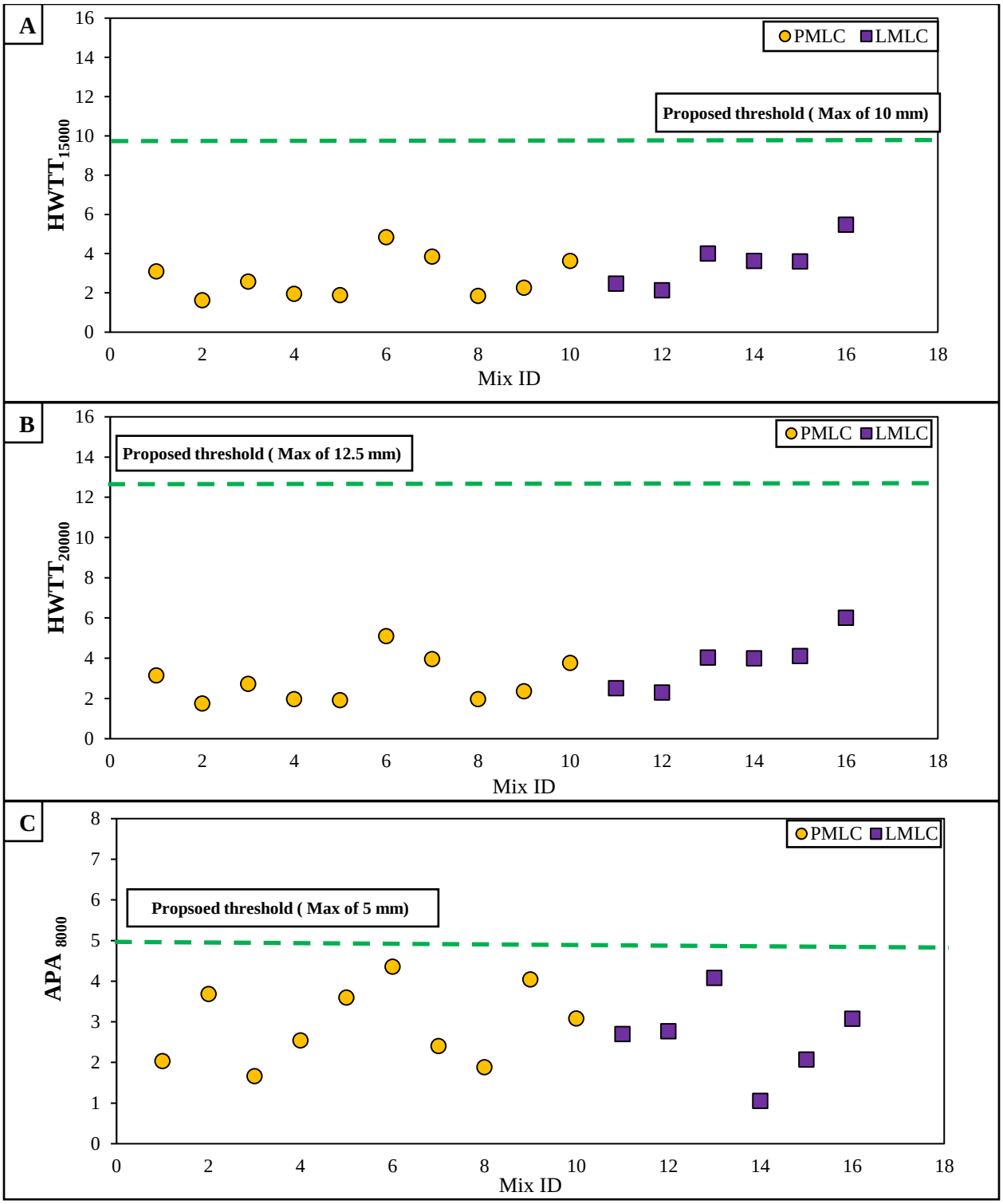


**Figure 6.12.** rut depth for all test mixes (LMLC, PMLC, and field cores) for A) $HWTT_{15000}$, B) $HWTT_{20000}$, and C) $APA_{8000}$

## 6.8. Summary and Conclusions

This study aimed to advance the implementation of the most promising wheel-tracking rutting assessment tests within the PEMD method. In order to achieve this goal, the study examined the validity of HWTT and APA rut test assessment tests and three rutting performance indicators derived from these tests. Three different asphalt mix types were evaluated (i.e., six LMLC, 10 PMLC, and 17 field projects) using both tests. Based on the findings of this study, the following conclusions can be made.

- The literature review indicated that most state DOTs prefer to conduct either HWTT or APA rut test at a fixed test temperature rather than a test temperature equivalent to the high binder PG.

- The HWTT and APA rutting indicators (i.e., $APA_{8000}$, $HWTT_{15000}$, and $HWTT_{20000}$) were both sensitive to the variation in binder content and binder PG. The $HWTT_{15000}$ and $HWTT_{20000}$ indicators provided the expected trends with the variation in binder content and grade PG, while the $APA_{8000}$ provided the expected trend for the variation in binder content only.

- The HWTT and APA rut test performance indicators (i.e., $APA_{8000}$, $HWTT_{15000}$, and $HWTT_{20000}$) were able to differentiate between field projects with different rutting resistance (e.g., good, and fair). A maximum rut depth of 10 mm for $HWTT_{15000}$, 12.5 mm for $HWTT_{20000}$, and 5 mm for $APA_{8000}$ were proposed.

- The laboratory evaluation of PMLC mixes demonstrated that the current practice of using APA rut test, and immersion compression test, and adding anti-strip agents during the asphalt mix design is an effective practice that should be maintained.

- Spearman ranking correlation showed an excellent ranking agreement between both HWTT indicators ($r_s = 0.98$). $APA_{8000}$ was also found to have poor ranking agreement with both $HWTT_{15000}$ and $HWTT_{20000}$ rutting indicators ($R_s = 0.14$ and 0.10 with $HWTT_{15000}$ and $HWTT_{20000}$, respectively).

- The variability of the test results indicated that the HWTT and APA rut test performance indicators had similar variability. $APA_{8000}$ results had low/moderate variability, while $HWTT_{15000}$ and $HWTT_{20000}$ had moderate variability. Also, $HWTT_{15000}$ and $HWTT_{20000}$ have similar average COV and range.

- The HWTT and APA rut test provided similar rutting assessment for the evaluated mixes. The authors recommend using HWTT over APA since HWTT provides an additional assessment to moisture damage. Also, since the two HWTT rutting performance indicators (e.g., $HWTT_{15000}$ and $HWTT_{20000}$) are highly correlated and thus using only one or the other would be sufficient. Since the $HWTT_{15000}$ requires a smaller number of passes which reduces the HWTT testing time, it is recommended over $HWTT_{20000}$.

## 6.9. References

[1] R.C. West, C. Rodenzo, F. Leiva, F. Yin, Development of a framework for balanced mix design, NCHRP project 20-07/task 406, 2018. http://apps.trb.org/cmsfeed/TRBNetProjectDisplay.asp?ProjectID=4324.

[2] B.K. Bairgi, I.A. Syed, R.A. Tarefder, Evaluation of rutting and stripping potential of WMA with different additives, (2017) 201–212. doi:10.1061/9780784481219.018.

[3] Texas Department of Transportation (TxDOT), Standard specifications for construction and maintenance of highways, streets, and bridges, 2014.

[4] Texas Department of Transportation (TxDOT), Test procedure for Hamburg Wheel-Tracking Test (Tex-242-F), 2014.

[5] Washington State Department of Transportation (WSDOT), Standard specifications for road, bridge, and municipal construction, 2016.

[6] Colorado Department of Transportation (CODOT), Standard method of test for Hamburg wheel-track testing of compacted bituminous mixtures (CP-L 5112), 2015.

[7] Louisiana Department of Transportation and Development (LaDOT), Louisiana Standard Specification for Roads and Bridges, 2016.

[8] Montana Department of Transportation (MTDOT), Standard Specifications for Road and Bridge Construction, 2014.

[9] Montana Department of Transportation (MTDOT), Method of Sampling and Testing Hamburg Wheel-Track Testing of Compacted Bituminous Mixtures, 2014.

[10] S.O.F. California, C. State, T. Agency, P. By, Standard Specifications 2018, (2018) 263–822.

[11] Iowa Department of Transportation (Iowa DOT), Moisture sensitivity testing of asphalt mixtures, (2017). https://www.iowadot.gov/erl/current/IM/content/319.htm.

[12] Iowa Department of Transportation (Iowa DOT), Section 2303. Flexible Pavement, (2019). https://www.iowadot.gov/erl/current/GS/content/2303.htm#Section230302E.

[13] Illinois department of transportation (IDOT), Standard specifications for road and bridge construction, (2016).

[14] Oklahoma department of transportation, Special provision for HAMBURG rut testing of hot mix asphalt, 2009.

[15] U.D. of T. (UDOT), Standard specifications for road and bridge construction, 2017.

[16] American Association of State Highway and Transportation (AASHTO), Standard Method of Test for Hamburg Wheel-Track Testing of Compacted Hot Mix Asphalt (HMA) ( AASHTO T324-14), 2015.

[17] J. Poorbaugh, Idaho Transportation System Pavement Performance-2017 Report, (2017).

[18] PathWay Services Incorporated Companies, Pavement profiler information- the PathRunner, (2019). http://www.pathwayservices.com/equipment-1/.

[19] Idaho Transportation Department (ITD DOT), Standard specifications for highway construction, 2012. http://apps.itd.idaho.gov/apps/manuals/SpecBook/files/SpecBinder.pdf.

[20] Idaho Transportation Department (ITD), Standard specification for highway construction, 2017.

[21] Washington State Department of Transportation (WSDOT), Standard specifications for road, bridge, and municipal construction, 2018.

[22] American Association of State Highway and Transportation (AASHTO), Standard Method of Test for Determining the Rutting Susceptibility of Asphalt Paving Mixtures Using the Asphalt Pavement Analyzer (APA) (AASHTO T340), 2015.

[23] Georgia Department of Transportation (GDOT), Hot mix asphalt level II quality control technician certification study guide, 2005.

[24] Georgia Department of Transportation (GDOT), Road standards-section 828 - hot mix asphaltic concrete mixtures-attachment, 2013.

[25] Alabama Department of Transportation (ALDOT), Rutting susceptibility determination of asphalt paving mixtures using the asphalt pavement analyzer, v, n.d. f.

[26] Alabama Department of Transportation(ALDOT), Standard Specifications-section 410 - Asphalt Pavements, 2013.

[27] Transportation Research Board, Application of asphalt mix specifications, 2014. doi:10.17226/22248.

[28] Virginia Department of Transportation (VDOT), Method of test for determining rutting susceptibility using the asphalt pavement analyzer – (asphalt lab) (Virginia Test Method -110), 2008.

[29] Virginia Department of Transportation (VDOT), Road and bridge specifications, 2016.

[30] T. Bennert, E. Sheehy, R. Blight, S. Gresavage, F. Fee, Implementation of performance-based specifications for asphalt mix design and production quality control for New Jersey, Transportation Research Board. (2014). doi:10.17226/22248.

[31] Alaska department of Transportation (ALDOT), Alaska test methods manual, 2018.

[32] Arkansas state highway and transportation department (ArDOT), Standard specifications for highway construction, 2014.

[33] Arkansas state highway and transportation department (ArDOT), Manual of Field Sampling and Testing Procedures, (2019) 222. https://www.arkansashighways.com/materials_division/A--FIELDMAN.pdf.

[34] North Carolina Department of transportation (NrDOT), Standard specifications for roads and structures, (2012).

[35] Ohio Department of Transportation (ODOT), Supplemental specification 856 Bridge Deck Waterproofing Asphalt Surface Course, 2017.

[36] Ohio Department of Transportation (ODOT), Supplement 1057 Loaded wheel tester asphalt mix rut testing method, 2016.

[37] O.D. of T. (ODOT), Contractor mix design guidlines for asphalt concrete, 207AD.

[38] South Carolina department Transportation (SCDOT), Supplemental technical specification for Hot-Mix Asphalt Material Properties, 2011.

[39] South Dakota Department of transportation (SDDOt, Standard Specifications for Roads and bridges, 2015.

# Chapter 7: Investigate the Applicability of Weibull Cracking Resistance Index Using Data Generated by Other Researchers and Reported in The Literature

Hamza Alkuime[1*]; Emad Kassem[1]; Fouad M.S. Bayomy[1] and Richard J. Nielsen[1]

(To be submitted to International Journal of Pavement Research and Technology)

## 7.1. Abstract

This study investigates the applicability of a newly proposed cracking performance indicator called Weibull Cracking Resistance Index ($Weibull_{CRI}$) as a unified approach to analyze the results of various monotonic assessment tests. The data used for this purpose was generated by other researchers and reported in the literature. The results showed that $Weibull_{CRI}$ is able to interpret the testing results of various tests including Indirect Tension Test [IDT] )-intermediate temperature, Semi-Circle Bending (SCB)-intermediate temperature, SCB-low temperature, Disk-Shaped Compact Tension (DCT), and Simple Punching Shear Test (SPST).$Weibull_{CRI}$ was also sensitive to variation in test conditions including specimen geometry, notch depth, thickness, and air void content. $Weibull_{CRI}$ was also sensitive to variation in mix proportions such as binder content, binder grade, aggregate type, NMAS, aging, rejuvenator dosages, and Recycled Asphalt Pavement (RAP). Furthermore, $Weibull_{CRI}$ was calculated from various displacement measurement methods including actuator vertical displacement and Crack Mouth Opening Displacement (CMOD) and provided similar cracking assessment. There was also good correlation between $Weibull_{CRI}$ and cyclic cracking tests. The results support the applicability of $Weibull_{CRI}$ as a unified analysis method for various monotonic cracking assessment tests.

Keywords: semi-circular bending; indirect tension test, performance-engineered mix design (PEMD); balanced mixed design (BMD)

[1] Department of Civil and Environmental Engineering, University of Idaho, Moscow, ID 83844 USA.

## 7.2. Introduction

Asphalt mixes are subjected to several distresses including cracking, rutting, and moisture damage. Proper evaluation of asphalt mixes is necessary to ensure that such mixes have adequate resistance to these distresses. The newly proposed Performance-Engineered Mix Design (PEMD) or Balanced Mix Design (BMD) incorporates performance assessment tests and thresholds in the design of asphalt mixes. Several tests are proposed and standardized in the literature to assess asphalt mix resistance to cracking, rutting, moisture damage, etc. However, assessment tests that incorporate monotonic loading are getting more attention than others. The monotonic tests use simple specimen geometry, require inexpensive testing equipment, can be completed in a short time, and they have low variability in the test results [1].

Several studies proposed various monotonic assessment tests to evaluate the resistance of asphalt mixes to intermediate-temperature cracking. These tests include Indirect Tension Test [IDT], Semi-Circle Bending [SCB]-Flexibility Index (SCB-FI), and Semi-Circle Bending-critical strain energy release rate [SCB-$J_c$]). Some of these tests were standardized such as ASTM D8044 (SCB-Jc), D6931 ($IDT_{Strength}$), and D8225 (IDEAL-$CT_{Index}$), and AASHTO TP124 (SCB-FI), TP105 (SCB-Low-temperature), and T283 ($IDT_{Moisture\ damage}$).

These monotonic tests have a similar loading concept (i.e., constant displacement rate) and test outputs (i.e., load-displacement curve). They evaluate the variation in the shape of the load-displacement curve to examine the change in mix resistance to cracking. Several performance indicators are proposed to interpret the variation in the load-displacement curve such as total fracture energy ($G_{fracture}$), indirect tensile strength ($IDT_{strength}$), critical strain energy release rate ($J_C$), cracking resistance index (CRI), indirect tensile asphalt cracking test (IDEAL-$CT_{Index}$), indirect tensile modulus ($IDT_{Modulus}$), flexibility index (FI), and Nflex factor [2–12]. However, none of these indicators is able to describe the entire load-displacement curve.

Recently, the authors proposed and evaluated a new performance indicator called Weibull Cracking Resistance Index ($Weibull_{CRI}$), that is able to describe the entire load-

displacement curve. The $Weibull_{CRI}$ was found to provide a good interpretation for the results of IDT and SCB tests to assess the cracking resistance of the laboratory prepared asphalt mixes. In addition, the $Weibull_{CRI}$ calculated from IDT test had the lowest variability (average Coefficient of Variability [COV]), the highest number of Tukey's HSD groups, the best correlation with cyclic cracking resistance assessment indicators as compared to the other monotonic performance indicators (Chapter 3 and Chapter 5) [14].

This study aimed to investigate the applicability of $Weibull_{CRI}$ as a unified approach to analyze the results of various monotonic cracking assessment tests using data generated by other researchers and reported in the literature.

### 7.3. Evaluation Plan and Weibull $_{CRI}$ Calculation

Figure 7.1 presents the aspects investigated in this study. Four different aspects were covered including:

(1) Ability to analyze the load-displacement curve of various monotonic assessment tests (e.g., low-temperature cracking monotonic assessment tests).

(2) Sensitivity to the change in testing conditions (e.g., specimen notch depth).

(3) Sensitivity to the change in mix properties proportions (e.g., Recycled Asphalt Pavement [RAP]).

(4) Correlation with cyclic cracking assessment tests.

The authors used the open-source data extraction tool WebPlotDigitizer version 4.1 to extract the load and displacement data from published resources in the literature. Figure 7.2 shows an example of data extraction process from a SCB test. It includes five main steps:

(1) Plot uploading and axis calibration.

(2) Curve selection.

(3) Data points identifications.

(4) Data extraction.

(5) Data plotting and analyzing.

Further details on data extraction procedures using the *WebPlotDigitize*r tool are provided by Rohatgi (2015) [15].

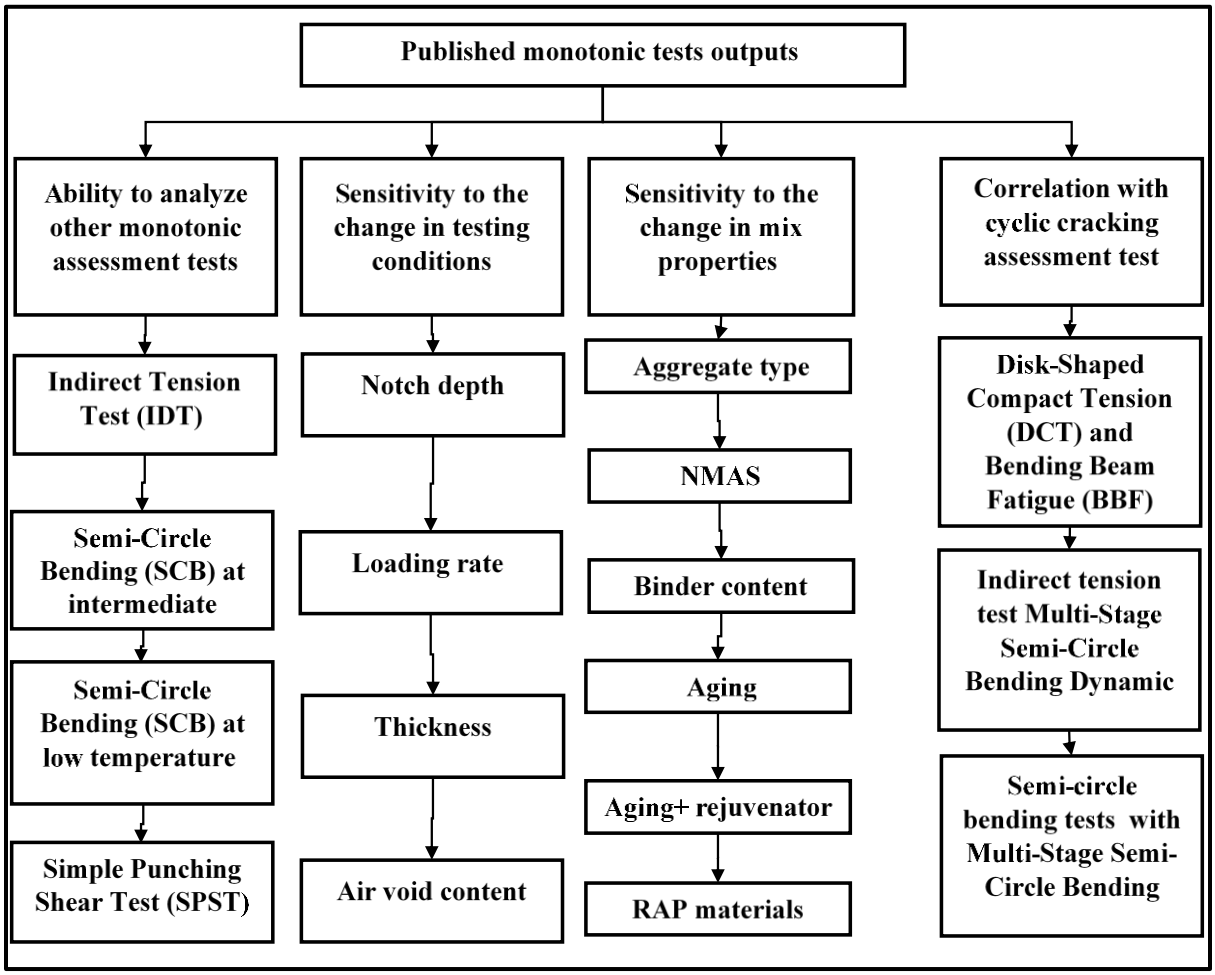


**Figure 7.1.** Research plan for Task

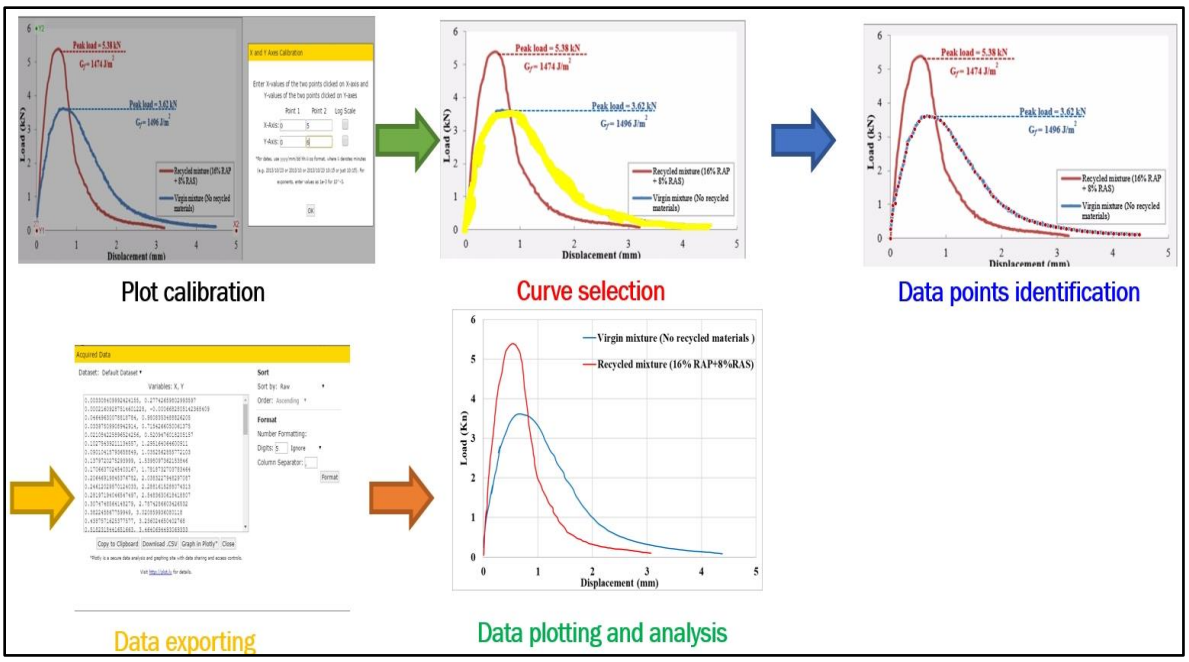


**Figure 7.2**. Data extraction procedure using WebPlotDigitizer

The extracted load-displacement curves are fitted using the modified Weibull function as shown in Equation 7.1. The fitting parameters ( $A$, $\beta$, and $\eta$) are used to determine the $\text{Weibull}_{\text{CRI}}$ using Equation 7.2. It should be noted that higher $\text{Weibull}_{\text{CRI}}$ values indicate improved mix performance. In this study, the load was expressed in Newton (N), while the displacement was expressed in mm. Further information about $\text{Weibull}_{\text{CRI}}$ is provided in (Chapter 2) [13].

$$P = A \times \left(\frac{\beta}{\eta}\right)\left(\frac{u}{\eta}\right)^{\beta-1} \times e^{-(\frac{u}{\eta})^{\beta}} \qquad 7.1$$

$$Weibull_{CRI} = \left(\frac{\eta}{\beta}\right) \times log[A] \qquad 7.2$$

where $P$ is the applied load or stress, $A$ is the area parameter (equivalent to the area under the load-displacement curve or stress-strain curve), $\beta$ is the shape parameter (Weibull slope), $\eta$ is the scale, $u$ is the measured displacement (vertical actuator displacement, LVDT or CMOD) or strain.

## 7.4. Analysis and Discussion

In this study, the investigation of the applicability of $Weibull_{CRI}$ as a unified approach covered four aspects including ability to analyze the load-displacement curve of various monotonic assessment tests, sensitivity to the change in testing conditions (e.g., specimen geometry),sensitivity to the change in mix properties (e.g., Recycled Asphalt Pavement [RAP]), and correlation with cyclic cracking assessment tests.

### *7.4.1. Ability to Analyze the Load-Displacement Curve of Various Monotonic Assessment Tests*

Monotonic tests have a similar loading concept (i.e., constant displacement rate) and test outputs (i.e., load-displacement curve), but it mainly has different testing conditions (e.g., loading rate). This section examines the ability of $Weibull_{CRI}$ to interpret the variation in the load-displacement curve obtained from various monotonic assessment tests to assess asphalt mixes resistance to various distress (i.e., intermediate-temperature cracking, low-temperature cracking, and rutting).

#### *7.4.1.1. Indirect Tension Test (IDT) to Assess Intermediate-Temperature Cracking*

In a previous study by the authors, $Weibull_{CRI}$ calculated from IDT test ($Weibull_{CRI}[IDT_{Intermediate\text{-}temperature}]$) was used to assess the resistance of 10 currently produced (Plant Produced-Laboratory Compacted [PMLC]) asphalt mixes in the state of Idaho to intermediate-temperature cracking (Chapter 2) [13]. The findings showed that $Weibull_{CRI}$ ($IDT_{Intermediate\text{-}temperature}$) had good agreement with the expected performance of PMLC mixes based on mix compositions, low variability (average COV < 15 %), and a good statistical grouping of mixes resistance to cracking. Further information about mix properties, specimen preparation, and testing conditions, procedures, and testing results is provided in (Chapter 2 and Chapter 6) [13,14].

#### *7.4.1.2. Semi-Circle Bending (SCB) to Assess Intermediate-Temperature Cracking*

Similarly, the authors in a previous study used $Weibull_{CRI}$ calculated from the SCB test ($Weibull_{CRI}[SCB_{Intermediate\text{-}temperature}]$) to assess the resistance of the same 10 PMLC mixes to

intermediate-temperature cracking (Chapter 2)[13]. The study findings showed that $Weibull_{CRI}$ ($SCB_{Intermediate\text{-}temperature}$) had good agreement with the expected performance of PMLC mixes based on mixes compositions, had moderate variability (15% < average COV < 25%), and had a good statistical grouping of mixes resistance to cracking. Further information about mix properties, specimen preparation, and testing conditions, procedures, and testing results is provided in (Chapter 2)[13].

#### *7.4.1.3. Semi-Circle Bending (SCB) Test to Assess Low-Temperature Cracking*

Moon et al. (2019) used the SCB-low-temperature ($SCB_{low\text{-}temperature}$) test to assess the resistance of asphalt mixes with high RAP materials to low-temperature cracking [19]. The study evaluated seven Laboratory Prepared-Laboratory Compacted (LMLC) asphalt mixes. Mixes were prepared using one binder grade (PG70-34), one NMAS (12.5 mm), and different percent of RAP materials and virgin aggregates (granite, and taconite) (Table 7.1). In addition, mix performance was examined under two different aging conditions (short- and long-term aging) and test temperatures (-12°C and -24°C). Further information about mix properties, specimen preparation, and testing conditions and procedures is provided by Moon et al. (2019) [19].

**Table 7.1** Properties of mixes evaluation by Moon et al. (2019) [19].

| Mix ID | Material contents | | |
|---|---|---|---|
| | Granite (%) | Taconite (%) | RAP materials (%) |
| Mix #1 | 100 | 0 | 0 |
| Mix #2 | 80 | 0 | 20 |
| Mix #3 | 65 | 0 | 35 |
| Mix #4 | 30 | 50 | 20 |
| Mix #5 | 0 | 65 | 35 |
| Mix #6 | 50 | 50 | 0 |
| Mix #7 | 50 | 0 | 50 |

Figure 7.3-A and Figure 7.3-B present the calculated $Weibull_{CRI}$ from $SCB_{low\text{-}temperature}$ ($Weibull_{CRI}$ [$SCB_{Low\text{-}temperature}$]) at -12°C and -24°C test temperatures, respectively. It can be observed that $Weibull_{CRI}$ ($SCB_{Low\text{-}temperature}$) results were in agreement with the expected low-temperature cracking resistance based on the composition of the evaluated asphalt mixes. For instance, Mix #1 had the lowest RAP content (i.e., 0%), thus it is expected to provide better resistance to low-temperature cracking (i.e., highest $Weibull_{CRI}$ [$SCB_{Low\text{-}temperature}$]) as

compared to other evaluated mixes. The $Weibull_{CRI}(SCB_{Low\text{-}temperature})$ results agree with this assumption (i.e., Mix #1 to provide the best resistance to low-temperature cracking) at all testing conditions (i.e., test temperatures [-12°C and -24°C] and aging [short- and long-term aging]) as shown in Figure 7.3.

In addition, Mix #1, Mix #2, and Mix #3 were prepared using the same aggregate type (i.e., granite), but with different RAP contents (Table 7.1). Mix #1 had 0% RAP content, Mix #2 had 20% RAP, and Mix #3 had 35% RAP. Therefore, it is expected that Mix #1 to provider better cracking resistance as compared to Mix #2 and Mix #3 while Mix #3 is expected to show the lowest resistance to low-temperature cracking. The $Weibull_{CRI}(SCB_{Low\text{-}temperature})$ findings agree with the expected trend. For instance, at a test temperature of -12°C and short-term aging testing conditions, Mix #1, Mix #2, and Mix #3 had $Weibull_{CRI}(SCB_{Low\text{-}temperature})$ of 0.70, 0.58, and 0.49, respectively. Higher $Weibull_{CRI}(SCB_{Low\text{-}temperature})$ values indicate better resistance to cracking. The same conclusions can be observed at the other test conditions (i.e., test temperatures [-12°C and -24°C] and aging [short- and long-term aging]) as shown in Figure 7.3.

Furthermore, $Weibull_{CRI}(SCB_{Low\text{-}temperature})$ results were in agreement with the expected effects of the variation in the testing conditions (i.e., test temperature and aging) on mix resistance to low-temperature cracking. The results demonstrated that test specimens subjected to long-term aging had less resistance to low-temperature cracking (i.e., lower $Weibull_{CRI}[SCB_{Low\text{-}temperature}]$) as compared to test specimens subjected to short-term aging at both test temperatures (i.e., -12 °C and -24 °C). In addition, the results demonstrated that mixes had better resistance to low-temperature cracking (i.e., higher $Weibull_{CRI}$[SCB-low temperature]) at -12 °C as compared to -24 °C.

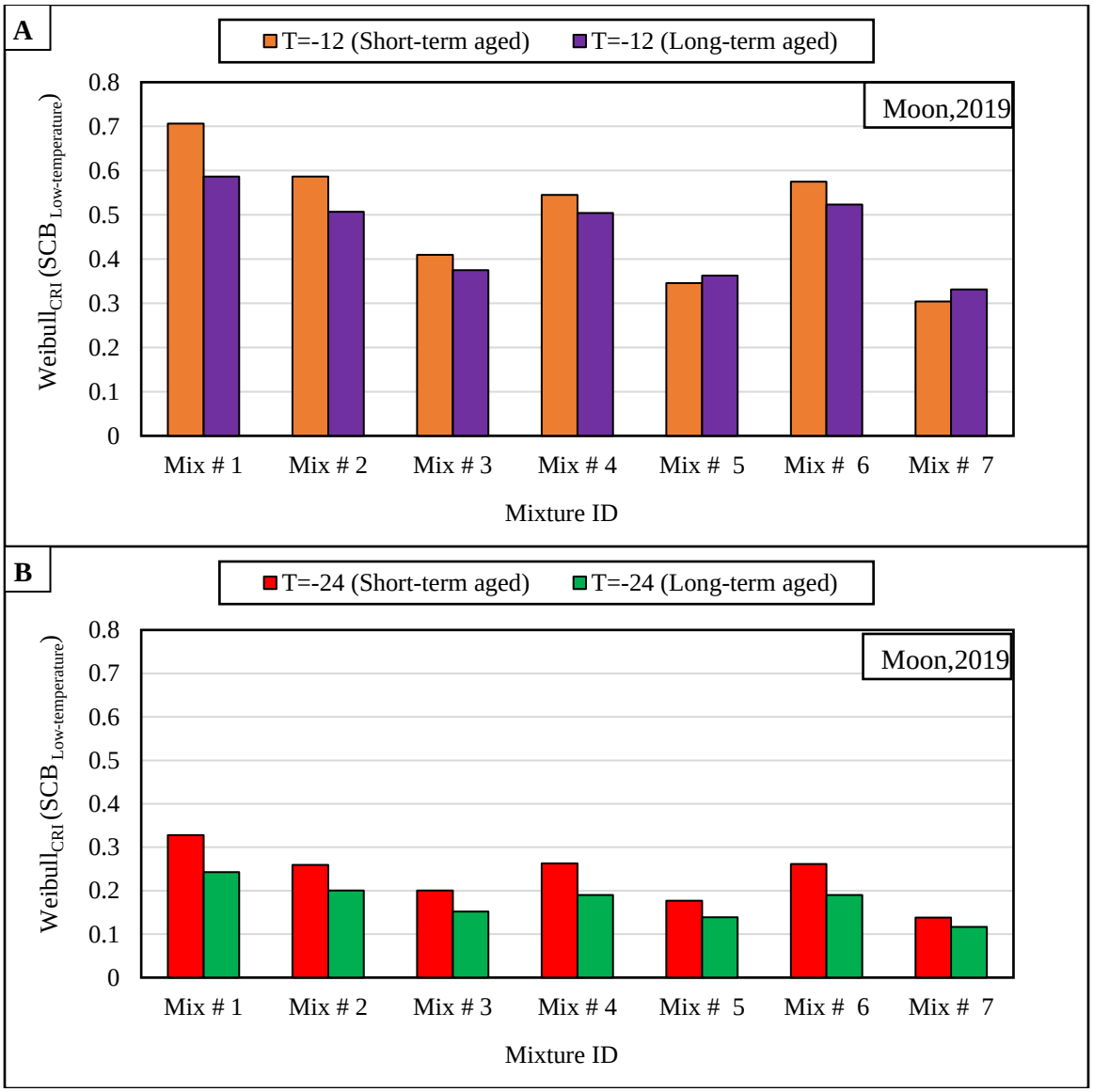


**Figure 7.3.** $Weibull_{CRI}(SCB_{Low\text{-}temperature})$ for mixes prepared with different RAP content at a test temperature of A) -12 °C and B) -24 °C using data published in [19].

*7.4.1.4. Simple Punching Shear Test (SPST)*

Faruk et al. (2015) used the Simple Punching Shear Test (SPST) to assess asphalt mix resistance to rutting ($SPST_{Rutting}$) [20]. They tested three different asphalt mixes prepared at three different binder contents including 1) Type D3 asphalt mix prepared at binder contents of 4.7%, 5.2%, and 5.7%, 2) Type D4 asphalt mix prepared at binder contents of 4.5%, 5.0%, and 5.5%, and 3) Type D5 asphalt mix prepared at binder contents of 6.1%, 6.6%, and 7.1%. Further information about mix properties, specimen preparation, and testing conditions and procedures is provided by Faruk et al. (2015) [20].

Figure 7.4 presents the variation in $Weibull_{CRI}$ determined from SPST test ($Weibull_{CRI}$ [$SPST_{Rutting}$]) for the evaluated mixes at different binder contents. In general, $Weibull_{CRI}$ ($SPST_{Rutting}$) decreased with the increase in binder content for all mixes (i.e., Type D3, D4, and D5). This observation is in good agreement with the expected impact of the increases in binder content on mix resistance to rutting. It is expected that mixes with higher binder content to have less resistance to rutting.

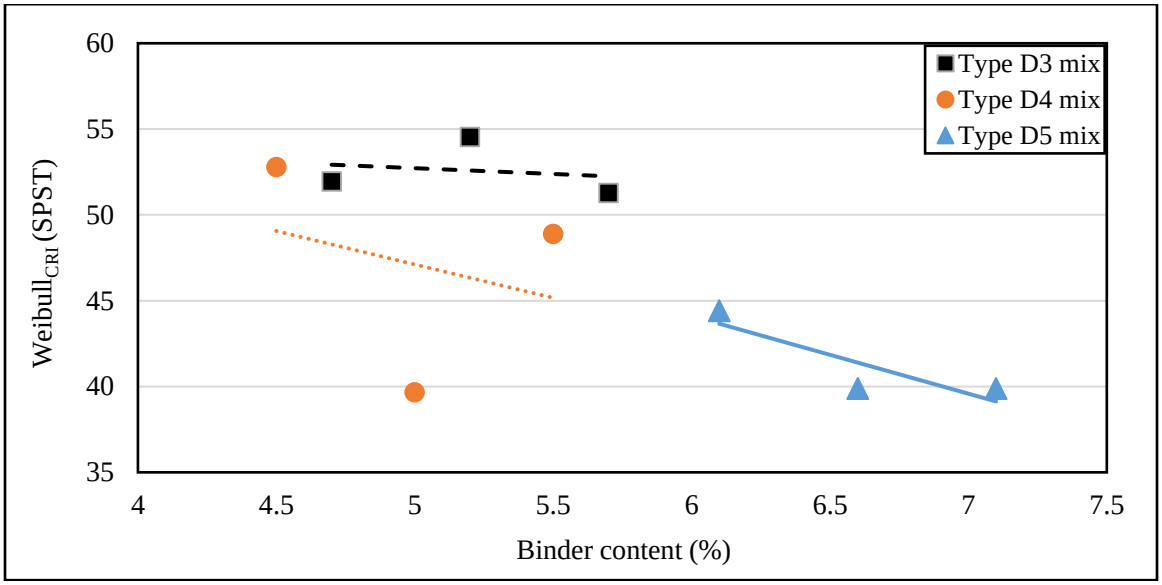


**Figure 7.4.** $Weibull_{CRI}$ from SPST using data collected from Faruk et al. (2015) [20]

*7.4.2. Sensitivity to the Change in Testing Conditions*

*7.4.2.1. Specimen Geometry and Displacement Measurement Method*

Son (2014) investigated the influence of specimen geometry and displacement measurement method on the resistance of asphalt mixes to low-temperature cracking [23]. This study examined the correlation between two different displacement measurement methods (Load Line Displacement [LLD] [or actuator displacement] and Crack Mouth Opening Displacement [CMOD]) and two specimen geometries (Semi-circle [SC] and Disk-shaped [DCT]) using four different asphalt mixes. Further information about mix properties, specimen preparation, and testing conditions and procedures is provided by Son (2014) [23].

Figure 7.5-A presents the correlation between $Weibull_{CRI}$ calculated from SC specimen using CMOD displacement ($Weibull_{CRI}$ [$SCB_{CMOD}$]) and LLD ($Weibull_{CRI}$

[$SCB_{LLD}$]. The indicators had an excellent correlation (coefficient of determination [$R^2$] of 0.89 [Figure 7.5-A]) and Pearson correlation coefficient (r) of 0.94. These findings demonstrate that $Weibull_{CRI}$ can be used as a tool to assess the resistance of asphalt mix to low-temperature cracking using LLD and CMOD data. Meanwhile, it should be noted that the LLD method is relatively simpler to perform compared to CMOD method.

Figure 7.5-B presents the correlation between $Weibull_{CRI}$ calculated from the DCT test using CMOD displacement ($Weibull_{CRI}$ [$DCT_{CMOD}$]) and $Weibull_{CRI}$ ($SCB_{CMOD}$) as well as the correlation between $Weibull_{CRI}$ ($DCT_{CMOD}$) and $Weibull_{CRI}$ ($SCB_{LLD}$). It can be observed that $Weibull_{CRI}$ ($DCT_{CMOD}$) had a good correlation with both $Weibull_{CRI}$ ($SCB_{CMOD}$) and $Weibull_{CRI}$ ($SCB_{LLD}$) with $R^2$ of 0.83 and 0.79, respectively. In addition, the results had an excellent Pearson correlation coefficient (r) of 0.91 and 0.89 between $Weibull_{CRI}$ ($DCT_{CMOD}$) and $Weibull_{CRI}$ (SCB-CMOD) and $Weibull_{CRI}$ (SCB-LLD), respectively. These findings demonstrated that both DCT and SCB tests provided a similar assessment of asphalt mix resistance to low-temperature cracking, therefore one test should be sufficient. Meanwhile, the SCB requires simpler specimen geometry compared to the DCT test.

#### *7.4.2.2. Specimen Initial Notch Depth*

Nsengiyumva (2015) and Rivera (2017) investigated the impact of variation in the initial notch depth of SCB test specimens on the test results. Nsengiyumva (2015) considered five different depths (i.e., 5, 15, 25, and 40 mm) while Rivera (2017) four different depths (i.e., 10, 15, 20, and 35 mm) [24,25]. Further information about mix properties, specimen preparation, and testing conditions and procedures is provided by Nsengiyumva (2015) and Rivera (2017) [24, 25].

Figure 7.6 presents the relationship between $Weibull_{CRI}$ (SCB) and initial notch depth. The $Weibull_{CRI}$ (SCB) decreased with the notch depth using data extracted from both studies. The data from Nsengiyumva showed that the un-notched specimen (i.e. 0 mm notch depth) had the highest $Weibull_{CRI}$ (SCB) of 3.38, while the specimen with 40 mm notch depth had the lowest $Weibull_{CRI}$ (SCB) of 1.90. Similar results were obtained using the data extracted from Rivera (2017) [25]. It should be noted that low $Weibull_{CRI}$ (SCB) indicates a decrease in mix resistance to cracking. These findings are in good agreement with the

expected effect of the increase in specimen initial notch depth. The cracking face area of a semi-circular specimen is equivalent to specimen thickness multiplied by the cracking ligament length. The ligament length is the difference between specimen diameter and notch depth. Therefore, the increase in specimen notch depth would decrease the specimen ligament length and cracking area, thus the specimen fractures faster indicating reduced resistance to cracking.

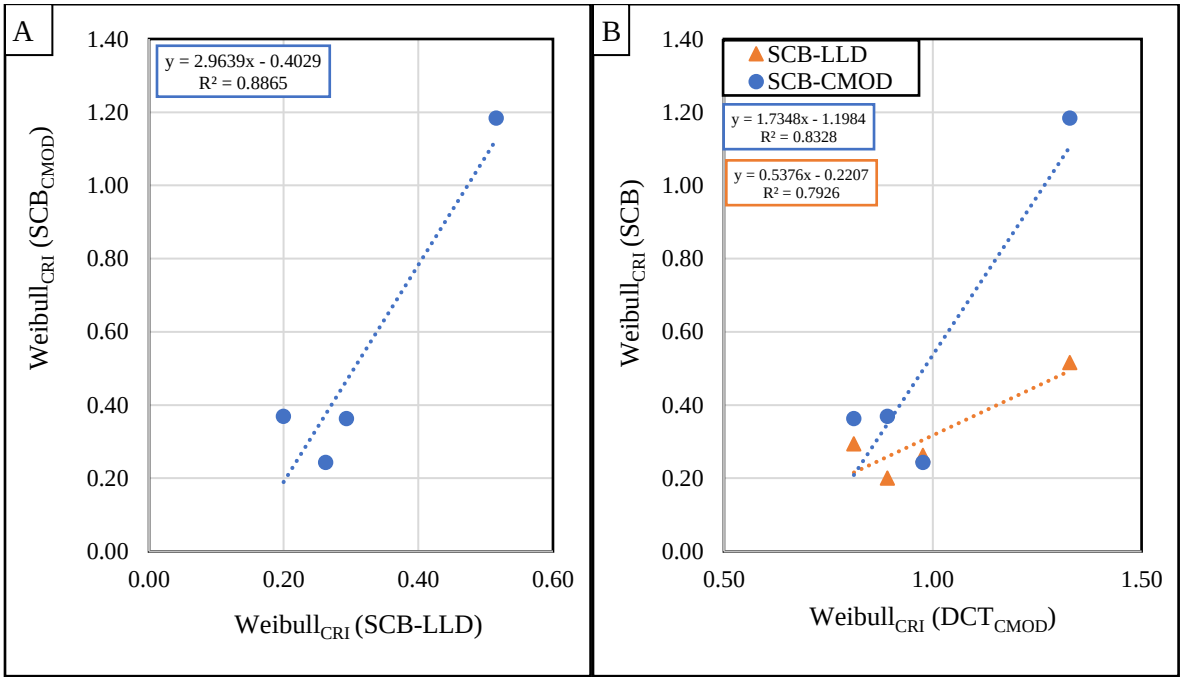


**Figure 7.5.** A) correlation between $Weibull_{CRI}(SCB_{CMOD})$ and $Weibull_{CRI}$ $(SCB_{LLD})$ and B) correlation between $Weibull_{CRI}(DCT_{CMOD})$ and $Weibull_{CRI}(SCB_{CMOD})$ and between $Weibull_{CRI}$ $(DCT_{CMOD})$ and $Weibull_{CRI}(SCB_{LLD})$ using data published in [23].

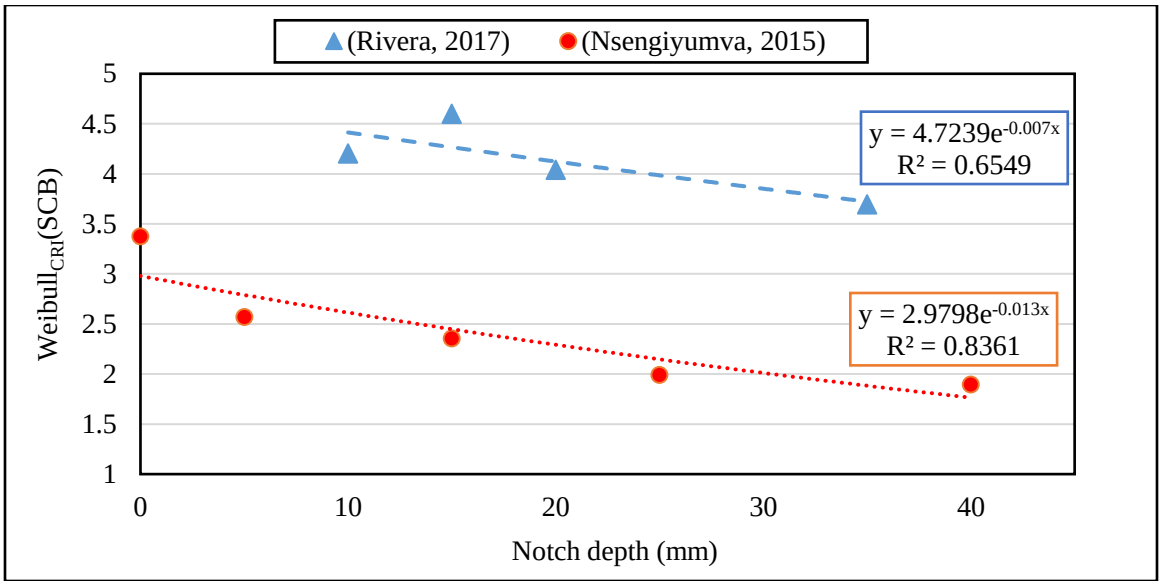


**Figure 7.6.** The sensitivity of $Weibull_{CRI}$ to the variation in specimen notch depth using data published in [24,25]

*7.4.2.3. Testing Loading Rate*

The monotonic cracking assessment tests are performed at a constant displacement rate. ASTM D8225, D6931 and AASHTO TP 124 are performed at a loading rate of 50 mm/min, while ASTM D8044 is performed at a loading rate of 0.5 mm/min. Several studies investigated the effect of loading rate on the testing results of monotonic tests. Nsengiyumva (2015), Rivera-Perez (2017), and Solaimanian and Chen (2017) examined the effects of various loading rates on the SCB test results [24-26]. Nsengiyumva (2015) considered five loading rates (0.1, 0.5, 1.0, 5.0, and 10 mm/min). Rivera-Perez (2017) included four loading rates (0.7, 6.25, 25, and 50 mm/min), while Solaimanian and Chen (2017) also evaluated four loading rates (1.0, 5.0, 25, and 50 mm/min). Further information about mix properties, specimen preparation, and testing conditions and procedures is provided in the respective reference [24-26].

The calculated $Weibull_{CRI}$ (SCB) and $Weibull_{CRI}$ fitting parameters ($A$, $\acute{\eta}$, and $\beta$) at various loading rates are summarized in Table 7.2. It can be observed that $Weibull_{CRI}$ (SCB) was not very sensitive to the variation in the test loading rate. For instance, Nsengiyumva (2015) data showed that the slowest loading rate (i.e., 0.1 mm/min) had $Weibull_{CRI}$ (SCB) of 2.33, while the fastest loading rate (i.e., 10 mm/min) had $Weibull_{CRI}$ (SCB) of 2.07. A similar conclusion can be observed for $Weibull_{CRI}$ (SCB) calculated using data extracted from the

other studies. Therefore, it can be concluded that $Weibull_{CRI}$ (SCB) is not sensitive to the SCB loading rate which could be an advantage for $Weibull_{CRI}$ (SCB).

This observation can be explained by examining the variation in $Weibull_{CRI}$ fitting parameters with the variation in the test loading rate. It can be observed from Table 7.2 that $\beta$ and ή fitting parameters were less sensitive to the variation in test loading rate as compared to the area parameter (i.e., *A*). For instance, Nsengiyumva (2015) data showed that the slowest loading rate (i.e., 0.1 mm/min) had *A*, $\acute{\eta}$, and $\beta$ of 1763, 1.54, and 2.15, respectively, while the fastest loading rate (i.e., 10 mm/min) had *A*, $\acute{\eta}$, and $\beta$ of 4376, 1.27, and 2.24, respectively. The *A*, $\acute{\eta}$, and $\beta$ had 90%, 9% and -18% change between these two loading rates (i.e., 0.1 and 10 mm/min). This finding indicates that the variation in the loading rate mainly influences the area under the load-displacement curve (or parameter *A*).

**Table 7.2.** The sensitivity of $Weibull_{CRI}$ to the variation in test loading rate using data published in [24–26]

| Reference | Loading rate (mm/min) | $Weibull_{CRI}$ fitting parameters | | | $Weibull_{CRI}$(SCB) |
|---|---|---|---|---|---|
| | | $\beta$ | ή | A | |
| Nsengiyumva, (2015) [24] | 0.1 | 2.15 | 1.54 | 1763 | 2.33 |
| | 0.5 | 2.31 | 1.53 | 2784 | 2.28 |
| | 1 | 2.73 | 1.88 | 3335 | 2.42 |
| | 5 | 2.34 | 1.69 | 3746 | 2.58 |
| | 10 | 2.24 | 1.27 | 4376 | 2.07 |
| Rivera-Perez, (2017) [25] | 0.7 | 1.85 | 2.25 | 2015 | 4.02 |
| | 6.25 | 1.83 | 2.09 | 3700 | 4.07 |
| | 25 | 2.05 | 1.65 | 5163 | 2.98 |
| | 50 | 1.65 | 1.74 | 6890 | 4.04 |
| Solaimanian and Chen, (2017) [26] | 1 | 2.00 | 2.22 | 2026 | 3.68 |
| | 5 | 1.93 | 2.27 | 3431 | 4.15 |
| | 25 | 1.94 | 2.28 | 5638 | 4.41 |
| | 50 | 2.04 | 2.31 | 7613 | 4.41 |

*7.4.2.4. Specimen Thickness*

Nsengiyumva (2015), Barry (2016), and Rivera-Perez (2017) examine the effect of variation in specimen thickness on the test results of the SCB test [24,25,27]. Nsengiyumva (2015) examined five different specimen thicknesses (30, 40, 50, and 60 mm), while Barry (2016) examined six different specimen thicknesses (10, 20, 30, 40, 50, and 60 mm) prepared

using two different NMAS (4.75 and 9.50 mm). Rivera-Perez (2017) examined six different specimen thicknesses (25, 30, 40, 45, 50, and 60 mm). Further information about mix properties, specimen preparation, and testing conditions and procedures is provided in the respective references [24, 25, 27].

Table 7.3 summarizes the calculated $Weibull_{CRI}$ (SCB) at different specimen thicknesses. The results demonstrated that $Weibull_{CRI}$ (SCB) increases with the increases in specimen thickness. For instance, Nsengiyumva (2015) data showed that the specimen with the 30 mm thickness had $Weibull_{CRI}$ (SCB) of 2.42, while the specimen with the 60 mm thickness had $Weibull_{CRI}$ (SCB) of 2.54. A similar conclusion can be observed for $Weibull_{CRI}$ (SCB) calculated using data extracted from the other studies. These findings are in agreement with the expected effect of the increase in specimen thickness. The cracking face area of a semi-circle specimen is equivalent to specimen thickness multiplied by the cracking ligament length. Therefore, the increase in specimen thickness will increase the cracking area, thus it will require more energy to fracture the specimen.

This observation can also be explained by examining the variation in $Weibull_{CRI}$ fitting parameters with the variation in specimen thickness. It can be observed from Table 7.3 that $\beta$ and $\acute{\eta}$ fitting parameters were less sensitive to the variation in specimen thickness as compared to the area parameter (i.e., *A*). For instance, Nsengiyumva (2015) data demonstrated that 30-mm thick test specimen had *A*, $\acute{\eta}$, and $\beta$ of 1448, 1.52, and 1.98, respectively, while 60-mm thick test specimen had *A*, $\acute{\eta}$, and $\beta$ of 3516, 1.50, and 2.10, respectively. The *A*, $\acute{\eta}$, and $\beta$ had 143%, 6% and -1% change between these thicknesses. This finding indicates that the variation in specimen thickness mainly affects the area under the load-displacement curve (or parameter *A*), which is the amount of work required to fracture the specimen.

Similar limitations (i.e., an illogical trend with the change in specimen thickness) were reported for other monotonic cracking performance assessment indicators [4,5,25,28]. However, this is an important issue and needs to be addressed, especially when evaluating extracted field cores. The extracted cores from field projects had different thickness depending on the structure design of the selected projects. Therefore, the monotonic cracking

performance indicators (e.g., $Weibull_{CRI}$ [SCB]) should be able to eliminate the effects of specimen thickness on testing results or it may mislead the findings of the correlation between laboratory testing results and observed field performance. Further discussion about this limitation and the proposed correction approaches were provided in a previous study by the authors (Chapter 6)[22].

**Table 7.3.** The sensitivity of $Weibull_{CRI}$ to the variation in specimen thickness using data published in [24,25,27]

| References | Specimen thickness (mm) | $Weibull_{CRI}$ fitting parameters | | | $Weibull_{CRI}$ (SCB) |
|---|---|---|---|---|---|
| | | $\beta$ | ή | A | |
| Nsengiyumva, (2015) [24] | 30 | 1.98 | 1.52 | 1448 | 2.42 |
| | 40 | 2.21 | 1.51 | 2448 | 2.32 |
| | 50 | 2.65 | 1.80 | 3293 | 2.39 |
| | 60 | 2.10 | 1.50 | 3516 | 2.54 |
| Rivera-Perez, (2017) [25] | 25 | 1.82 | 1.94 | 3588 | 3.79 |
| | 30 | 1.75 | 2.16 | 4065 | 4.46 |
| | 40 | 1.77 | 2.03 | 5349 | 4.26 |
| | 45 | 1.71 | 1.95 | 5770 | 4.30 |
| | 50 | 1.87 | 1.89 | 6399 | 3.85 |
| | 60 | 1.76 | 1.96 | 7677 | 4.32 |
| Barry, 2016 (4.75 mm NMAS) [27] | 10 | 1.54 | 1.75 | 1365 | 3.57 |
| | 20 | 1.72 | 1.55 | 2479 | 3.06 |
| | 30 | 1.71 | 1.45 | 3830 | 3.02 |
| | 40 | 1.75 | 1.73 | 5853 | 3.73 |
| | 50 | 1.77 | 1.73 | 7139 | 3.75 |
| | 60 | 1.81 | 1.62 | 8261 | 3.51 |
| Barry, 2016 (9.5 mm NMAS) [27] | 10 | 1.54 | 1.01 | 791 | 1.90 |
| | 20 | 1.59 | 1.14 | 1754 | 2.32 |
| | 30 | 1.66 | 1.38 | 2951 | 2.88 |
| | 40 | 1.73 | 1.28 | 3561 | 2.63 |
| | 50 | 1.75 | 1.37 | 5049 | 2.89 |
| | 60 | 1.82 | 1.32 | 5520 | 2.73 |

#### *7.4.2.5. Specimen Air Void Content*

Barry (2016), Rivera-Perez (2017), and Solaimanian and Chen (2017) examined the influence of variation in air void content on the results of SCB test [25–27]. Barry (2016) examined eight different air void contents ([3%, 5%, 7.7%, and 9.8%] and [4%, 5.8%, 7.5%, and 9.7%] prepared with NMAS of 4.75 mm and 9.5 mm, respectively), Rivera-Perez (2017)

examined five different air void contents (2%, 4%, 6%, 8%, and 10%), while Solaimanian and Chen (2017) examined three different air void contents (2%, 4%, and 7%). Further information about mix properties, specimen preparation, and testing conditions and procedures is provided in the respective references [24,25,27].

Table 7.4 summarizes the calculated $Weibull_{CRI}$ (SCB) at various specimen air void contents for the selected studies. The results demonstrated that $Weibull_{CRI}$ (SCB) increases with the increases in specimen air void content. For instance, Nsengiyumva (2015) data showed that the specimen with the 4.0% air void content had $Weibull_{CRI}$ (SCB) of 3.08, while the specimen with the 9.7% air void content had $Weibull_{CRI}$ (SCB) of 4.22. Similar observations can be made for $Weibull_{CRI}$ (SCB) calculated using the data extracted from other studies. These findings indicated that the resistance of asphalt mix to cracking is improved with the increase in specimen air void content which contradicts the expected performance of the influence of air void on mix resistance to cracking [29,30].

Such observations can also be explained by examining the variation in $Weibull_{CRI}$ fitting parameters with the variation in air void content (Table 7.4). It can be observed that the area parameter ($A$) is responsible for providing the illogical trend with the variation in air void content. The shape parameter ($\beta$) decreased while the scale parameter ($\eta$) increased with the increase in air voids which indicates reduced resistance to cracking resistance (i.e., a logical trend). The area parameter ($A$) increased with the increase in air void content, which indicates improved mix resistance to cracking (i.e., illogical trend). $Weibull_{CRI}$ (SCB) results were mainly controlled by the area parameter ($A$) and provided an illogical trend.

Similar limitations (i.e., an illogical trend with the variation in specimen air void content) were reported for other monotonic cracking performance assessment indicators [4,5,25,28]. However, it is important that these indicators provide a logical trend with the variation in air void content, especially when evaluating extracted field cores. The field cores are expected to have a wide range of air void content, which may provide misleading cracking assessment evaluation. Further discussion about this limitation and proposed correction approaches were provided in Chapter 6 [22].

**Table 7.4**. The sensitivity of WeibullCRI to the variation in specimen air void content using data published in [25–27]

| References | Specimen air void content (%) | $Weibull_{CRI}$ fitting parameters | | | $Weibull_{CRI}$ (SCB) |
|---|---|---|---|---|---|
| | | $\beta$ | ή | A | |
| Barry, 2016 (4.75 mm NMAS) [27] | 4.0 | 1.85 | 1.47 | 7555 | 3.08 |
| | 5.8 | 1.79 | 1.66 | 7565 | 3.60 |
| | 7.5 | 1.74 | 1.78 | 7008 | 3.92 |
| | 9.7 | 1.73 | 1.92 | 6337 | 4.22 |
| Barry, 2016 (9.5 mm NMAS) [27] | 3.0 | 2.14 | 1.13 | 5131 | 1.95 |
| | 5.0 | 1.86 | 1.27 | 5177 | 2.54 |
| | 7.7 | 1.85 | 1.29 | 4513 | 2.56 |
| | 9.8 | 1.77 | 1.65 | 4946 | 3.45 |
| Rivera-Perez, 2017 [25] | 2.0 | 2.35 | 0.91 | 6019 | 1.47 |
| | 4.0 | 1.99 | 1.14 | 7709 | 2.23 |
| | 6.0 | 1.96 | 1.48 | 8073 | 2.95 |
| | 8.0 | 1.95 | 1.38 | 6781 | 2.71 |
| | 10.0 | 1.64 | 1.86 | 7425 | 4.38 |
| Solaimanian and Chen, 2017 [26] | 2.0 | 2.06 | 1.75 | 8278 | 3.33 |
| | 4.0 | 2.05 | 1.80 | 7166 | 3.40 |
| | 7.0 | 1.95 | 2.20 | 6459 | 4.30 |

### *7.4.3. Sensitivity to Change in Mix Properties*

#### *7.4.3.1. Sensitivity to Binder Content and Grade*

Alkuime et al. (2019) and Solaimanian and Chen (2017) examine the influence of variation in binder content on the results of different monotonic tests to assess asphalt mix resistance to intermediate-temperature cracking [13,26]. Alkuime et al. (2019) examined the effects of three binder contents (4.25%, 5.00%, and 5.75%) using two binder grades (PG 70-28 and PG 58-34) on the testing results of IDT and SCB tests, while Solaimanian and Chen (2017) examined four binder contents (4.70%, 5.20%, 5.70%, and 6.20%) on SCB test results. Further information about mix properties, specimen preparation, and testing conditions and procedures is provided by Alkuime et al. (2019) and Solaimanian and Chen (2017) [13,26].

Figure 7.7 presents the calculated $Weibull_{CRI}$ at various binder contents examined in each study. $Weibull_{CRI}$ calculated from the IDT test ($Weibull_{CRI}$ [IDT]) and the SCB test ($Weibull_{CRI}$ [SCB]) increased with binder content for the data extracted from each study. These findings are in good agreement with the expected influence of the increase in binder

content on mix resistance to cracking. Mixes with higher binder content are expected to be more flexible and provide better resistance to cracking.

The data from Alkuime et al. (2019) was used to examine the sensitivity of $Weibull_{CRI}$ (IDT) and $Weibull_{CRI}$ (SCB) to the variation in binder PG. $Weibull_{CRI}$ (SCB) indicated that specimens prepared with the softer binder (PG 58-34) showed better resistance to cracking compared to the stiffer binder (PG 70-28) at the corresponding binder content. Meanwhile, $Weibull_{CRI}$ (IDT) indicated a similar trend at 5.0% binder content only. Softer binders are expected to improve the resistance of asphalt mixtures to cracking compared to stiffer binders. Furthermore, $Weibull_{CRI}$ (IDT) and $Weibull_{CRI}$ (SCB) test results had low variability (Average COV < 15%) and moderate variability (15% < average COV < 25%), respectively. $Weibull_{CRI}$ (IDT) had an average COV of 7.4% and ranged between 0.6% and 19.8 %, while $Weibull_{CRI}$ (SCB) had an average COV of 16.4% and ranged between 5.3% and 34.7%.

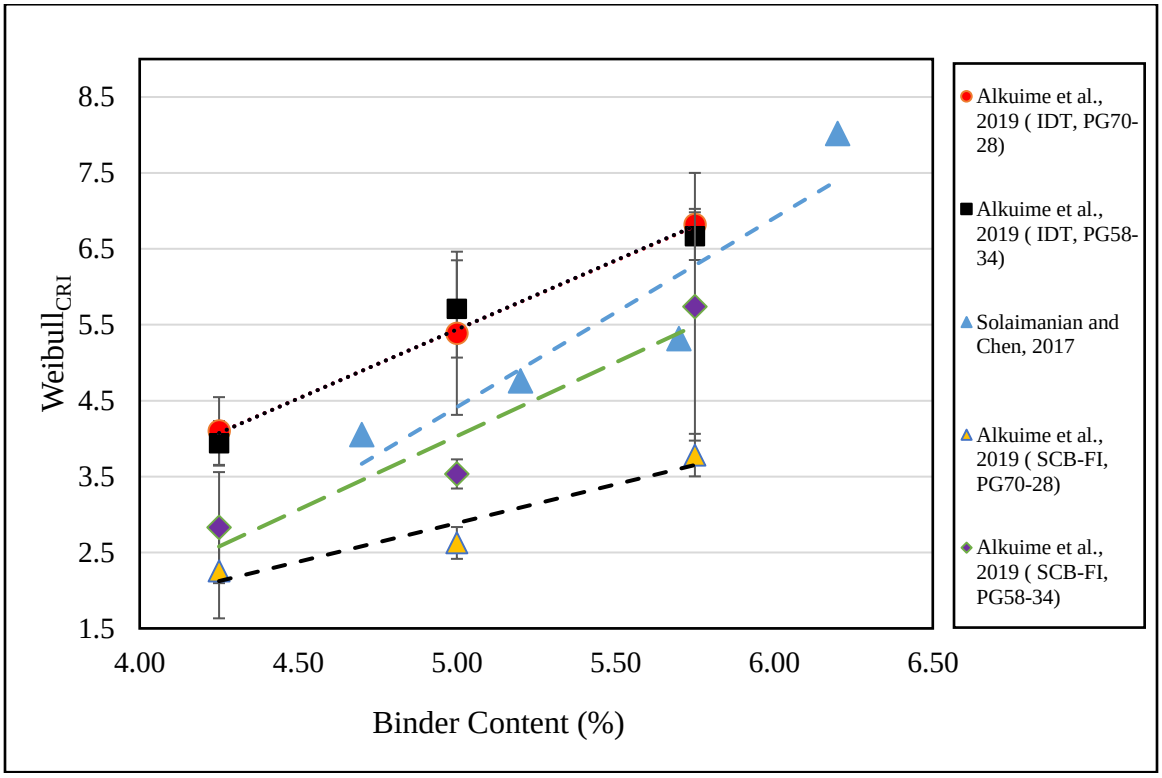


**Figure 7.7.** The sensitivity of $Weibull_{CRI}$ to the variation in binder content using data published in [13,26]

#### *7.4.3.2. Sensitivity to Aggregate Type and Binder Grade*

Barros (2018) examined the influence of aggregate type (dolomite and granite) and binder grade (PG 64-22, PG 70-22, and PG 76-22) on asphalt mix resistance to intermediate-temperature cracking using the IDT test [18]. Information about mix properties, specimen preparation, and testing conditions and procedures is provided by Barros (2018) [18]. Figure 7.8 presents the calculated $Weibull_{CRI}$ from IDT ($Weibull_{CRI}$ [IDT]) test with aggregate type and binder grade. It can be observed that test specimens prepared with granite aggregate had better cracking resistance compared to the ones prepared with dolomite aggregate at PG 70-22 and PG 76-22. However, an opposite trend was observed at binder PG 64-22. This finding is in agreement with the expected performance of each aggregate type. The granite aggregate had a lower crushing value thus, it is expected to provide better strength as compared to the dolomite aggregate.

Figure 7.8 also presents the change in $Weibull_{CRI}$ (IDT) with binder grade. The test specimens prepared with dolomite aggregate indicated that specimens with the stiffer binder grade had less resistance to cracking as compared to specimens prepared with the softer binder. For instance, specimens prepared with PG 64-22 and PG 76-22 binders had $Weibull_{CRI}$ (IDT) of 6.29 and 5.22, respectively. Similarly, test specimens prepared with granite aggregate provided a logical trend between PG 70-22 and PG 76-22 only.

Furthermore, the $Weibull_{CRI}$ (IDT) results had low variability. Specimens prepared with dolomite aggregates had average COV of 7.3% and ranged between 3.9% and 10.3%, while specimens prepared with granite aggregates had average COV of 7.5% and ranged between 5.3% and 10.2%.

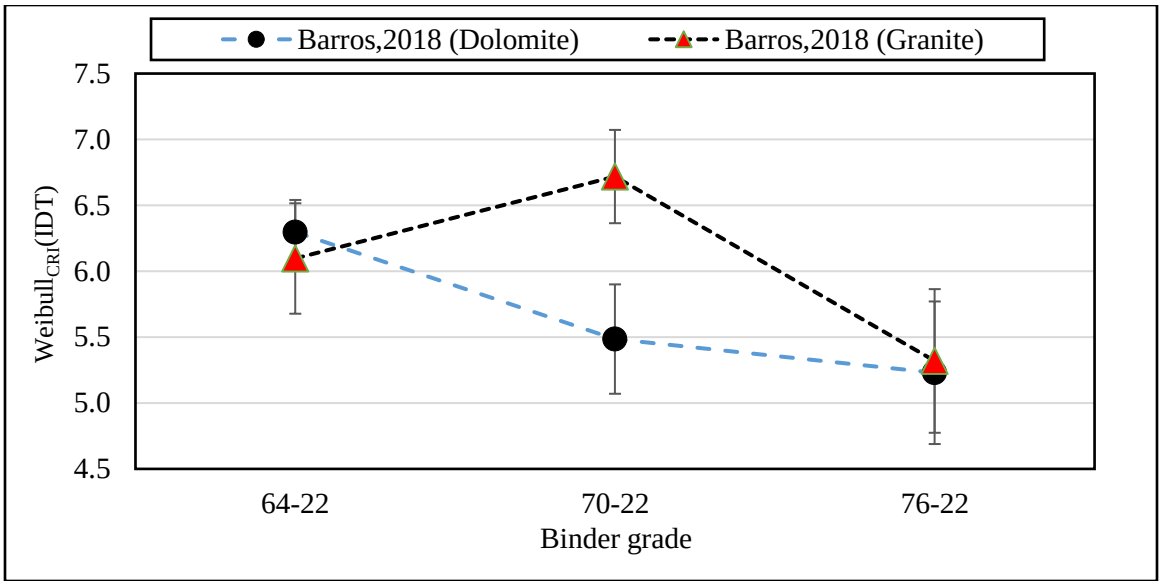


**Figure 7.8.** The sensitivity of Weibull$_{CRI}$ to the variation in aggregate type and binder grade using data published in [18].

*7.4.3.3. Sensitivity to Nominal Maximum Aggregate Size*

Barry (2016) examined the influence of the variation in Nominal Maximum Aggregate Size (NMAS) on the SCB test results to assess intermediate-temperature cracking [27]. Specimens were prepared with two different NMAS (4.75 mm and 9.50 mm) and various thicknesses and air void content. Further information about mix properties, specimen preparation, and testing conditions and procedures is provided by Barry (2016) [27].

Figure 7.9 presents the calculated Weibull$_{CRI}$ from the SCB test (Weibull$_{CRI}$ [SCB]) with NMAS. It can be observed that specimens prepared with the small NMAS (i.e., 4.75 mm) had higher Weibull$_{CRI}$ (SCB) as compared to specimens prepared with larger NMAS (i.e., 9.50 mm). Higher Weibull$_{CRI}$ (SCB) indicates better resistance. This finding is in agreement with the expected effect of NMAS on mix resistance to cracking. Mixes prepared with low NMAS require higher binder content as compared to mixes prepared with high NMAS, thus it is expected that to have better resistance to cracking [31].

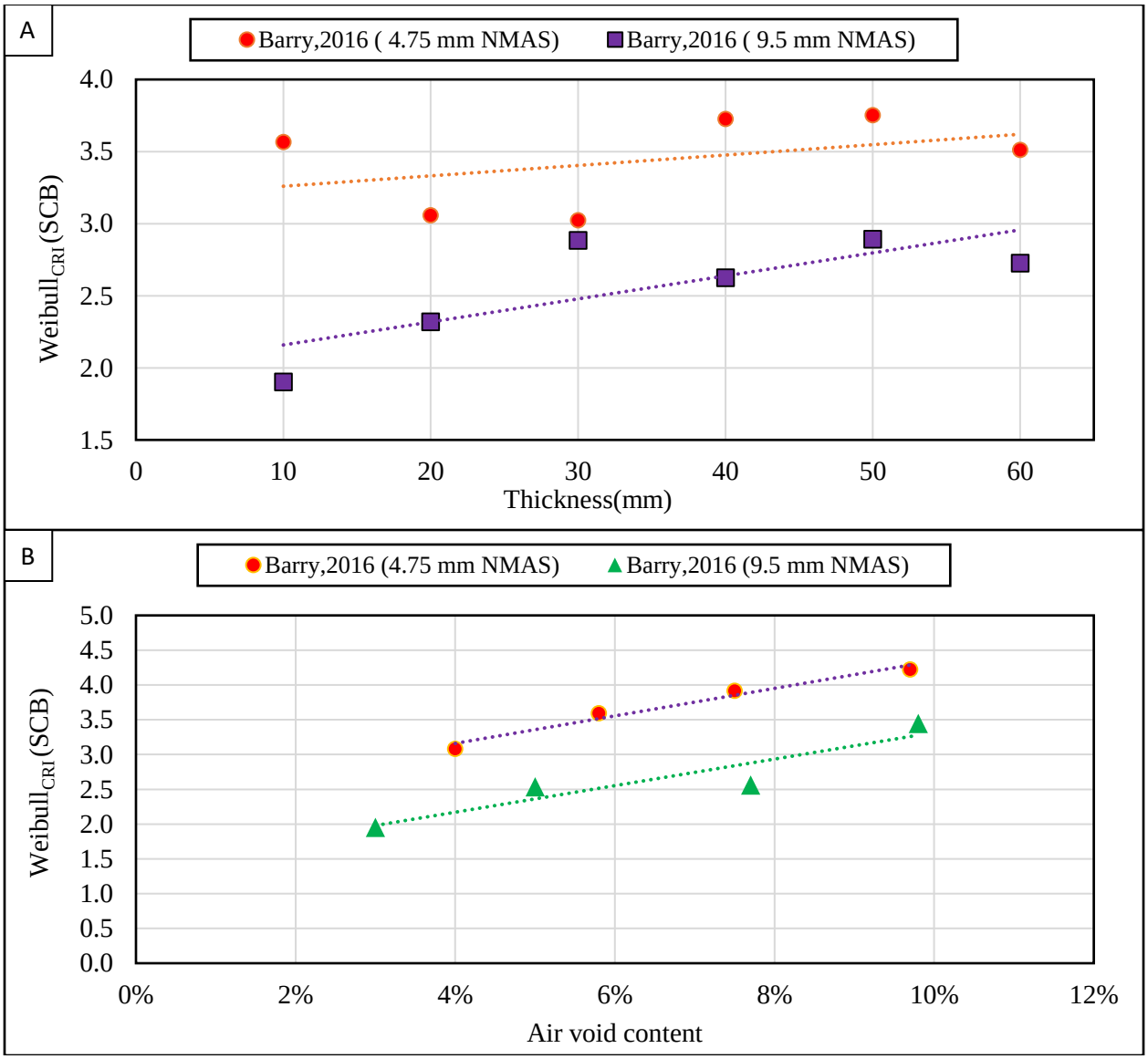


**Figure 7.9**. The sensitivity of Weibull$_{CRI}$ to the variation in NMAS at A) different specimen thickness and B) at different specimen air void content using data published in [27]

*7.4.3.4. Sensitivity to Mix Aging*

Zhu et al. (2019) examined the influence of aging on the SCB test results to assess asphalt mix resistance to intermediate-temperature cracking [32]. The study evaluated three different aging conditions (unaged, aged for one day at 95 °C, and aged for five days at 85 °C). Further information about mix properties, specimen preparation, and testing conditions and procedures is provided by Zhu et al. (2019) [32].

Figure 7.10 represents the calculated $Weibull_{CRI}$ from SCB ($Weibull_{CRI}$ [SCB ]) at different aging conditions. It can be observed that $Weibull_{CRI}$ (SCB ) decreased with aging time. The unaged, aged for one day at 95 °C, and aged for five days at 85 had $Weibull_{CRI}$ (SCB ) of 4.46, 3.47, and 2.72, respectively. This finding is in good agreement with the expected influence of the increase in specimen aging on mix resistance to cracking. The aged mix is often stiffer than the unaged mix, thus it would have less resistance to cracking.

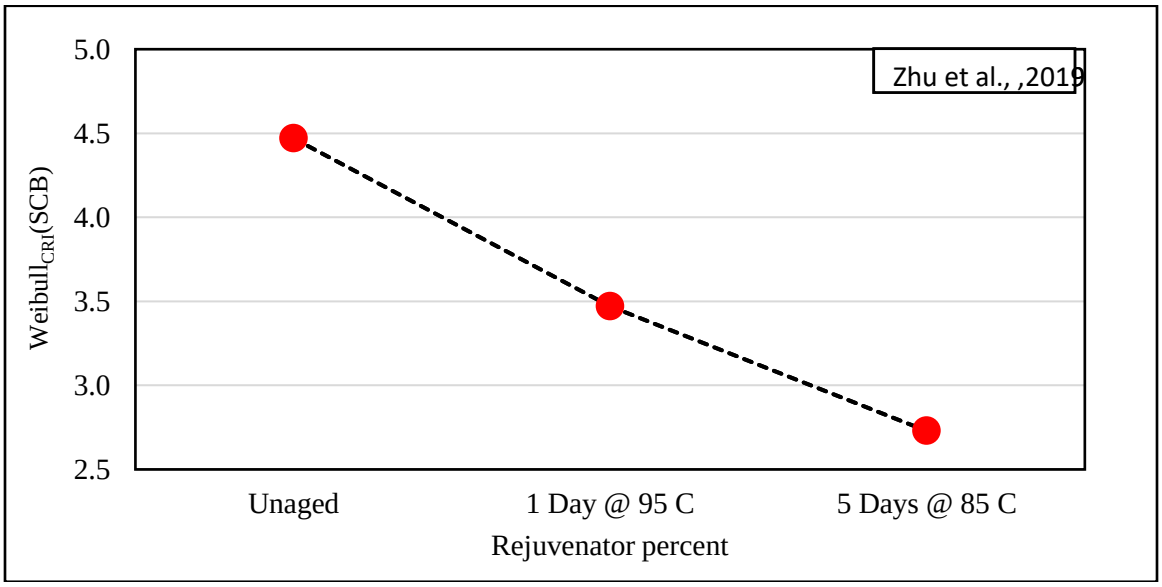


**Figure 7.10.** The sensitivity of $Weibull_{CRI}$ to the variation in aggregate type and binder grade using data published in [32]

*7.4.3.5. Sensitivity to the Use of Rejuvenators*

Barry (2016) examined the influence of the use of rejuvenator on the SCB test results to assess intermediate-temperature cracking [27]. The study prepared specimens with four different rejuvenator dosages (0%, 5%, 10%, and 15%) as a percent of total binder weight. The study also evaluated specimens with and without rejuvenator at three different aging durations (0 days, 4 days, and 10 days) at 85 °C. Further information about mix properties, specimen preparation, and testing conditions and procedures is provided by Barry (2016) [27].

Figure 7.11-A presents the calculated $Weibull_{CRI}$ from the SCB test ($Weibull_{CRI}$ [SCB]) at various rejuvenator dosages. It can be observed that $Weibull_{CRI}$ (SCB) increased with the increase in rejuvenator dosage which indicates improved mix resistance to cracking.

Specimens prepared with 0%, 5%, 10%, and 15% had $Weibull_{CRI}$ (SCB) of 0.9, 1.8, 2.1, and 3.03, respectively. These findings are in agreement with the expected effect of adding rejuvenator on mix resistance to cracking. Rejuvenators help to restore the ratio of asphaltene to maltene in asphalt binder which reduces mix stiffness and improves mix resistance to cracking.

Figure 7.11-B presents the calculated $Weibull_{CRI}$ (SCB) at different aging durations. It can be observed that the increase in aging duration reduced the $Weibull_{CRI}$ (SCB) for both specimens prepared with and without rejuvenators. It also can be observed that specimens with rejuvenator had higher $Weibull_{CRI}$ (SCB) as compared to specimens without rejuvenator at the corresponding aging time. In addition, specimens prepared with rejuvenator had a lower reduction rate in $Weibull_{CRI}$ (SCB) with the aging time as compared to specimens prepared without rejuvenator. These findings are in agreement with the impact of rejuvenator materials and specimen aging on mix resistance to cracking.

#### *7.4.3.6. Sensitivity to the Use of Recycled Asphalt Pavement Materials*

Al-Qadi, et al. (2015), Barros (2018), and Kaseer et al. (2018) examined the influence of using RAP materials on the IDT and SCB test results [2,4,18]. Barros (2018) evaluated IDT specimens prepared using two aggregate types (dolomite and granite) and four different Recycled Binder Replacement (RBR) percentages (0% [no RAP), 15%, 30%, and 45%). Al-Qadi, et al. (2015) and Kaseer et al. (2018) evaluated SCB specimens prepared using two RBR percentages (0% and 15 %). Further information about mix properties, specimen preparation, and testing conditions and procedures is provided by the respective references [2,4,18].

Figure 7.12 presents $Weibull_{CRI}$ at different RBR percentages using data collected from the previous sources. The test results of Al-Qadi, et al. (2015) and Kaseer et al. (2018) indicated that mix resistance to cracking is reduced (i.e., lower $Weibull_{CRI}$ [SCB]) with the increased percentage of RAP materials, while Barros (2018) results indicated unclear trends. For instance, $Weibull_{CRI}$ (IDT) decreased when RBR was between 0% and 30% RAP content for both aggregates, but it increased when RBR reach 45%. The findings from of Al-Qadi, et al. (2015) and Kaseer et al. (2018) are in agreement with the effects of using RAP materials

on the cracking resistance of asphalt mixes or increases the RBR percentages. In addition, the test results of Barros (2018) mixes indicated that $Weibull_{CRI}$ results had low variability. Mixes prepared with dolomite aggregate had an average COV of 5.7% and range between 3.9% and 8.8%. In addition, mixes prepared with granite aggregate had an average COV of 8.6% and range between 5.4% and 10.3 %.

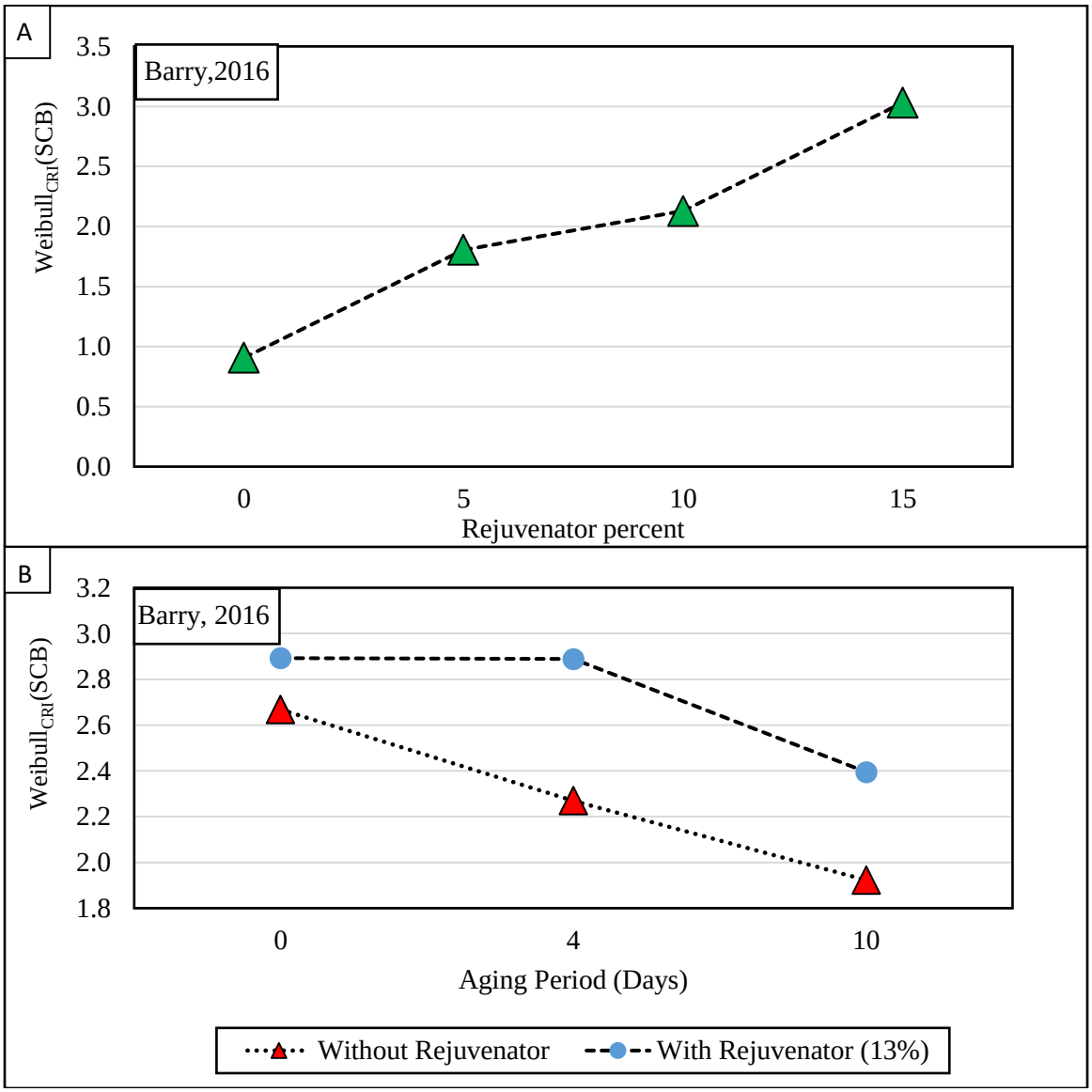


**Figure 7.11.** The sensitivity of $Weibull_{CRI}$ to A) different rejuvenator dosages and B) rejuvenator and aging effects using data published in [27]

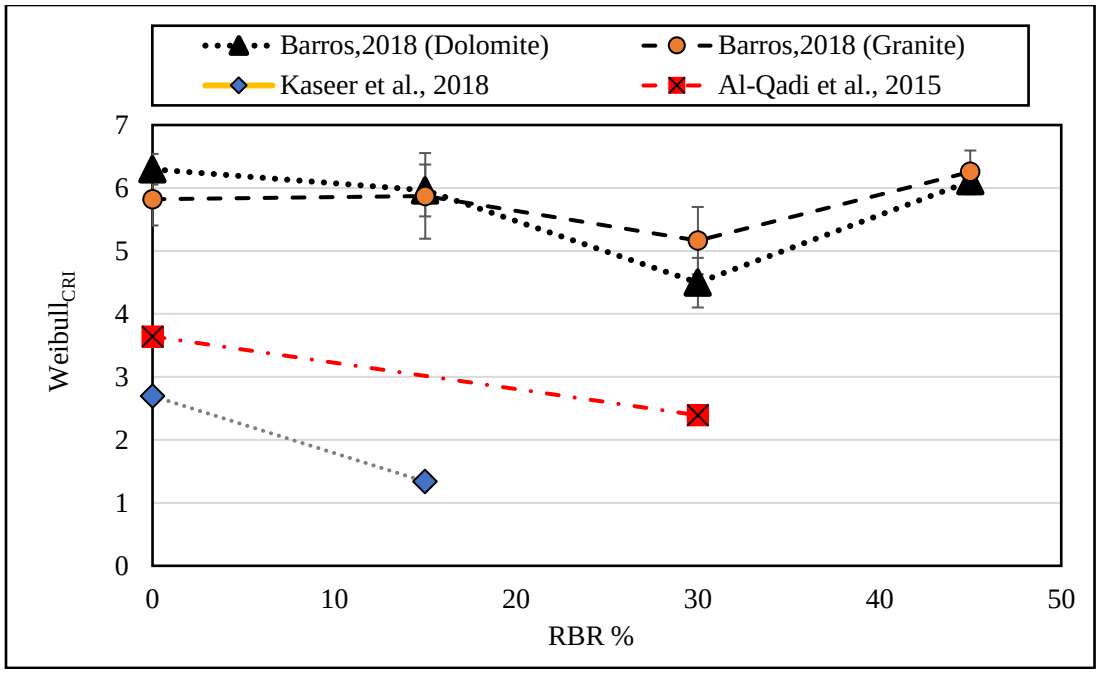


**Figure 7.12.** The sensitivity of Weibull$_{CRI}$ to the variation in Recycled Binder Replacement (RBR) percentages using data published in [2,4,18].

### *7.4.4. Correlation with Cyclic Cracking Assessment Tests*

Although monotonic tests are preferred over the cyclic cracking assessment tests, the cyclic tests simulate fatigue damage under repeated traffic loads in the field better than the monotonic tests. Therefore, it is important that the selected monotonic tests and performance indicators to have good correlation (or similar cracking assessment) with cyclic assessment tests. This section examines the ability of Weibull$_{CRI}$ obtained from different monotonic tests to correlate with different cyclic cracking assessment tests.

#### *7.4.4.1. Correlation between Disk-Shaped Compact Tension (DCT) and Bending Beam Fatigue (BBF) test*

Chiangmai (2010) used the Disk-Shaped Compact Tension (DCT) to predict the correlation with the Bending Beam Fatigue (BBF) test [21]. The study used five PMLC mixes with various properties to determine the appropriate monotonic performance indicators calculated from the DCT test that well correlated with the cyclic performance indicators calculated from the BFF test. Further information about mix properties, specimen preparation, and testing conditions and procedures is provided by Chiangmai (2010) [21].

Figure 7.13 presents $Weibull_{CRI}$ determine from Disk-Shaped Compact Tension (DCT) ($Weibull_{CRI}$ [DCT]) results for the evaluated PMLC mixes. It can be observed that $Weibull_{CRI}$ (DCT) had a moderate variability. The $Weibull_{CRI}$ (DCT) had an average COV of 22.5% and ranged between 14% and 32%.

Figure 7.14 presents the correlation between $Weibull_{CRI}$ (DCT) and cyclic performance indicators calculated from BFF test (fatigue life at 50 % reduction in mix initial stiffness [$Nf_{50}$], and the Plateau Value [PV]) at two different strain rate levels (700 and 1000 microstrain/second). The results demonstrate that $Weibull_{CRI}$ (DCT) to have good correlation with both cyclic performance indicators at different strain levels. For instance, $Weibull_{CRI}$ (DCT) had coefficient of determination ($R^2$) of 0.87 and 0.91 with $Nf_{50}$ and PV, respectively at a strain rate of 1000 microstrain/second. Similarly, $Weibull_{CRI}$ (DCT) had $R^2$ of 0.52 and 0.74 with $Nf_{50}$ and PV, respectively at a strain rate of 700 microstrain/second.

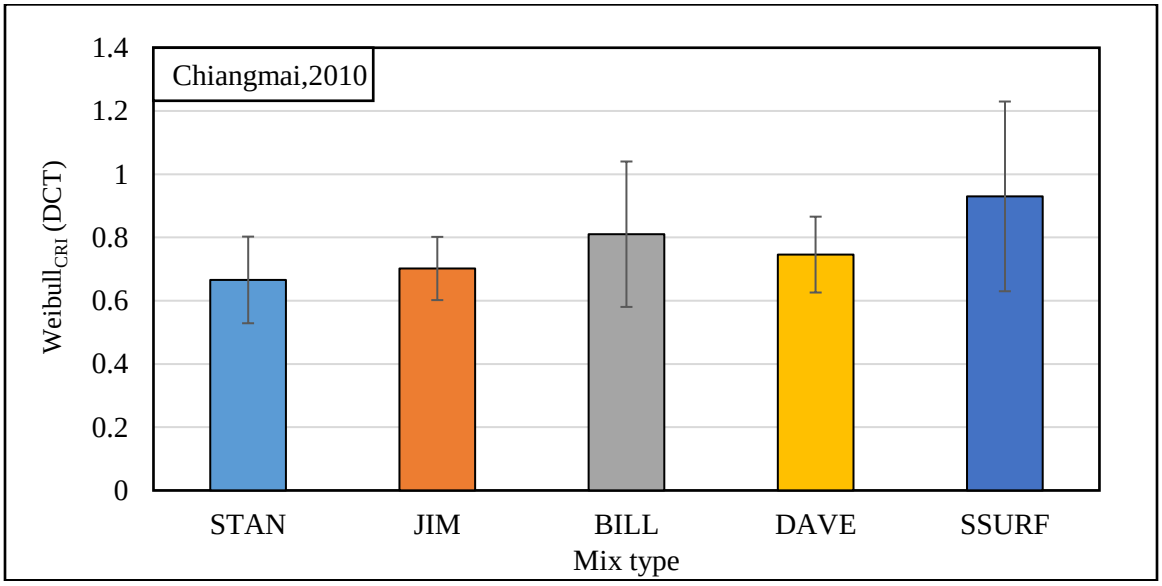


**Figure 7.13.** $Weibull_{CRI}$ from the Disk-shaped compact tension using data collected from Chiangmai, (2010) [21]

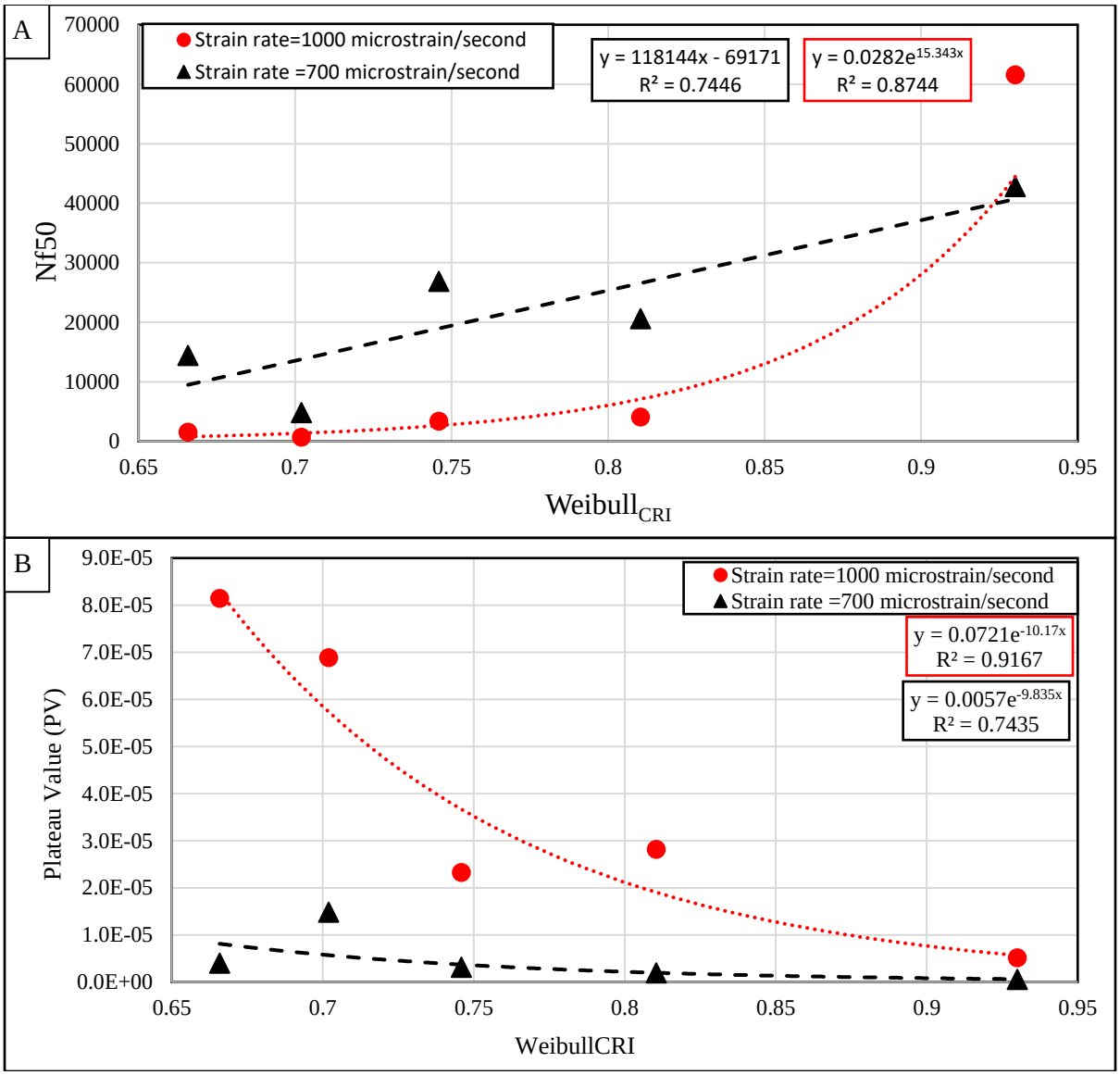


**Figure 7.14.** Correlation between $Weibull_{CRI}$ for the Disk-shaped compact tension and A) $Nf_{50}$ and B) PV using data collected from Chiangmai, (2010) [21]

### *7.4.4.2. Correlation between IDT and SCB tests with Multi-Stage Semi-Circle Bending Dynamic Test*

In this study, the authors examined the correlation between $Weibull_{CRI}$ calculated from IDT ($Weibull_{CRI}$ [IDT]) and SCB ($Weibull_{CRI}$ [SCB]) tests with the cyclic performance indicators obtained from the newly developed Multi-Stage Semi-Circle Dynamic Test (MSSD). The MSSD incorporates two performance indicators to assess asphalt mix resistance to intermediate temperature including the slope ($z$) and Abs (log $H$). Further detailed information about these indicators is provided in Chapter 4. A total number of 10 PMLC

mixes with different properties were examined and tested using the selected tests. Further detailed information about mix properties, specimen preparation, testing conditions and procedures, testing results, and the calculated performance indicators is provided in Chapter 2 and Chapter 5.

Figure 7.15 represents the correlation between different performance indicators. It can be observed that $Weibull_{CRI}$ (IDT) had a better correlation with both cyclic indicators (i.e., slope [$z$] and Abs [log $H$]) compared to $Weibull_{CRI}$ (SCB). For instance, the results showed that $Weibull_{CRI}$ (IDT) and $Weibull_{CRI}$ (SCB) had good and poor correlation with the slope ($z$) with $R^2$ of 0.80 and 0.15, respectively (Figure 7.15-A). Similarly, $Weibull_{CRI}$ (IDT) and $Weibull_{CRI}$ (SCB) had fair and poor correlation with the Abs (log $H$) with $R^2$ of 0.51 and 0.1, respectively (Figure 7.15-B). Therefore, $Weibull_{CRI}$ (IDT) is recommended over $Weibull_{CRI}$ (SCB). $Weibull_{CRI}$ (IDT) had the best correlation with MSSD indicators compared to various performance indicators used in the literature as discussed in Chapter 6.

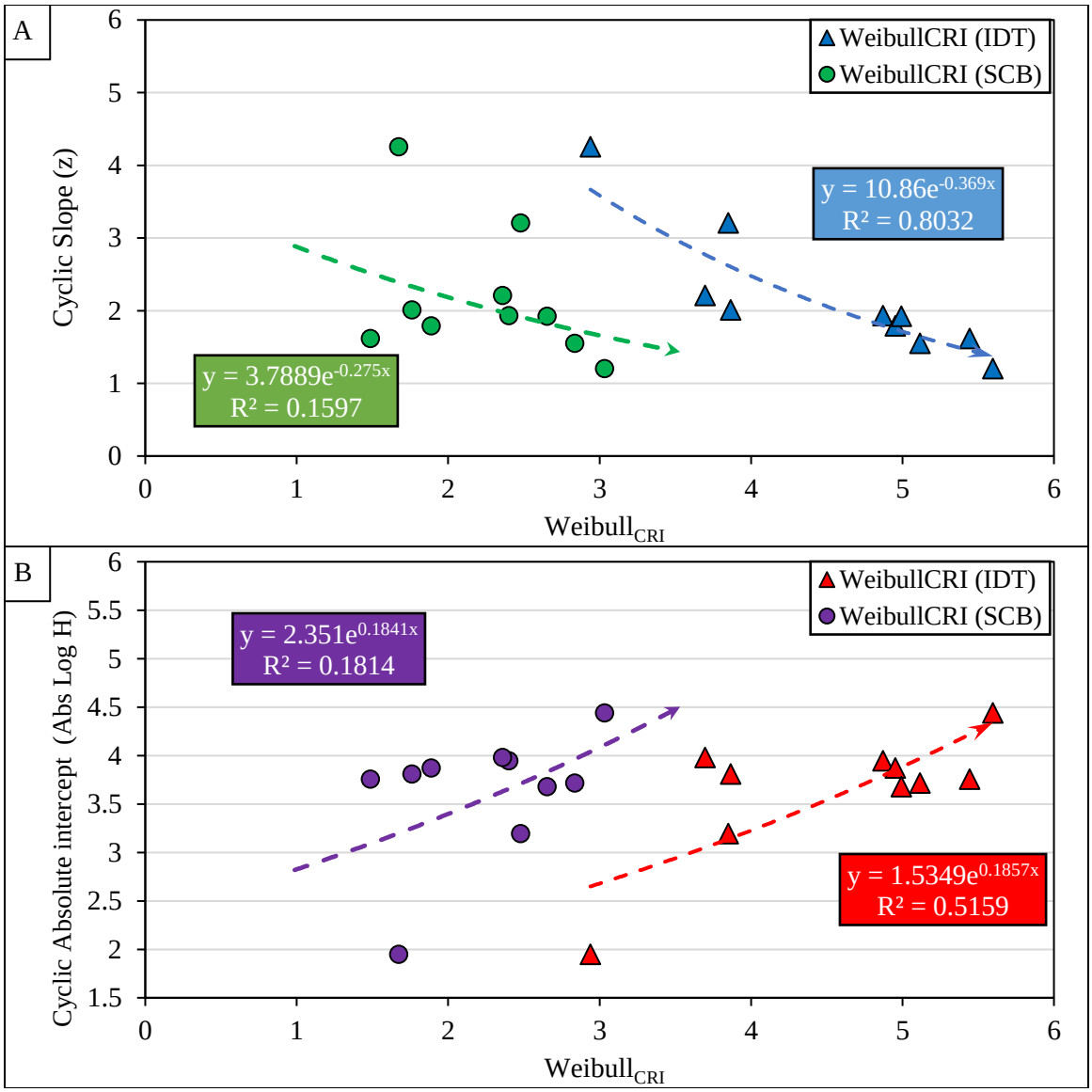


**Figure 7.15.** Correlation between $Weibull_{CRI}$ from IDT and SCB tests with MSSD performance indicators [13,14,22]

## 7.5. Conclusions

This study aimed to investigate the applicability of $Weibull_{CRI}$ as a unified approach to analyze the results of various monotonic cracking assessment tests using data generated by other researchers and reported in the literature. The evaluation covered four aspects including ability to analyze the load-displacement curve of various monotonic assessment tests, sensitivity to the change in testing conditions (e.g., specimen geometry), sensitivity to the change in mix properties (e.g., [percent RAP, percent binder, aggregate type]), and

correlation with cyclic cracking assessment tests. In addition, the variability of $Weibull_{CRI}$ was examined as data is available.

The study findings showed that $Weibull_{CRI}$ was able to interpret the results of IDT and SCB tests to assess asphalt mix resistance to intermediate-temperature cracking. In addition, SCB and DCT tests results were used to assess the resistance of asphalt mixtures to low-temperature cracking. The SPST test data was also used to assess asphalt mix resistance to rutting. $Weibull_{CRI}$ was found to be sensitive to the variation in specimen notch depth, thickness, and air void content. $Weibull_{CRI}$ also provided logical trends with the variation in binder content, binder grade, aggregate type, NMAS, aging, rejuvenator dosages, and RAP materials. Also, the results showed that $Weibull_{CRI}$ to have good correlation with the cyclic performance indicators from BFF and MSSD tests. Overall, $Weibull_{CRI}$ results had low variability.

## 7.6. References

[1] F. Zhou, D. Newcomb, C. Gurganus, S. Banihashemrad, M. Sakhaeifar, E.S. Park, R.L. Lytton, Field Validation of Laboratory Tests to Assess Cracking Resistance of Asphalt Mixtures: An Experimental Design, 2016. doi:10.17226/23608.

[2] I. Al-Qadi, H. Ozer, J. Lambros, A. El Khatib, D. Singhvi, Testing Protocols to Ensure Performance of High Asphalt Binder Replacement Mixes Using RAP and RAS (Report No. R27-128), Urbana, IL: Illinois Center for Transportation, Illinois Dept. of Transportation. (2015).

[3] R.C. West, C. Van Winkle, S. Maghsoodloo, S. Dixon, Relationships between simple asphalt mixture cracking tests using ndesign specimens and fatigue cracking at FHWA's accelerated loading facility, Road Materials and Pavement Design. 86 (2017) 579–602. doi:10.1080/14680629.2017.1389083.

[4] F. Kaseer, F. Yin, E. Arámbula-Mercado, A.E. Martin, J.S. Daniel, S. Salari, Development of an index to evaluate the cracking potential of asphalt mixtures using the semi-circular bending test, Construction and Building Materials. 167 (2018) 286–298. doi:10.1016/j.conbuildmat.2018.02.014.

[5] F. Zhou, S. Im, L. Sun, T. Scullion, Development of an IDEAL cracking test for asphalt mix design and QC/QA, Asphalt Paving Technology: Association of Asphalt Paving Technologists-Proceedings of the Technical Sessions. 86 (2017) 549–577. doi:10.1080/14680629.2017.1389082.

[6] F. Bayomy, A. abdo Ahmad, M. Ann Mull, Evaluation of hot mix asphalt ( HMA ) fracture resistance using the critical strain energy release rate, 2006.

[7] W.G. Buttlar, R. Roque, N. Kim, Accurate asphalt mixture tensile strength, in: Proceedings of the Materials Engineering Conference, 1996.

[8] AASHTO, Standard method of test for determining the creep compliance and strength of hot mix asphalt (HMA) using the indirect tensile test device AASHT322-07:, Washington D.C., 2011.

[9] A.A.A. Molenaar, A. Scarpas, X. Liu, S.M.J.G. Erkens, Semi-circular bending test; simple but useful, Asphalt Paving Technology: Association of Asphalt Paving Technologists. (2002). https://trid.trb.org/view.aspx?id=698764.

[10] L. Huang, K. Cao, M. Zeng, Evaluation of semicircular bending test for determining tensile strength and stiffness modulus of asphalt mixtures, Journal of Testing and Evaluation. 37 (2009) 122–128.

[11] R. Hofman, B. Oosterbaan, S.M.J.G. Erkens, J. Van der Kooij, Semi-circular bending test to assess the resistance against crack growth, 6th International Rilem Symposium. (2003) 257–263.

[12] R.C. West, A. Copeland, High RAP asphalt pavements: Japan practice-lessons learned, National Asphalt Pavement Association. 139 (2015) 62.

[13] H. Alkuime, E. Kassem, F. Bayomy, Development of a new performance indicator to evaluate the resistance of asphalt mixes to intermediate temperature cracking., Journal of Transportation Engineering, Part B: Pavements. (2019).

[14] H. Alkuime, E. Kassem, F.M. Bayomy, R. Nielsen, Development and evaluation of Multi-Stage Semi-circle bending Dynamic (MSSD) test to assess the cracking resistance of asphalt mixes., Construction and Building Materials. (2019).

[15] A. Rohatgi, WebPlotDigitizer User Manual, 2015.

[16] Y.R. Kim, H. Wen, Fracture energy from indirect tension testing, in: Asphalt Paving Technology, 2002: pp. 779–793.

[17] L.F. Walubita, V. Umashankar, X. Hu, B. Jamison, F. Zhou, T. Scullion, A.E. Martin, S. Dessouky, New Generation Mix-Designs: Laboratory Testing and Construction of the Apt Test Section, 2010.

[18] L. Barros, Influence of mix design parameters on performance of balanced asphalt concrete, University of Texas at El Paso, 2018.

[19] K.H. Moon, A. Cannone Falchetto, D. Wang, Y.S. Kim, Experimental Investigation on Fatigue and Low Temperature Properties of Asphalt Mixtures Designed with Reclaimed Asphalt Pavement and Taconite Aggregate, Transportation Research Record. (2019). doi:10.1177/0361198119835525.

[20] A.N.M. Faruk, S.I. Lee, J. Zhang, B. Naik, L.F. Walubita, Measurement of HMA shear resistance potential in the lab: The simple punching shear test, Construction and Building Materials. 99 (2015) 62–72. doi:10.1016/j.conbuildmat.2015.09.006.

[21] C.N. Chiangmai, Fatigue-fracture relation on asphalt concrete mixtures, University of Illinois at Urbana-Champaign, 2010.

[22] H. Alkuime, E. Kassem, F. Bayomy, Development of performance-engineered mix design (PEMD) specifications for intermediate temperature monotonic cracking assessment tests and performance indicators, Road Materials and Pavement Design. (2019).

[23] S. Son, Development of a phenomenological constitutive model for fracture resistance degradation of asphalt concrete with damage growth due to repeated loading, University of Illinois at Urbana-Champaign, 2014.

[24] G. Nsengiyumva, Development of Semi-Circular Bending ( SCB ) Fracture Test for Bituminous Mixtures, University of Nebraska, 2015.

[25] J. Rivera-Perez, Effects of speciemn geometry and test configuration on the fracture process zone for asphalt materials, University of Illinois at Urbana-Champaign, 2017.

[26] M. Solaimanian, X. Chen, Semi-Circular Bending Beam Test : Effect of Loading and Mix Parameters, in: Notrh East Asphalt User/Producer Group ( NEAUPG) Annual Meeting, 2017.

[27] M. Barry, An analysis of impact factors on the Illinois flexibility index test, University of Illinois at Urbana-Champaign, 2016.

[28] I. Al-Qadi, H. Ozer, J. Lambros, D. Lippert, A. El Khatib, T. Khan, P. Singh, J.J. Rivera-Perez, Testing protocols to ensure performance of high asphalt binder replacement mixes using RAP and RAS, 2015.

[29] R.N. Linden, J. Mahoney, N.C. Jackson, Effect of Compaction on Asphalt Concrete Performance, Transportation Research Board. (1989).

[30] N. Tran, P. Turner, J. Shambley, Enhanced compaction to improve durability and extend pavement service life : a literature review (NCAT Report 16-02R), 2016.

[31] M. Zaumanis, L.D. Poulikakos, M.N. Partl, Performance-based design of asphalt mixtures and review of key parameters, Materials and Design. 141 (2018) 185–201. doi:10.1016/j.matdes.2017.12.035.

[32] Z. Zhu, P. Singhvi, A.F. Espinoza-Luque, H. Ozer, I.L. Al-Qadi, Influence of mix design parameters on asphalt concrete aging rate using I-FIT specimens, Construction and Building Materials. 200 (2019) 181–187. doi:10.1016/j.conbuildmat.2018.12.099.

# Chapter 8: Recommendations and Guidelines for PEMD Implementation

In this research study, several cracking and rutting performance assessment tests and indicators were evaluated and validated. This chapter provides recommendations of the appropriate testing standards, performance indicators as well as performance specifications to assess asphalt mix resistance to cracking and rutting. In addition, this chapter provides guidelines to demonstrate the use of the proposed tools during the design and/or production of asphalt mix. It also proposes standard test procedures for the newly developed $Weibull_{CRI}$ indicator and MSSD test.

## 8.1. Recommendations

Based on the results of this study, the author recommends using the IDT testing standard and $Weibull_{CRI}$ (IDT) to assess asphalt mix resistance to cracking using monotonic cracking assessment tests. In addition, the MSSD test and slope (*z*) are selected to assess asphalt mix resistance to cracking using a dynamic cracking assessment test. For rutting evaluation, the author recommends the use of HWTT and $HWTT_{15000}$ to assess asphalt mix resistance to rutting.

The results of this study clearly showed that $Weibull_{CRI}$ is the only monotonic performance indicator that can describe the entire load-displacement curve of various monotonic cracking tests. In addition, the laboratory evaluation results indicated that $Weibull_{CRI}$ was found to be sensitive to variation in binder content and binder PG. In addition, the results of $Weibull_{CRI}$ were in good agreement with expected cracking resistance based on the composition of PMLC mixes. Also, $Weibull_{CRI}$ had the lowest variability and the highest number of Tukey's HSD groups. In addition, it had the best correlation with dynamic fatigue cracking parameters compared to other monotonic performance indicators. Furthermore, the investigation using data generated by other researchers and reported in the literature indicated that $Weibull_{CRI}$ can be used as a unified approach to analyze the results of various monotonic cracking assessment tests. $Weibull_{CRI}$ was able to interpret the testing results of various monotonic performance assessment tests (i.e., IDT, SCB, DCT, and SPST), various displacement measurement methods (i.e., actuator vertical displacement and

CMOD). In addition, it was sensitive to the variation in test conditions (i.e., specimen notch depth, thickness, and air void content) and mix composition (i.e., binder content, binder grade, aggregate type, NMAS, aging, rejuvenator dosages, and RAP materials).

The results of laboratory testing indicated that the IDT test and $Weibull_{CRI}$ (IDT) were recommended to assess asphalt mix resistance to cracking over the SCB test and $Weibull_{CRI}$ (SC). The IDT specimens are easier to prepare compared to the SC specimens. $Weibull_{CRI}$ (IDT) results were in better agreement with the expected cracking performance based on the composition of PMLC mixes. It also had a higher number of Turkey's HSD statistical groups and lower variability compared to $Weibull_{CRI}$ (SC) results. Therefore, the author selected IDT test and $Weibull_{CRI}$ (IDT) and proposed three pass/fail performance assessment thresholds (or PEMD specifications) for $Weibull_{CRI}$ (IDT) including, good cracking resistance group ($Weibull_{CRI} > 4.7$), fair cracking resistance group ($3.57 < Weibull_{CRI} \leq 4.7$), and poor cracking resistance group ($Weibull_{CRI} < 3.57$).

This study also developed and proposed the MSSD test and its performance indicators (i.e., slope [$z$] and Abs [log $H$]) to assess asphalt mix resistance to cracking. The MSSD has advantages over the available monotonic and dynamic cracking assessment tests and addresses the major concerns to implement the PEMD (i.e., performance test validity, specimen preparation, and testing time). The developed MSSD test simulates the repeated loading (dynamic) in a reasonable testing time (less than 9 hours per test regardless of mix type), has a fixed loading sequence that works for mixes with different characteristics (e.g., mix composition, percent air void content, thickness, etc.), and it utilizes testing equipment and specimen geometry similar to that used in monotonic tests. The results showed that the MSSD performance indicators correlated well with the observed cracking performance in the field and were able to differentiate between mixes with good and poor observed field cracking resistance. The research proposed three thresholds to distinguish between mixes resistance to cracking; good cracking resistance ($z \leq 1.9$) or (Abs [log $H$] > 3.60), fair cracking resistance ($1.9 < z \leq 2.9$) or ($3.0 <$ Abs [log $H$] $\leq 3.60$), and poor cracking resistance ($z > 2.9$) or (abs [log $H$] <3.0).

This study also examined the validity of HWTT and APA rut test and three rutting performance indicators (i.e., $HWTT_{15000}$, $HWTT_{20000}$, and $APA_{8000}$) to assess the resistance of asphalt mixes to rutting. The results showed that the indicators were sensitive to the variation in binder content and binder PG. $HWTT_{15000}$ and $HWTT_{20000}$ indicators provided an expected trend with the variation in binder content and PG, while the $APA_{8000}$ trend was expected for the variation in binder content only. In addition, the three indicators (i.e., $HWTT_{15000}$, $HWTT_{20000}$, and $APA_{8000}$) had similar variability and statistical grouping of PMLC mixes and were able to differentiate between field projects with different rutting resistance. Although both HWTT and APA rut test provided similar rutting assessment for the evaluated mixes, HWTT is recommended over APA since HWTT can be also used to assess resistance to moisture damage. In addition, $HWTT_{15000}$ is recommended over $HWTT_{20000}$ since it requires a smaller number of passes which reduces the testing time. The research proposed a pass/fail rutting performance assessment threshold for $HWTT_{15000}$ of maximum rut depth of 10 mm to differentiate between mixes with good/fair and poor/very poor performance groups.

## 8.2. Proposed Standard Test Method Drafts

In this study, two new innovative assessment tools were developed and evaluated to assess asphalt mix resistance to intermediate temperature cracking; Weibull Cracking Resistance Index ($Weibull_{CRI}$) derived from monotonic loading cracking assessment tests (Chapter 2) and Multi-Stage Semi-circle bending Dynamic (MSSD) test (Chapter 5). As discussed in the previous section, $Weibull_{CRI}$ indicator and MSSD test overcome the limitations of the current monotonic and dynamic cracking assessment indicators and test, respectively. They also address the concerns of state DOTs and contractors to evaluate the resistance of asphalt mix to cracking. The findings of the laboratory evaluation indicated that both of them have advantages over other indicators or tests. Therefore, this study developed two testing procedure drafts in accordance with ASTM test standard format including 1) *Standard Test Method for Determination of Weibull Cracking Resistance Index to Evaluate the Resistance of Asphalt Mixtures to Intermediate Temperature Cracking using Monotonic Loading Cracking Assessment tests* (Appendix E) and 2) *Standard Test Method for Evaluation of Asphalt Mixture Resistance to Intermediate Temperature Cracking using Multi-Stage Semi-Circle Bending Dynamic Test* (Appendix F). The first standard draft describes the

calculations of $Weibull_{CRI}$ from the load-displacement (or stress-strain) curve obtained from various monotonic cracking assessment tests using either a cylindrical or notched Semi Circular (SC), however, the author recommended using IDT test. The second draft covers the MSSD test procedure and determining its performance indicators (i.e., the slope [z] and Abs Log [*H*]) performance indicators using a notched SC specimen.

### 8.3. Implementation Guidelines

As highlighted in Chapter 1, state DOTs and contractors highlight the need to develop training materials and recommended plans for PEMD implementation. This section presents guidelines to demonstrate the use of the recommended performance assessment tests, indicators, and PEMD specifications to assess asphalt mix resistance to cracking and rutting during the design and/or production of asphalt mix.

Figure 8.1 illustrates the concept of implementing the proposed cracking and rutting performance assessment thresholds during mix design process using $Weibull_{CRI}$ and $HWTT_{15000}$ performance indicators. This example shows that the cracking resistance is improved (i.e., higher $Weibull_{CRI}$ [IDT]) while the rutting resistance declined (i.e., rut depth increases) with the increase in binder content. For PEMD design, the binder content is initially determined using the Superpave volumetric procedures then it can be optimized to achieve balanced (or engineered) mix design with improved performance.

In fact, the binder content parameter in the previous example can be replaced with any other mix proportions such as RAP content, recycled asphalt shingles (RAS), rejuvenators, etc. For instance, RAP content can be optimized to produce asphalt mixes that have adequate resistance to both cracking and rutting. Also, combined parameters can be optimized (e.g., binder content, RAP, RAS, rejuvenators) to allow the use of higher RAP or RAS in asphalt mixes yet meeting the performance specifications. A similar approach can be implemented for MSSD performance indicators as an alternative for $Weibull_{CRI}$ to assess asphalt mix resistance to cracking.

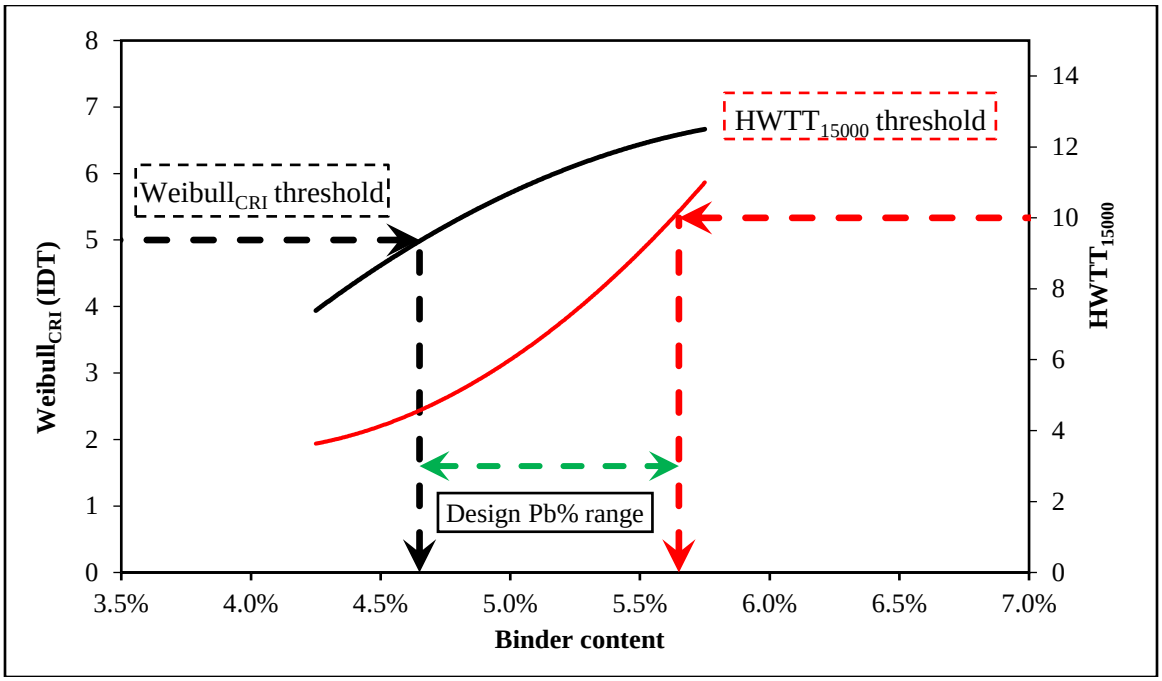


**Figure 8.1.** Schematic of implementation of the proposed HWTT rutting and cracking thresholds

In addition, the proposed performance thresholds can also be used as a quality control tool during the production and placement of asphalt mixes in the field (Figure 8.2). The performance of asphalt mix changes with the variation in mix proportions such as binder content. The performance assessment tests can be used to ensure that the produced mixes have similar performance to the accepted original mix design. In this concept, loose mixes are collected during the construction and test specimens are prepared and tested for rutting and cracking using the recommended performance assessment tests and indicators. The developed PEMD specifications (i.e., pass/fail performance thresholds) are used as quality control. For instance, if the accepted original mix designed with binder content (B.C.) of 5.75% but the produced mix in the field had a lower binder content (i.e., 5.00% or 4.25%). The PEMD performance assessment tests and indicators can easily capture such change in mix proportions by comparing the cracking and rutting performance of the produced mixes to the performance of the original design mix as shown in Figure 8.2. Figure 8.2 showed asphalt mixtures produced with different binder contents. As the binder content changes, the resistance to cracking/rutting changes accordingly, thus such change can be captured using

the proposed performance thresholds. A similar approach can be used to capture the variation in other mix proportions such as RAP.

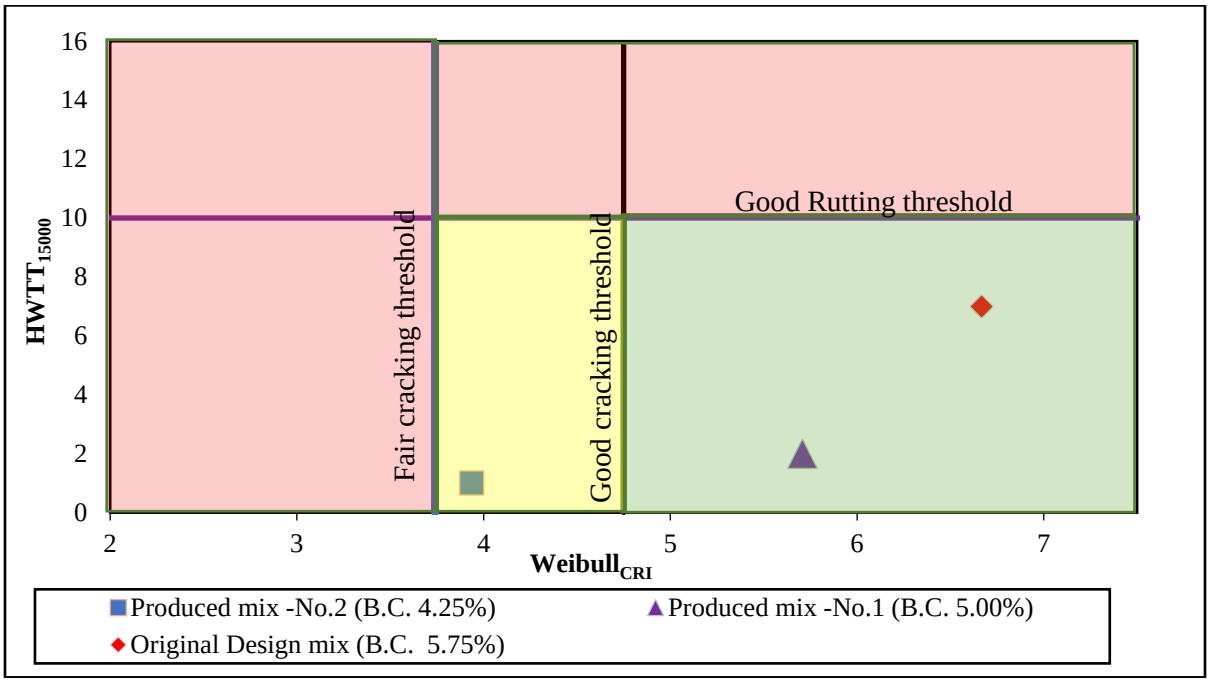


**Figure 8.2.** Implementation of performance tests as quality control tools

# Chapter 9: Conclusions

This chapter provides summary of the main findings of this study and recommendations for future research.

## 9.1. Conclusions

### *9.1.1. Development of New Performance Indicator to Evaluate the Resistance of Asphalt Mixes to Cracking*

This study developed and introduced a new performance indicator called Weibull Cracking Resistance Index ($Weibull_{CRI}$) that describes the entire load-displacement curve and can be used to evaluate the resistance of asphalt mixes to cracking. An extensive laboratory evaluation that included 16 different asphalt mixes (6 LMLC and 10 PMLC) using two different testing protocols (i.e., ASTM D6931 and AASHTO TP 125) was conducted. The main findings of this part of the study can be summarized as follows:

- The study investigated the fundamental meaning of the change in the load-displacement curve shape with variation in mix composition. It was found that the curve peak, the pre-peak, and post-peak slopes increase with the reduction in binder content while the termination displacement increases with binder content.

- $Weibull_{CRI}$ was found to be sensitive to variation in binder content and binder grade. In addition, the $Weibull_{CRI}$ results were in good agreement with the expected cracking resistance based on PMLC mix composition.

- The study showed that $Weibull_{CRI}$ (IDT) and $Weibull_{CRI}$ (SC) had a good correlation ($r = 0.74$) and good mix cracking resistance ranking agreements based on Spearman ranking analysis ($r_s = 0.65$). Also, the findings showed that the $Weibull_{CRI}$ (IDT) results had lower variability compared to $Weibull_{CRI}$ (SC).

- The IDT test standard and $Weibull_{CRI}$ (IDT) are recommended to assess asphalt mix resistance to cracking over the SCB test standard and $Weibull_{CRI}$ (SC). The IDT test specimen is easier to prepare compared to the SC specimen. The $Weibull_{CRI}$ (IDT)

results were in better agreement with expected cracking performance based on the composition of PMLC mixes. Also, the $Weibull_{CRI}$ (IDT) had a higher number of Turkey's HSD statistical groups and lower variability as compared to $Weibull_{CRI}$ (SC) results.

### *9.1.2. Review and Evaluation of Cracking Testing Standards and Performance Indicators for Asphalt Mixes*

This study also reviewed the most promising monotonic cracking performance assessment tests and indicators. In addition, a comprehensive laboratory evaluation was performed to investigate the validity of various cracking tests and indicators using laboratory-prepared specimens. A total number of 12 performance indicators were evaluated and compared in different aspects including sensitivity to mix compositions, variability, statistically grouping as well as performance ranking and the correlation between various performance indicators. The main findings of this study can be summarized as followed:

- The review indicated that $G_{fracture,}$ $IDT_{strength}$, $IDT_{Modulus}$, and $J_c$, CRI, FI, IDEAL-$CT_{Index}$, Nflex factor, and $Weibull_{CRI}$ were found to be the most promising monotonic cracking indicators.

- Several performance indicators including CRI (IDT), CRI (SCB-FI), FI (IDT), FI (SCB-FI), IDEAL-$CT_{Index}$, Nflex factor, and $Weibull_{CRI}$ showed that the cracking resistance is improved with the increase in binder content. Other performance indicators including $G_{fracture}$ (IDT), $G_{fracture}$ (SCB-FI), $IDT_{strength}$, $IDT_{Modulus}$, and $J_c$ showed mixed trends with increased binder content.

- The results of $G_{fracture}$ (IDT), $G_{fracture}$ (SCB-FI), $IDT_{strength}$, $IDT_{Modulus}$, and $J_c$ indicate that mixes with PG 70-28 binder are expected to provide better cracking resistance when compared to mixes prepared with PG 58-34 binder. Other performance indicators (e.g., CRI (IDT), CRI (SCB-FI), FI (IDT), FI (SCB-FI), IDEAL-$CT_{Index}$, Nflex factor) showed that mixes with PG 58-34 binder are expected to provide better cracking resistance when compared to mixes prepared with PG 70-28 binder.

- There was good agreement between mix cracking resistance based on the shape of the load-displacement curve and mix composition.

- The $Weibull_{CRI}$ had the lowest average COV, while FI calculated from the SCB-FI test had the highest average. Performance indicators with low variability (COV < 10%) included $Weibull_{CRI,}$ $IDT_{strength,}$ and CRI (IDT). Other indicators had a moderate variability (15% < average COV < 35%). Also, it was observed that performance indicators calculated from the IDT test data exhibited lower variability compared to indicators calculated from the SCB test data.

- Among all examined indicators, CRI (IDT), FI (IDT), Nflex factor, $Weibull_{CRI}$(IDT) were able to provide reasonable cracking resistance assessment compared to expected performance and were sensitive to binder content and binder PG. CRI (IDT) and $Weibull_{CRI}$(IDT) had the highest number of Tukey's HSD groups (4 groups) and the lowest variability in test results which offers advantage over the other performance indicators. Based on the results of this study, the $Weibull_{CRI}$ is recommended to evaluate the cracking resistance of asphalt mixtures. Each indicator uses one or more elements of the load-displacement curve, while $Weibull_{CRI}$ describes the entire load-displacement curve.

### *9.1.3. Development and Evaluation of Multi-Stage Semi-circle bending Dynamic (MSSD) Test to Assess the Cracking Resistance of Asphalt Mixes*

This study developed, evaluate, and validate a new dynamic test called Multi-Stage Semi-circle bending Dynamic (MSSD) test. The MSSD has advantages over the available monotonic and dynamic cracking assessment tests and addresses major concerns to implement the Balanced Mix Design (BMD) (i.e., performance test validity, specimen preparation, and testing time). The main findings of this study as follows:

- The MSSD performance indicators correlated well with the observed field cracking performance and were able to differentiate between mixes with good and poor cracking resistance based on field performance. The results demonstrated that mixes with lower slope ($z$) and higher Abs (log $H$) showed better cracking resistance

compared to mixes with higher slope (*z*) and lower Abs (log *H*). In addition, it had good agreement between expected cracking performance and composition of PMLC mixes.

- Three performance thresholds were proposed to distinguish between mixes; good cracking resistance ($z \leq 1.9$) or (Abs [log *H*] > 3.60), fair cracking resistance ($1.9 < z \leq 2.9$) or ($3.0 <$ Abs [log *H*] $\leq 3.60$), and poor cracking resistance ($z > 2.9$) or (abs [log H] <3.0).

- The results of the PMLC and field projects showed that there is a direct relationship between both performance indicators (i.e, slope [*z*] and abs [log H]). The field project had a coefficient of determination ($R^2$) of 0.80, while it was 0.75 for PMLC mixes.

- The findings indicated that Abs (log *H*) had a low variability (average COV <10%), while the slope (*z*) had moderate variability (15% < average COV < 35%) for both field cores and PMLC mixes. Overall, the MSSD performance indicators had lower variability compared to other dynamic tests and comparable variability to that of monotonic performance indicators.

### *9.1.4. Evaluation, and Development of Performance-Engineered Specifications for Cracking Assessment Monotonic Loading Tests*

This study also investigated the validity of the monotonic cracking resistance assessment tests and performance indicators in terms of the correlation with the observed field cracking and to develop pass/fail performance assessment thresholds in order to advance the implementation of PEMD or monotonic cracking performance assessment tests. A total number of 17 field projects with different observed field cracking performance were selected across the state of Idaho. Based on the findings of this study, the following conclusions can be made:

- None of the monotonic cracking resistance indicators was able to correlate with the observed field cracking performance or to distinguish between the subjective observed field cracking performance groups (i.e., good, fair, and poor performance

groups). The cracking resistance groups were overlapping; thus, it was not possible to identify the appropriate cut-off value to propose the performance thresholds.

- It was found that the monotonic performance assessment tests and indicators have shortcomings when assessing the extracted field cores. The authors believe that the wide range of air void contents and thicknesses of the extracted field cores influence the performance results of various monotonic cracking tests and indicators.

- The study proposed, evaluated, and validated an alternative approach to develop appropriate performance thresholds for monotonic performance indicators. The approach was able to propose performance assessment thresholds for several monotonic performance indicators. Also, it was found that the proposed performance indicators thresholds were comparable to the ones proposed by other researchers for the respective tests. Among all monotonic performance indicators, $Weibull_{CRI}$ determined from IDT test had the best correlation with MSSD slope parameter ($R^2$ of 0.8), which is expected to provide more reliable performance thresholds.

- The authors recommend the selection of IDT and $Weibull_{CRI}$ as monotonic performance assessment test and indicator, respectively to assess cracking resistance of asphalt mixes. Three thresholds for $Weibull_{CRI}$ were proposed, good cracking resistance ($Weibull_{CRI} > 4.7$), fair cracking resistance ($3.57 < Weibull_{CRI} \leq 4.7$), and poor cracking resistance ($Weibull_{CRI} < 3.57$).

### *9.1.5. Comprehensive Evaluation of Wheel-Tracking Rutting Performance Assessment Tests*

This study also examined the validity of HWTT and APA rut test rutting assessment tests and three rutting performance indicators derived from these tests. Based on the findings of this study, the following conclusions can be made:

- The HWTT and APA rut test rutting indicators were sensitive to variation in binder content and binder PG and were able to differentiate between field projects with different rutting resistance (e.g., good and fair). In addition, $APA_{8000}$ results had low/moderate test variability, while $HWTT_{15000\ and}$ $HWTT_{20000}$ had moderate test variability.

- The results showed excellent ranking correlation between both HWTT indicators (i.e., $HWTT_{15000\ and}$ $HWTT_{20000}$) ($r_s = 0.98$), while $APA_{8000}$ was found to have poor ranking agreement with both $HWTT_{15000}$ and $HWTT_{20000}$ rutting indicators.

- HWTT and APA rut test provided similar rutting assessment for the evaluated mixes. The authors recommend using HWTT over APA since HWTT can be used also to evaluate the resistance of asphalt mixes to moisture damage. Also, since the two HWTT rutting performance indicators (e.g., $HWTT_{15000}$ and $HWTT_{20000}$) are highly correlated and thus using only one would be sufficient. Since the $HWTT_{15000}$ requires a smaller number of passes which reduces the HWTT testing time, the authors recommend it to interpret the HWTT test results.

### *9.1.6. Investigate the Applicability of Weibull Cracking Resistance Index Using Data Generated by Other Researchers and Reported in The Literature*

In addition, this research investigated the applicability of $Weibull_{CRI}$ as a unified approach to analyze the results of various monotonic cracking assessment tests using data generated by other researchers and reported in the literature. The evaluation covered four aspects including 1) ability to analyze the load-displacement curve of various monotonic assessment tests, 2) sensitivity to the change in testing conditions (e.g., specimen geometry), 3) sensitivity to the change in mix properties (e.g., Recycled Asphalt Pavement [RAP]), and 4) correlation with cyclic cracking assessment tests. The main findings of this study can be summarized as follows:

- The study findings showed that $Weibull_{CRI}$ was able to interpret the testing results of Indirect Tension Test [IDT], and Semi-Circle Bending (SCB) used to assess asphalt mix resistance to intermediate-temperature cracking, in addition to SCB-low-temperature and Disk-Shaped Compact Tension (DCT) used to evaluate the resistance of asphalt mixtures to low temperature cracking. The Simple Punching Shear Test (SPST) data used to assess asphalt mix resistance to rutting was also analyzed. Furthermore, $Weibull_{CRI}$ had good correlation with the performance indicators of Bending Beam Fatigue (BBF) and MSSD tests.

- The study findings also indicated that $Weibull_{CRI}$ was sensitive to variation in specimen notch depth, thickness, and air void content. $Weibull_{CRI}$ results provided logical trends with variation in binder content, binder grade, aggregate type, Nominal Maximum Aggregate Size (NMAS), aging, rejuvenator dosages, and Recycled Asphalt Pavement (RAP).

- The study showed that $Weibull_{CRI}$ was able to be determined from various displacement measurement method including actuator vertical displacement, Load Line Displacement (LLD) and Crack mouth opening displacement (CMOD).

## 9.2. Research Significance and Contributions to Knowledge

The outcomes of this research are expected to advance the implementation of performance-engineered design approach and specifications to extend the service life of asphalt pavements. The main outcomes are as follows:

(1) The comprehensive laboratory evaluation of the selected cracking and rutting testing standards and indicators addresses state DOTs and contractor's concerns in terms of the validity of current performance assessment tests.

(2) The developed monotonic cracking assessment performance indicator overcomes the limitations of the available indicators and can be used to interpret various monotonic performance tests.

(3) The developed dynamic cracking assessment test addresses the concern of state DOTs and contractors related to the complex specimen preparation and long testing time of the current dynamic cracking assessment tests.

(4) The developed monotonic cracking performance indicator and dynamic cracking assessment test have advantages over the current monotonic indicators and dynamic tests, respectively. Therefore, it is expected to provide a better assessment of asphalt mix to cracking resistance.

(5) The proposed alternative approach to develop PEMD specifications for monotonic cracking assessment tests and indicators was able to overcome the limitations of monotonic tests.

(6) The proposed PEMD specifications (i.e., pass/fail performance thresholds) should ensure that a given asphalt mix has adequate resistance to cracking and rutting which would extend the service life of asphalt pavements.

(7) The developed guidelines and recommendations shall guide state DOT to implement PEMD specifications.

## 9.3. Future Recommendations

- The study developed initial cracking performance thresholds that were proposed using the testing results of PMLC mixes for various performance indicators. However, these thresholds need further validation and calibration by monitoring the cracking performance of these PMLC mixes in the field.

- Further research investigation is recommended to reduce the testing time of the developed MSSD test. Currently, this test can take up to 9 hours.

- Further investigation of MSSD and $Weibull_{CRI}$ using different asphalt mixes and field projects is recommended.

# Appendix A - Detailed Example of Statistical Analysis Results

In this dissertation, the t-test and One-Way Analysis of Variance (ANOVA) were used to examine if the groups (mixes) means are different from one another. The t-test was used to compare the means of two groups (i.e., two mixes), while the one-way ANOVA test was used to compare the means of more than two groups (i.e., two mixes). However, the ANOVA test informs only if there is a significant difference or not between the mixes, but it does not locate which mixes are different. Therefore, a post-hoc test (i.e., Tukey's Honestly Significant Difference [Tukey's HSD]) test was performed. Tukey's HSD compared the means of all studied groups (mixes) to the mean of every other group to determine which specific mixes are different from one another.

The t-test was used to evaluate the sensitivity of performance indicators to binder PG, while ANOVA and Tukey' HSD tests were used to evaluate the sensitivity for the composition of PMLC mixes and the binder content. Both tests (t-test, ANOVA, and Tukey's HSD) were performed at 95% confidence interval using Minitab software. The statistical analysis results were included in the form of letters or numbers at the bottom of each bar. Mixes that do not share the same letter/number were significantly different in terms of results. This section provides a detailed analysis example of each test.

## A.1 T-test to study performance indicators sensitivity to binder content

In this study, two binder grades were evaluated; PG 70-28 and PG 58-34 at three different binder contents (i.e., 4.25%, 5.00%, and 5.75%). The t-test was used to examine the sensitivity of performance indicators to binder PG at the three different binder content. This section provided an example of t-test results to study the difference of $Weibull_{CRI}$ (IDT) between PG 70-28 and PG58-34 at 4.25 % binder content.

(1) The hypothesis

- $\mu_1$: mean of $Weibull_{CRI}$ (IDT) when Binder grade = PG58-34, 4.25%
- $\mu_2$: mean of $Weibull_{CRI}$ (IDT) when Binder grade = PG70-28, 4.25%

- Difference: $\mu_1 - \mu_2$

(2) Descriptive Statistics

| Binder grade | N | Mean | StDev | SE Mean |
|---|---|---|---|---|
| PG58-34, 4.25% | 3 | 5.720 | 0.785 | 0.45 |
| PG70-28, 4.25% | 3 | 4.100 | 0.546 | 0.32 |

(3) Estimation for Difference

| Difference | 95% CI for Difference |
|---|---|
| 1.620 | (-0.138, 3.377) |

(4) T- test

- Null hypothesis $H_0$: $\mu_1 - \mu_2 = 0$

- Alternative hypothesis $H_1$: $\mu_1 - \mu_2 \neq 0$

| Binder grade | T-Value | DF | P-Value | Decision |
|---|---|---|---|---|
| PG58-34, 4.25% | 2.93 | 3 | 0.061 | P- |
| PG70-28, 4.25% | | | | |

(5) Decision

- P-value =0.06 >0.05, thus $Weibull_{CRI}$ (IDT) when Binder grade = PG58-34, 4.25% is not statically different from $Weibull_{CRI}$ (IDT) when Binder grade = PG70-28, 4.25%.

(6) Results reporting

Since the mixes have an insignificant difference, thus it will share the same letter (I) as can be shown in Figure A.1

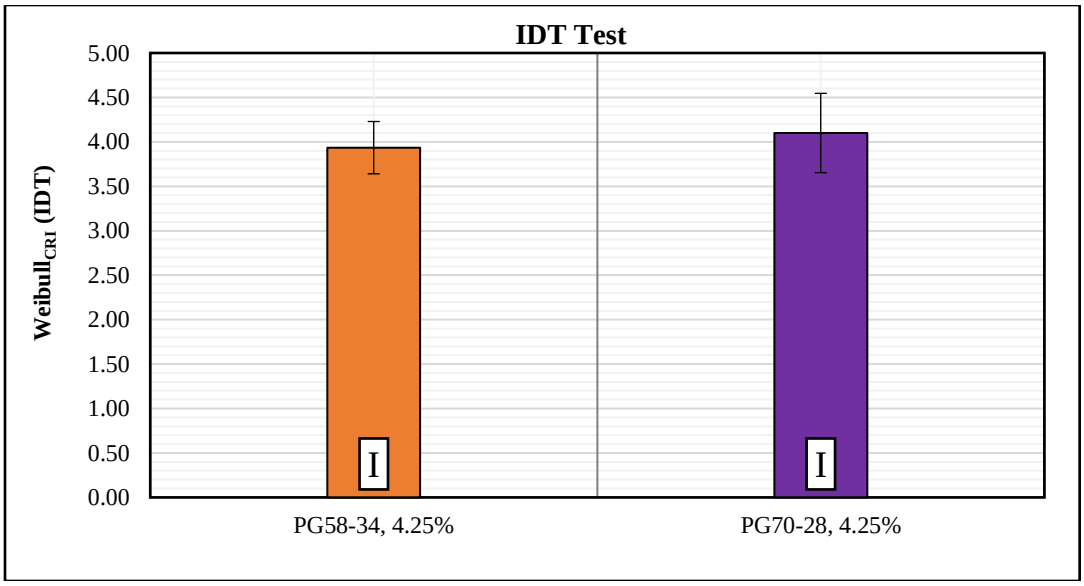


**Figure A.1** Sensitivity of Weibull$_{CRI}$ from IDT test for PG

## A.2 One-way ANOVA and Tukey's

In this study, two binder grades were evaluated; PG 70-28 and PG 58-34 at three different binder contents (i.e., 4.25%, 5.00%, and 5.75%). The ANOVA and Tukey's test were used to examine the sensitivity of performance indicators to binder content at different binder PG. Also, it was used to study the sensitivity of performance indicators to the composition of PMLC mixes.

### A.2.1 Performance indicators sensitivity to binder content

This section provided an example of ANOVA and Tukey's test results to study the difference of Weibull$_{CRI}$ (SCB) between 4.25 %, 5.00%, and 5.75 % binder content at PG 58-34 binder PG.

(1) The hypothesis

- Null hypothesis All means are equal
- Alternative hypothesis Not all means are equal
- Significance level $\alpha = 0.05$

(2) Factor information

| Factor | Levels | Values |
|---|---|---|
| Binder content | 3 | PG58-34,4.25, PG58-34,5.0, PG58-34,5.75 |

(3) Analysis of Variance (ANOVA)

| Source | DF | Adj SS | Adj MS | F-Value | P-Value |
|---|---|---|---|---|---|
| BINDER CONTENT | 2 | 20.23 | 10.116 | 6.18 | 0.020 |
| Error | 9 | 14.72 | 1.636 | | |
| Total | 11 | 34.96 | | | |

- P-value =0.02 < 0.05, thus there is a significant different between $Weibull_{CRI}$ (IDT) results at different binder content

(4) Means

| Binder Content | N | Mean | StDev | 95% CI |
|---|---|---|---|---|
| PG58-34,4.25 | 4 | 2.875 | 0.844 | (1.428, 4.322) |
| PG58-34,5.0 | 4 | 3.537 | 0.222 | (2.091, 4.984) |
| PG58-34,5.75 | 4 | 5.90 | 2.04 | (4.45, 7.35) |

(5) Tukey Simultaneous Tests for Differences of Means

| Difference of Levels | Difference of Means | SE of Difference | 94% CI | T-Value |
|---|---|---|---|---|
| PG58-34,5.0 - PG58-34,4.25 | 0.662 | 0.904 | (-1.755, 3.080) | 0.73 |
| PG58-34,5.75 - PG58-34,4.25 | 3.025 | 0.904 | (0.608, 5.443) | 3.35 |
| PG58-34,5.75 - PG58-34,5.0 | 2.363 | 0.904 | (-0.054, 4.780) | 2.61 |

(6) Grouping Information Using the Tukey Method and 94% Confidence

| Binder Content | N | Mean | Grouping | |
|---|---|---|---|---|
| PG58-34,4.25 | 3 | 2.875 | A | |
| PG58-34,5.0 | 3 | 3.537 | A | B |
| PG58-34,5.75 | 3 | 5.90 | | B |

(7) Results reporting

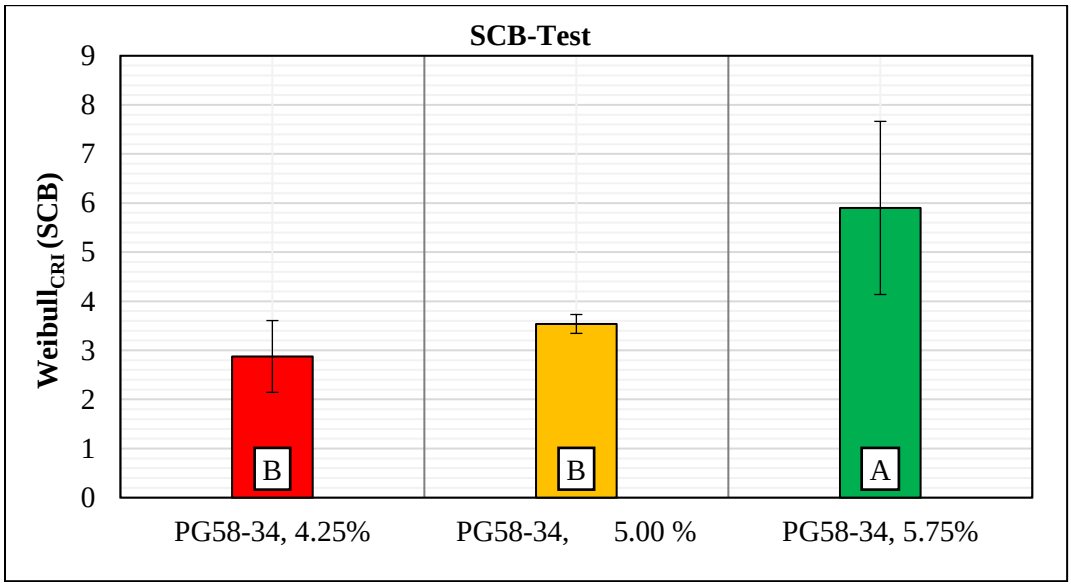


**Figure A.2** Sensitivity of Weibull$_{CRI}$ from IDT test for PG

**A.2.2 Performance indicators sensitivity to PMLC mixes.**

This section provided an example of ANOVA and Tukey's test results to study the difference of Weibull$_{CRI}$ (IDT) for PMLC mixes

(1) The hypothesis

- Null hypothesis All means are equal
- Alternative hypothesis Not all means are equal
- Significance level $\alpha = 0.05$

(2) Factor information

| Factor | Levels | Values |
|---|---|---|
| PMLC mixes | 3 | PG58-34,4.25, PG58-34,5.0, PG58-34,5.75 |

(3) Analysis of Variance (ANOVA)

| Source | DF | Adj SS | Adj MS | F-Value | P-Value |
|---|---|---|---|---|---|
| PMLC mixes | 9 | 19.637 | 2.1818 | 9.04 | 0.000 |
| Error | 16 | 3.862 | 0.2414 | | |
| Total | 25 | 23.498 | | | |

- P-value =0.02 < 0.05, thus there is a significant different between $Weibull_{CRI}$ (IDT) results at different binder content

(4) Means

| Binder Content | N | Mean | StDev | 95% CI |
|---|---|---|---|---|
| PG58-34,4.25 | 4 | 2.875 | 0.844 | (1.428, 4.322) |
| PG58-34,5.0 | 4 | 3.537 | 0.222 | (2.091, 4.984) |
| PG58-34,5.75 | 4 | 5.90 | 2.04 | (4.45, 7.35) |

(5) Tukey Simultaneous Tests for Differences of Means

| # | Difference of Levels | Difference of Means | SE of Difference | 95% CI | T-Value | Adjusted P-Value |
|---|---|---|---|---|---|---|
| 1 | D2L1 - D1L1 | 0.083 | 0.491 | (-1.706, 1.872) | 0.17 | 1.000 |
| 2 | D2L2 - D1L1 | 0.727 | 0.448 | (-0.906, 2.360) | 1.62 | 0.821 |
| 3 | D3L1 - D1L1 | -1.930 | 0.448 | (-3.564, -0.297) | -4.30 | 0.014 |
| 4 | D3L2 - D1L1 | 0.246 | 0.448 | (-1.387, 1.880) | 0.55 | 1.000 |
| 5 | D3L3 - D1L1 | -1.020 | 0.491 | (-2.809, 0.769) | -2.08 | 0.566 |
| 6 | D3L4 - D1L1 | -1.173 | 0.448 | (-2.806, 0.460) | -2.61 | 0.285 |
| 7 | D3L5 - D1L1 | -1.005 | 0.491 | (-2.794, 0.784) | -2.05 | 0.583 |
| 8 | D5L1 - D1L1 | 0.122 | 0.448 | (-1.511, 1.755) | 0.27 | 1.000 |
| 9 | D6L1 - D1L1 | 0.573 | 0.448 | (-1.061, 2.206) | 1.28 | 0.945 |
| 10 | D2L2 - D2L1 | 0.644 | 0.448 | (-0.989, 2.277) | 1.44 | 0.898 |
| 11 | D3L1 - D2L1 | -2.014 | 0.448 | (-3.647, -0.380) | -4.49 | 0.010 |
| 12 | D3L2 - D2L1 | 0.163 | 0.448 | (-1.470, 1.796) | 0.36 | 1.000 |
| 13 | D3L3 - D2L1 | -1.103 | 0.491 | (-2.892, 0.686) | -2.24 | 0.468 |
| 14 | D3L4 - D2L1 | -1.256 | 0.448 | (-2.889, 0.377) | -2.80 | 0.215 |
| 15 | D3L5 - D2L1 | -1.089 | 0.491 | (-2.878, 0.700) | -2.22 | 0.484 |
| 16 | D5L1 - D2L1 | 0.039 | 0.448 | (-1.594, 1.672) | 0.09 | 1.000 |
| 17 | D6L1 - D2L1 | 0.489 | 0.448 | (-1.144, 2.122) | 1.09 | 0.979 |
| 18 | D3L1 - D2L2 | -2.657 | 0.401 | (-4.118, -1.197) | -6.62 | 0.000 |
| 19 | D3L2 - D2L2 | -0.481 | 0.401 | (-1.941, 0.980) | -1.20 | 0.962 |
| 20 | D3L3 - D2L2 | -1.747 | 0.448 | (-3.380, -0.113) | -3.89 | 0.031 |
| 21 | D3L4 - D2L2 | -1.900 | 0.401 | (-3.360, -0.439) | -4.74 | 0.006 |
| 22 | D3L5 - D2L2 | -1.732 | 0.448 | (-3.366, -0.099) | -3.86 | 0.033 |
| 23 | D5L1 - D2L2 | -0.605 | 0.401 | (-2.066, 0.856) | -1.51 | 0.871 |
| 24 | D6L1 - D2L2 | -0.154 | 0.401 | (-1.615, 1.306) | -0.39 | 1.000 |
| 25 | D3L2 - D3L1 | 2.177 | 0.401 | (0.716, 3.638) | 5.43 | 0.002 |
| 26 | D3L3 - D3L1 | 0.911 | 0.448 | (-0.722, 2.544) | 2.03 | 0.592 |
| 27 | D3L4 - D3L1 | 0.758 | 0.401 | (-0.703, 2.218) | 1.89 | 0.676 |
| 28 | D3L5 - D3L1 | 0.925 | 0.448 | (-0.708, 2.558) | 2.06 | 0.573 |
| 29 | D5L1 - D3L1 | 2.053 | 0.401 | (0.592, 3.513) | 5.12 | 0.003 |
| 30 | D6L1 - D3L1 | 2.503 | 0.401 | (1.042, 3.964) | 6.24 | 0.000 |
| 31 | D3L3 - D3L2 | -1.266 | 0.448 | (-2.899, 0.367) | -2.82 | 0.208 |
| 32 | D3L4 - D3L2 | -1.419 | 0.401 | (-2.880, 0.042) | -3.54 | 0.061 |
| 33 | D3L5 - D3L2 | -1.252 | 0.448 | (-2.885, 0.381) | -2.79 | 0.218 |
| 34 | D5L1 - D3L2 | -0.124 | 0.401 | (-1.585, 1.337) | -0.31 | 1.000 |
| 35 | D6L1 - D3L2 | 0.326 | 0.401 | (-1.135, 1.787) | 0.81 | 0.997 |
| 36 | D3L4 - D3L3 | -0.153 | 0.448 | (-1.786, 1.480) | -0.34 | 1.000 |
| 37 | D3L5 - D3L3 | 0.014 | 0.491 | (-1.775, 1.803) | 0.03 | 1.000 |
| 38 | D5L1 - D3L3 | 1.142 | 0.448 | (-0.491, 2.775) | 2.55 | 0.315 |
| 39 | D6L1 - D3L3 | 1.592 | 0.448 | (-0.041, 3.225) | 3.55 | 0.059 |
| 40 | D3L5 - D3L4 | 0.167 | 0.448 | (-1.466, 1.801) | 0.37 | 1.000 |
| 41 | D5L1 - D3L4 | 1.295 | 0.401 | (-0.166, 2.756) | 3.23 | 0.105 |
| 42 | D6L1 - D3L4 | 1.745 | 0.401 | (0.285, 3.206) | 4.35 | 0.013 |
| 43 | D5L1 - D3L5 | 1.128 | 0.448 | (-0.506, 2.761) | 2.51 | 0.330 |
| 44 | D6L1 - D3L5 | 1.578 | 0.448 | (-0.055, 3.211) | 3.52 | 0.063 |
| 45 | D6L1 - D5L1 | 0.450 | 0.401 | (-1.010, 1.911) | 1.12 | 0.975 |

(6) Grouping Information Using the Tukey Method and 94% Confidence

| Binder Content | Mean | Grouping | | | |
|---|---|---|---|---|---|
| D2L2 | 5.5970 | A | | | |
| D6L1 | 5.443 | A | B | | |
| D3L2 | 5.116 | A | B | C | |
| D5L1 | 4.992 | A | B | C | |
| D2L1 | 4.953 | A | B | C | |
| D1L1 | 4.8700 | A | B | C | |
| D3L5 | 3.865 | | B | C | D |
| D3L3 | 3.8505 | | B | C | D |
| D3L4 | 3.697 | | | C | D |
| D3L1 | 2.940 | | | | D |

(7) Results reporting

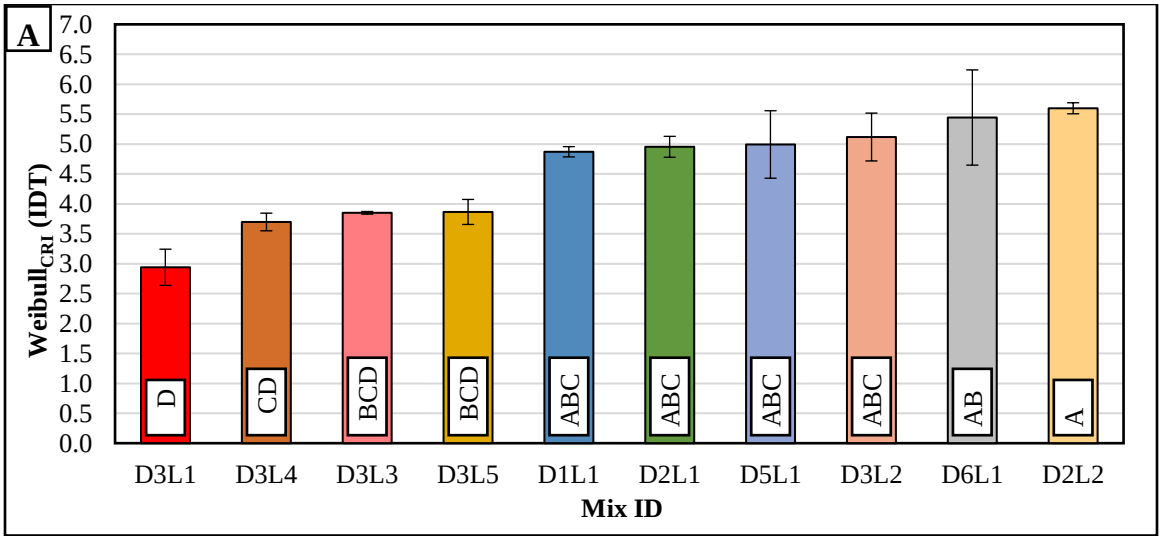


**Figure A.3** Sensitivity of Weibull$_{CRI}$ from IDT test for PG

# Appendix B - Sensitivity of Monotonic Indicators for Binder Content and PG

Figures B.1 to B.12 provide the sensitivity results of the selected performance indicators to the variation in binder content and binder PG. The error bars represent ± one standard deviation from the average value. Sensitivity to binder content was evaluated using a statistical ANOVA and Tukey's Honestly Significant Difference (Tukey's HSD) at each binder PG (three binder content groups at each binder PG). Sensitivity for binder PG was evaluated using a statistical t-test at each binder content (two binder PG groups at each binder content). Both tests (Tukey's HSD and t-test) were performed at 95% confidence interval (i.e., $\alpha = 0.05$). The statistical analysis results are included in the form of letters or numbers at the bottom of each bar. Mixes that do not share the same letter/number are significantly different in terms of their fracture energy.

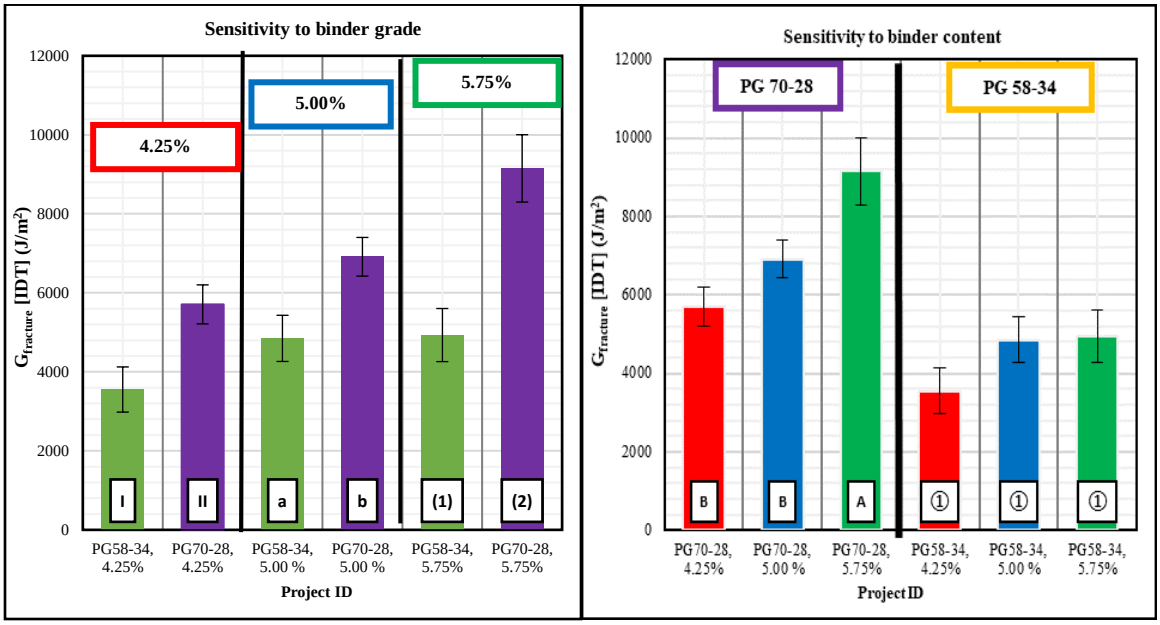


**Figure B.1** Sensitivity of total fracture energy from IDT test for PG and binder content $G_{fracture}$ (IDT)

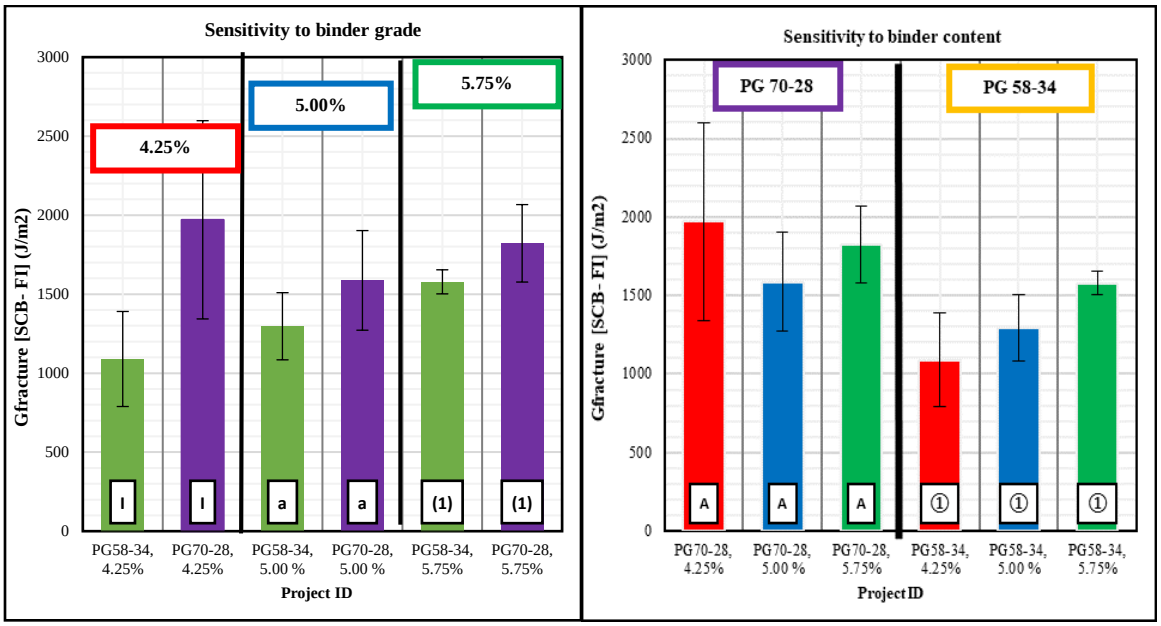


**Figure B.2** Sensitivity of total fracture energy from SCB-FI test for PG and binder content

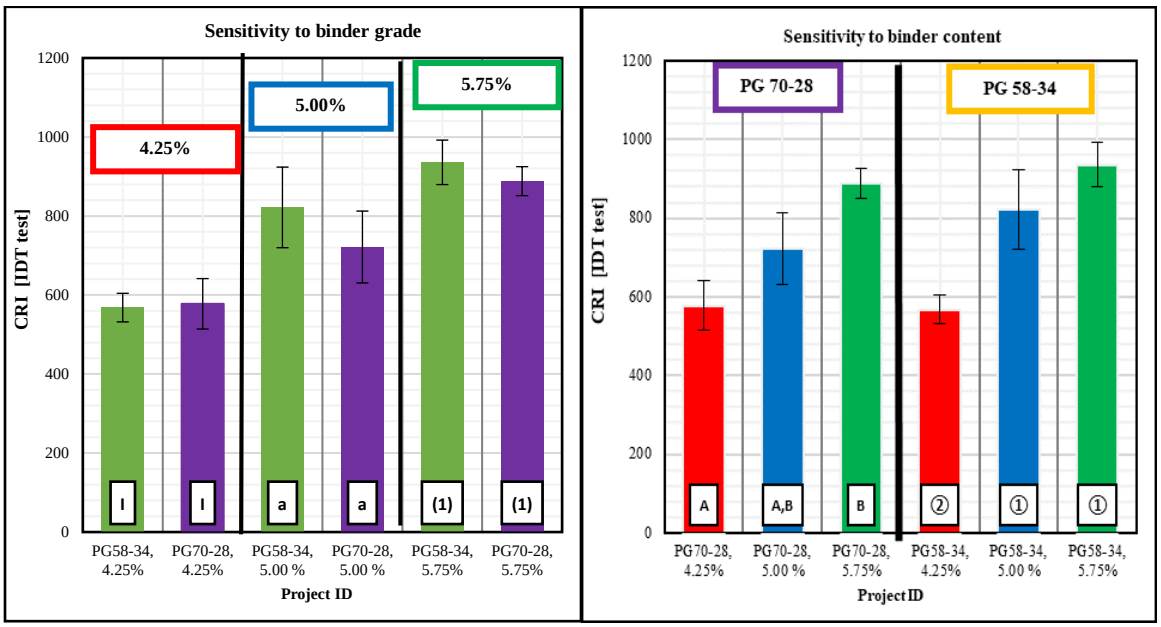


**Figure B.3** Sensitivity of CRI from IDT test for binder grade

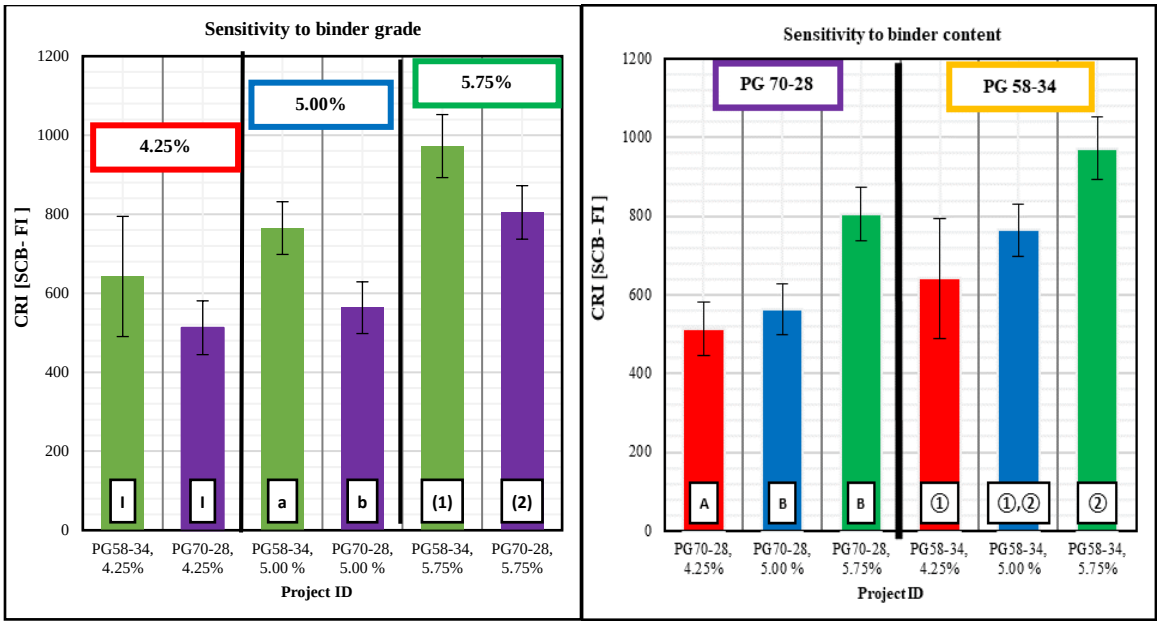


**Figure B.4** Sensitivity of CRI from SCB-FI test for PG and binder content

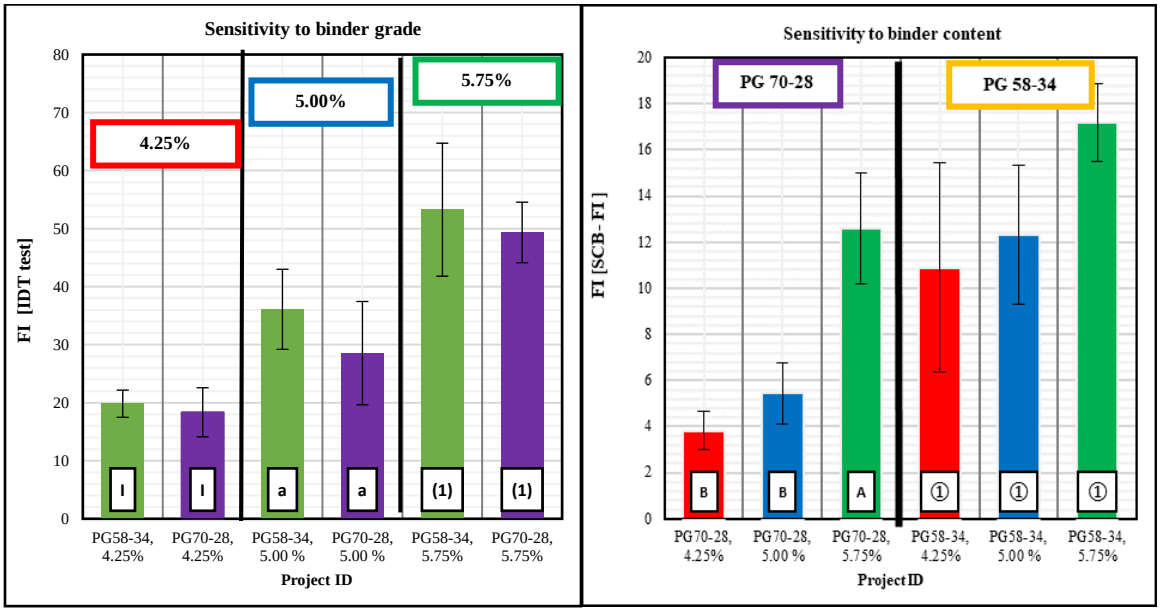


**Figure B.5** Sensitivity of FI from IDT test for PG and binder content

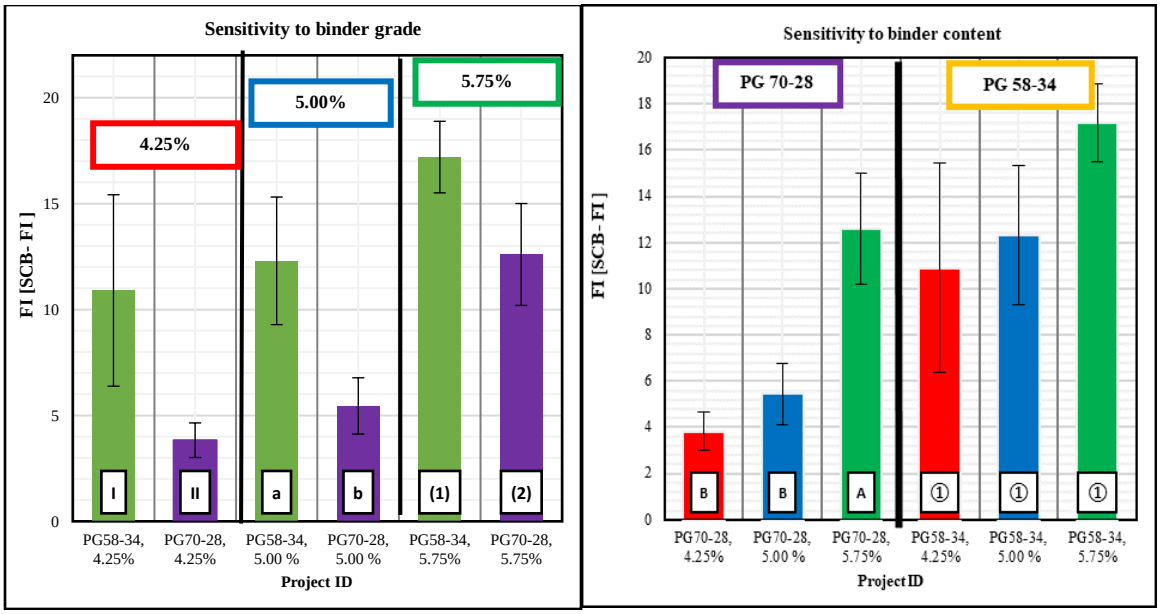


**Figure B.6** Sensitivity of FI from SCB-FI test for PG and binder content

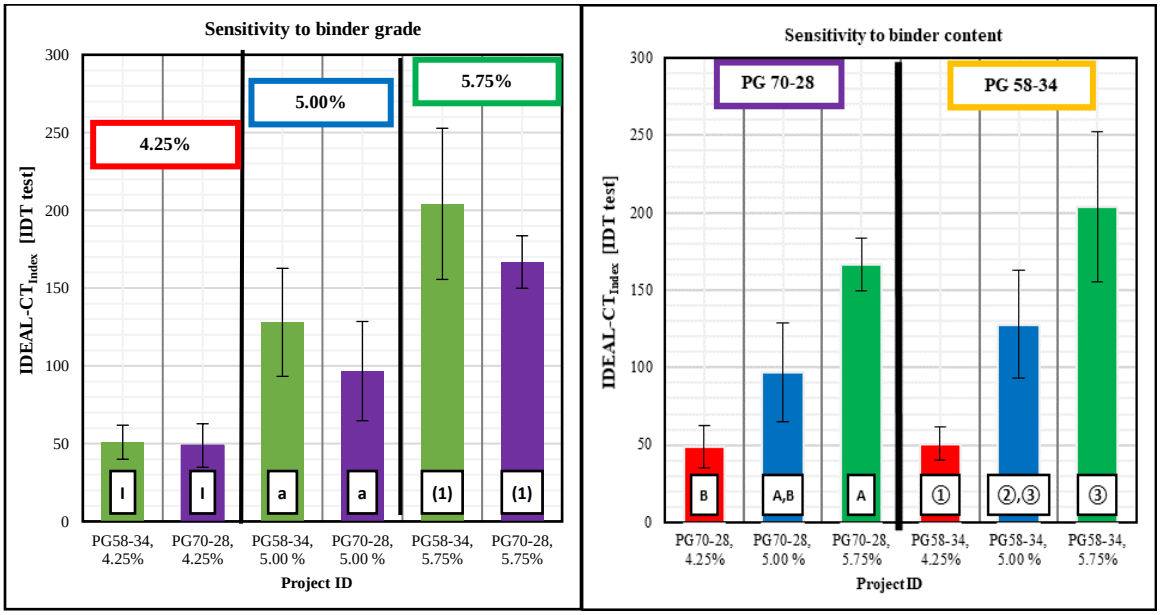


**Figure B.7** Sensitivity of IDEAL-CT$_{Index}$ from IDT test for PG and binder content

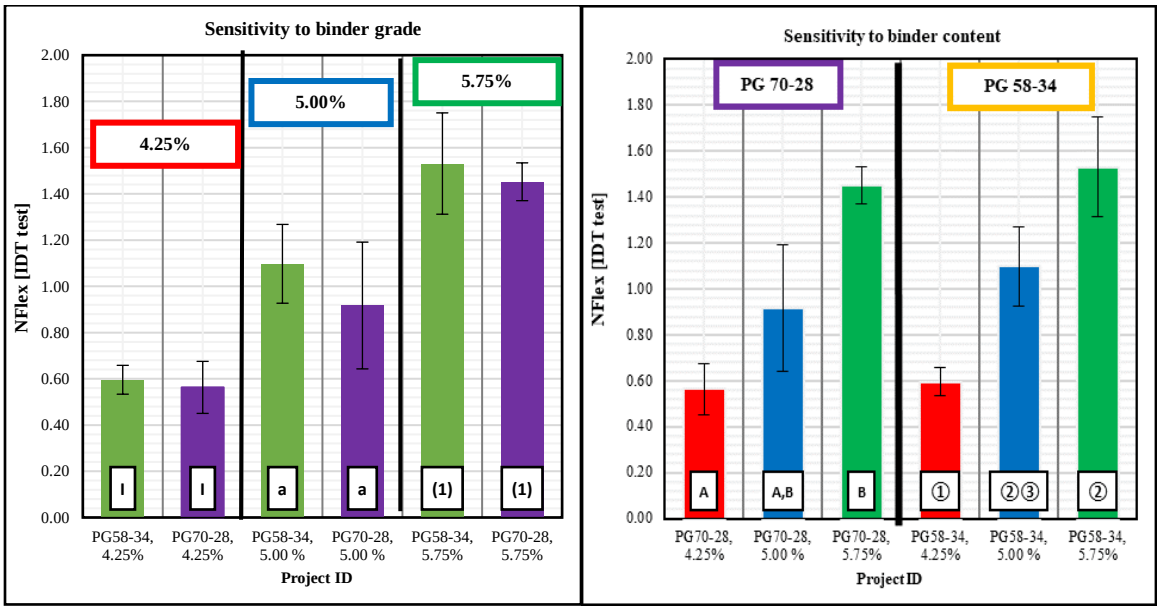


**Figure B.8** Sensitivity of Nflex from IDT test for PG and binder content

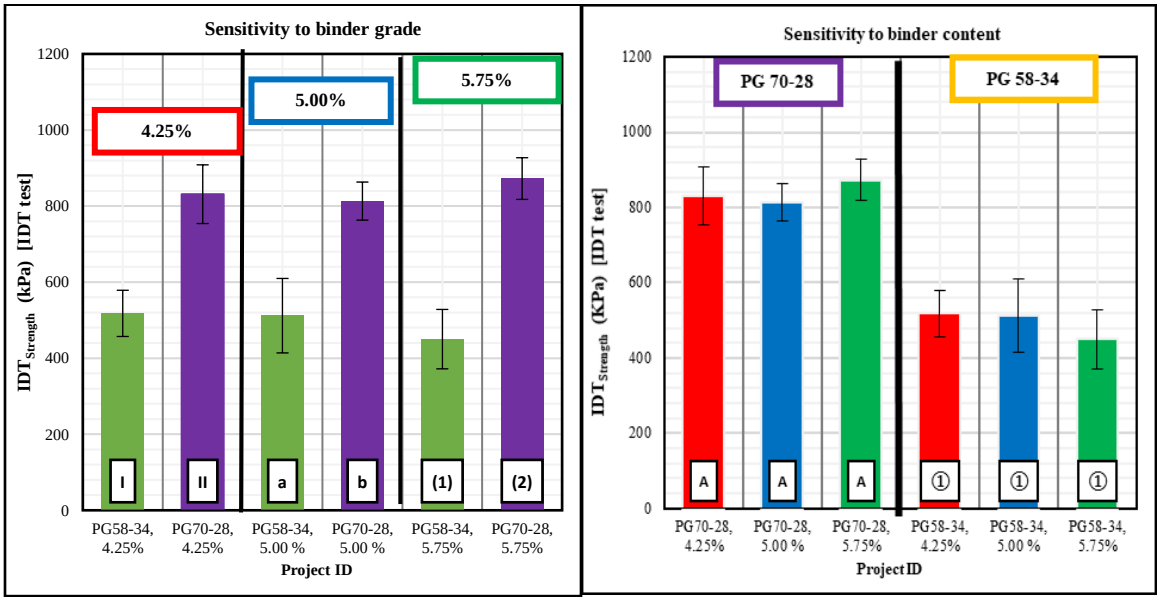


**Figure B.9** Sensitivity of $IDT_{strength}$ from IDT test for PG and binder content

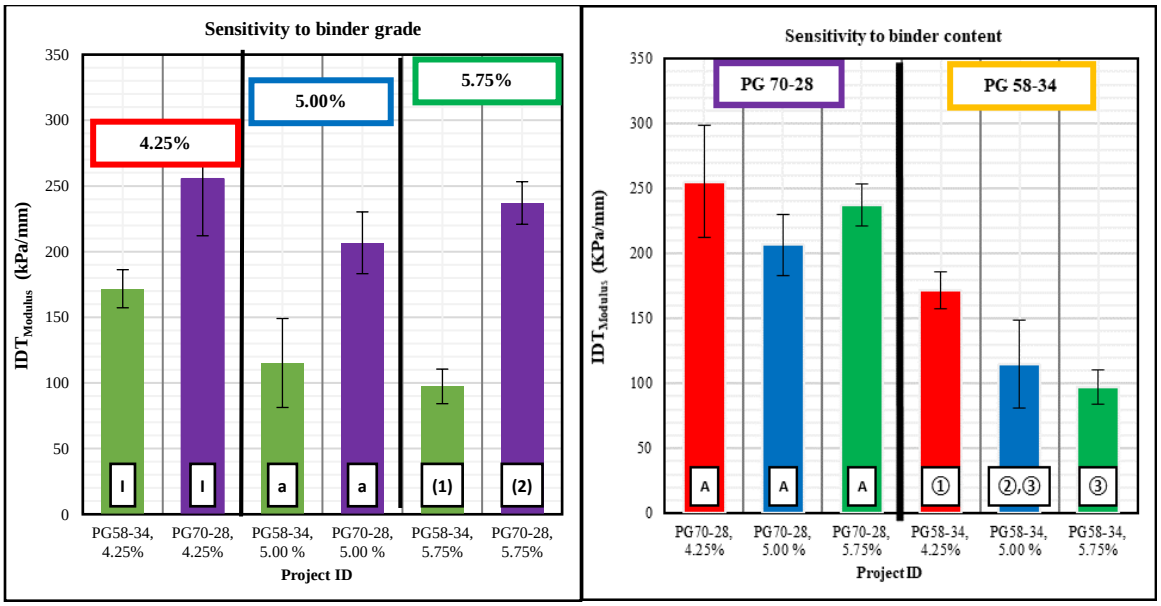


**Figure B.10** Sensitivity of $IDT_{Modulus}$ from IDT test for PG and binder content

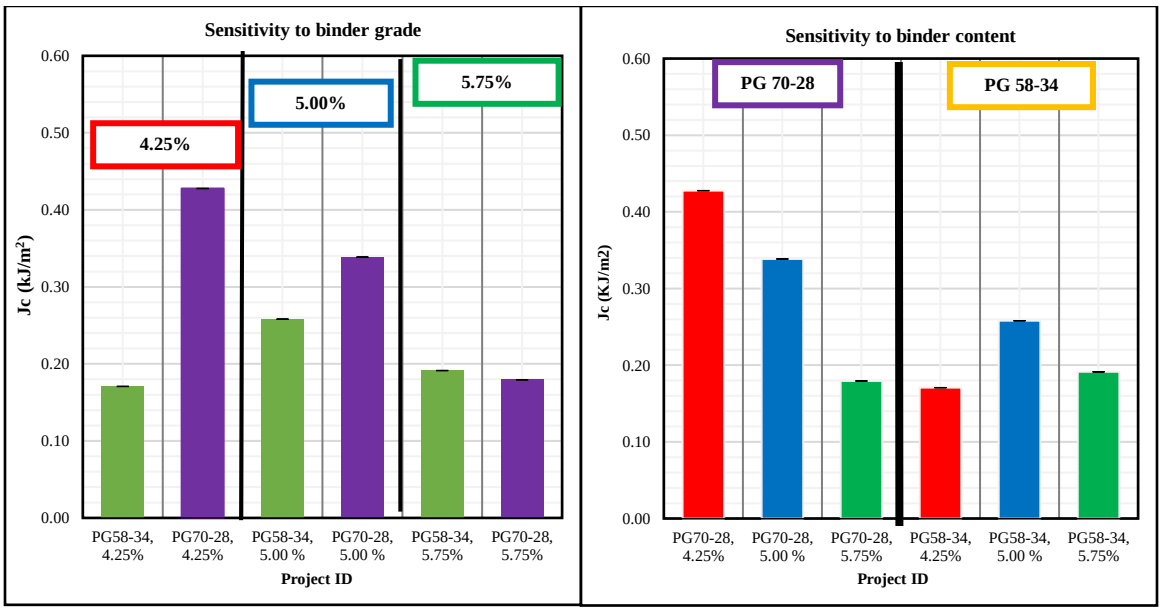


**Figure B.11** Sensitivity of $J_c$ from IDT test for PG and binder content

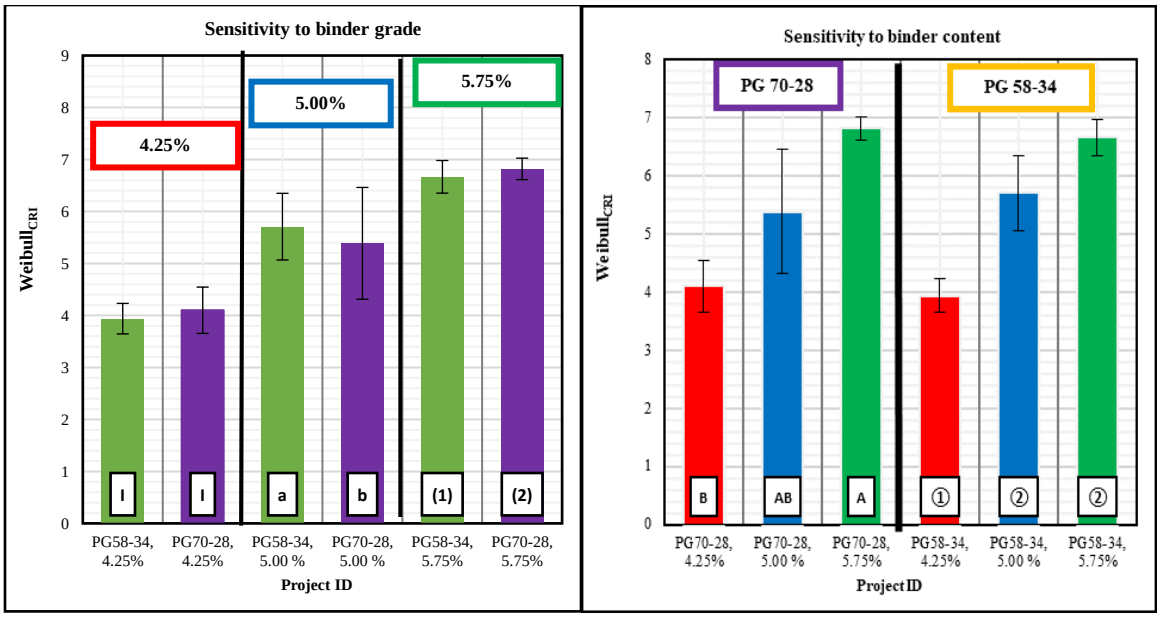


**Figure B.12** Sensitivity of Weibull$_{CRI}$ from IDT test for PG and binder content

# Appendix C - Correlation between Field Cracking Resistance and Monotonic Indicators

Figures C.1 to C.22 present the direct correlations between the laboratory testing results of the selected monotonic performance indicators and subjective cracking performance grouping of the selected field projects. In these figures, the performance groups were represented using bar colors. Field projects with good, fair, and poor observed field cracking resistance were represented in green, yellow, and red bars, respectively. In addition, the mean values of various performance indicators were. The error bars represent ± one standard deviation (SD) from the mean value. Both tests (Tukey's HSD and t-test) were performed at 95% confidence interval (i.e., $\alpha = 0.05$). The statistical analysis results are included in the form of letters or numbers at the bottom of each bar. Mixes that do not share the same letter/number are significantly different in terms of their fracture energy.

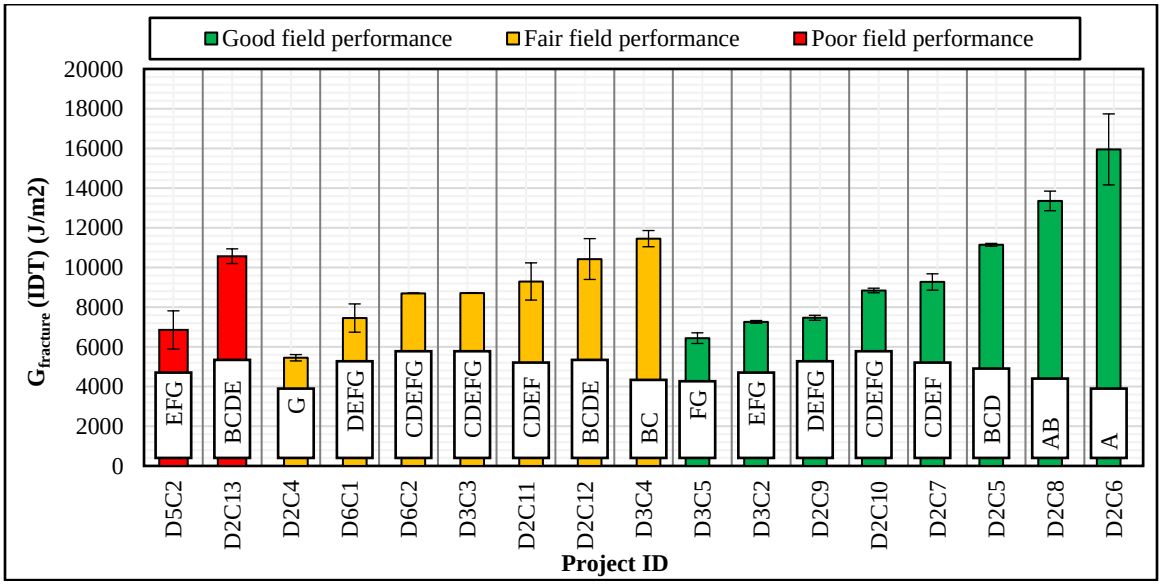


**Figure C.1** Correlation between total fracture energy from IDT test with field project performance ($G_{fracture}$ [IDT])

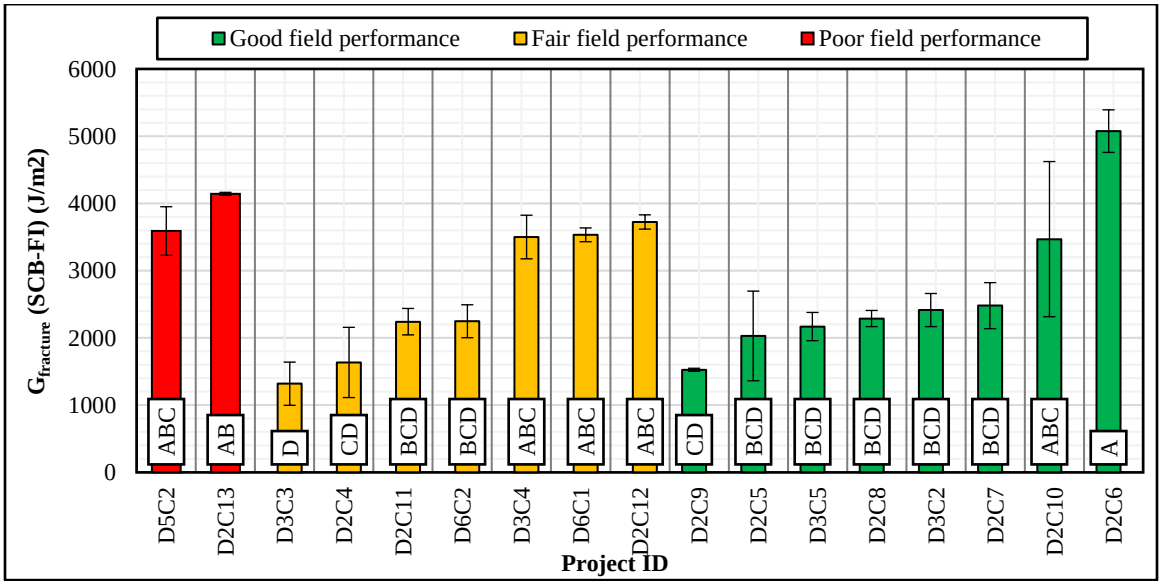


**Figure C.2** Correlation between total fracture energy from SCB test with field project performance ($G_{fracture}$ [SCB])

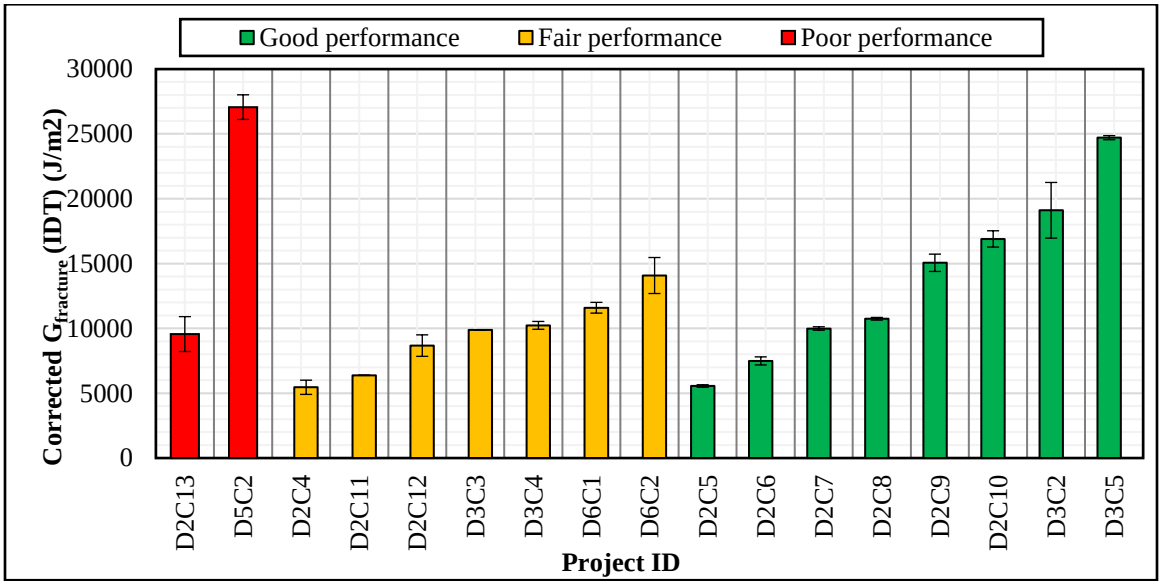


**Figure C.3** Correlation between corrected total fracture energy from IDT test with field project performance ($G_{fracture}$ [IDT])

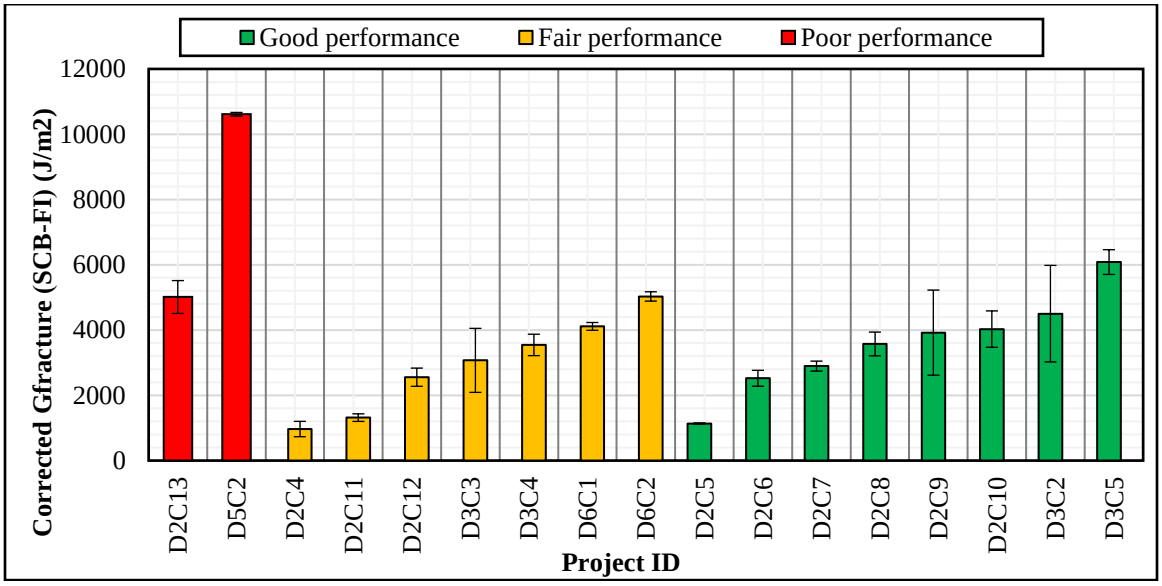


**Figure C.4** Correlation between corrected total fracture energy from SCB test with field project performance ($G_{fracture}$ [SCB])

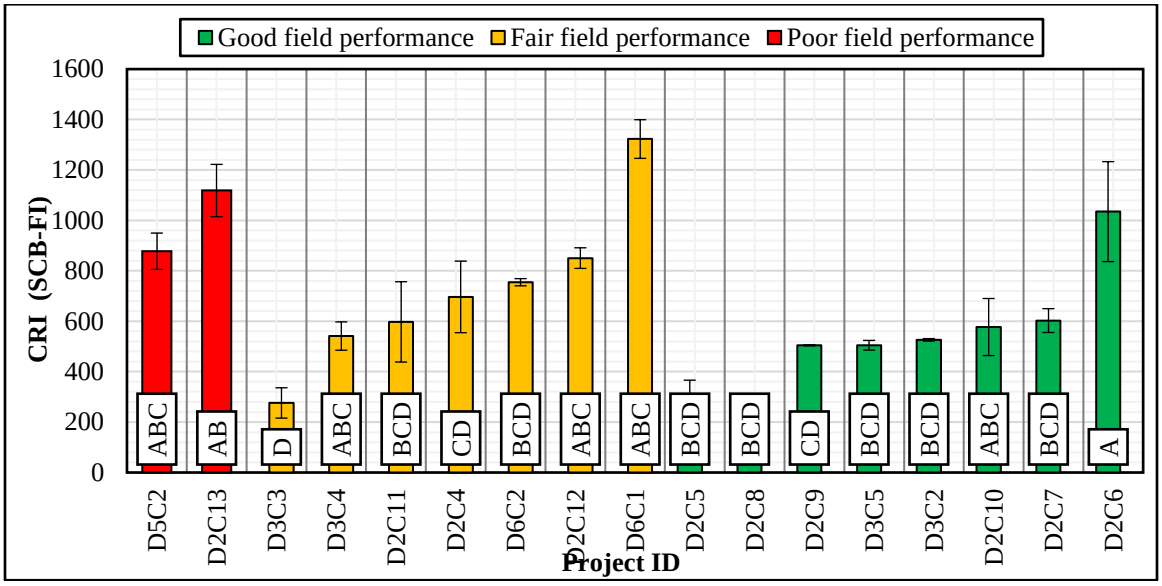


**Figure C.5** Correlation between CRI from computed from SCB test with field project performance

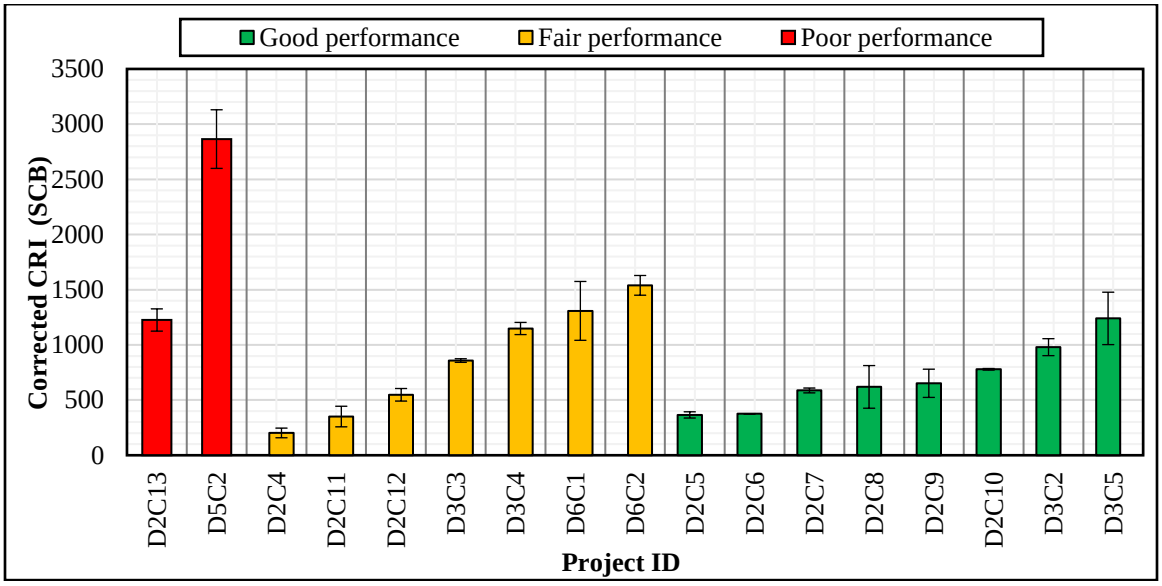


**Figure C.6** Correlation between Corrected CRI computed from IDT test with field project performance

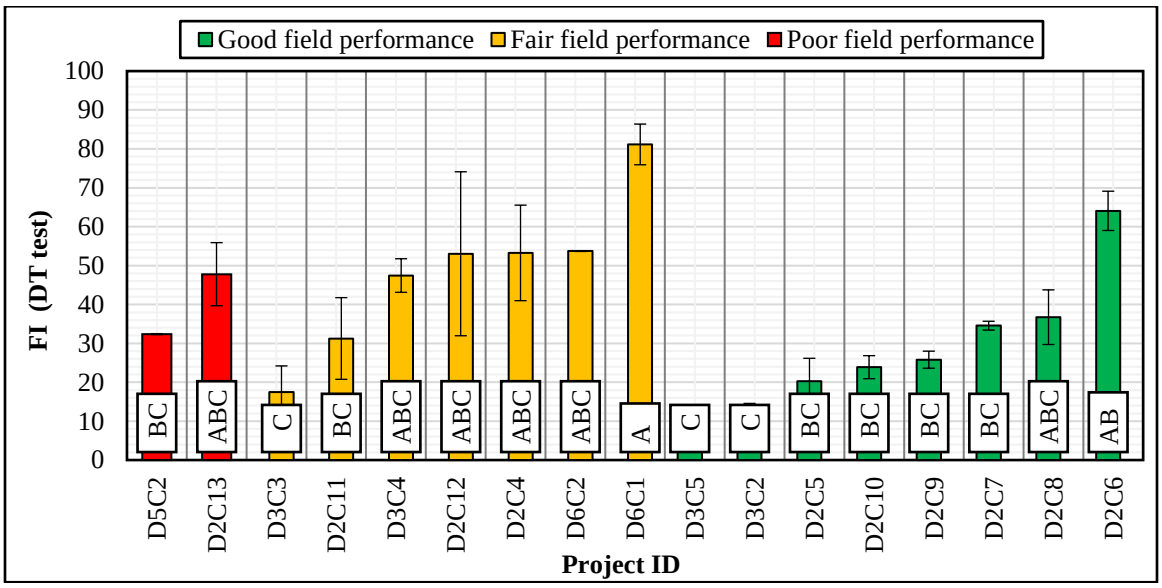


**Figure C.7** Correlation between FI computed from IDT test with field project performance

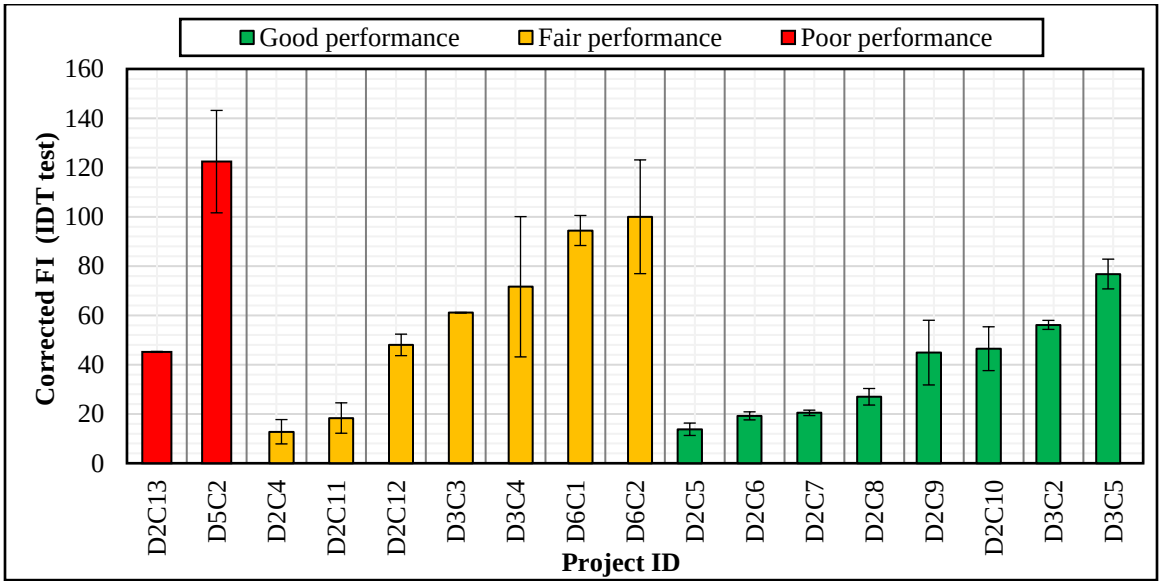


**Figure C.8** Correlation between FI from computed from SCB test with field project performance

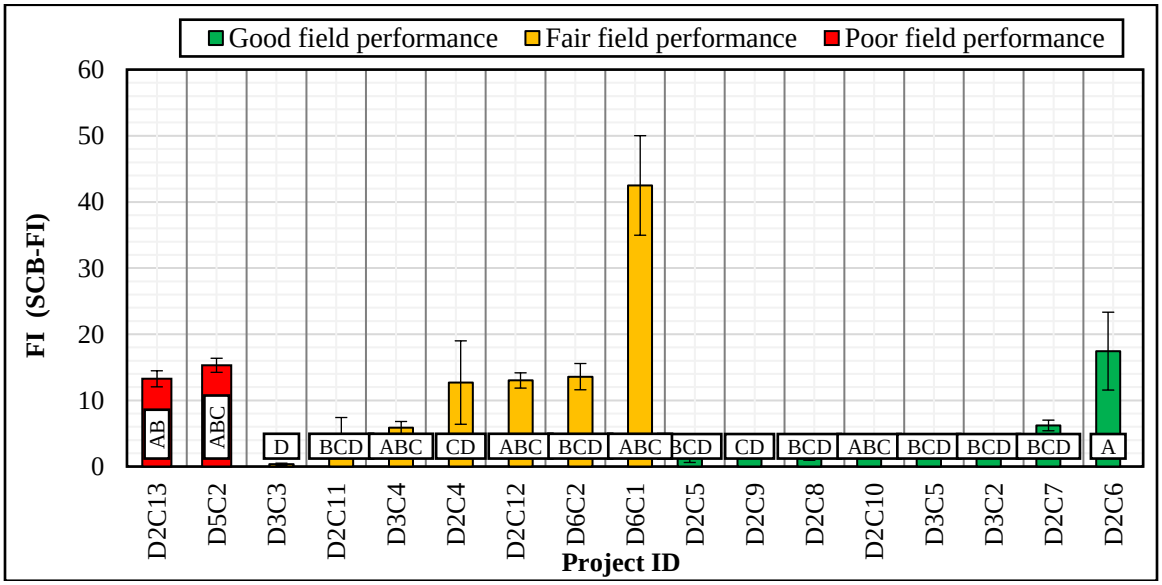


**Figure C.9** Correlation between corrected FI computed from IDT test with field project performance

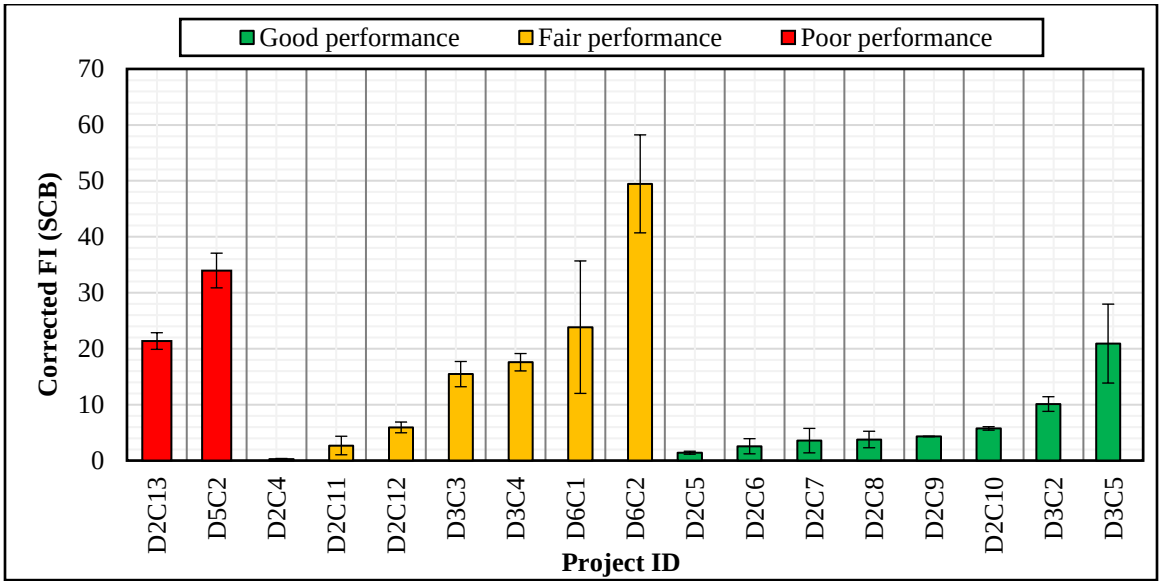


**Figure C.10** Correlation between corrected FI from computed from SCB test with field project performance

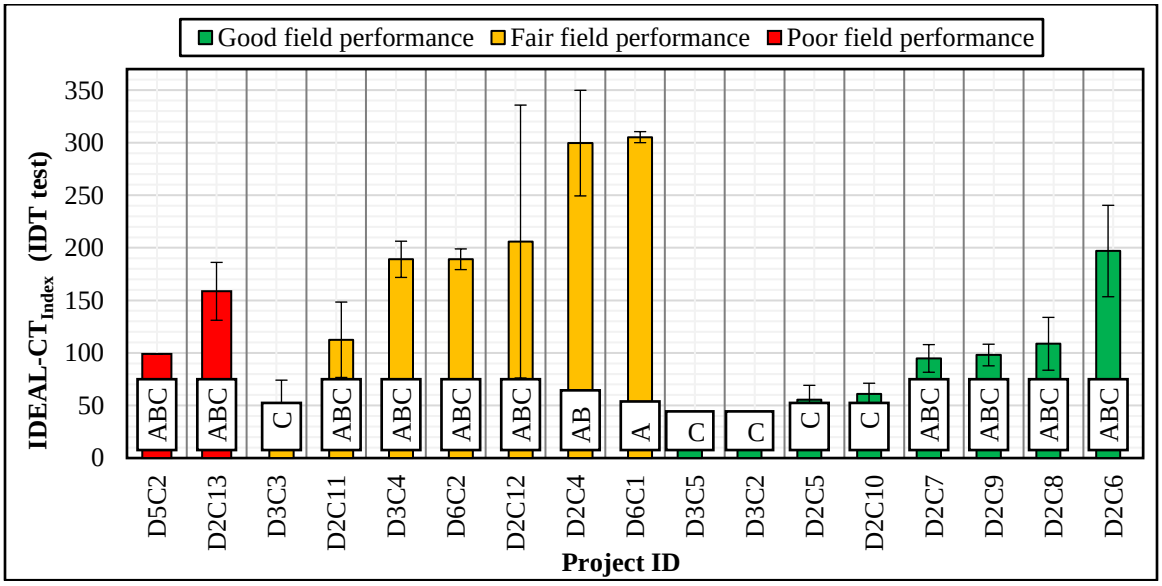


**Figure C.11** Correlation between IDEAL-$CT_{Index}$ from computed from SCB test with field project performance

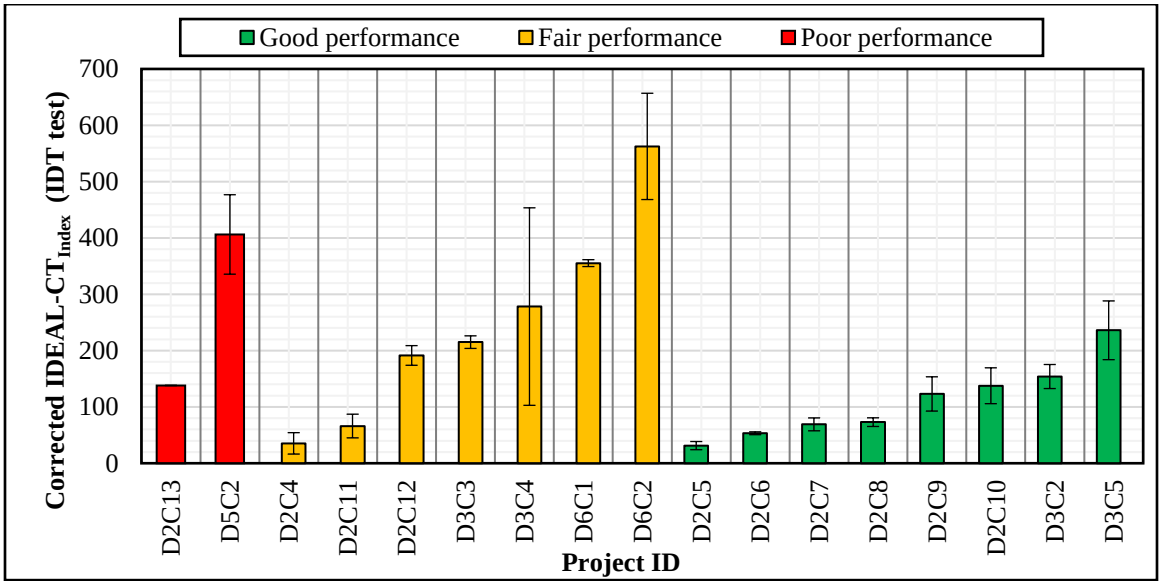


**Figure C.12** Correlation between corrected IDEAL-$CT_{Index}$ from computed from SCB test with field project performance

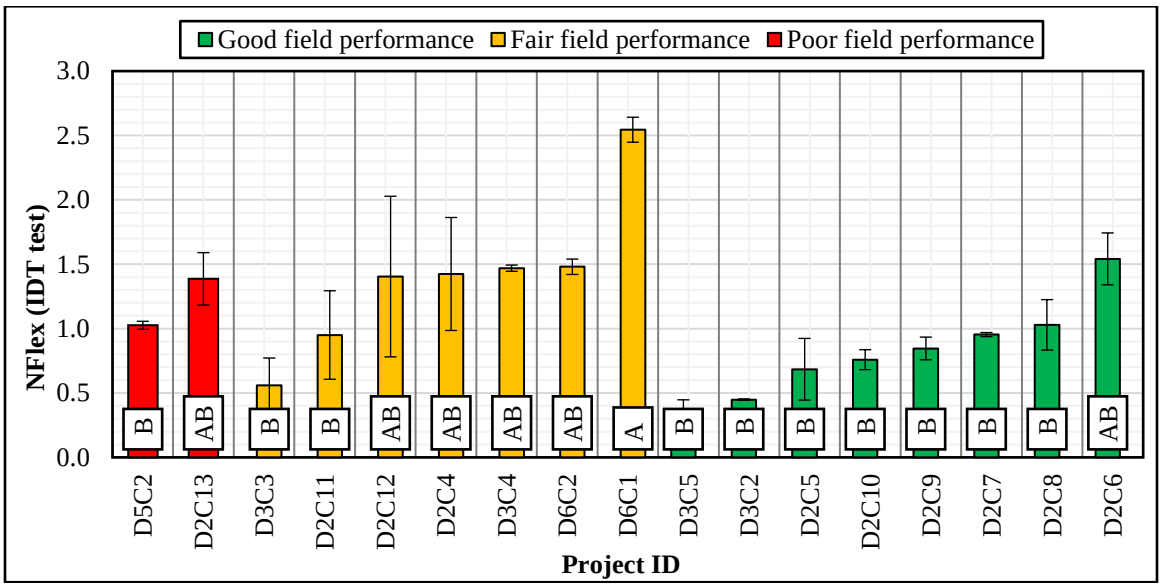


**Figure C.13** Correlation between Nflex from computed from SCB test with field project performance

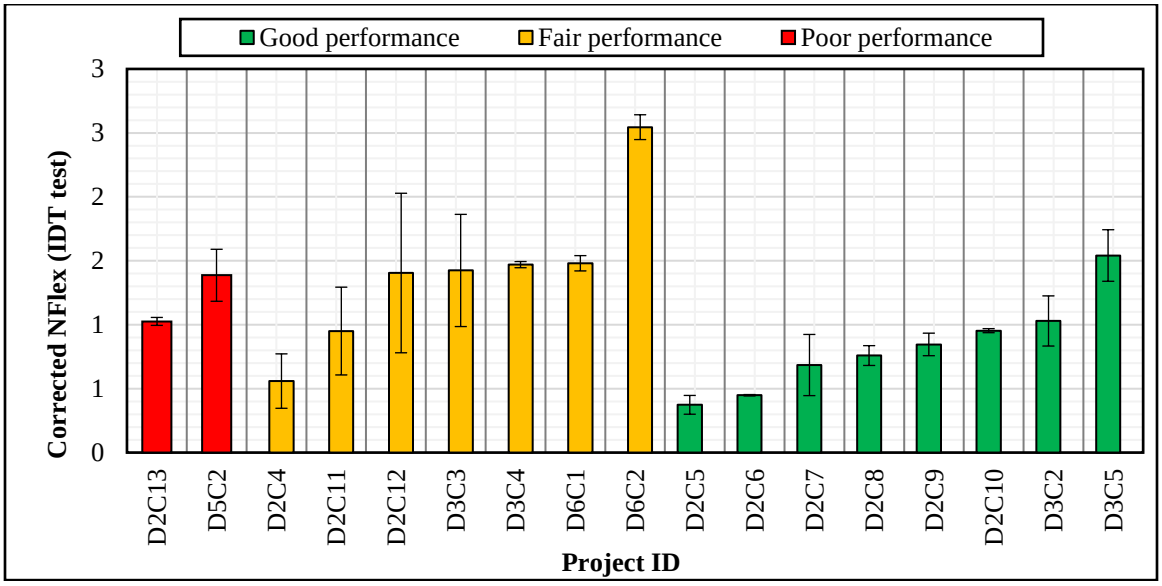


**Figure C.14** Correlation between corrected Nflex from computed from SCB test with field project performance

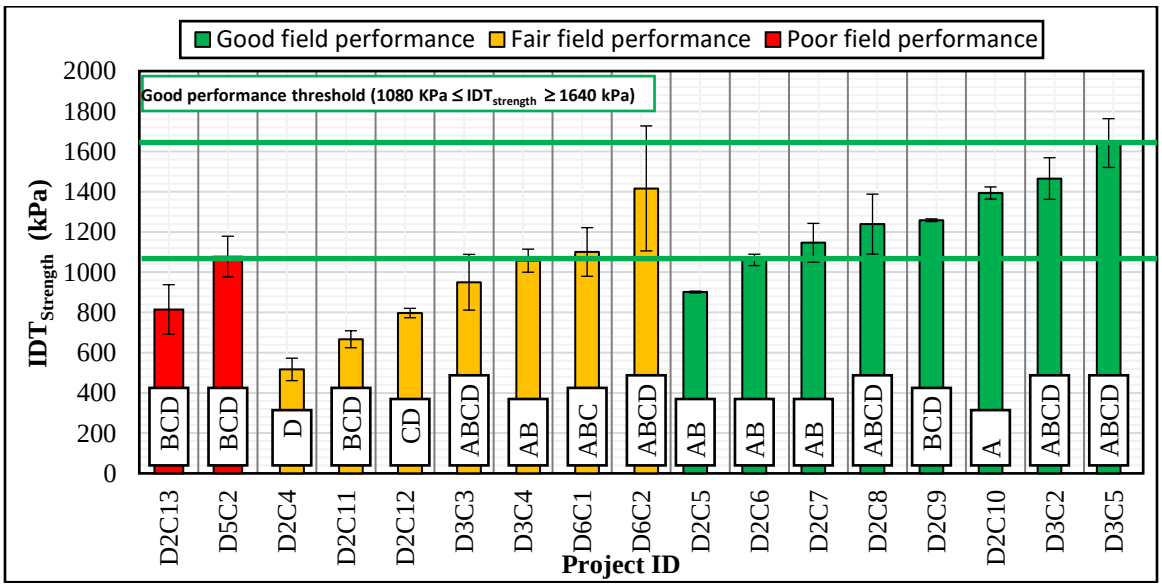


**Figure C.15** Correlation between $IDT_{strength}$ from computed with field project performance

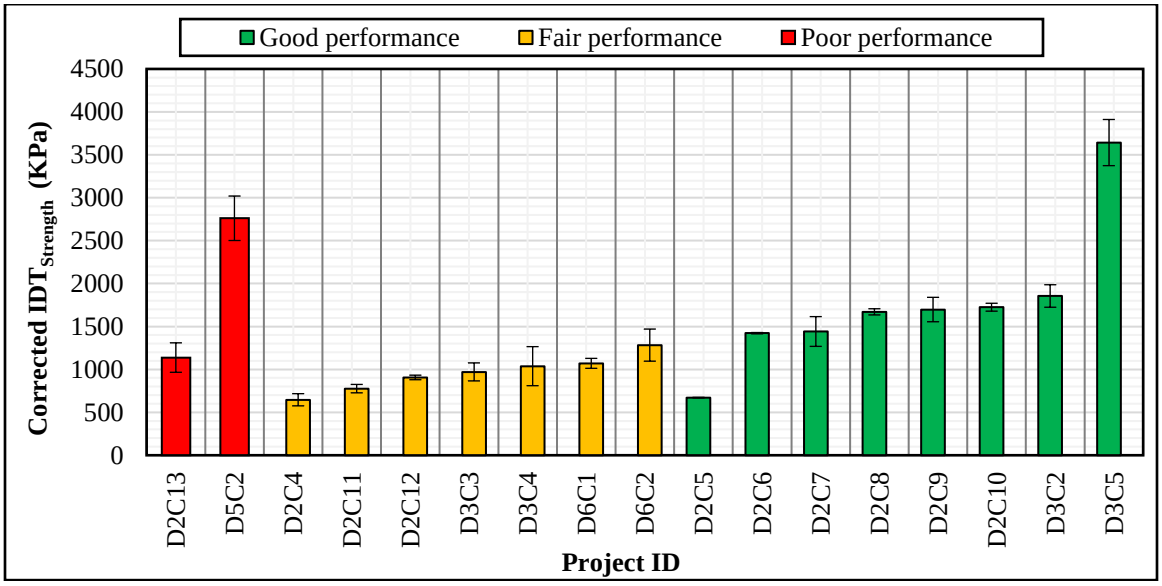


**Figure C.16** Correlation between corrected $IDT_{strength}$ from computed with field project performance

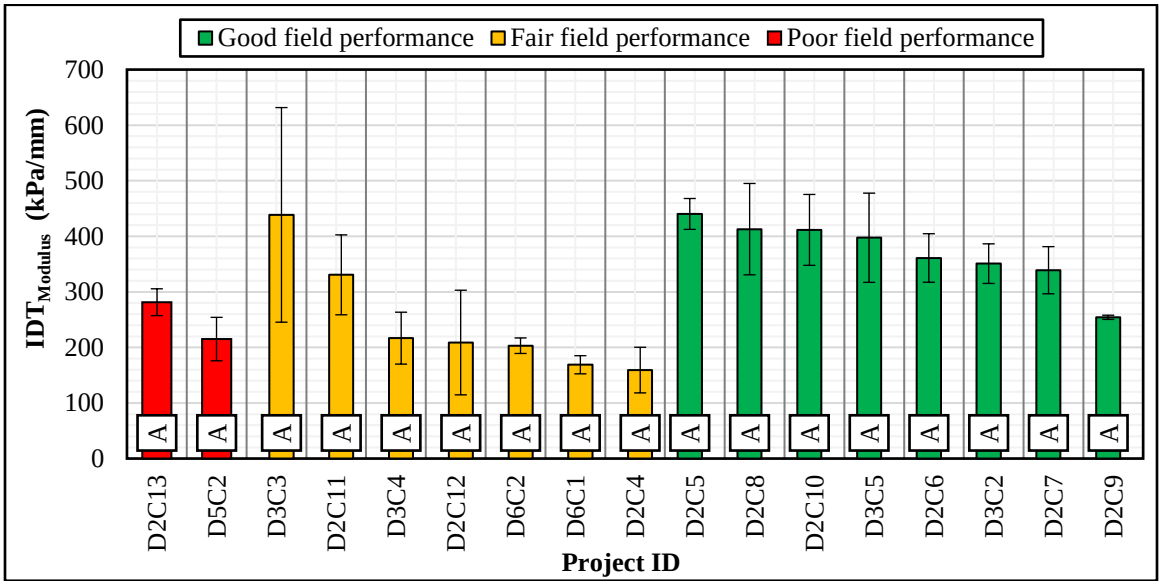


**Figure C.17** Correlation between $IDT_{Modulus}$ from computed with field project performance

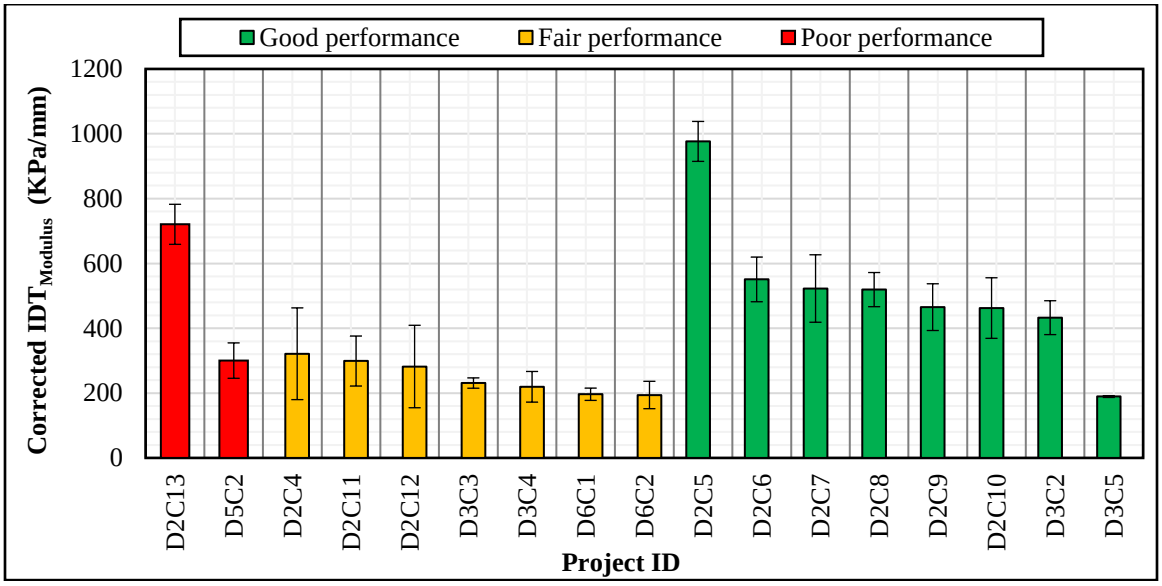


**Figure C.18** Correlation between corrected $IDT_{Modulus}$ from computed with field project performance

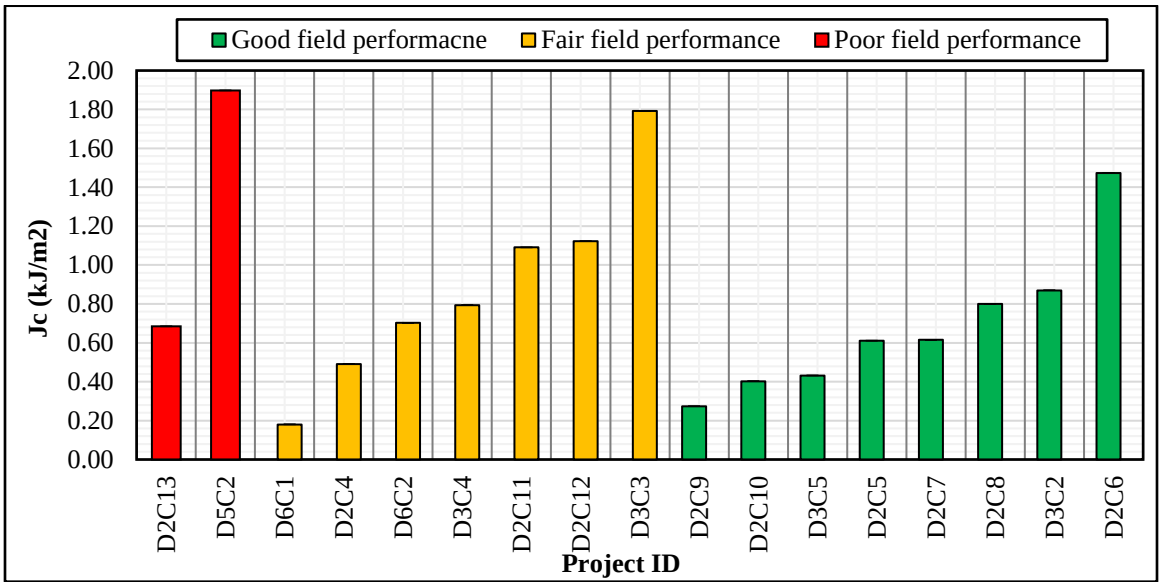


**Figure C.19** Correlation between $J_c$ with field project performance

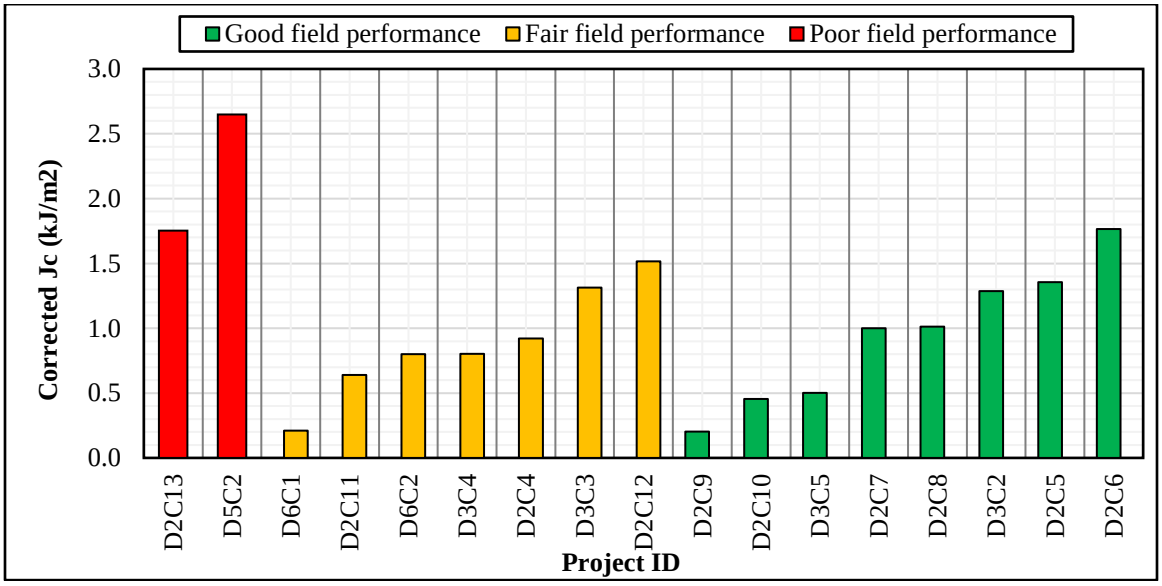


**Figure C.20** Correlation between corrected $J_c$ with field project performance

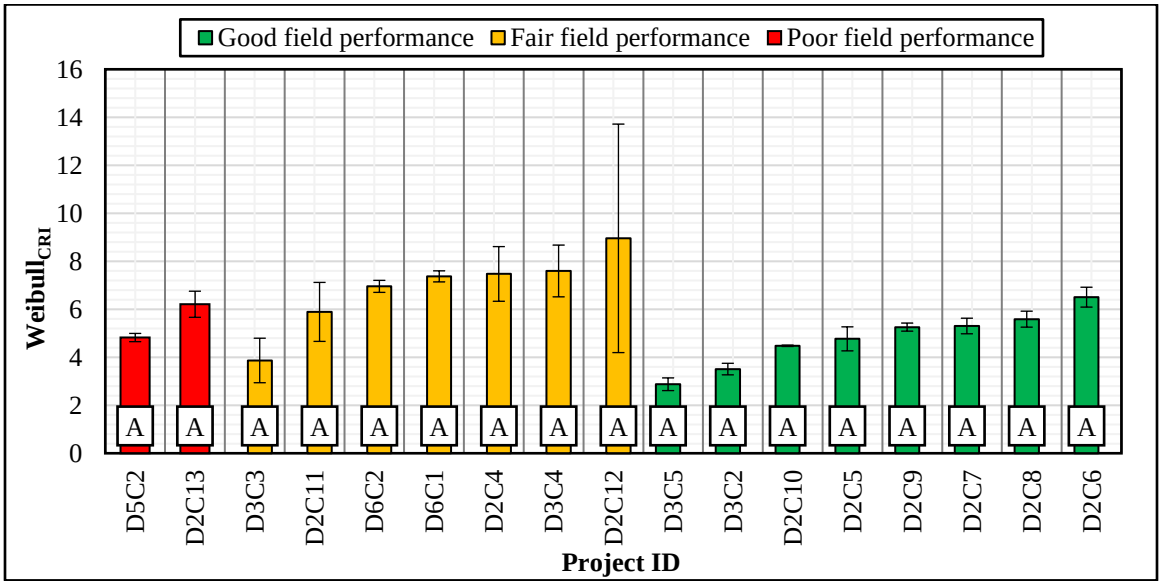


**Figure C.21** Correlation between $Weibull_{CRI}$ with field project performance

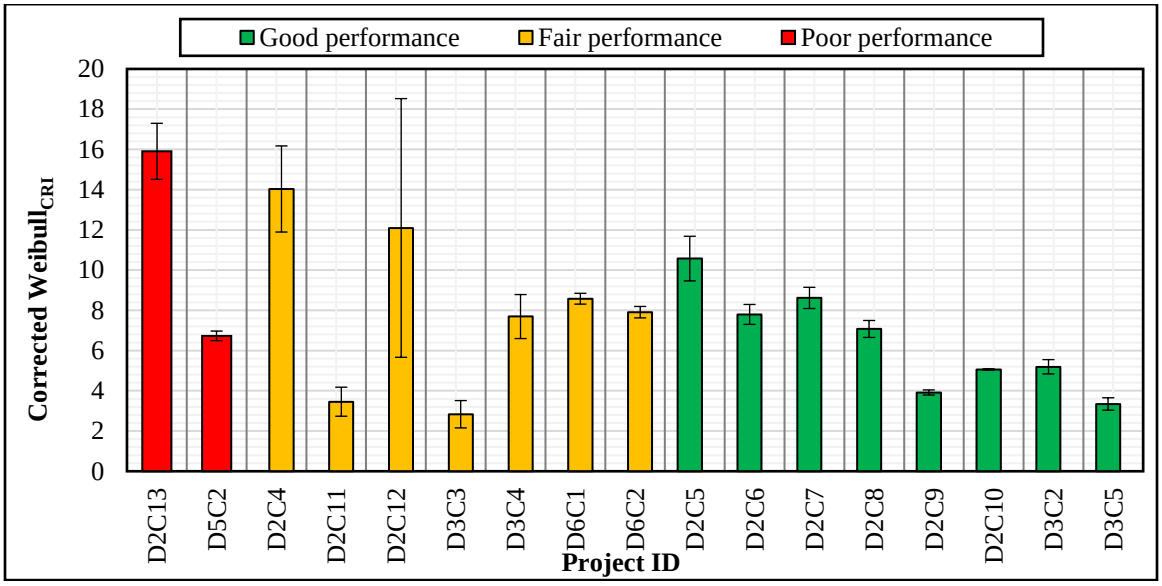


**Figure C.22** Correlation between corrected Weibull$_{CRI}$ with field project performance

# Appendix D - Correlation Between Monotonic and MSSD Performance Indicators

Figures D.1 to D.12 present the correlation between MSSD performance indicators (i.e., slope [*z*] and Absolute intercept [Abs {log *H*}]) and the selected monotonic performance indicators.

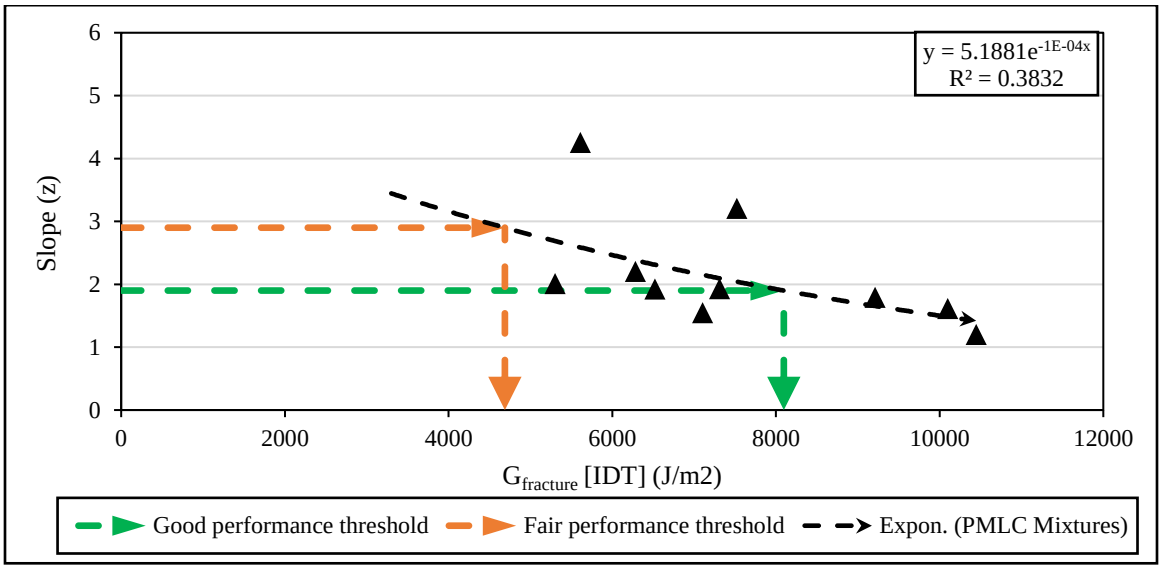


**Figure D.1** Correlation between $G_{fracture}$ (IDT) and the slope (*z*) parameter

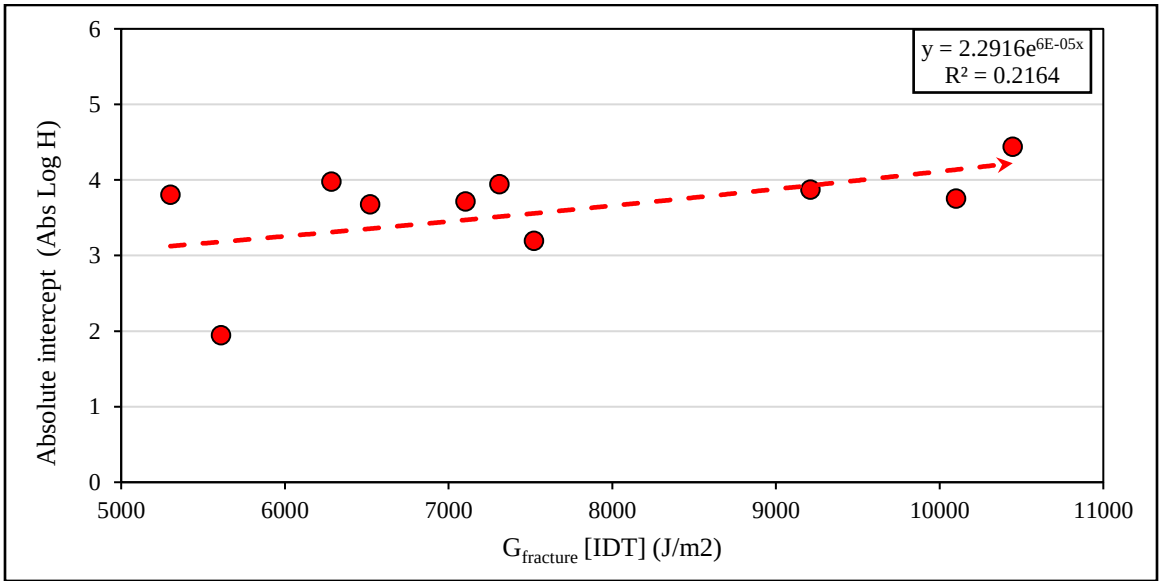


**Figure D.2** Correlation between $G_{fracture}$ (IDT) and Abs (log *H*) parameter

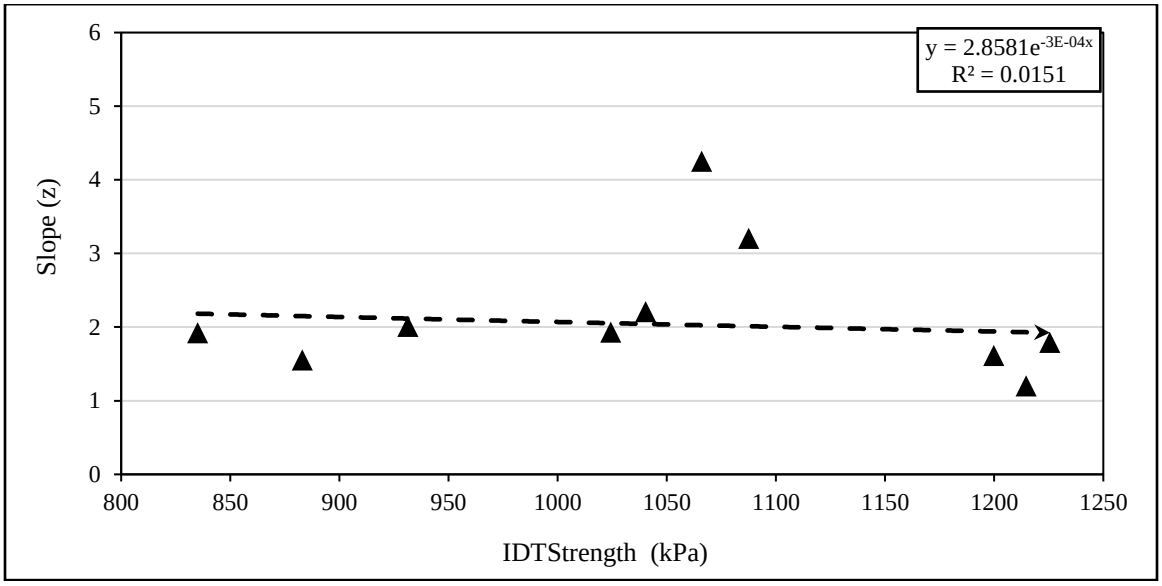


**Figure D.3** Correlation between $IDT_{Strength}$ and the slope (z) parameter

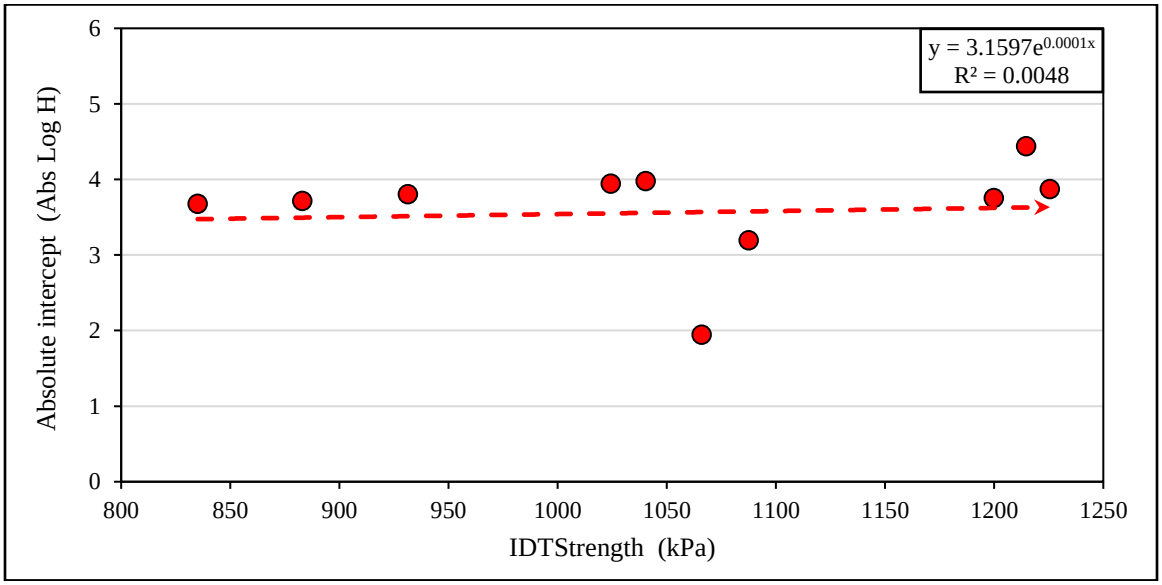


**Figure D.4** Correlation between $IDT_{Strength}$ and Abs (log *H*) parameter

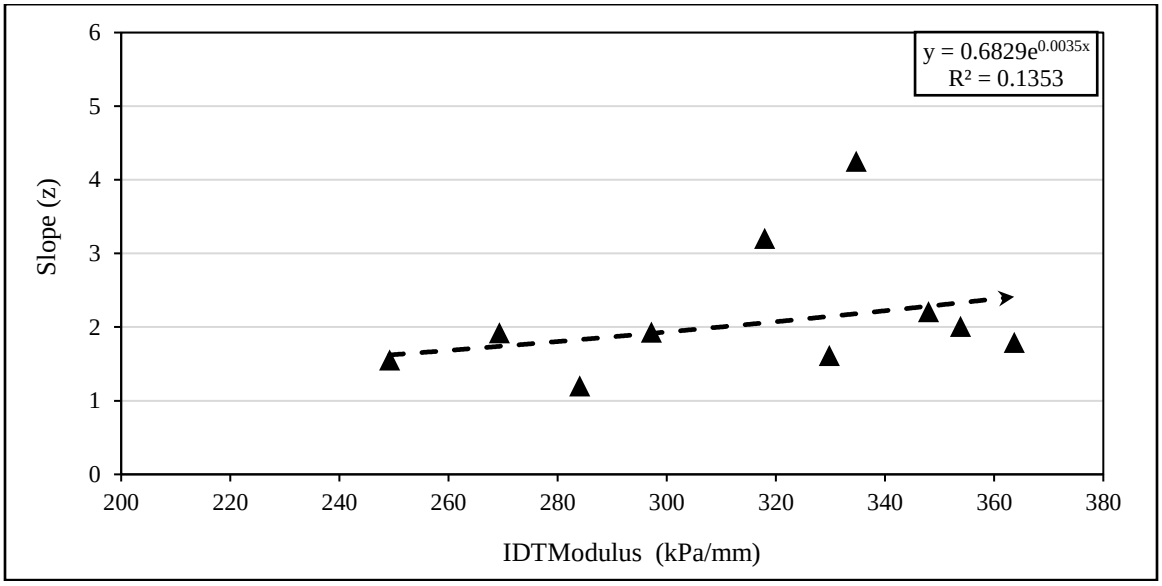


**Figure D.5** Correlation between $IDT_{Modulus}$ and the slope (*z*) parameter

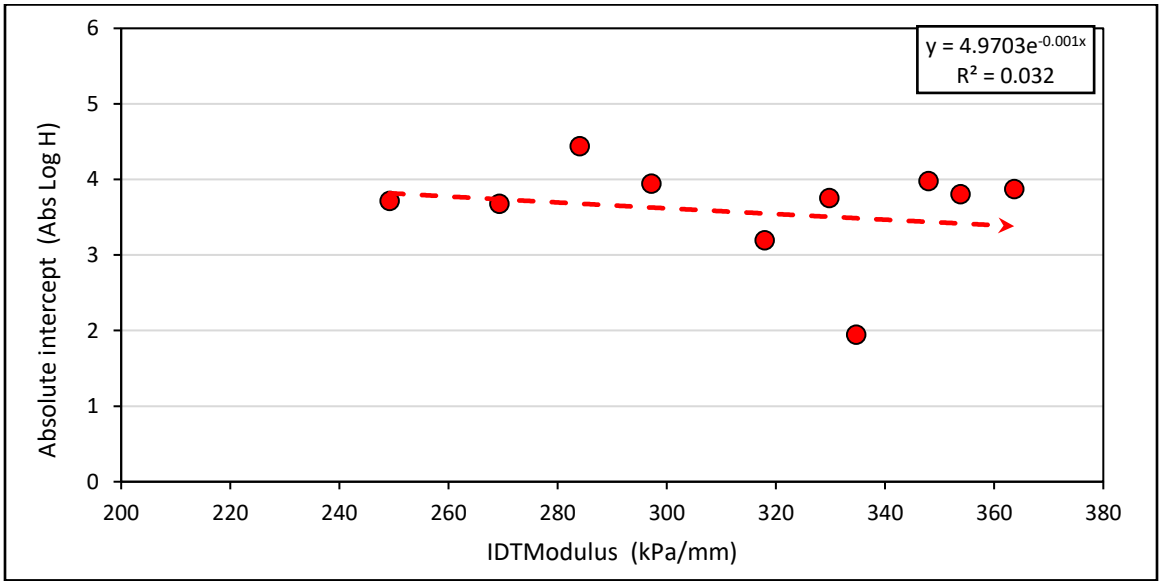


**Figure D.6** Correlation between $IDT_{Modulus}$ and Abs (log *H*) parameter

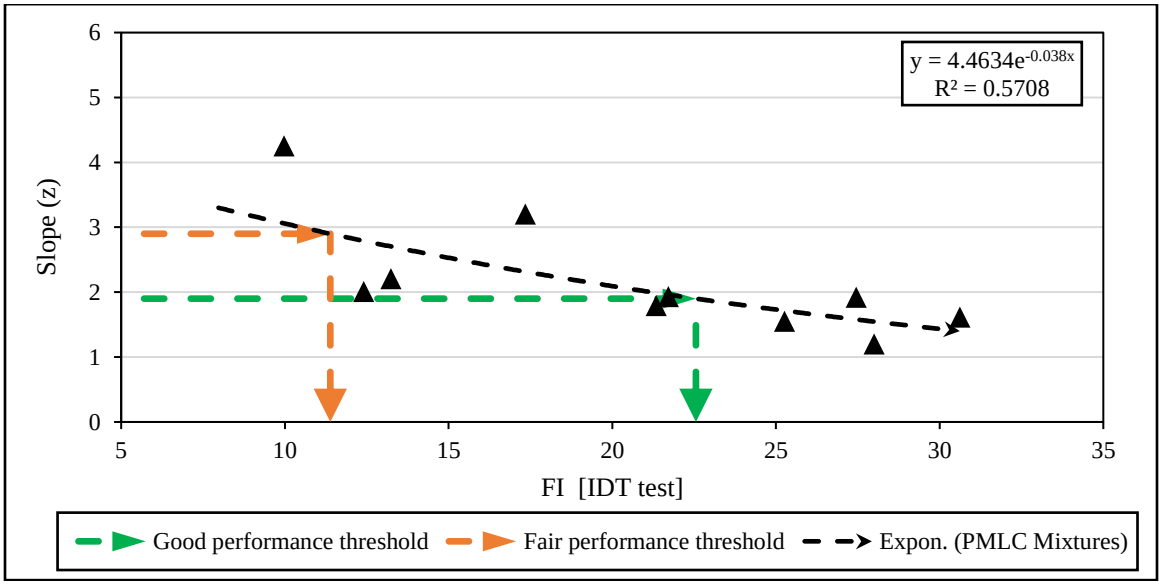


**Figure D.7** Correlation between FI [IDT test] and the slope (*z*) parameter

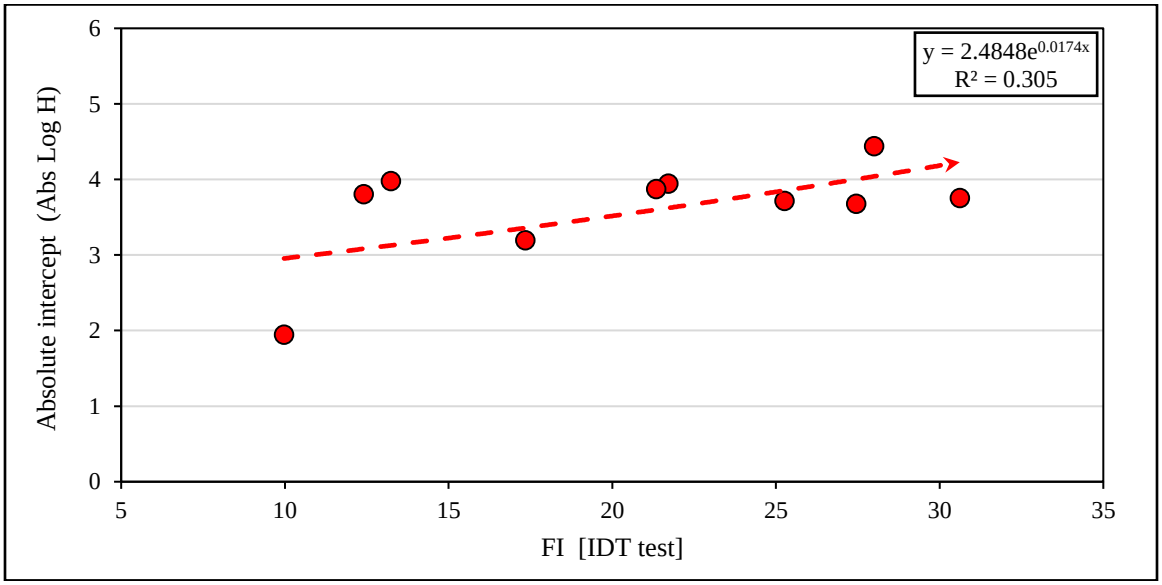


**Figure D.8** Correlation between FI [IDT test] and Abs (log *H*) parameter

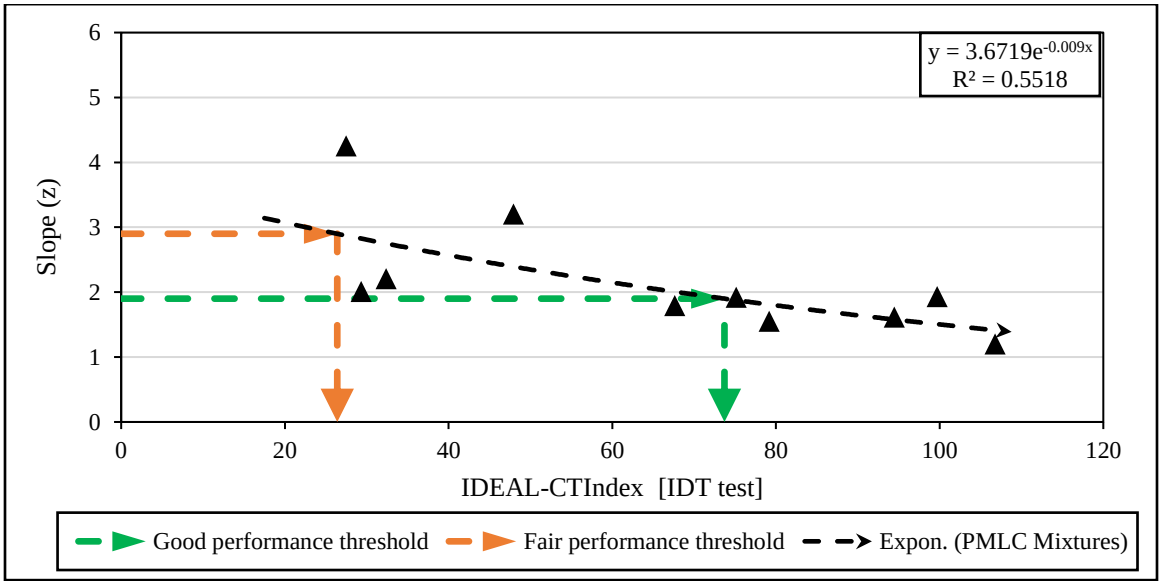


**Figure D.9** Correlation between IDEAL-$CT_{Index}$ [IDT test] and the slope (*z*) parameter

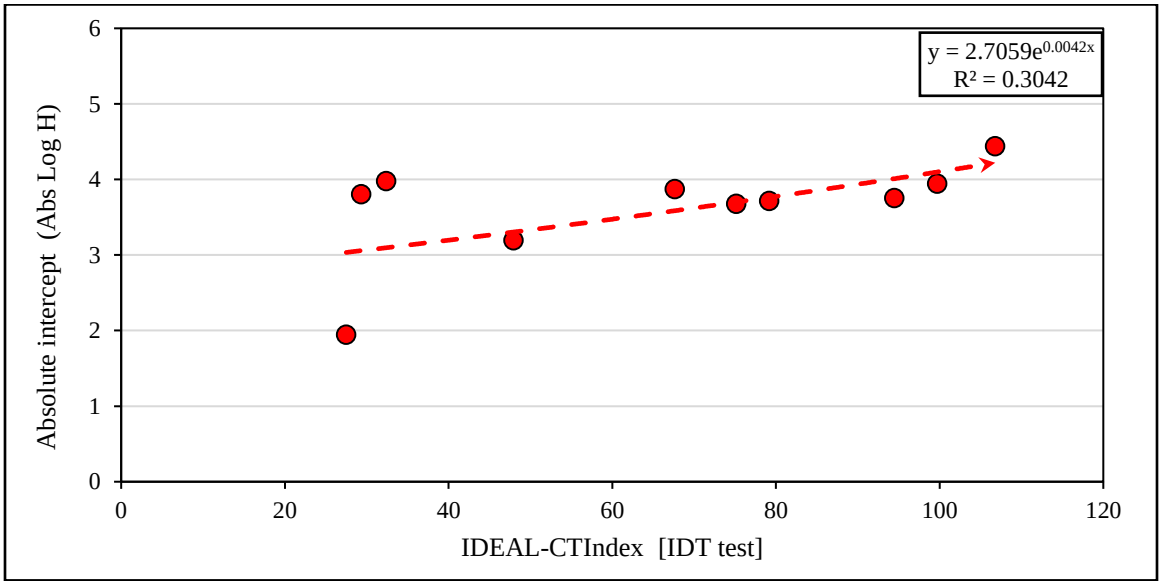


**Figure D.10** Correlation between IDEAL-$CT_{Index}$ (IDT test) and Abs (log *H*) parameter

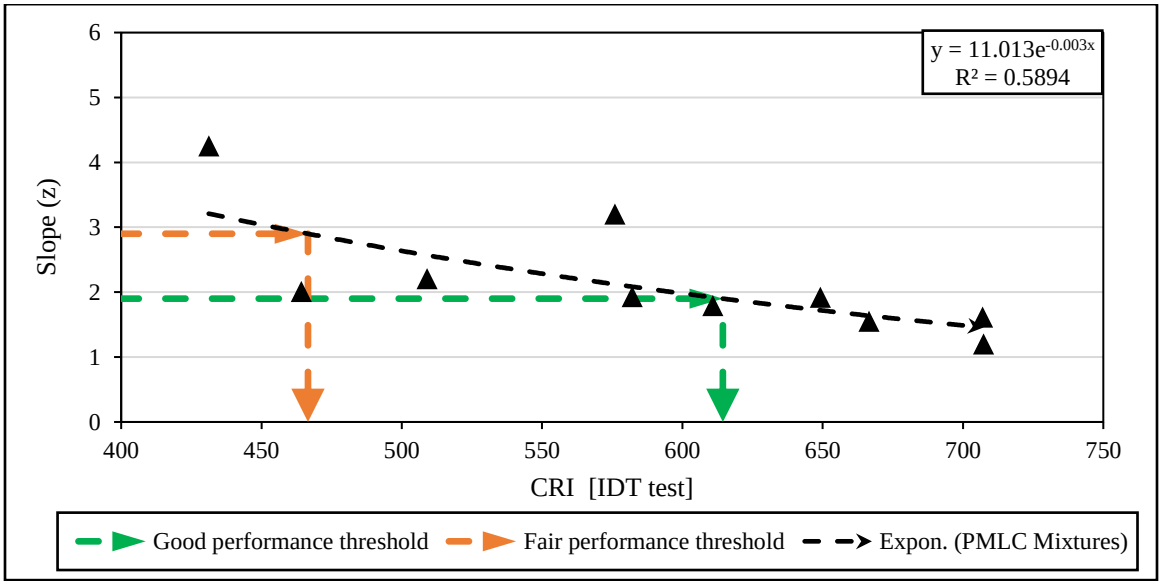


**Figure D.11** Correlation between CRI (IDT test) and the slope (*z*) parameter

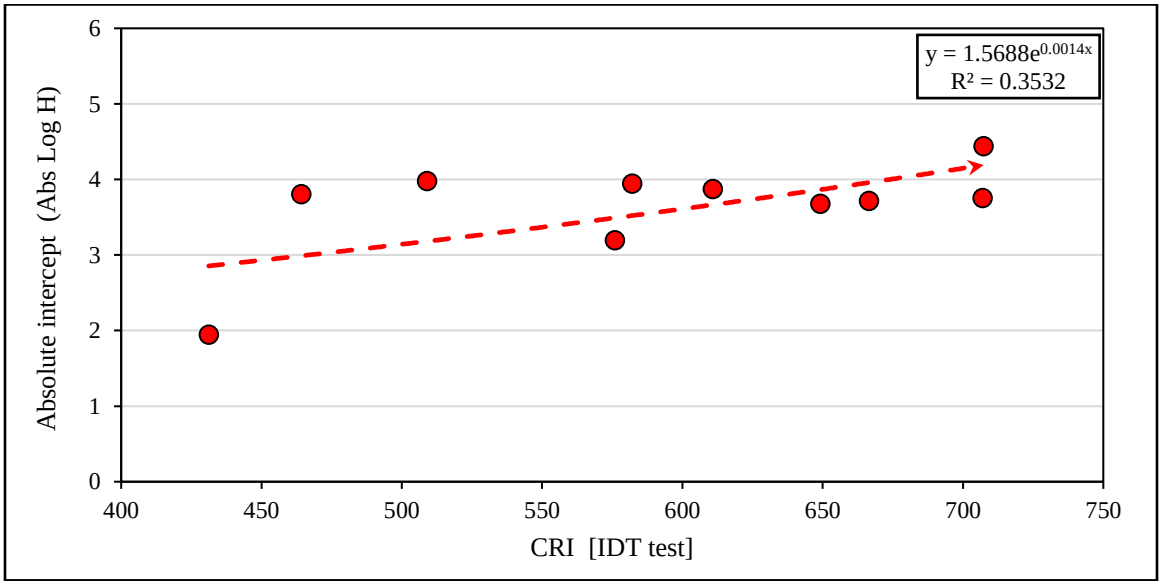


**Figure D.12** Correlation between CRI (IDT test) and Abs (log *H*) parameter

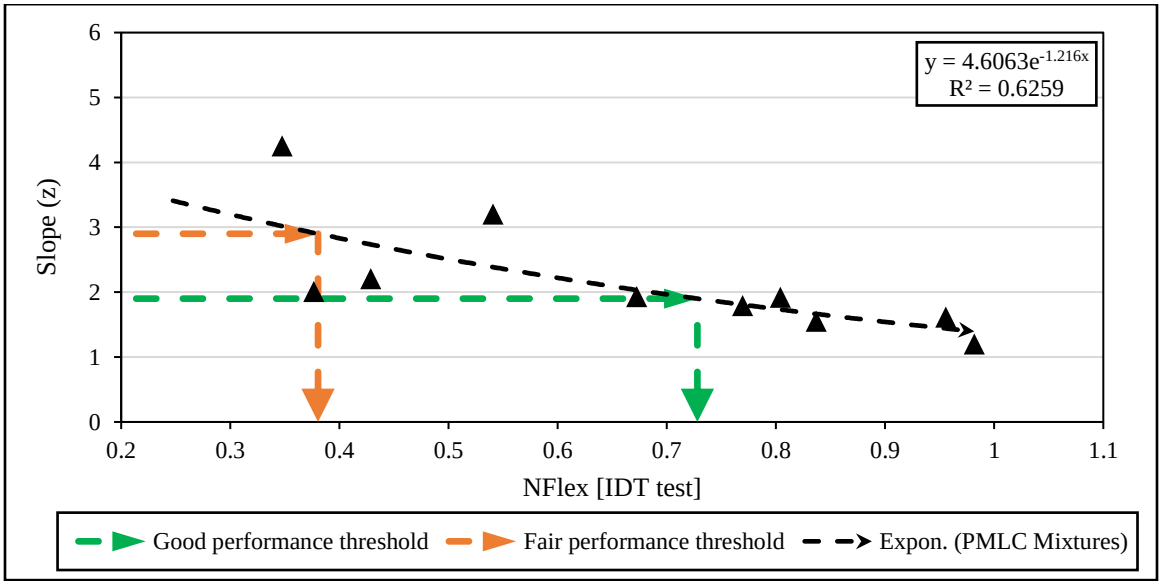


**Figure D.13** Correlation between NFlex (IDT test) and the slope (*z*) parameter

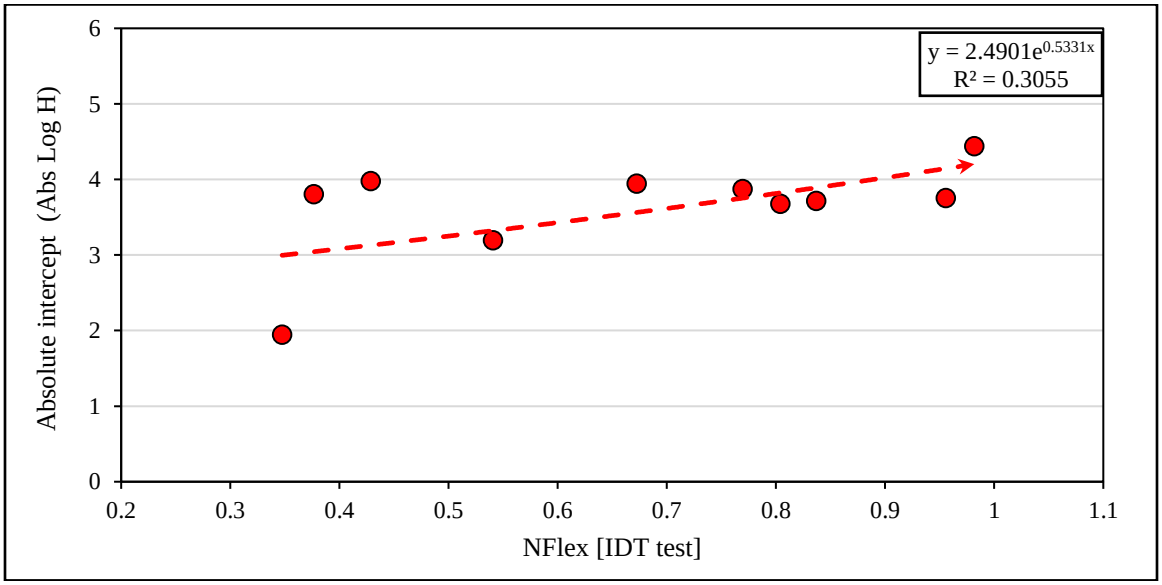


**Figure D.14** Correlation between NFlex (IDT test) and Abs (log *H*) parameter

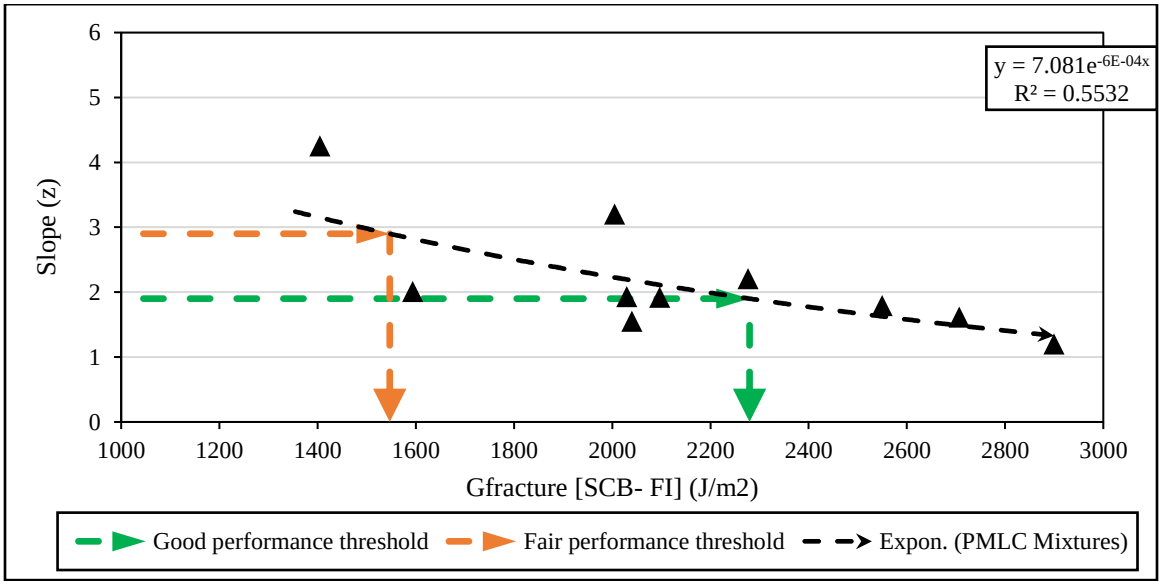


**Figure D.15** Correlation between $G_{fracture}$ (SCB- FI) and the slope ($z$) parameter

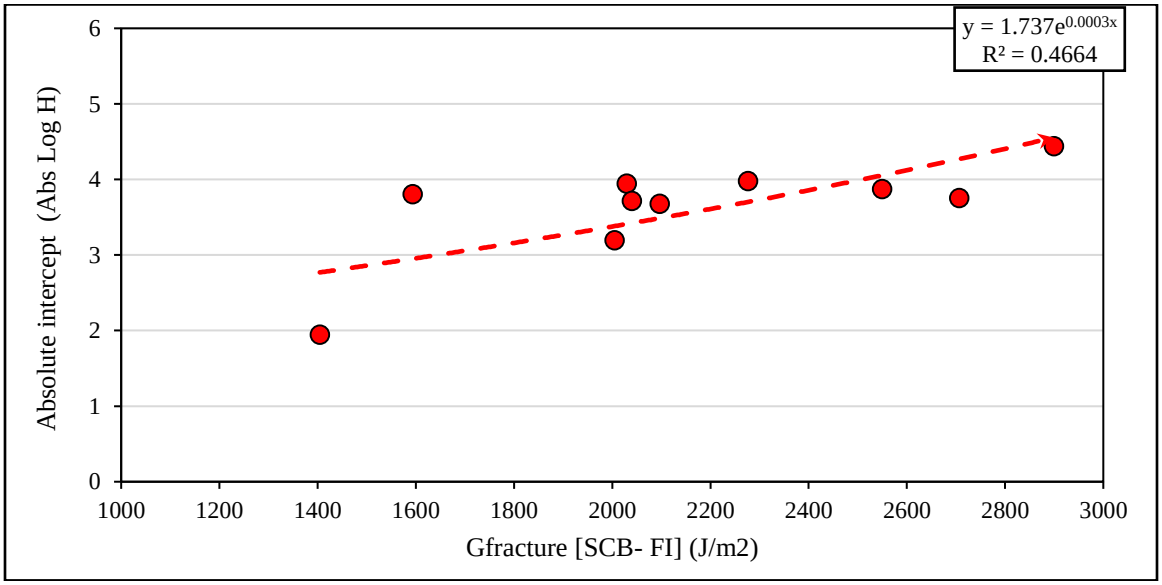


**Figure D.16** Correlation between $G_{fracture}$ (SCB- FI) and Abs (log $H$) parameter

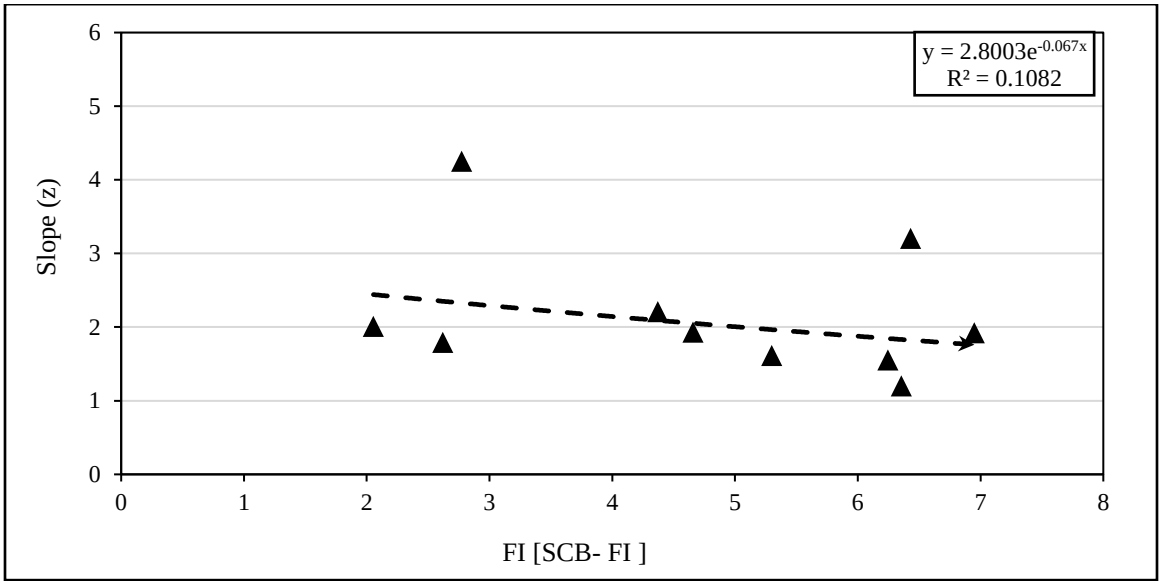


**Figure D.17** Correlation between FI (SCB- FI) and the slope (*z*) parameter

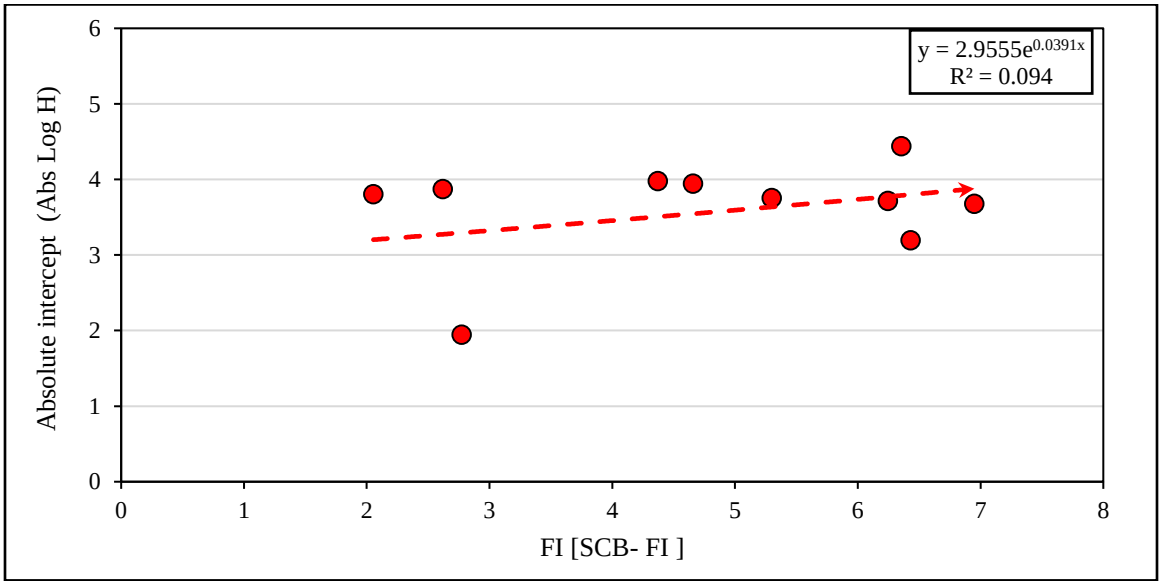


**Figure D.18** Correlation between FI (SCB- FI) and Abs (log *H*) parameter

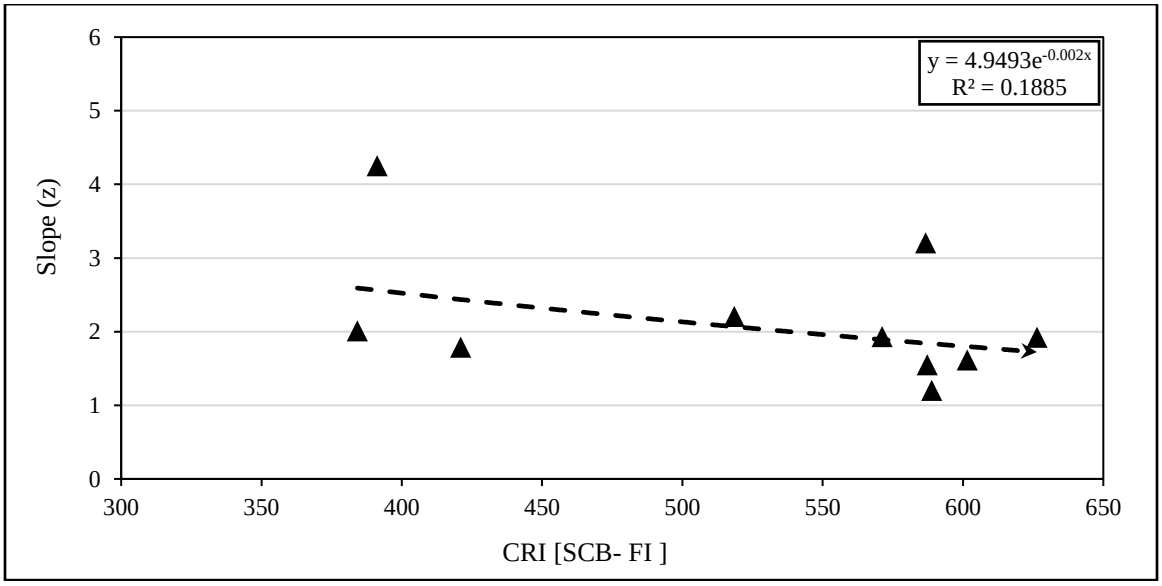


**Figure D.19** Correlation between CRI (SCB- FI) and the slope (*z*) parameter

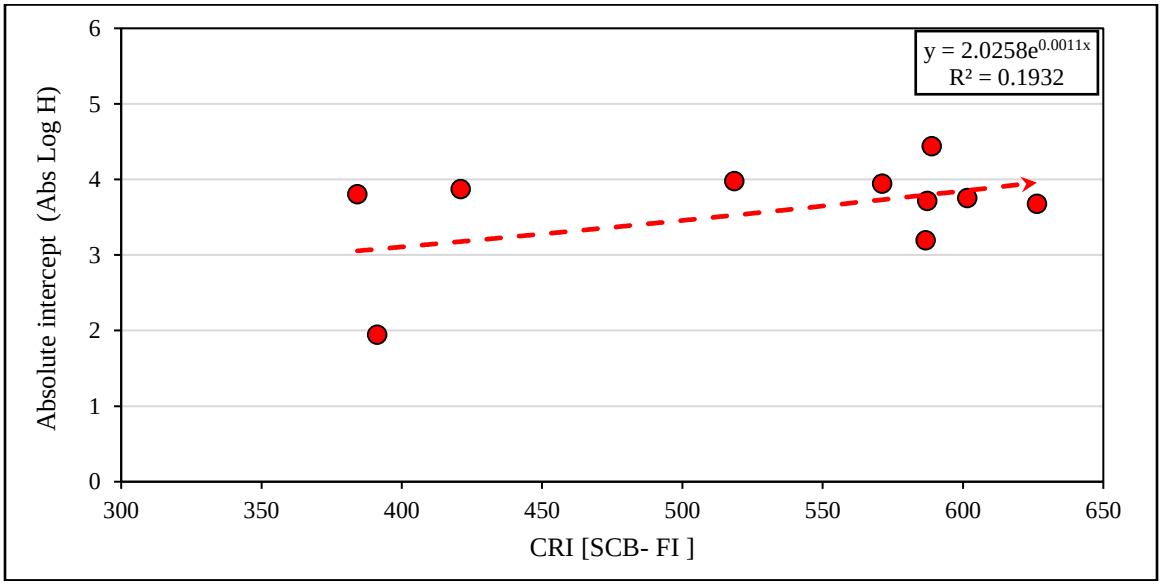


**Figure D.20** Correlation between CRI (SCB- FI) and Abs (log *H*) parameter

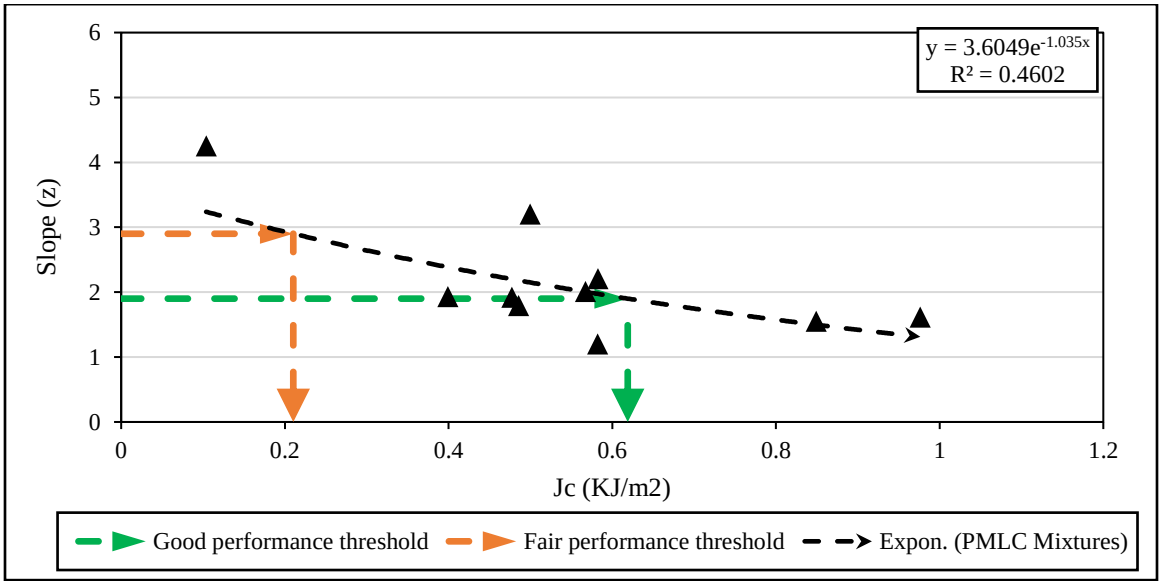


**Figure D.21** Correlation between $J_c$ and the slope ($z$) parameter

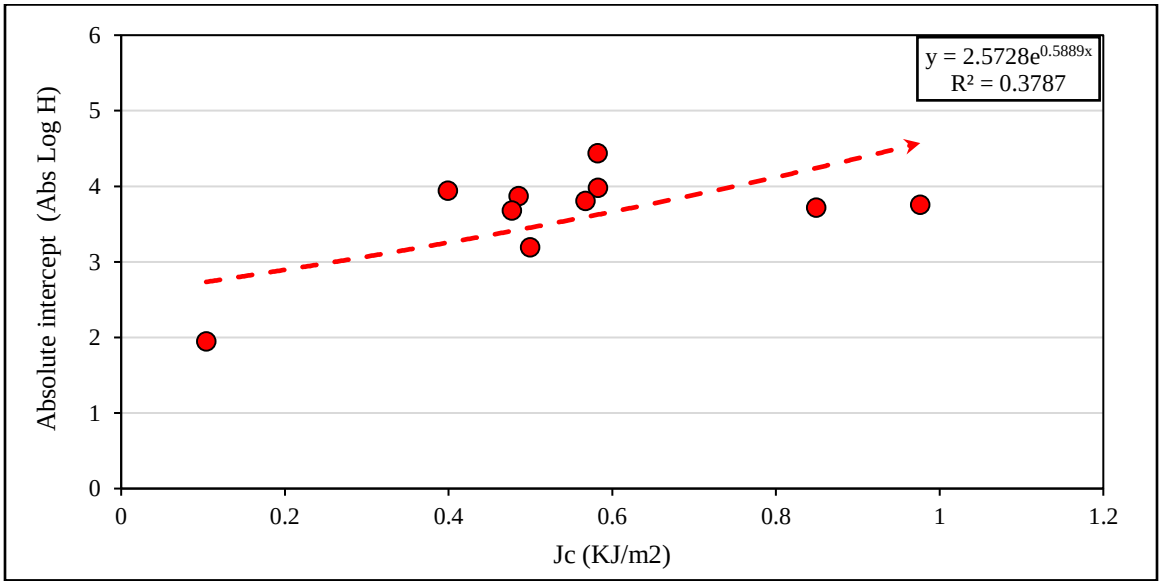


**Figure D.22** Correlation between $J_c$ and Abs (log $H$) parameter

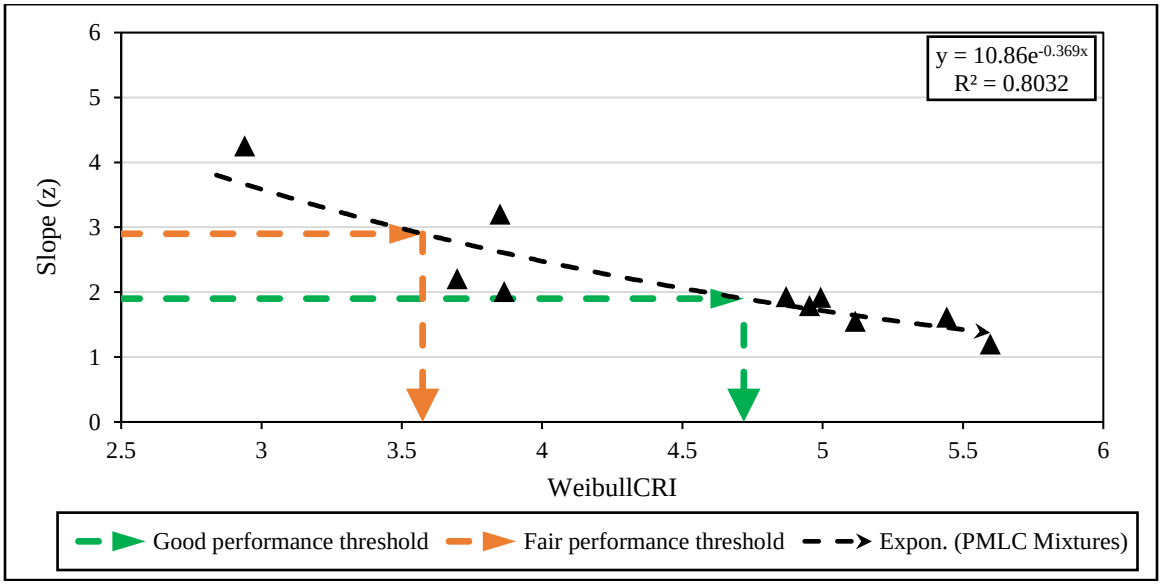


**Figure D.23** Correlation between $\text{Weibull}_{\text{CRI}}$ and the slope ($z$) parameter

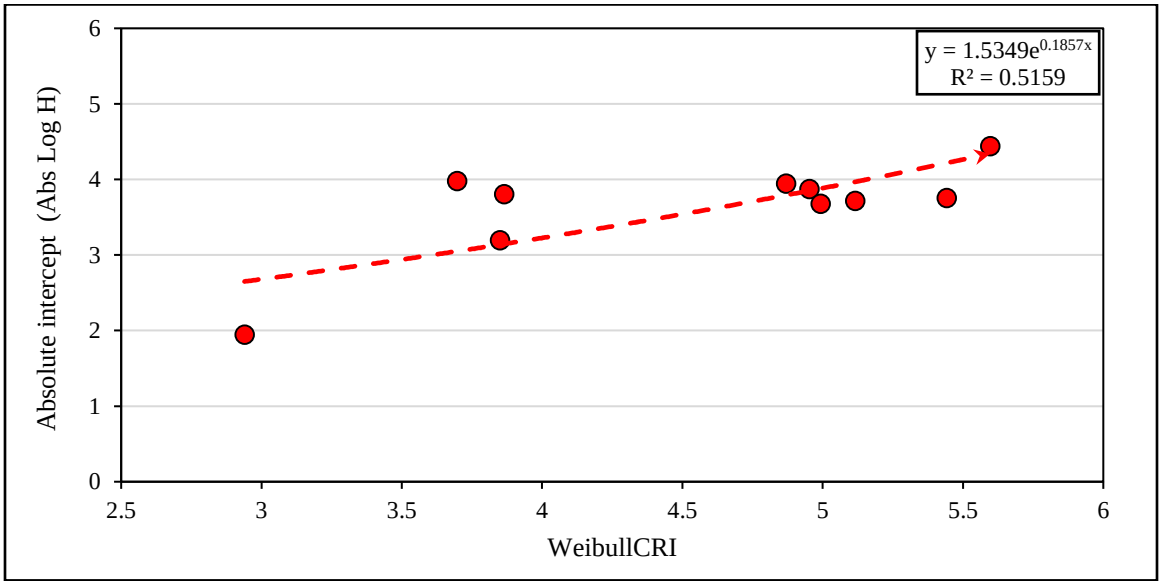


**Figure D.24** Correlation between $\text{Weibull}_{\text{CRI}}$ and Abs (log $H$) parameter

# Appendix E - Standard Test Method for Determination of Weibull Cracking resistance Index to Evaluate the Resistance of Asphalt Mixtures to Intermediate Temperature Cracking using Monotonic Loading Cracking Assessment tests

**Designation: DXXXX− 19**

## Standard Test Method for
**Determination of Weibull Cracking resistance Index to Evaluate the Resistance of Asphalt Mixtures to Intermediate Temperature Cracking using Monotonic Loading Cracking Assessment tests**

### 1. Scope

**1.1** This test method contains procedures set out to assess asphalt mix resistance to intermediate temperature cracking using a cylindrical or notched Semi Circular (SC) specimens.

1.2 The test method describes the determination of Weibull Cracking Resistance Index ($Weibull_{CRI}$) from the load-displacement (or stress-strain) curve obtained from various monotonic cracking assessment tests.

1.3 $Weibull_{CRI}$ can be used to interpret the variation in the load-displacement curve of various monotonic tests and describe the variation in mix resistance to cracking.

1.4 The values stated in SI units are to be regarded as standard.

1.5 *This standard does not purport to address all of the safety concerns, if any, associated with its use. It is the responsibility of the user of this standard to establish appropriate safety and health practices and determine the applicability of regulatory limitations prior to use.*

### 2. Referenced Documents

2.1 ASTM Standards:[1]

D8 Terminology Relating to Materials for Roads and Pavements

D6931 Indirect Tensile (IDT) Strength of Bituminous Mixtures

D8225 Determination of Cracking Tolerance Index of Asphalt Mixture Using the Indirect Tensile Cracking Test at Intermediate Temperature

D6925 Test Method for Preparation and Determination of the Relative Density of Asphalt Mix Specimens by Means of the Superpave Gyratory Compactor

2 AASHTO Standards:[2]

AASHTO T166 Bulk Specific Gravity (Gmb) of Compacted Hot Mix Asphalt (HMA) Using Saturated Surface-Dry Specimens

AASHTO T124 Determining the Fracture Potential of Asphalt Mixtures Using the Flexibility Index Test (FIT)

AASHTO R 30 Mixture Conditioning of Hot Mix Asphalt (HMA)

AASHTO T312 Preparing and Determining the Density of Asphalt Mixture Specimens by Means of the Superpave Gyratory Compactor

[1] For referenced ASTM standards, visit the ASTM website, www.astm.org, or contact ASTM Customer Service at service@astm.org. For *Annual Book of ASTM Standards* volume information, refer to the standard's Document Summary page on the ASTM website.

[2] Available from American Association of State Highway and Transportation Officials (AASHTO), 444 N. Capitol St., NW, Suite 249, Washington, DC 20001, ttp://www.transportation.org.standards, visit the ASTM

## 3. Summary of Test Method

3.1 A cylindrical specimen or notched semi-circular specimen is loaded in compression at a constant vertical actuator displacement rate of 50 mm/min and test temperature of 25 °C until fracture. The time, load and displacement are collected during the test and are used to calculate the $Weibull_{CRI}$ to assess mix resistance to cracking.

## 4. Significance and Use

4.1 The monotonic cracking assessment tests use the variation in the load-displacement curve to assess the variation in mix resistance to cracking. Several performance indicators derived from the load-displacement curve were proposed to assess the resistance of asphalt mix to cracking. While these methods have their own merits, none of them can describe the overall variation in the load-displacement curve except $Weibull_{CRI}$[3].

4.2 $Weibull_{CRI}$ was able to interpret the testing results of various monotonic cracking assessment tests such as Indirect Tension Test [IDT] in accordance with D8225 or D6931 and Semi-Circle Bending (SCB) in accordance with AASHTO TP124 to assess asphalt mix resistance to cracking. However, IDT test is recommended.

4.3 $Weibull_{CRI}$ was found to be sensitive to the variation in specimen notch depth, thickness, and air void content and provided logical trends with the variation in binder content, binder grade, aggregate type, NMAS, aging, rejuvenator dosages, and Recycled Asphalt Pavement (RAP). In addition, it had the good correlation with cyclic cracking assessment tests and low variability [3,4,5].

## 5. Apparatus

5.1 The testing system shall include

5.1.1 *Axial loading device* — The testing system shall be able to apply the loading in compression with minimum capacity of 10 KN. Also, it shall maintain a constant vertical actuator displacement rate of 50 mm/min.

5.1.2 *Loading cell* — The testing system shall have a loading cell with a minimum capacity of 10 kN and resolution of 10 N.

*5.1.3 Testing fixture* — The testing system shall have a suitable testing fixture for either the cylindrical or notched SC specimens. The test fixture for cylindrical specimen shall follow the requirement in D6931 or D8225. The test fixture for a semi-circular specimen shall follow the requirements in AASHTO TP124.

5.1.4 *Displacement measuring device* — The testing system shall have an internal/external displacement measuring device.

5.1.5 *Data acquisition system* — The testing system shall have a data acquisition system able to collect time, load, and the displacement (internal or external) during the test at a minimum data sampling frequency of 20 Hz.

5.2 *Gyratory compactor* — A gyratory compactor is needed to prepare test specimens.

[3] H. Alkuime, F. Tousif, E. Kassem, F. Bayomy, Review and evaluation of intermediate temperature cracking testing standards and performance indicators for asphalt mixes., Construction and Building Materials. (2019).

[4] H. Alkuime, E. Kassem, F. Bayomy, Development of a new performance indicator to evaluate the resistance of asphalt mixes to intermediate temperature cracking., Journal of Transportation Engineering, Part B: Pavements. (2019).

[5] H. Alkuime, E. Kassem, F. Bayomy, Development of performance-engineered mix design (PEMD) specifications for intermediate temperature monotonic cracking assessment tests and performance indicators, Road Materials and Pavement Design. (2019).

*5.3 Conditioning Chamber* — The testing system shall have an environmental chamber able to maintain the temperature of the test specimen at the required testing temperature during the test.

5.3 *Specimen measurement device* — A caliper shall be used to measures specimen diameter and thickness. In addition, the notch depth and length of the notched SC specimen.

5.4 *Saw* — A laboratory saw capable to make a notch on the semicircular specimen and trimming the extracted field cores is needed

**6. Hazards**

6.1 Standards Laboratory caution should be exercised when handling, mixing, compacting, and preparing asphalt mixtures and test specimens.

**7. Specimen Preparation**

7.1 The monotonic test may be conducted on laboratory-prepared specimens or extracted field cores from constructed test sections.

7.2 Laboratory prepared specimen

7.2.1 *Asphalt mix*—Laboratory prepared specimen is prepared either from Laboratory Mixed-Laboratory Compacted (LMLC) or Plant Mixed-Laboratory Compacted (PMLC) asphalt mixes.

7.2.2 *Specimen geometry*— Specimen shall have 150 ± 2 mm diameter and 50 ±1 mm thickness. The notched SC specimen requires additional notch making with 15 ±1 mm length and 1.5 ±1 mm width.

7.2.3 *Aging* — Specimen prepared from LMLC mixes shall be short-term aged in aged in accordance with AASHTO R30. No short-term aging is required for specimens prepared from PMLC mixes.

7.2.4 *Air void content* — Test specimens shall be compacted to a target air void content of 7 ±0.5% in accordance with AASHTO T 312 at the required *thickness*

7.3 *Extracted field cores*

7.3.1 Field cores shall be extracted using a 150-mm coring bit.

7.3.2 *Specimen geometry* — The extracted field cores shall have 150 mm diameter and a minimum thickness of 30 mm. The notched SC specimen requires additional notch making with 15 ±1 mm length and 1.5 ±1 mm width.

7.3.3 *Air Void content* — The air void content of the extracted field cores shall be measured prior to testing

**8. Testing procedures**

8.1 Place the specimen in the test fixture inside the testing system.

8.2 Precondition the test specimen *for a minimum of 2 hours at 25 ℃ prior to testing.*

8.3 Test the specimen at a constant displacement loading rate of 50 mm/min. The test shall be stopped when the load reaches 0.1 kN. The time, applied load, and displacement shall be measured during the test.

**9. Data interpretation**

9.1 The determination of WeibullCRI requires is performed in two steps; steps-1 and steps-2.

9.1.1 *Step-1* — Fitting of the load-displacement curve

9.1.1.1 The modified Weibull probability density function (Equation E.1) is used to fit the load-displacement curve.

$$P = A \times \left(\frac{\beta}{\eta}\right)\left(\frac{u}{\eta}\right)^{\beta-1} \times e^{-(\frac{u}{\eta})^{\beta}} \qquad \text{E.1}$$

where:

| | | |
|---|---|---|
| $P$ | = | The applied load (N or KN) |
| A | = | The area parameter |

$\beta$ = The shape parameter

$\eta$ = The scale parameter

$u$ = The measured displacement (mm)

9.1.1.2 The load-displacement curve fitting is performed using the Nonlinear Least Square Fitting (NLSF) regression method.

9.1.1.2.1 The NLSF fitting can be performed using commercial software (e.g., OriginLab) or using Excel's SOLVER tool

9.1.1.2.2 The NLSF fitting is optimized to provide a minimum Sum of Squared Errors (SSR) between the measured and the predicted load values (Equation E.2).

9.1.1.2.2 The fitting accuracy is checked using the Standard Error (SE), the coefficient of determination ($R^2$), and the 95% Confidence Intervals (CI) as presented in Equations E.3, E.4, and E.5, respectively.

$$\text{SSR} = \sum_{i=1}^{n} \left[P_{measured} - P_{predicted}\right]^2 \qquad \text{E.2}$$

$$\text{SE} = \frac{SSR}{df} \qquad \text{E.3}$$

$$R^2 = 1 - \frac{SSR}{\sum_{i=1}^{n} [P_{measured} - P_{mean}]^2} \qquad \text{E.4}$$

$$\text{CI} = t_{critial} \times SE \qquad \text{E.5}$$

where:

$SSR$ = The sum of squared error

$P_{measured}$ = The measured load (N or kN)

$P_{predicted}$ = The predicted load (N or kN)

$i$ = Counter

$n$ = The number of measured data points

$df$ = The degrees of freedom ($df = n - 3$)

$P_{mean}$ = The average value of the measured load

$t_{critial}$ = The critical t-value at 95% confidence interval.

9.1.1.2.4 Figure 1 shows an example of using the modified Weibull function (Equation 9.1) to fit the load-vertical actuator displacement curve generated from IDT test data. The function fits the entire curve data with excellent accuracy (coefficient of determination [$R^2$] = 0.997). In addition, Figure 1 demonstrates that the 95% CI bands provide an accurate estimation

9.1.2 *Step-2* — Determination of Weibull Cracking Resistance Index ($\text{Weibull}_{\text{CRI}}$)

9.1.2.1 The fitting parameters is used to determine Weibull Cracking Resistance Index using Equation E.6.

$$Weibull_{CRI} = \left(\frac{\eta}{\beta}\right) \times log[A] \qquad \text{E.6}$$

where:

$\beta$ = The shape parameter

$\eta$ = The scale parameter

A = The area parameter

**10 Report**

10.1 Report the following information

10.1.1 Test temperature

10.1.2 Specimen geometry type

10.1.3 Specimen air void content

10.1.4 Specimen Thickness (mm)

10.1.5 Specimen Notch depth (mm)

10.1.6 Specimen diameter (mm)

10.1.7 Asphalt mix type

10.1.8 Measured Load unit (N or kN)

10.1.9 Measured displacement (mm)

10.1.10 $Weibull_{CRI}$

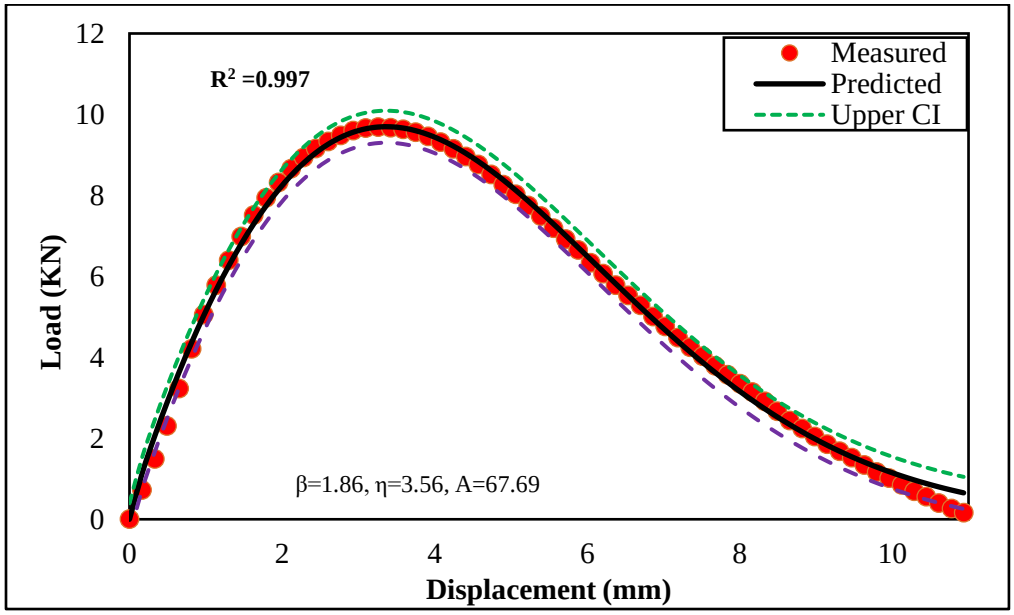


**Figure 1.** Fitting the Load-displacement curve using the modified Weibull function

# Appendix F - Standard Test Method for Evaluation of Asphalt Mixture Resistance to Intermediate Temperature Cracking using Multi-Stage Semi-Circle Bending Dynamic Test

**Designation: DXXXX− 19**

## Standard Test Method for
## Evaluation of Asphalt Mixture Resistance to Intermediate Temperature Cracking using Multi-Stage Semi-Circle Bending Dynamic Test

### 1. Scope

1.1 This test method covers procedures set out to determine the Slope (s) and Absolute Log (H) performance indicators of the Multi-Stage Semi-circle bending Dynamic (MSSD) test to evaluate asphalt mixes resistance to intermediate temperature cracking

1.2 This test standard is applicable to notched Semi Circular (SC) specimen prepared from Laboratory Mixed-Laboratory Compacted (LMLC), Plant Mixed-Laboratory Compacted (PMLC) asphalt mixes or extracted field cores.

1.3 The values stated in SI units are to be regarded as standard.

1.4 *This standard does not purport to address all of the safety concerns, if any, associated with its use. It is the responsibility of the user of this standard to establish appropriate safety and health practices and determine the applicability of regulatory limitations prior to use.*

### 2. Referenced Documents

2.1 ASTM Standards:[1]

D8 Terminology Relating to Materials for Roads and Pavements
D3549 Test Method for Thickness or Height of Compacted Bituminous Paving Mixture Specimens
D5361 Standard Practice for Sampling Compacted Bituminous Mixtures for Laboratory Testing
D6931 Indirect Tensile (IDT) Strength of Bituminous Mixtures
D8225 Determination of Cracking Tolerance Index of Asphalt Mixture Using the Indirect Tensile Cracking Test at Intermediate Temperature
D6925 Test Method for Preparation and Determination of the Relative Density of Asphalt Mix Specimens by Means of the Superpave Gyratory Compactor

2 AASHTO Standards:[2]

AASHTO T166 Bulk Specific Gravity (Gmb) of Compacted Hot Mix Asphalt (HMA) Using Saturated Surface-Dry Specimens

AASHTO T124 Determining the Fracture Potential of Asphalt Mixtures Using the Flexibility Index Test (FIT)
AASHTO R 30 Mixture Conditioning of Hot Mix Asphalt (HMA)
AASHTO T312 Preparing and Determining the Density of Asphalt Mixture Specimens by Means of the Superpave Gyratory Compactor

---

[1] For referenced ASTM standards, visit the ASTM website, www.astm.org, or contact ASTM Customer Service at service@astm.org. For *Annual Book of ASTM Standards* volume information, refer to the standard's Document Summary page on the ASTM website.

[2] Available from American Association of State Highway and Transportation Officials (AASHTO), 444 N. Capitol St., NW, Suite 249, Washington, DC 20001, http://www.transportation.org.tandards, visit the ASTM

**3. Summary of Test Method**

3.1 The MSSD applies a series of compressive loads that produce a predetermined series of SIFs in a notched Semi-Circular (SC) test specimen at a test temperature of 25 °C until fracture.

3.2 Ten predetermined Stress Intensity Factors (SIFs) associated with ten loading stages, including one conditioning stage (Stage-0) and nine loading stages (Stage-1 to Stage-9), were selected. Each loading stage applies a continuous haversine loading wave with a frequency of 1Hz.

3.3 The Number of cycles, load and displacement are collected during the test and are used to determine the Slope (s) and Absolute Log (H) performance indicators

**4. Significance and Use**

4.1 The MSSD has advantages over the available monotonic and dynamic cracking assessment tests and addresses major concerns to implement the Balanced Mix Design (BMD) (i.e., performance test validity, specimen preparation, and testing time).

4.2 The developed MSSD test simulates the repeated loading (dynamic) in a reasonable testing time (less than 9 hours per test regardless of mix type), has a fixed loading sequence that works for mixes with different characteristics (e.g., mix composition, percent air void content, thickness, etc.) and utilizes testing equipment and specimen geometry similar to that used in monotonic tests[3].

**5. Apparatus**

5.1 *Asphalt Mixture Performance Test (AMPT) —an* Asphalt Mixture Performance Test (AMPT) machine or other servohydraulic testing system (e.g., Universal Testing Machine [UTM], or Material Testing System [MTS]).

5.2 *Testing fixture* — The testing system shall have a suitable testing fixture for notched SC specimens follows the requirements in AASHTO TP124.

5.3 *Displacement measuring device* — The testing system shall have an internal/external displacement measuring device.

5.4 *Data acquisition system* — The testing system shall have a data acquisition system able to collect the number of cycles, load, and the displacement (internal or external) during the test at minimum data sampling frequency of 20 Hz.

5.5 *Specimen measurement device* — A caliper shall be used to measures specimen diameter and thickness as well as the notch depth and length.

5.6 *Saw* — A laboratory saw to make a notch in the semicircular specimen and trim the extracted field cores is needed.

5.7 *Gyratory compactor* — A gyratory compactor is needed to compact the test specimens.

**6. Hazards**

6.1 Standards Laboratory caution should be exercised when handling, mixing, compacting, and preparing asphalt mixtures and test specimens.

**7. Specimen Preparation**

7.1 The MSSD test may be conducted on laboratory-prepared specimens or extracted field cores from constructed test sections.

[3] H. Alkuime, E. Kassem, F.M. Bayomy, R. Nielsen, Development and evaluation of Multi-Stage Semi-circle bending Dynamic (MSSD) test to assess the cracking resistance of asphalt mixes., Construction and Building Materials. (2019).

7.2 Laboratory prepared specimen

7.2.1 *Asphalt mix*—Laboratory prepared specimen is prepared either from Laboratory Mixed-Laboratory Compacted (LMLC) or Plant Mixed-Laboratory Compacted (PMLC) asphalt mixes.

7.2.2 *Specimen geometry*— Specimen shall have 150 ± 2 mm diameter and 50 ±1 mm thickness and *a* notch *that is* 15 ±1 mm *in* length and 1.5 ±1 mm *in* width.

7.2.3 *Aging* — Specimen prepared from LMLC mixes shall be short-term aged in accordance with AASHTO R30. No short-term aging is required for specimens prepared from PMLC mixes.

7.2.4 *Air void content* — Test specimens shall be compacted to a target air void content of 7 ±0.5% in accordance with AASHTO T 312 at the required *thickness*

7.3 *Extracted field cores*

7.3.1 Field cores shall be extracted using a 150-mm coring bit.

7.3.2 *Specimen geometry* — The extracted field cores shall have 150 mm diameter and minimum thickness of 30 mm and *a* notch *that is* 15 ±1 mm *in* length and 1.5 ±1 mm *in* width

7.3.3 *Air Void content* — The air void content of the extracted field cores shall be measured prior to testing.

**8. Testing procedures**

8.1 Identify the required applied load for each loading stage.

8.1.1 The MSSD tests applied ten predetermined SIFs associated with ten loading stages, including one conditioning stage (Stage-0) and nine loading stages (Stage-1 to Stage-9) were selected.

8.1.2 Each loading stage applies a continuous haversine loading wave with a frequency of 1Hz (Figure F.1)

8.1.3. Each wave resulted in a change in SIF (ΔK) of $K_{max}$-$K_{min}$ where $K_{max}$ is the SIF associated with maximum applied load and $K_{min}$ is the stress intensity factor associated with the setting load (Figure F.1)

8.1.4 In the MSSD test, the $K_{min}$ and $K_{max}$ were predetermined for each loading stage. Figure F.2 shows $K_{min}$, $K_{max}$, and ΔK for each loading stage of the nine stages of the test.

8.1.5 These stress intensity values in addition to specimen geometry were used to back-calculate the required compressive applied load using Equations D.1-D.4

$$K_{IC} = \left(Y_{1_{(0.8)}}\right) \times \left(\sigma_{max}\sqrt{\pi a}\right); \qquad \text{F.1}$$

$$Y_{1_{(0.8)}} = 4.782\text{-}1.219\left(\frac{a}{r}\right) + 0.063exp\left(7.045\left(\frac{a}{r}\right)\right) \qquad \text{F.2}$$

$$\sigma_{max} = \frac{P_{max}}{D \times t} \qquad \text{F.3}$$

$$P_{stage-i} = \left[\frac{24 \times (\%K_{IC\,stage-i})}{\left(Y_{1_{(0.8)}}\right) \times (\sqrt{\pi a})}\right] \times (D \times t) \qquad \text{F.4}$$

Where:

| | | |
|---|---|---|
| KIC | = | The fracture toughness (N/mm3/2) |
| $P_{stage-i}$ | = | The required load for stage-i |
| $P_{max}$ | = | The maximum load (N) |
| t | = | Specimen thickness (mm) |
| %KICU | = | The percentage of fracture toughness |

for stage-i (N/mm$^{3/2}$)

$\sigma_{max}$ = The maximum tensile stress (N/mm$^2$)

D = Specimen diameter (mm)

8.2 8.2 Place the specimen in the test fixture inside the testing system for preconditioning for minimum of 2 hours at 25 °C prior to testing.

8.4 Test the specimen following the require loading stages until fracture. The number of cycles, applied load, and displacement shall be measured during the test

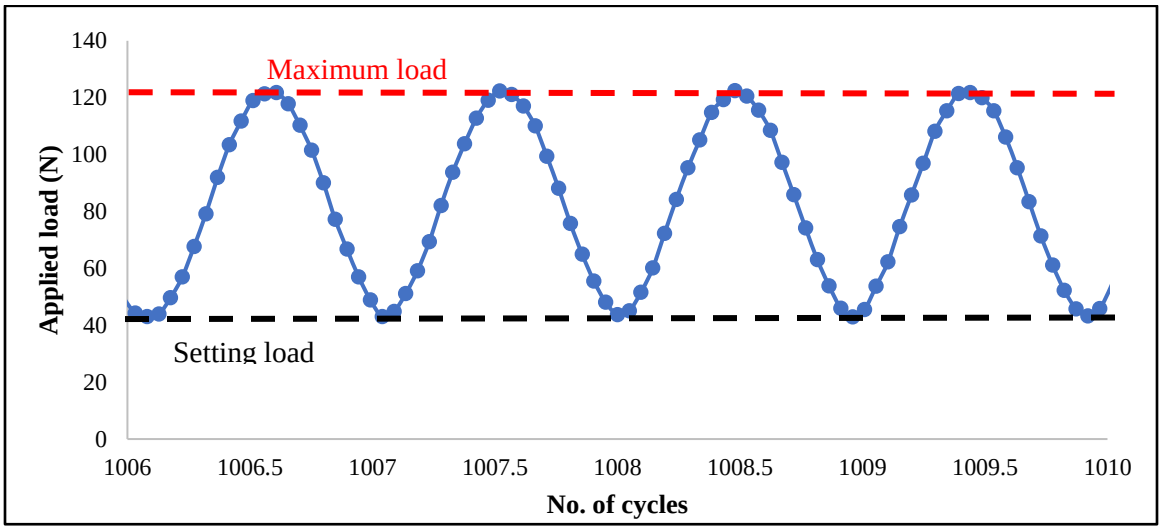


**Figure F.1**. MSSD continuous haversine loading wave

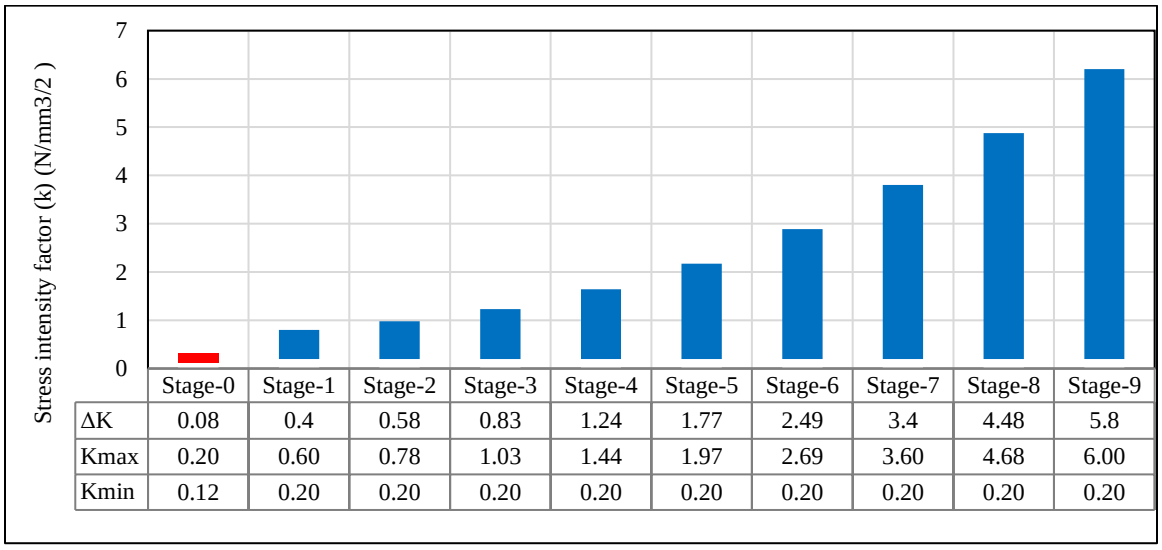


| | Stage-0 | Stage-1 | Stage-2 | Stage-3 | Stage-4 | Stage-5 | Stage-6 | Stage-7 | Stage-8 | Stage-9 |
|---|---|---|---|---|---|---|---|---|---|---|
| ΔK | 0.08 | 0.4 | 0.58 | 0.83 | 1.24 | 1.77 | 2.49 | 3.4 | 4.48 | 5.8 |
| Kmax | 0.20 | 0.60 | 0.78 | 1.03 | 1.44 | 1.97 | 2.69 | 3.60 | 4.68 | 6.00 |
| Kmin | 0.12 | 0.20 | 0.20 | 0.20 | 0.20 | 0.20 | 0.20 | 0.20 | 0.20 | 0.20 |

**Figure F.2** ΔK, Kmax, and Kmin for each load

## 9. Data interpretation

9.1 Figure F.3 shows the collected data in the MSSD test, including the applied load, the actuator vertical displacement, and the number of loading cycles

9.2 Two performance indicators were proposed to analyze the MSSD data including the slope (z) and Abs (log *H*).

9.3 The intercept (log *H*) reflects the initial rate of displacement per cycle, while the slope (*z*) reflects the increment in the displacement rate with the change in SIF.

9.4 The higher slope indicates a faster rate of damage. A higher slope is associated with a lower absolute intercept (Abs [log *H*]). Therefore, mixes with a lower slope (z) and higher Abs (log *H)* are expected to exhibit higher resistance to cracking.

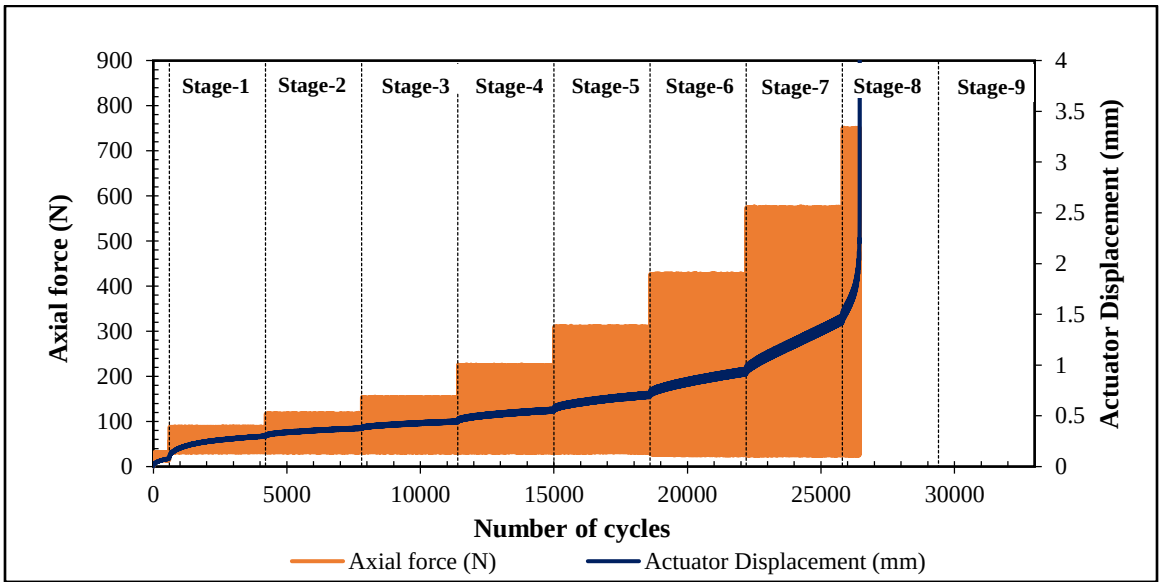


**Figure D.3** MSSD test typical output

9.5 The MSSD performance indicators (H and z) can be determined by performing the following steps:

9.5.1 Plot the vertical actuator displacement ($v$) versus the number of loading cycles ($N$) (Figure D.4)

9.5.2 Fit the curve from Step No. 1 with a 6th-degree polynomial function (Figure D.4).

9.5.3 Determine the rate of change in vertical actuator displacement with the number of cycles ( $\frac{dv}{dN}$ ) at the end of each testing stage and the failure cycle.

9.5.4 Determine the change in SIF (ΔK) for each testing stage (Figure D.4).

9.5.5 Plot ΔK versus the associated $\frac{dv}{dN}$ on a log-log scale (Figure D.5).

9.5.6 Determine the MSSD performance indicators (H and z) by fitting the data using a power function using Equation F.5

$$\frac{dv}{dN} = H\,(\Delta K)^z \qquad \text{F.5}$$

where:

| | | |
|---|---|---|
| v | = | Vertical actuator displacement (mm) |
| N | = | Number of loads cycles (Cycle) |
| *dv*/*dN* | = | The rate of vertical actuator displacement to the number of cycles |
| ΔK | = | Mode I SIF range ($K_{max}$ - $K_{min}$) |
| *H* and *z* | = | *F*itting constants for |

the MSSD model.

## 10 Report

10.1 Report the following information

10.1.1 Test temperature

10.1.2 Asphalt mix type

10.1.3 Specimen air void content

10.1.4 Specimen Thickness (mm)

10.1.5 Specimen Notch depth (mm)

10.1.6 Specimen diameter (mm)

10.1.7 Measured Load unit (N or kN)

10.1.8 Measured displacement (mm)

10.1.9 slope (z)

10.1.10 Abs [log *H*]

## 11 Keywords

11.1 asphalt mix racking resistance; balanced mixed design; semi-circular bending; performance-engineered mix design, fatigue cracking; intermediate temperature cracking

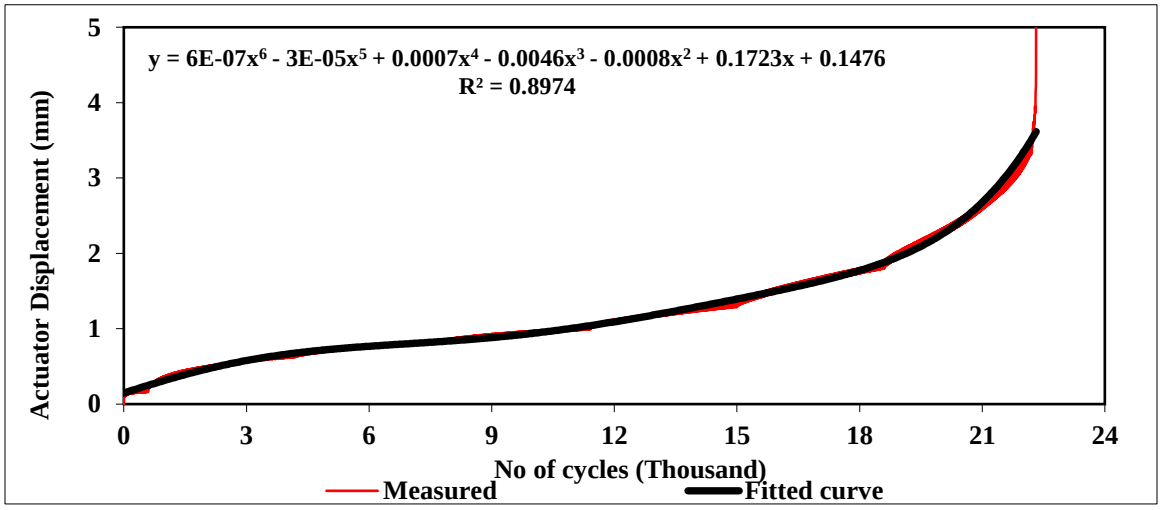


**Figure F4**. Fitting the S-curve with a 6th-degree polynomial function

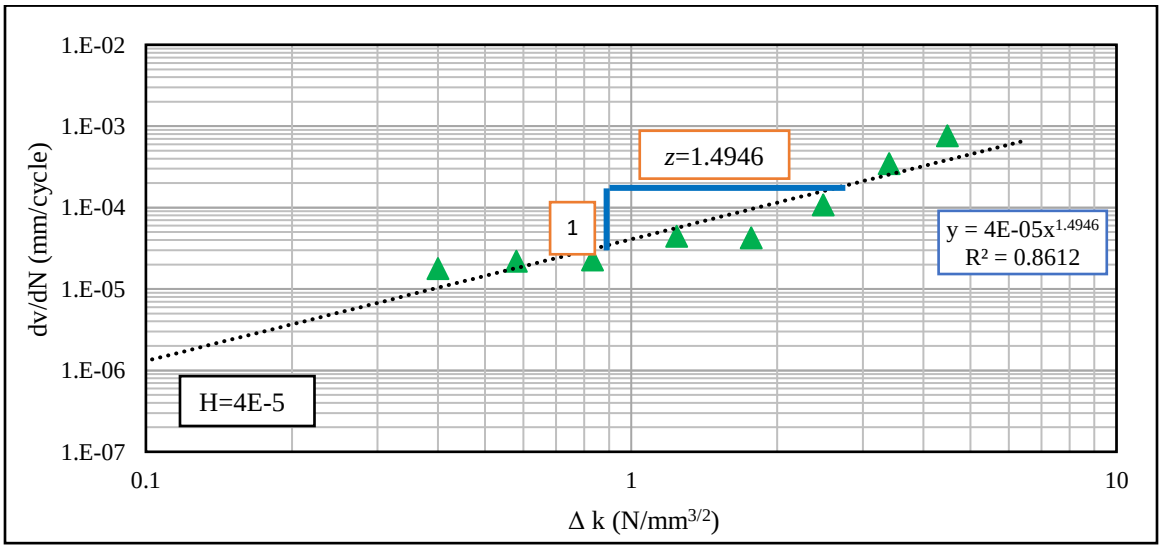


**Figure F5**. Determination of MSSD performance indicator

# Appendix G - Permissions

The National Academies of
SCIENCES • ENGINEERING • MEDICINE

**National Academies Press**
**Rights & Permissions**

November 7, 2019 **Reference #: 11071900**

Hamza Alkuime
Graduate Student, Civil and Environmental Engineering
University of Idaho
875 Perimeter Drive MS 1022
Moscow, ID 83844-1022

Dear Ms. Alkuime:

You have requested permission to reproduce the following material copyrighted by the National Academy of Sciences in a dissertation:

***Exhibits 2-3, 2-15, 2-18, and 3-2, Development of a Framework for Balanced Mix Design. Contractor's final report for NCHRP Project 20-07, Task 406, 2018***

Your request is granted for the material cited provided that credit is given to the copyright holder. Nonexclusive rights are extended for noncommercial use of this material.

Suggested credit (example):
Transportation Research Board. West, R., C. Rodezno, F. Leiva, F. Yin. 2018. *Development of a Framework for Balanced Mix Design. Contractor's final report for NCHRP Project 20-07, Task 406*. Reproduced with permission from the National Academy of Sciences, Courtesy of the National Academies Press, Washington, D.C.

Thank you,

Barbara Murphy

Barbara Murphy
Permissions Coordinator
National Academies Press

500 Fifth Street, NW, Washington, DC 20001
Phone 202.334.1902 Fax 202.334.2793 E-mail Bmurphy@nas.edu www.nationalacademies.org